Charles University

First Faculty of Medicine

Cell Biology and Pathology

Joao Victor de Sousa Cabral, MD

Použití regenerativní medicíny pro rekonstrukce na povrchu oka: Léčba deficience limbálních kmenových buněk pomocí moderní buněčné terapie

Regenerative Medicine in Ocular Surface Reconstruction: Advancing Cell-Based Therapies for Limbal Stem Cell Deficiency

Doctoral Thesis

Supervisor: Prof. Mgr. Kateřina Jirsová, Ph.D.

Prague, 2023

Declaration

I, Joao Victor de Sousa Cabral, hereby solemnly declare that I have prepared this final work independently and have taken care to meticulously provide references to all the sources and literature that I have consulted throughout the course of this research.

Furthermore, I would like to reiterate that this work has not been submitted or used to obtain any other university degree. Nonetheless, it is important to note that I have also contributed to a research paper, which has been published and is mentioned in this work. Specifically, I acted as the co-author, but my contribution was equivalent to that of the first author, as is mentioned in the published paper (**Appendix 3: Interleukin-13 increases the stemness of limbal epithelial stem cells cultures**). My former colleague did not use the paper for his own doctoral thesis, and it was originally appended to this thesis.

I agree with the permanent archiving of the electronic version of my theses in the database system interuniversity project Theses.cz in order to allow permanent inspection of the resemblance of qualification work.

In Prague, 11.08.2023

_____

Joao Victor de Sousa Cabral, MD

Identification record

CABRAL, Joao Victor. *Použití regenerativní medicíny pro rekonstrukce na povrchu oka: Léčba deficience limbálních kmenových buněk pomocí moderní buněčné terapie. [Regenerative Medicine in Ocular Surface Reconstruction: Advancing Cell-Based Therapies for Limbal Stem Cell Deficiency]*. Prague, 2023. 246 pages, 7 appendices. Doctoral Thesis (Ph.D.). Charles University, First Faculty of Medicine, Institute of Biology and Medical Genetics, Supervisor Jirsová, Kateřina.

Dedication

I wholeheartedly dedicate this dissertation to my beloved mom, the pillar of strength and unwavering support. I am profoundly grateful for her guidance, love, and belief in my potential, which have been pivotal in shaping the person I am today. Her wise counsel and guidance have been my compass during challenging times, guiding me toward achieving my aspirations. This dissertation celebrates her enduring impact on my life, and I am forever grateful for that.

Acknowledgment

I want to express my deepest gratitude to my esteemed supervisor, Professor Mgr. Kateřina Jirsová, Ph.D., whose guidance, expertise, and encouragement have been invaluable throughout this research journey. Your unwavering support and insightful feedback have helped shape this thesis into its final form.

I am also indebted to my colleagues, who have played a crucial role in this research endeavor. Thank you, Mgr. Peter Trošan, Ph.D., for your patience in teaching me many of the methods I have used for this work. Thank you, Eleni Voukali, Ph.D., for your assistance and collaboration in applying molecular biology methods in this work. My gratitude also to MUDr. Viera Veselá, Ing. Jiří Trousil, Ph.D., Lukáš Balogh, Assoc. Prof. RNDr. Jan Bednár, Ph.D., Mgr. Nikola Chmúrčiaková, Tijana Šopin, M.Sc., Magui Khazaal, MSc., Mgr. Ingrida Šmeringaoivá, Ph.D., Šárka Kalašová, Simona Krausová, Ing. Tereza Fenclová, Ph.D., MUDr. Karolína Kučerová, MUDr. Natália Smorodinová, Ph.D., Dagmar Hrabánková, and Mgr. Denisa Németová, Ph.D., for your valuable contributions, assistance with experiments, and for keeping me motivated.

My sincere appreciation goes to our collaborators, MUDr. Adam Šafanda, MUDr. Michaela Bártů, Ph.D., RNDr. Soňa Vodenková, Ph.D., Mgr. Kristýna Tomášová, Catherine Jackson, Ph.D., Dr. Prof. Tor Paaske Utheim, Ph.D., assoc. Prof. MUDr. Pavel Studený, Ph.D., Ing. Hana Studenovská, Ph.D., Ing. Tomáš Vacík, Ph.D., Dr. Evgeny Smirnov, Ph.D., and doc. RNDr. Dušan Cmarko, Ph.D., for their partnership, which has enriched this thesis with diverse perspectives and ideas, and also who collaborated on some of the methods and papers included in this work. I would also like to express my gratitude for the assistance and kindness provided by the staff and personnel of the Institute of Biology and Medical Genetics, First Faculty of Medicine, Charles University. To name a few, I extend my thanks to Prof. MUDr. Ondřej Šeda, Ph.D., and Ivana Karbusová.

I cannot overlook my friends and family's unwavering support and love. Your belief in me and your encouragement has been instrumental in overcoming the challenges along this journey. Last, I want to extend my heartfelt thanks to my partner, whose support, patience, and understanding have sustained me during the highs and lows of pursuing a Ph.D. And, of course, a special mention to my loyal companion, my dog, Rico, whose companionship has provided comfort during long hours of research and writing.

Thank you all.

Financial support

Abstract

Limbal stem cell deficiency is a disease caused by the impairment of limbal epithelial stem cells (LESCs), leading to the replacement of the corneal surface with nontransparent conjunctiva, and its treatment is not standardly available worldwide. This work focuses on preparing cells for treating both uni- and bilateral forms of the disease using advanced cell-based therapy. It investigates LESCs in various scaffolds (fibrin, nanofibers) and explores non-limbal cell sources like oral mucosal epithelial cells (OMECs) under standard complex and xenobiotic-free culture conditions. The study uses immunofluorescence and gene expression to detect stem cell markers, proliferation, and differentiation capacity of cultured cells. Moreover, long-term OMECs storage with different media and cryoprotective agents and the healing properties of the amniotic membrane (AM) were also examined.

We found that adding interleukin-13 to the culture media enhanced LESCs' stemness. LESCs on fibrin gels showed higher expression of stemness markers, while those on polymers expressed more mesenchymal ones. Using standard and xeno-free media, we successfully prepared OMEC-containing cell sheets on fibrin gel substrates. The cultured cells exhibited high expression of stemness genes (*ΔNp63α*, *NGFR*, *KLF4*) and decreased levels of differentiation (lower *KRT13* expression). Keratins related to basal layer and progenitor cells (*KRT14*, *KRT15*, *KRT17*, *KRT19*) were highly expressed in both conditions. The cells in complex media had a higher proliferation rate, evidenced by the upregulation of *MKI67*, with an earlier onset of the growth and reaching confluence sooner than xeno-free cultures. OMECs formed a confluent cell sheet even after storage in liquid nitrogen. Better outcomes (confluence, viability) were observed for OMECs stored in complex media alone or with 5% glycerol, compared to complex media with 10% glycerol or 10% dimethyl sulfoxide, particularly when stored after the first passage instead of using primary cells. Lastly, we showed that cryopreserved AM is a safe and effective treatment for non-healing wounds, with consistent interplacental quality among AM grafts and a strong analgesic effect.

In conclusion, we have prepared and finalized protocols for cultivating limbal and oral mucosa cells. The cell culture can now be transferred to the cleanroom conditions of the tissue bank for verification, and the protocols can be forwarded to the State Institute for Drug Control for approval for clinical use.

Keywords: limbal stem cell deficiency, stem cells, ocular surface, oral mucosa, cell culture, amniotic membrane, transplantation

Abstrakt

Deficience limbálních kmenových buněk je onemocnění způsobené poškozením limbálních epiteliálních kmenových buněk (LESC), které vede k přerůstání průhledné rohovky netransparentní spojivkou a ztrátě zraku. Léčba není standardně dostupná. Tato práce se věnuje přípravě buněk pro léčbu jedno- i oboustranné formy deficience pomocí moderní buněčné terapie. Zkoumá růst LESC na různých substrátech (fibrin, nanovlákna), dále buňky epitelu bukální sliznice (OMEC), kultivované ve standardním komplexním médiu i v podmínkách bez xenobiotik. K detekci markerů kmenových buněk, stanovení proliferační a diferenciační kapacity kultivovaných buněk byla použita imunocytochemie a genová exprese. Kromě toho byl hodnocen vliv dlouhodobého skladování OMEC v médiích s různými kryoprotektivními látkami. Součástí teze bylo i hodnocení hojivých vlastností amniové membrány (AM).

Zjistili jsme, že přidání interleukinu-13 do kultivačního média zvýšilo kmenovost LESC. LESC pěstované na fibrinu více exprimovaly márkry kmenovosti, buňky na nano-vlákenných polymerech exprimovaly více márkrů mezenchymálních. Na fibrinu se nám kultivací ve standardním komplexním médiu, ale i v prostředí bez cizorodých látek (xeno-free) podařilo připravit kultury OMEC. Buňky vykazovaly vysokou expresi kmenových márkrů (*ΔNp63α*, *NGFR*, *KLF4*) a sníženou diferenciaci do fenotypu epitelu bukální sliznice (nižší exprese *KRT13*). Keratiny typické pro bazální vrstvou a progenitorové buňky (*KRT14*, *KRT15*, *KRT17*, *KRT19*), byly exprimovány v obou podmínkách. Buňky v komplexním médiu rostly rychleji (upregulace *MKI67*). Tyto buňky také dosáhly ve srovnání s buňkami kultivovanými v xeno-free médiu rychleji 100% konfluenci. OMEC vytvořily souvislou vrstvu buněk i po kryokonzervaci. Lepší výsledky (konfluence, viabilita) byly pozorovány u OMEC skladovaných v komplexním médiu bez kryoprotektiv, nebo v komplexním médiu s 5% glycerolem ve srovnání s komplexním médiem s 10% glycerolem nebo 10% dimethylsulfoxidem, zejména pokud byly mrazeny po první pasáži. Prokázali jsme, že kryokonzervovaná AM je bezpečná a účinná v léčbě dlouhodobě se nehojících ran, že má silný analgetický účinek, a že mezi AM štěpy není patrný rozdíl v intenzitě hojení.

Závěrem: připravili jsme postupy pro kultivaci limbálních buněk a epitelových buněk ústní sliznice. Kultivace lze nyní přenést do podmínek čistých prostor tkáňové banky k ověření, a protokoly předat Státnímu ústavu pro kontrolu léčiv ke schválení klinického hodnocení.

Klíčová slova: deficience limbálních kmenových buněk, kmenové buňky, povrch oka, bukální sliznice, kultivace buněk, amniová membrána, transplantace.

Table of Contents

Abbreviations

AA	Antibiotic-Antimycotic Solution
ABCB5	ATP-Binding Cassette, Sub-Family B, Member 5
ABCG2	ATP-Binding Cassette, Subfamily G, Member 2
ACTA2	Actin alpha 2, smooth muscle
ALDH3A1	Aldehyde dehydrogenase 3 family member A1
ALS	Alkali Labile Sites
AM	Amniotic Membrane
AMT	Amniotic Membrane Transplantation
ANOVA	Analysis of Variance
BSA	Bovine Serum Albumin
CEBPD	CCAAT enhancer binding protein delta
CFA	Colony Forming Assay
CLAU	Conjunctival Limbal Autograft
CLET	Cultivated Limbal Epithelial Transplantation
COM	Complex Medium
COM_L	Complex Medium for Limbal Explant Culture
COMET	Cultivated Oral Mucosal Epithelial Transplant
CPA	Cryoprotective Agent
dAM	Deepithelized Amniotic Membrane
DMEM	Dulbecco's Modified Eagle Medium
DMSO	Dimethyl Sulfoxide
dps	Days Post-Seeding
EDTA	Ethylenediaminetetraacetic Acid
EGF	Epidermal Growth Factor
FBLN1	Fibulin 1
FBS	Fetal Bovine Serum
FDA	Food and Drug Administration
FPG	Formamidopyrimidine DNA Glycosylase
HE	Hematoxylin-Eosin
HPRT1	Hypoxanthine phosphoribosyltransferase 1
HS	Human Serum
IGFBP5	Insulin-like growth factor binding protein 5
IL13	Interleukin-13
ITGB1	Integrin subunit beta 1
ITS	Insulin-Transferrin-Selenium
K	Keratin

KRT3	Keratin 3 (gene)
KRT7	Keratin 7 (gene)
KRT8	Keratin 8 (gene)
KRT12	Keratin 12 (gene)
KRT13	Keratin 13 (gene)
KRT14	Keratin 14 (gene)
KRT15	Keratin 15 (gene)
KRT17	Keratin 17 (gene)
KRT19	Keratin 19 (gene)
KLAL	Keratolimbal Allograft
KLF4	Krüppel like factor 4
LECs	Limbal Epithelial Cells
LESCs	Limbal Epithelial Stem Cells
LMP	Low Melting Point
lr-CLAL	living-related-Conjunctival Limbal Allograft
LRIG1	Leucine-rich repeats and immunoglobulin-like domains 1
LSCD	Limbal Stem Cell Deficiency
MKI67	Marker of proliferation Ki-67
MSCs	Mesenchymal Stem Cells
NANOG	Nanog homeobox
NGFR	Nerve growth factor receptor
NHW	Non Healing Wounds
OCT	Optimal Cutting Temperature
OCT4	POU class 5 homeobox 1
OMECs	Oral Mucosa Epithelial Cells
P	Passage
PAX6	Paired box 6
PBS	Phosphate Buffered Saline
PCNA	Proliferating Cell Nuclear Antigen
PCR	Polymerase Chain Reaction
PDLLA	Poly(L-lactide-*co*-DL-lactide)
RPL32	Ribosomal Protein L32
RT-qPCR	Reverse Transcription Quantitative Real-time Polymerase Chain Reaction
S	Specimen
SBs	Single-Strand Breaks
SD	Standard Deviation
SLET	Simple Limbal Epithelial Transplantation
SOX2	SRY-box transcription factor 2

TA	Tranexamic Acid
TACs	Transient Amplifying Cells
THY1	Thy-1 cell surface antigen
VSX2	Visual system homeobox 2
XF	Xenobiotic-free
ΔNp63a	ΔN p63 Transcription Factor Alpha Isoform

Preface

Limbal stem cell deficiency (LSCD), a condition affecting the cornea, is the impetus for this doctoral dissertation, aiming to provide a comprehensive understanding of it and explore alternative treatment options in the field of advanced therapy medicinal products. The initial section of the introduction sheds light on the nature of LSCD, elucidating the intricacies of this disorder that motivated the research endeavor. An overview of the currently available treatment options for LSCD is presented, highlighting their limitations and paving the way for examining an alternative approach, culturing oral mucosal cells. Moreover, an in-depth examination of limbal epithelial cells is provided to establish a foundation for comprehending the subsequent discussions.

The introduction proceeds by offering a concise overview of the cornea and the epithelium to facilitate a holistic comprehension of the research focus. As LSCD primarily affects the anterior segment of the eye, it becomes essential to acquaint the reader with the structure and significance of the cornea, which acts as the primary site for the pathological manifestation. The role of the corneal epithelium, responsible for the barrier function and maintenance of corneal integrity, is also elaborated upon to provide a context for understanding the impact of LSCD on the corneal tissue.

Furthermore, the mechanisms involved in corneal repair and the existing treatment modalities are explored. By investigating the repair mechanism of corneal damage, the introduction seeks to enhance the reader's comprehension of the challenges encountered in addressing LSCD and the importance of exploring alternative approaches.

The subsequent sections of the introduction delve into the rationale behind utilizing the culture of oral mucosal cells as an alternative treatment strategy for LSCD. The dissertation offers fresh insights into the field by providing a comprehensive justification for this therapeutic avenue, including the search for a culture technique that avoids animal components. Additionally, histological and morphological details pertaining to the oral mucosa are outlined, elucidating the unique properties that make it suitable for cellular therapy in LSCD, an alternative option when autologous limbal stem cells (LSCs) are not available.

Recognizing the importance of sample preservation for future use, especially in the context of potential secondary transplants in the same patient, the dissertation delves into the cryopreservation of tissues. By exploring the principles and techniques of cryopreservation,

the feasibility and challenges of storing oral mucosal cell samples for subsequent use are assessed. This discussion provides valuable insights into the practical considerations of utilizing oral mucosal cells in clinical settings.

Lastly, it highlights the standard use of amniotic membranes (AM) as a supporting substrate for cell culture, establishing an intersection between the main topic of LSCD and the use of AM for the treatment of chronic non-healing wounds. Additionally, this section provides a broader perspective on the applications of amniotic membranes and their potential synergies with the main research topic.

By examining the pathophysiology of LSCD, the cornea, and its epithelium, the repair mechanisms, and the existing treatments, the groundwork is laid for the subsequent examination of the potential of oral mucosal cell culture. The following sections of the dissertation will expand upon these introductory concepts, providing detailed analyses, methodological approaches, and key findings to advance the understanding and potential treatment strategies for LSCD.

1. Introduction

1.1. Limbal Stem Cells Deficiency

Limbal stem cell deficiency (LSCD) is a disease of the ocular surface that results from the destruction or dysfunction of the limbal epithelial stem cells (LESCs), leading to a loss of the corneal epithelium's barrier function (Ahmad, 2012; Yin & Jurkunas, 2018). This is usually caused by injuries, chemical burns, thermal burns, inflammation, and inherited diseases (Ahmad, 2012; Bonnet, Roberts, & Deng, 2021). The deficiency of the limbal stem cells results in the replacement of the corneal surface by not transparent conjunctival tissue (conjunctivalization), **Figure 1**, which eventually leads to the vascularization and opacification of the cornea (Masood et al., 2022), **Figure 2**. Other signs of LSCD include persistent or recurrent epithelial defects, ocular surface inflammation, and scarring (Deng et al., 2019). Decreased or loss of vision and discomfort are frequent symptoms that lower health-related quality of life (Deng et al., 2019).
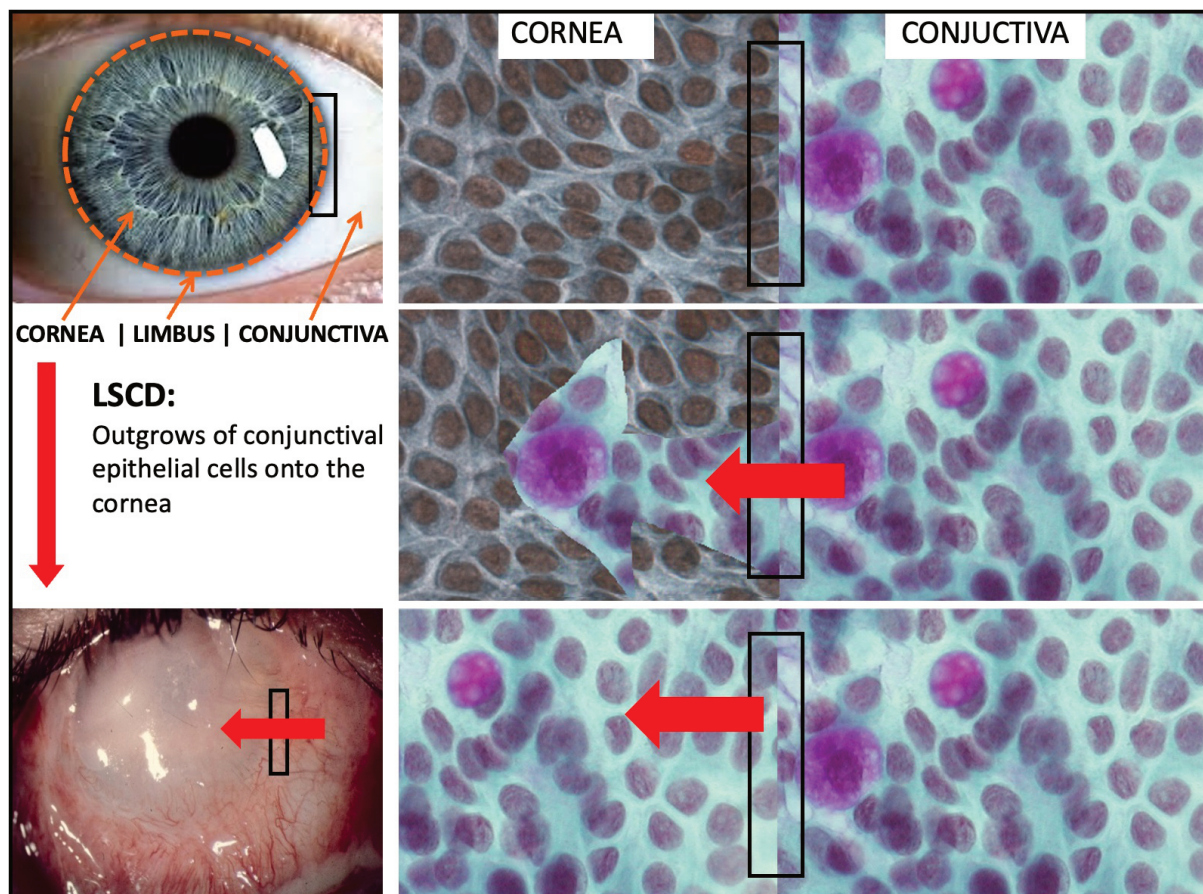
FIGURE 1: Representation of the conjunctival epithelium ingrowths onto the surface of the

cornea (red arrows), known as conjunctivalization. Such a condition originates as a result of progressive depletion or dysfunction of the limbal epithelial stem cell (LESCs) population. Image from the author's archive.
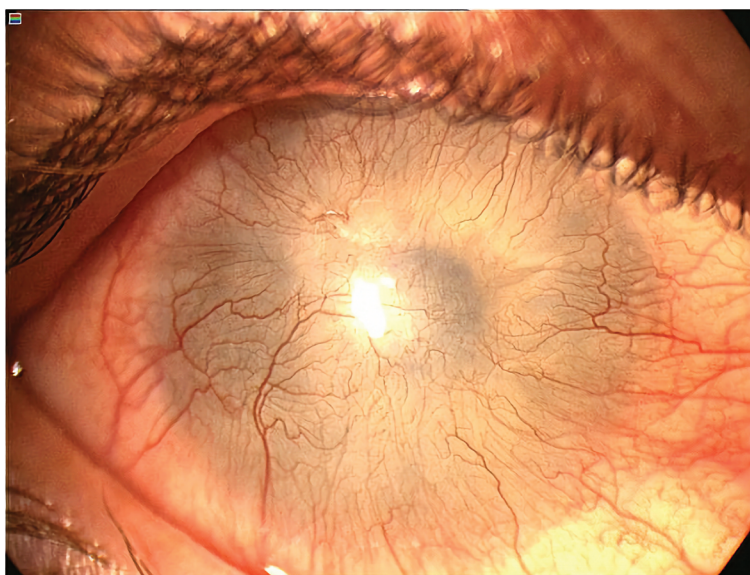
FIGURE 2: The vascularized conjunctival epithelium covering the ocular surface in a patient with limbal stem cell deficiency (LSCD). Image from the laboratory archive.

1.1.1. Treatment and Advanced Therapy Medicinal Products for LSCD

The choice of treatment depends on whether LSCD is unilateral or bilateral, the extent of damage (partial or total), and the overall health of the patient (Ruan et al., 2021; Elhusseiny et al., 2022), **Figure 3**. Conjunctival limbal autograft (CLAU) was first described as a therapy for unilateral total LSCD by Kenyon and Tseng in the late 1980s (Kenyon & Tseng, 1989); however, it increases the risk of iatrogenic LSCD in the healthy donor eye (Elhusseiny et al., 2022). Based on advancements in cell culture techniques, Pellegrini et al. (Pellegrini et al., 1997) described cultivated limbal epithelial transplantation (CLET) for unilateral LSCD, in which a small limbal tissue was taken from the patient's healthy eye and utilized to manufacture corneal epithelial cell sheets *in vitro*. The cultured cell sheet may be transplanted onto the recipient's eye using a carrier, such as an amniotic membrane (AM) or fibrin gel, a biodegradable material, and Food and Drug Administration (FDA)-approved commercial product (Eslani, Baradaran-Rafii, & Ahmad, 2012; Spotnitz, 2014; Nguyen et al., 2018). More recently, Sangwan et al. (Sangwan et al., 2012) introduced simple limbal epithelial transplantation (SLET) as an alternative to CLET.
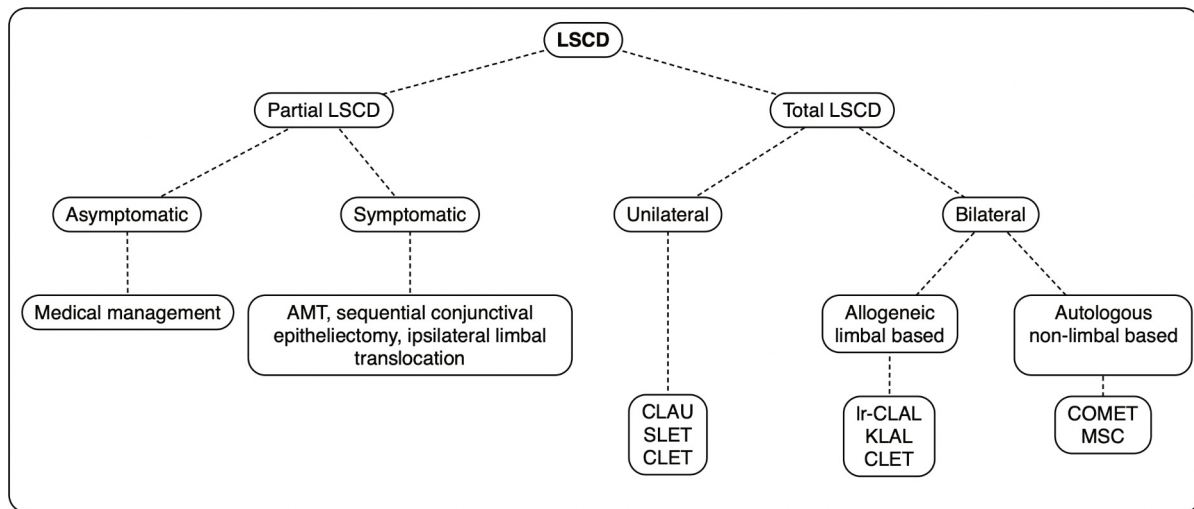
FIGURE 3: A diagram with current therapeutic options for limbal stem cell deficiency (LSCD). CLAU, conjunctival limbal autograft, KLAL, keratolimbal allograft, Ir-CLAL, living-related conjunctival limbal allograft, SLET, simple limbal epithelial transplantation, COMET, cultivated oral mucosal epithelial transplantation, AMT, amniotic membrane transplantation, MSCs, mesenchymal stem cells. Based on Elhusseiny et al. (Elhusseiny et al., 2022).

Bilateral total LSCD has traditionally been treated with allogeneic limbal grafts from cadavers or living donors (Yazdanpanah et al., 2019). Both keratolimbal allograft (KLAL) and living-related-conjunctival limbal allograft (lr-CLAL) are examples of these procedures (Yazdanpanah et al., 2019; Elhusseiny et al., 2022), both requiring long-term systemic immunosuppression to prevent graft rejection (Yazdanpanah et al., 2019).

Researchers have looked into non-limbal autologous sources of epithelial grafts for bilateral total LSCD due to the scarcity of allogeneic limbal tissue and the difficulties brought on by an immunological rejection of allografts (Haagdorens et al., 2016). Nakamura et al. (Nakamura et al., 2004) introduced autologous cultivated oral mucosal epithelial transplant (COMET) in 2004 to treat bilateral LSCD. They demonstrated the viability of transplanting cultured autologous oral epithelial cells on an AM substrate to provide the advantages of autologous transplants to patients lacking an existing population of healthy LESCs (Nakamura et al., 2004).

Additional potential sources of non-limbal cells have been researched over the past few years with varying degrees of success (Haagdorens et al., 2016; Lachaud, Hmadcha, & Soria, 2019; Ghareeb, Lako, & Figueiredo, 2020; Nosrati et al., 2021). To date, oral mucosa epithelial cells (OMECs) and mesenchymal stem cells (MSCs) have been shown to be safe and effective for treating patients with ocular surface failure caused by LSCD (Calonge et al.,

2019; Calonge et al., 2021).

The advancements in the treatment options for LSCD led to the first stem cell-based therapy approved for commercial use in the European Union, Holoclar® (Chiesi Farmaceutici), in 2015, representing a significant advancement in regenerative medicine (Pellegrini et al., 2018). To create a graft grown *ex vivo*, Holoclar® employs a patient's LESCs from the unaffected eye. A normal transparent corneal surface can be made after graft transplantation into the injured eye because it expands the LESC population (Pellegrini et al., 2018). In 2021, Holoclar® was also approved for treating patients in the Czech Republic. Later, Ocural® was introduced in Japan in 2021 as the first product in the world for bilateral LSCD treatment using COMET (Toshida et al., 2023).

In this context of ocular surface reconstruction, the AM has contributed to its development. De Rotth et al. (de Rotth, 1940) proposed the AM's first ocular indication in 1940. Since then, several uses have been documented for treating ocular surface disorders. Amniotic membrane transplantation (AMT) can be carried out alone (cryopreserved or dehydrated), in combination with various tissue transplants (CLAU, lr-CLAL, and KLAL), acting as a cell carrier (CLET and COMET) (Grueterich, Espana, & Tseng, 2003a; Nakamura et al., 2004; Ma et al., 2009), or even establishing an environment that permits the in-vivo expansion of LESCs (SLET) (Sangwan et al., 2012). AMT may be utilized in any of these situations with various objectives (temporary patch or permanent graft). Still, due to its anti-inflammatory, antiangiogenic, anti-scarring, and antibacterial qualities, it may always work to mitigate the negative consequences of LSCD (Sabater & Perez, 2017).

The present study will go through the therapeutic range of LSCD in the sense that it will showcase the culture of LESCs and its optimization with interleukin-13 (IL13) and the comparison of growth in nanofibrous polymer membrane and fibrin gel; the research on alternative non-limbal cell source, OMECs, and their cultivation in different culture conditions to analyze which favors the preparation of cell sheet graft containing putative stem cells. This work aims to broaden the availability of advanced therapy medicinal products and offer an alternative treatment to those who suffer from bilateral LSCD. Lastly, the AM's anti-inflammatory, antiangiogenic, anti-scarring, and antibacterial properties will be evaluated by studying the healing of chronic non-healing wounds. Worth mentioning that the AM was also considered as culture support for OMECs, and AM's properties were assessed on the healing of chronic wounds.

The following chapters will go in-depth into the anatomy and physiology of the relevant structures for an overall understanding of the topic.

1.2. Cornea and Limbus

1.2.1. Cornea

The cornea, a transparent and avascular structure, composes the eye's outermost layer (DelMonte & Kim, 2011). Its primary physiological role is to allow external light to enter the eye and to contribute to its focus on the retina (Spadea et al., 2016). In fact, it provides more than two-thirds of the total refractive power of the eye and is the major refracting lens (Secker & Daniels, 2008; Nishida, Saika, & Morishige, 2021). The cornea also serves as a barrier that protects the eye from losing fluids (Gonzalez-Andrades, Argüeso, & Gipson, 2019). These essential functions are due to the corneal structure composed of six layers (Nishida, Saika, & Morishige, 2021), from anterior to posterior: corneal epithelium, epithelial basement membrane, Bowman's layer, the stroma, Descemet membrane, and endothelium, **Figure 4**.
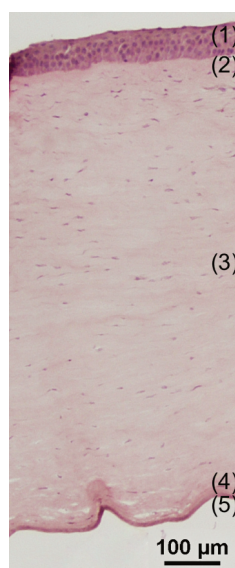
FIGURE 4: Histology of the cornea: epithelium and epithelial basement membrane (1), Bowman's layer (2), stroma (3), Descemet membrane (4), and endothelium (5). Image from the author's archive.

The cornea lacks lymphatic and blood arteries and thus has an angiogenic privilege against neovascularization in response to minor wounds, ensuring that corneal transparency is

constantly preserved (Ghafar, Jalil, & Kamarudin, 2021). Besides, the corneal stroma is exceptional in its uniform distribution of 25 – 30 nm-diameter fibrils that are consistently packed into lamellae (Hassell & Birk, 2010). This configuration reduces light scattering and enables transparency (Hassell & Birk, 2010). Moreover, the endothelium regulates the movement of fluid through membrane pumps (Srinivas, 2010), also ensuring the transparency of the cornea (Osei-Bempong, Figueiredo, & Lako, 2013).

1.2.1.1. Corneal Epithelium

The corneal epithelium has a thickness of around 50 μm and is made up of four to six layers of nonkeratinized, stratified squamous epithelial cells (Sridhar, 2018), including flattened apical squamous cells, subapical cells that have winglike structures – called "wing cells" – and a basal columnar cell layer (Gonzalez-Andrades, Argüeso, & Gipson, 2019). The specialized basal cell layer offers a tight anchorage of the epithelium to the underlying stroma through small stud-like structures called hemidesmosomes, whose main component is α6β4 integrin (Torricelli et al., 2013; Castro-Muñozledo et al., 2017).

The corneal epithelium is renewed within 7 to 14 days (West, Dorà, & Collinson, 2015). These cells originate from the LESCs, which reside in the corneoscleral limbus in an undifferentiated state (Schlötzer-Schrehardt & Kruse, 2005). The self-renewal capacity of LESCs is unlimited, and their mitotic activity is low (Gonzalez-Andrades, Argüeso, & Gipson, 2019). More details about corneal epithelium regeneration are explained further.

1.2.2. Limbus

The limbus is a 1.5 – 2.0 mm-wide transition zone between the cornea and sclera (Bonnet et al., 2021). It comprises an epithelium (between the corneal epithelium and the conjunctival epithelium) and a stroma containing vessels and different types of cells, such as MSCs and melanocytes (Schlötzer-Schrehardt & Kruse, 2005; Dziasko, Tuft, & Daniels, 2015; Funderburgh, Funderburgh, & Du, 2016).

Extensive research on the phenotype and function of corneal stem cells has strongly suggested that the basal layer of the limbus is the prime location of epithelial stem cells in the cornea, commonly referred to as LESCs (Schermer, Galvin, & Sun, 1986; Cotsarelis et al., 1989; Pellegrini et al., 1999; Lavker, Tseng, & Sun, 2004). Less than 10% of basal limbal epithelial cells (LECs) are classified as LESCs (Schlötzer-Schrehardt & Kruse, 2005).

The limbal subepithelial connective tissue contains papilla-like structures known as

the palisades of Vogt, which are interspaced by limbal epithelial crypts that project upwards from the stroma deep into the epithelium, and where the LESCs are situated (Goldberg & Bron, 1982; Townsend, 1991; Bizheva et al., 2017), **Figure 5**. LESCs are shielded from shear stress by these structures, providing them with nutrition from nearby blood veins (West et al., 2015; Gonzalez-Andrades, Argüeso, & Gipson, 2019).
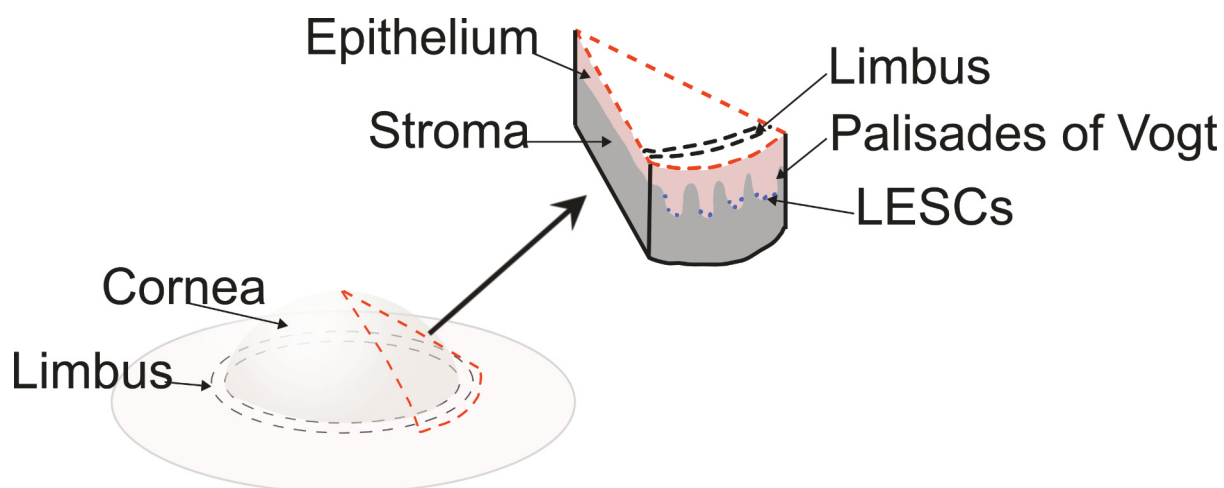
FIGURE 5: Illustration of the human cornea and limbus in a schematic form. A cross-section showing where the cornea, limbus, and palisades of Vogt, situated at the eye's cornea-limbal-scleral intersection. Limbal epithelial stem cells (LESCs) are situated in the basal layer of the palisades of Vogt. Illustration by the author.

1.2.2.1. LESCs and Cornea Regeneration

LESCs are essential for maintaining corneal transparency and vision as they are self-renewing cells that restore the corneal epithelium throughout life (Ebrahimi, Taghi-Abadi, & Baharvand, 2009). LESCs are typically mitotically inactive (Barbaro et al., 2007; Chen et al., 2015), and cuboidal in shape with a smaller volume than the basal cells of the central and peripheral cornea (Chen et al., 2004).

LESCs nuclei are heterochromatin-rich and have a high nucleus-to-cytoplasm ratio, but their nucleoli are poorly defined (Lehrer, Sun, & Lavker, 1998; Romano et al., 2003; Chen et al., 2004; Schlötzer-Schrehardt & Kruse, 2005). *In vivo* confocal microscopy studies have shown that limbal basal cells have a smaller diameter (around 10 μm in all studies) and higher cell density than central corneal or limbal suprabasal cell layers (Romano et al., 2003; Kobayashi & Sugiyama, 2005; Patel, Sherwin, & McGhee, 2006; Shortt et al., 2007).

The core principle of corneal homeostasis states that because the mass of the corneal epithelium is constant, the rate of cell gain and loss must be equal (Sharma & Coles, 1989).

The "X, Y, Z" hypothesis, put forth by Thoft and Friend in 1983 (Thoft & Friend, 1983), is the most widely accepted theory for corneal homeostasis.

These undifferentiated LESCs in the limbal epithelial crypts' basal epithelial layer have high proliferative potential (Lavker & Sun, 2000). They can divide symmetrically (in the horizontal plane) into two identical cells or asymmetrically to produce another LESC and a transient amplifying cell (TAC) in both vertical and horizontal planes (Sangwan, 2001; Kaplan et al., 2019). Early TACs multiply and move centripetally to occupy the corneal epithelial periphery. These cells lose some of their capacity for regeneration as more mature TACs replace the early TACs (Beebe & Masters, 1996; Lehrer et al., 1998). Then, as TACs move centripetally (towards the central cornea's cuboidal basal layer), TACs divide into postmitotic cells. The terminally differentiated cells migrate outward into the wing-shaped suprabasal layer, producing multiple layers of flattened, squamous superficial cells that are eventually sloughed off from the ocular surface (Pellegrini et al., 1999; Secker & Daniels, 2008; Yoon, Ismail, & Sherwin, 2014; Islam, Sharifi, & Gonzalez-Andrades, 2019; Masood et al., 2022), **Figure 6.**
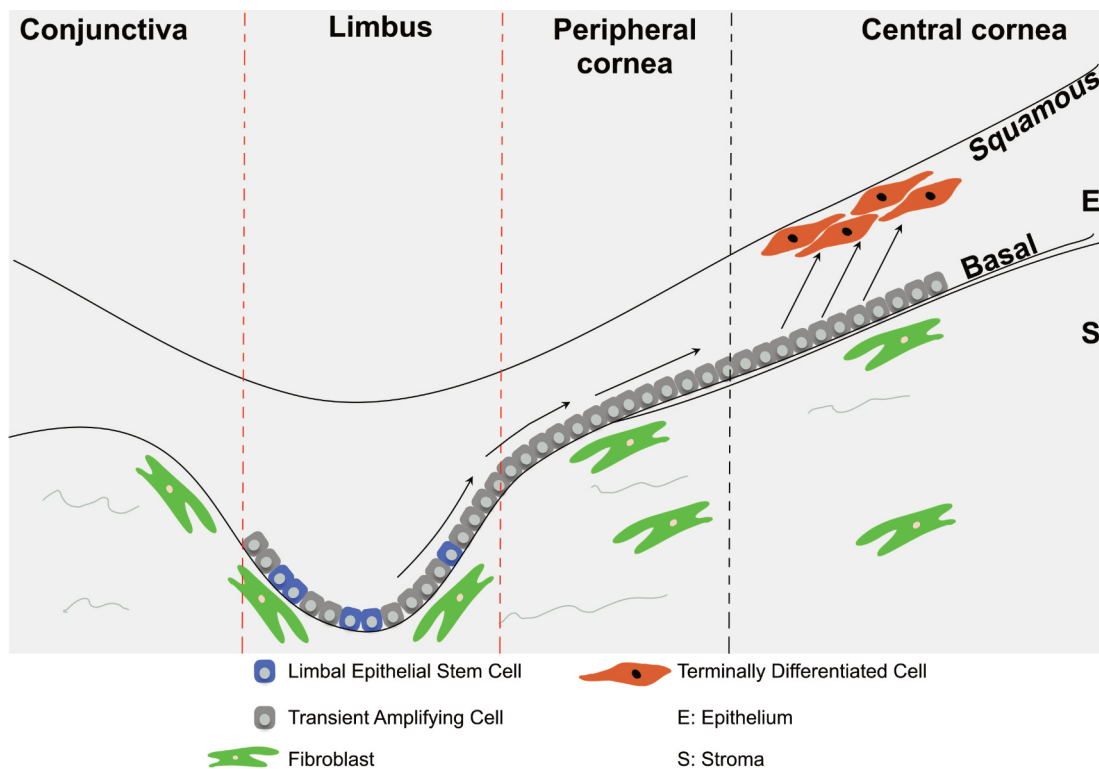
FIGURE 6: LESCs divide to produce TACs which migrate toward the apical layers of the corneal epithelium and eventually become terminally differentiated cells. Illustration by the

author, based on Masood et al. (Masood et al., 2022).

LESCs' capacity to restore corneal epithelium in both homeostatic and pathological conditions highlights the significance of these cells and suggests the existence of specific regulatory mechanisms that control LESCs proliferation and phenotype (Beebe & Masters, 1996). The regular death and desquamation of corneal epithelial cells and their replenishment through division from stem cells in the limbus all contribute to a net movement of epithelial cells in an apical direction (Eghrari, Riazuddin, & Gottsch, 2015).

1.2.2.2. Characterization of LESCs

Many molecules have been proposed to identify the basal cell layer of the limbal epithelium or cell clusters within it and are thought to identify LESCs along with early TACs (Takács et al., 2009). On the other hand, differentiation markers that are not present in limbal basal epithelial cells can be used as negative markers for LESCs. Typically, a combination of these markers is used to identify putative stem cells in the limbal epithelium (Takács et al., 2009). The detection of LESCs is still largely dependent on the presence or absence of particular biomarkers. However, none of the putative biomarkers have been shown to be LESC-specific, making it challenging to develop a reliable technique to identify LESCs (Guo et al., 2018).

According to research by Pellegrini et al. (Pellegrini et al., 2001), basal cells of the limbal epithelium produce the nuclear p63 transcription factor (specifically the isoform ΔNp63α), a p53 homolog connected to epithelial regeneration proliferation, both *in vivo* and *in vitro*, but not expressed by TACs, thus differentiating LESCs from TACs (Koster et al., 2004). The stem cell factor ΔNp63 is assumed to be in charge of keeping cells with the capacity for regeneration in an uncommitted state (Yang et al., 1998; Senoo et al., 2007). Expression of Δ*Np63α* was specifically detected in the limbal basal cells, which indicated that ΔNp63α might be a putative biomarker of LESCs (Saghizadeh et al., 2011). A hallmark study from Rama et al. (Rama et al., 2010) showed that more than 3% of p63-positive cells from total clonogenic cells in the grafted cell sheet led to successful transplantation (78%) in patients with LSCD, and this 3% threshold has been considered in multiple studies for defining the quality of the transplanted cell sheet (Calonge et al., 2021).

Another stemness marker is the ATP-binding cassette, subfamily G, member 2 (ABCG2) (de Paiva et al., 2005), which has been proposed as a universal and conserved

marker for stem cells from various tissues (Ebrahimi et al., 2009). Immunofluorescence staining by De Paiva et al. (de Paiva et al., 2005) revealed ABCG2+ cells among limbal basal cells, and these same cells were later demonstrated to have stem cell characteristics, confirming their identification as LESCs. As a result, ABCG2 was presumed to be a biomarker of LESCs (Ebrahimi et al., 2009).

In the study by De Paiva et al. (De Paiva, Pflugfelder, & Li, 2006), cells of the smallest size (10 – 16 μm) expressed the highest levels of the putative stem cell markers ΔNp63 and ABCG2 at both mRNA and protein levels. They also contained the highest number of label-retaining cells (side population) and had the highest clonogenic capacity in culture (De Paiva, Pflugfelder, & Li, 2006). ATP-Binding Cassette, Sub-Family B, Member 5 (ABCB5) has been identified as a gene required for LESCs development and repair (Ksander et al., 2014). Moreover, it was discovered that p63α and ABCB5 are coexpressed in LESCs. Because basal limbal epithelium contained ABCB5+ cells, ABCB5 may be a potential biomarker for LESCs (Ksander et al., 2014). Also, leucine-rich repeats and immunoglobulin-like domains 1 (LRIG1) has emerged as a key regulator of stem cell behavior due to its function in growth factor receptor regulation (Gur et al., 2004). The Krüppel-like factor 4 (KLF4), is a marker of pluripotency (Cieślar-Pobuda et al., 2016), and it suppresses epithelial-mesenchymal transition (Tiwari et al., 2017).

Regarding proliferation markers, Proliferating Cell Nuclear Antigen (PCNA) has a half-life exceeding 20 hours, allowing it to be detected in cells that are in the resting (G0-phase) state (Ohta & Ichimura, 2000). Furthermore, cultures generated by TACs express *PCNA* but not *p63* (Pellegrini et al., 2001). On the other hand, Ki-67, encoded by the gene *MKI67*, is a nuclear antigen found in proliferating cells, but not in resting cells (Gerdes et al., 1983; Gerdes et al., 1984; Gerdes et al., 1991; Scholzen & Gerdes, 2000; Sun & Kaufman, 2018). In the cell culture of limbal explants, there is an increase in the *MKI67* expression among both basal and suprabasal epithelial cells (Joseph et al., 2004).

When culturing LECs, it is also essential to assess their differentiation and characterization, as there are keratins specific for the limbus, cornea, and conjunctiva (Moll, Divo, & Langbein, 2008; Merjava et al., 2011b). As the expected outcome of grafting the cell sheet to the ocular surface is to reconstruct the corneal epithelium, it is acceptable that these cultured cells differentiate towards the corneal phenotype while in culture. However, it is crucial to maintain the stem cell pool during the culturing process to ensure the long-term

sustainability of corneal regeneration (Rama et al., 2010).

The corneal epithelium's specific and differentiation-related keratin (K) pair is K3/K12 (Moll, Divo, & Langbein, 2008), which is expressed across all layers of the corneal epithelium; however, only the suprabasal cells and basally situated corneal stem cells are positive in the limbus (Pitz & Moll, 2002; Moll, Divo, & Langbein, 2008). As basal limbal cells do not express K3, it is possible to distinguish between them and cells from the upper limbal layers in addition to distinguishing between corneal and limbal cells, which is important for the diagnosis of LSCD (Merjava et al., 2011b).

K7 is overexpressed in the surface epithelial layer of the conjunctiva but is absent in the superficial layer of the limbus and cornea (Merjava et al., 2011b). K8 is a primary keratin of simple epithelial cells (Moll et al., 2008), and it is expressed in limbal epithelial cells (Merjava et al., 2011a; Schreurs et al., 2020). Merjava et al. (Merjava et al., 2011a) showed that K8 was present in the basal layer of the limbal crypts, extending into the suprabasal and superficial epithelial layers of the limbus and cornea, with a gradual decrease in signal intensity.

K5/K14 is specifically expressed in the limbal epithelial basal cells; thus, it functions as a putative LESCs biomarker (Zhao et al., 2008; Richardson et al., 2017). LESCs might be precisely identified using K5+/K14+ and K3-/K12- (Zhao et al., 2008). Yet, a study has shown that K5/K14 is an unreliable maker for undifferentiated LESCs *ex vivo* (Chen et al., 2010), as K14 is also detected in cells of the superficial corneal layer (Merjava et al., 2011b).

K15, a minor cytoskeletal component of stratified tissue (Moll et al., 1982), is present in the basal cells of the limbus and conjunctiva (Merjava et al., 2011b). K15 is an important keratin that is not expressed in differentiated corneal epithelium, unlike K14. It is also useful in distinguishing the limbal phenotype from the conjunctiva (Yoshida et al., 2006). Elder et al. (Elder, Hiscott, & Dart, 1997) showed that K17 was present throughout the whole corneal, limbal, and conjunctival epithelium, but in Merjava et al. (Merjava et al., 2011b), K17 was not present in these structures.

According to reports, K19 is a putative biomarker of LESCs and is expressed in limbal epithelial basal cells (Larouche et al., 2005; Larouche et al., 2010). Its specificity, nevertheless, is debatable. Chen et al. (Chen et al., 2004) discovered that corneal epithelial cells and LECs both expressed K19. Similarly to this, Ramirez-Miranda et al. (Ramirez-Miranda et al., 2011) found that limbal and conjunctival epithelial cells both expressed K19,

particularly close to corneal borders.

1.2.2.3. LESCs and Interleukin-13

Based on previous work from our group (Stadnikova et al., 2019), IL13, one of the anti-inflammatory interleukins and a T helper 2-type cytokine (Junttila, 2018), has a favorable effect on the proliferation and expression of the *ΔNp63a* gene in the conjunctival epithelium produced from limbal explants. We then hypothesized that IL13 would have a similar effect on the expansion of LESCs from limbal explants, preserving their stemness. Much research has not been done on how IL13 affects LESCs or stem cells in general. It makes IL13 a promising stem cell research target when combined with our finding of the function of IL13 in the stemness of conjunctival epithelial cells.

1.3. Oral Mucosa

The oral buccal mucosa consists of squamous stratified epithelium (Brizuela & Winters, 2022). This tissue is highly structured, avascular, semipermeable, and non-keratinized (Brizuela & Winters, 2022). The stratified epithelium of the oral mucosa comprises two layers, epithelial cells with a basement membrane and an underlying connective tissue, the lamina propria, which supports the oral epithelium (Squier & Kremer, 2001). The stratified squamous epithelium comprises many layers of elliptical-shaped cells, known as the *stratum spinosum*, which is followed by a layer of basal cells known as *stratum basal* (Dabelsteen, 1991; Squier & Kremer, 2001), **Figure 7**. The lamina propria contains minor salivary glands, structural fibers, blood vessels, fibroblasts, and other cell types (e.g., histiocytes, mast cells, lymphocytes) (Collins & Dawes, 1987; Squier & Kremer, 2001; Richard & Pillai, 2010; Squier & Brogden, 2011; Nguyen et al., 2012; Abdulmajeed, Dalley, & Farah, 2013).

The lamina propria and the epithelium are connected by an interdigitated interface. Its histological structure involves epithelial undulations known as *rete ridges* (or *rete pegs*), which protrude downward into the lamina propria (Brizuela & Winters, 2022). Dermal papillae, which are upward extensions of the lamina propria that resemble fingers, are produced as a result (Brizuela & Winters, 2022). The epithelium is firmly attached to the non-cellular basement membrane that separates these two tissues (Ali, Farooq, & Mohammed, 2021; Brizuela & Winters, 2022).
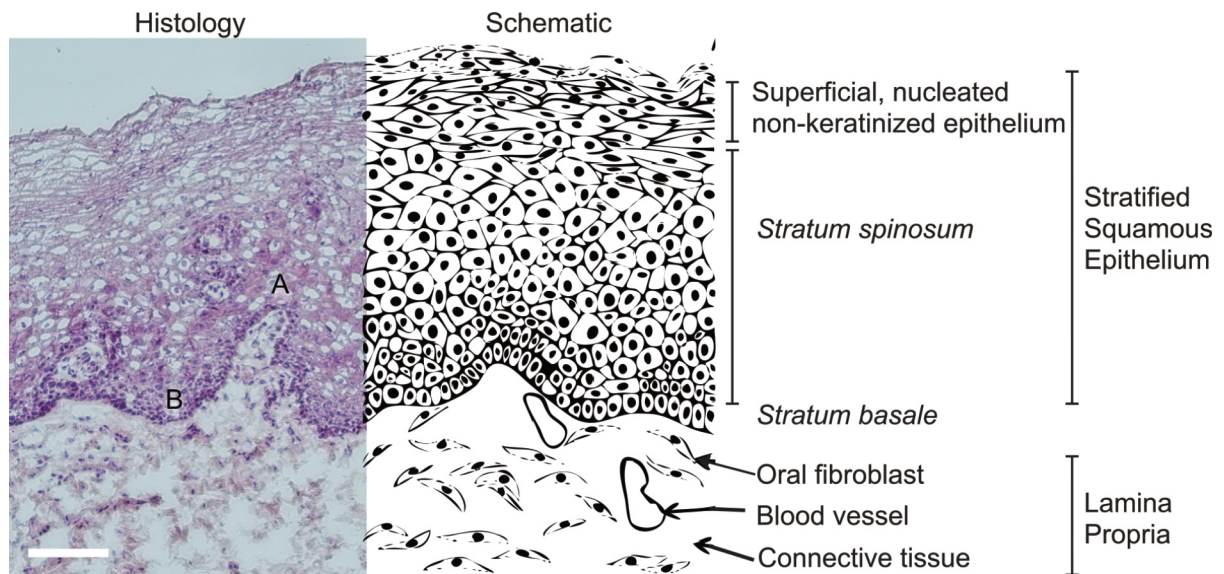
FIGURE 7: Oral buccal mucosa in a histological and schematic image. In the histological image, A represents the base of the rete ridge, and B the tip. Scale bar = 100 μm. Image from the author's archive and illustration by the author.

The squamous epithelium relies on epithelial stem cells for tissue renewal (Iglesias-Bartolome, Callejas-Valera, & Gutkind, 2013). Cell division in oral mucosa epithelium mainly occurs in the basal layer, which contains the stem cell compartment from which the oral mucosa is regenerated (Nguyen et al., 2012; Papagerakis et al., 2014). After dividing, the committed cells undergo differentiation, leading to the expression of structural keratin proteins and the loss of internal organelles as cells move superficially, start to flatten, and eventually slough off the surface (Dale, Salonen, & Jones, 1990; Fuchs, 1995; Winning & Townsend, 2000; Squier & Kremer, 2001). Basal cells are a heterogenous population composed of stem cells and TACs with slow and fast proliferative capacities, respectively. Transmigrating via the suprabasal layers, cells from the basal layer go through terminal differentiation (Oda & Watson, 1990). Although having a limited capacity for self-renewal, TACs are crucial for the growth of the cell population. TACs go through terminal differentiation once they have reached their proliferative potential (Nakamura, Endo, & Kinoshita, 2007a). In the oral epithelium, it takes 14 – 24 days for a stem cell to divide and the progeny to traverse through the entire thickness of the epithelium (turnover time) (Richard & Pillai, 2010).

1.3.1. OMECs for Treating LSCD

Oral buccal mucosa shares structural similarities with other stratified epithelia in that it comprises many layers of cells that gradually specialize as they approach the tissue surface, as evidenced by the expression of particular keratins and the loss of organelles. A few characteristics make them suitable for use in ocular surface reconstruction (Ramachandran et al., 2014), such as: requiring less time to grow in culture, do not undergo keratinization when maintained in culture, scarring of the biopsy location is inconspicuous, and, most importantly, they lack secondary structures like hair follicles and sweat glands (Juhl, Reibel, & Stoltze, 1989; Hata et al., 1995), and contain epithelial stem cells with similar characteristics to LESCs, which readily express markers for corneal determination (López et al., 2021).

The use of OMECs as a source of stem cells for treating LSCD has gained significant attention in recent years (Guérin et al., 2021), as it has several advantages, including the ability to obtain a large number of cells, the ease of harvesting, and the low risk of immune rejection (Hancox et al., 2020). Stem cells found in the basal layer of oral mucosa express markers associated with limbal stem cells and can be transdifferentiated into cells resembling corneal epithelial cells (Nakamura et al., 2007a; Hancox et al., 2020). A schematic approach to tissue retrieval, culture, and transplantation is shown in **Figure 8**.
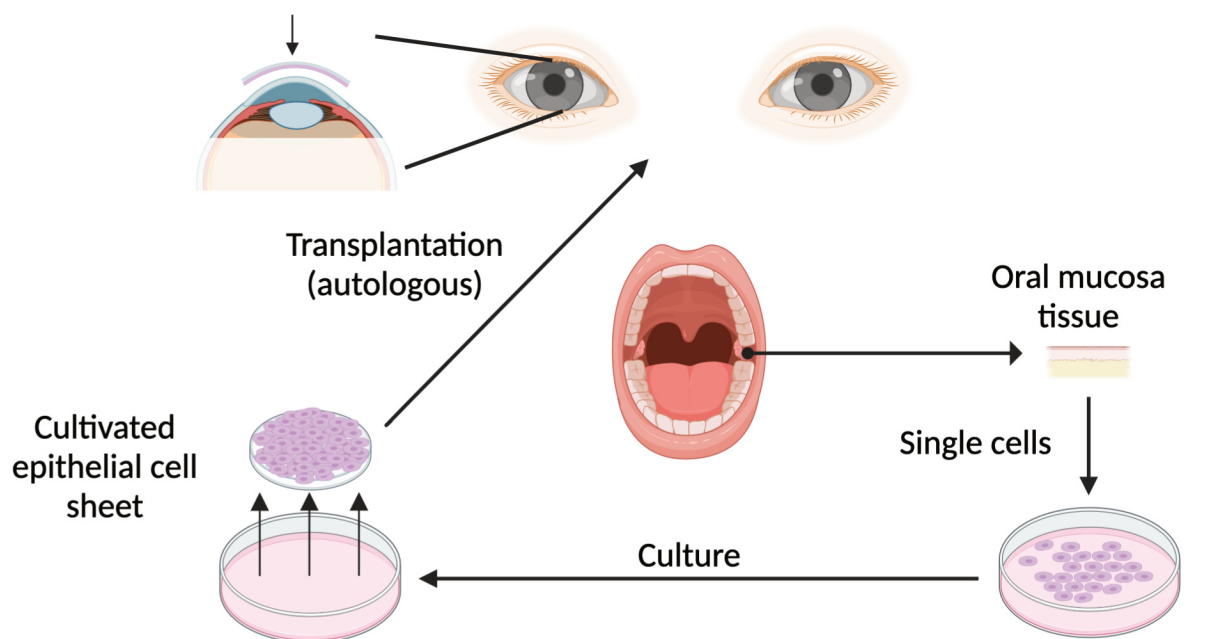
FIGURE 8: Schematic steps on the use of autologous oral mucosal cells for the treatment of bilateral limbal stem cell deficiency (LSCD). Oral mucosa tissue is collected from the buccal mucosa and used to prepare a cell suspension for cell culture. Subsequently, the engineered epithelial sheet is transferred to the ocular surface for the treatment of LSCD. Created with BioRender.com

Currently, the main concern is finding a marker to distinguish oral mucosal tissue from ocular surface epithelia to characterize transplants in patients accurately (Kolli et al., 2014). A clear marker for the oral mucosa would clarify the mechanism of action and help drive therapeutic choices (Kolli et al., 2014). Stimulation of resident corneal tissue implies the presence of residual limbal stem cells that can still interact with surrounding tissues, despite the clinical phenotype of the eye. A combination of the two processes or the transdifferentiation theory could also be considered (Attico, Galaverni, & Pellegrini, 2021).

It has been demonstrated that human oral keratinocyte stem/progenitor cell phenotypes could be characterized by their expression of p75NTR, a low-affinity neurotrophin receptor (Nakamura et al., 2007a). p75NTR was shown by Nakamura et al. (Nakamura et al., 2007a) to be expressed in the buccal mucosa's papillae. The p75NTR-positive cells were smaller and more capable of proliferating *in vitro* (Nakamura et al., 2007a). The putative stem cell marker p63 is observed in oral mucosal tissue's basal to suprabasal cell layers (Kasai et al., 2016).

In the literature, various markers have been used to distinguish between the three possible epithelial tissues on the ocular surface following COMET: oral mucosa, cornea, and conjunctiva (Inatomi et al., 2006; Nakamura et al., 2007b; Chen et al., 2009; Gaddipati et al., 2014; Kim et al., 2018). The keratin expression profile serves as a unique identifier to determine the origin of these epithelial cells (Moll et al., 2008). Specific keratins act as putative markers of stemness (K8, K14, K15, K17, K19) (Chen et al., 2004; Schlötzer-Schrehardt & Kruse, 2005; Yoshida et al., 2006; Figueira et al., 2007; Merjava et al., 2011a; Saghizadeh et al., 2014). Other keratins are linked to basal limbal epithelial cells (K8, K14, and K15) (Figueira et al., 2007; Merjava et al., 2011a), differentiated corneal epithelial cells (K3, K12) (Schermer et al., 1986), conjunctival cells (K7, K13, K19) (Poli et al., 2011; Jirsova et al., 2011) and differentiated oral mucosal cells (K4, K13) (Groeger & Meyle, 2019). Although keratin expression alone is insufficient to identify stem cells or progenitor TACs, combining the expression profiles of key keratins (e.g., *KRT14*, *KRT15*, *KRT17*, and *KRT19*) with other known potential markers (ABCG2, p63) can aid in the identification of

stem cells (Pathak et al., 2016).

Regarding the characterization of the oral mucosa, the pair K4/K13, mucosal stratified squamous epithelial cell markers (Kasai et al., 2016), for instance, is present in the suprabasal to the upper cell layers but not in the basal cell layer in both keratinized and non-keratinized oral epithelium (Moll et al., 2008; Squier & Brogden, 2011; Rao, Patil, & Ganavi, 2014; Kasai et al., 2016; Groeger & Meyle, 2019), while K14, K15, K19 are expressed by basal cells in the non-keratinized oral epithelium (Presland & Jurevic, 2002; Squier & Brogden, 2011; Kasai et al., 2016). K8, the primary keratin of simple epithelial cells (Moll et al., 2008), exhibits intense staining in the basal and parabasal layers, and stained single cells distributed throughout the *stratum spinosum*, with weak cytoplasmic staining in most other epithelial layers (Schreurs et al., 2020). On the other hand, K5 and K7 expressions are observed from the basal cell layer to the upper layer (Kasai et al., 2016).

1.4. Culture of LESCs and OMECs

1.4.1. Culture Media for *in vitro* Expansion of LESCs and OMECs

For the cultivation of LESCs, complex medium (COM) is usually employed, and media with very similar compositions are frequently used (Ramírez et al., 2015; Pellegrini et al., 2018). Fetal bovine serum (FBS, also known as fetal calf serum, but for standardization purposes, we will use FBS herein), antibiotic-antimycotic solution (AA), epidermal growth factor (EGF), hydrocortisone, insulin-transferrin-selenium (ITS), cholera toxin, and adenine are frequently included in COM for LESCs culture (Tsai, Li, & Chen, 2000; Meller, Pires, & Tseng, 2002; Brejchova et al., 2018).

According to previous studies, FBS increases the proliferation of limbal epithelial cells (Kruse & Tseng, 1992). However, it has been demonstrated that it is possible to culture LECSs without the use of serum in the medium (Lekhanont et al., 2009; Mimura et al., 2010). AA is added to prevent biological contamination from bacteria, yeast, and fungi (Weiskirchen et al., 2023). EGF increases clonogenic potential (Meyer-Blazejewska et al., 2010), and hydrocortisone plays an important role in keratinocyte proliferation and maintaining distinct epithelial colonies (Rheinwald & Green, 1975). ITS is employed as a basal medium supplement to lessen or completely replace the quantity of animal serum needed (Mainzer et al., 2014). Cholera toxin significantly promotes colony growth from a

small number of cultured human epidermal keratinocytes by an increase in intracellular cyclic AMP level (Okada, Kitano, & Ichihara, 1982; González, Chen, & Deng, 2017), while the addition of adenine to the culture media enhances the ability of epithelial cells to form colonies (Flaxman & Harper, 1975; Allen-Hoffmann & Rheinwald, 1984).

Regarding the culture of OMECs, its standard COM constituents follow a similar pattern as seen above, also including triiodothyronine, which has been shown to be helpful in the cultivation of keratinocytes by lowering the requirement for FBS in epithelial cultures to low levels (Hayashi, Larner, & Sato, 1978).

Media containing FBS or other questionable components (cholera toxin) (Yu et al., 2016) have been employed successfully for stem cell therapy in several countries (Ramírez et al., 2015). While the use of FBS is effective in promoting the growth of these cells *in vitro*, it is important to note that this product carries the risk of transmitted diseases, tumorigenesis, or precipitation of immunologic rejection, as well as biologic variability (Dua et al., 2005; Schwab, Johnson, & Harkin, 2006; Shortt et al., 2007; Shahdadfar et al., 2012; Llames et al., 2015).

Currently, reducing the usage of animal-derived products is a major goal of cell therapy development; for that, often-used chemicals are being replaced with those of human origin (Sharma et al., 2012). One alternative is to use human serum (HS) instead of FBS (Witzeneder et al., 2013; Utheim, 2015). This method has the advantage of being less xenogeneic and, thus, less likely to cause immunologic rejection or other adverse side effects (Tekkatte et al., 2011). In the present study, one of the main aims is to culture OMECs in xenobiotic-free (XF) media (containing HS) and produce a viable cell sheet. A protocol free of FBS and other animal-derived components is preferred for several reasons in the context of advanced stem cell therapies, as low-level contamination could go unnoticed even in Good Manufacturing Practice facilities (Erickson, Bolin, & Landgraf, 1991; Schwab, Johnson, & Harkin, 2006; Mannello & Tonti, 2007).

1.4.2. Substrates for *in vitro* Expansion of LESCs and OMECs

AM is the substrate most frequently used in clinical trials for treating LSCD using expanded cultured cells, both LESCs and OMECs (Utheim et al., 2016; Nguyen et al., 2018). AM has been utilized in both intact and deepithelialized (denuded) forms, each presenting its benefits and drawbacks (Utheim et al., 2016; Nguyen et al., 2018). Intact AM preserves

native amniotic epithelia in a devitalized state, promoting the deposition of basement membrane proteins. This, in turn, helps to keep stem cells in a partially undifferentiated state (Li et al., 2006). Nonetheless, using intact AM substrates also increases the possibility of immunological reactions (Nguyen et al., 2018). Another option, which appears to be the preferred choice when using AM, is to cultivate cells on the AM that has been stripped of its native epithelial cells, deepithelialized AM (dAM) (Riau et al., 2010; Utheim et al., 2016). But AM requires costly donor screening for microbial infections and storage, a skilled preparation, and the final product may exhibit variable thickness and transparency (Ma et al., 2002). More about the AM's properties will be explained in further detail in **1.7 Amniotic Membrane in Regenerative Medicine, page 40**.

Other substrates include fibrin gel, pioneered by Rama et al. (Rama et al., 2001) and have since been translated into the first commercial product for patients with LSCD, Holoclar®, which contains autologous expanded LESCs on a fibrin substrate (Pellegrini et al., 2018). The fibrin sealant from Tisseel (Baxter, Westlake Village, CA), which is prepared from human pooled plasma, is an FDA-approved commercial product, and fibrin sealant is the only agent presently approved as a hemostat, sealant, and adhesive (Spotnitz, 2014).

Fibrin gel, a biopolymeric material, is effective in treating patients with LSCD, and it is easy to prepare and handle (Rama et al., 2001; Di Iorio et al., 2010; Sheth et al., 2015; Nguyen et al., 2018; Pellegrini et al., 2018). Fibrin gel offers several advantages over synthetic materials when used as a tissue engineering scaffold and a cell carrier, as its excellent biocompatibility facilitates cell attachment (Li et al., 2015). Furthermore, fibrin gel mimics the natural blood-clotting process and self-assembles into a polymer network (Li et al., 2015). The gel is biodegradable, non-toxic, and inhibits fibrosis, tissue necrosis, and inflammation (Tuan et al., 1996; Radosevich, Goubran, & Burnouf, 1997; Weisel, 2005). However, there is a need to control the rate of fibrin degradation when seeding cells on this substrate, which is currently being addressed by using anti-fibrinolytic agents (Sheth et al., 2015). *In vivo*, the gel is completely resorbed and ultimately replaced by matrix components such as collagen (Tuan et al., 1996). One drawback of fibrin as a substrate is that it encourages angiogenesis (Dvorak et al., 1987), which is undesirable since the cornea is avascular (Gonzalez-Andrades, Argüeso, & Gipson, 2019). However, the gel is resorbed within days to weeks after transplantation, minimizing this effect (Radosevich, Goubran, & Burnouf, 1997).

The use of synthetic scaffolds presents promising opportunities to address clinical shortcomings related to culturing limbal and non-limbal epithelial stem cells (Nguyen et al., 2018). For instance, fibrous polymeric membranes have been utilized as scaffolds for eye tissue cell cultivation (Pellegrini et al., 2018), with high permeability being a crucial factor for successful eye graft functioning (Stanzel et al., 2014; Hotaling et al., 2016). Electrospun membranes made from biodegradable polymers offer several advantages, such as high porosity, large pore size, and low thickness. Zdraveva et al. (Zdraveva et al., 2023) studied electrospun scaffolds made from biocompatible polylactic acid modified with silk fibroin and gelation, which demonstrated improved adherence of LESCs and were confirmed to support cell growth, proliferation and corneal epithelial differentiation by the expression of specific marker analysis.

An ideal substrate meets specific requirements, such as availability, transparency, and ease of manipulation (Utheim et al., 2016). Additionally, it should be able to promote cell proliferation and viability. However, various culture methods have been used to demonstrate transplant success, and the most effective method for corneal regeneration has yet to be established. Finding appropriate substrates and protocols could lead to developing standardized and effective regenerative therapies for LSCD (Utheim et al., 2016).

1.4.3. Feeder layer

Although different media and substrates are used to grow cells, most researchers use 3T3 feeder cells (cell line of mouse embryonic fibroblasts), which are several cell lines of mouse embryonic fibroblasts (Mora, Brady, & Smith, 1970), to coculture the epithelium (limbal and oral mucosa) (Sharma et al., 2012), particularly in the cell suspension method (Schwab, Reyes, & Isseroff, 2000; Rama et al., 2001; Nishida et al., 2004a; Nishida et al., 2004b; Daya et al., 2005; Nakamura et al., 2006; Meyer-Blazejewska et al., 2010). Scientific evidence has demonstrated that utilizing a 3T3 feeder layer can enhance the properties of stem cells during the cultivation process (Rheinwald & Green, 1975; Pellegrini et al., 1999; Grueterich, Espana, & Tseng, 2003b). The main problem with this technique in clinical application is that the epithelial sheets 3T3 cocultured are xenogeneic (Martin et al., 2005).

Aiming to achieve a cell sheet product that could be used in clinical practice and commercialized, for this study, limbal and oral mucosa cells will be cultured on a feeder layer-free culture system, which has already been proven to produce cell sheets successfully

(Ilmarinen et al., 2013; Hongisto et al., 2017).

1.5. Genotoxicity

For ocular surface transplantation, the analysis of DNA damage in cultured cells is essential to ensure the procedure's safety and efficacy, as the long-term renewal of the epithelium following transplant surgery relies heavily on the presence of a functional pool of stem cells (Lorenzo et al., 2018).

Various factors, such as the composition of the medium and the duration of time in culture, influence the stability of the genome, levels of oxidative damage, and the efficiency of antioxidant defense and repair mechanisms (Shahdadfar et al., 2005; Lorenzo et al., 2009; Pathak et al., 2016). It has been indicated that assessing the levels of DNA single-strand breaks (SBs) and oxidative damage to DNA purine bases can provide valuable insights into the quality of a culture system (Lorenzo et al., 2009; Haug et al., 2013; Øsnes-Ringen et al., 2013).

The comet assay is a technique widely used to determine the presence of DNA SBs, including alkali-labile sites (ALS) such as baseless sugars, which are converted to breaks during alkaline incubation and electrophoresis (thus, SBs + ALS). The comet assay can be used to assess the genotoxicity of the cells before transplantation, ensuring that they do not carry significant DNA damage that could potentially lead to adverse effects (Rojas et al., 2014). First, cells are embedded in agarose and lysed, leaving the DNA as supercoiled loops attached to the nuclear matrix, forming a nucleoid. Electrophoresis is then performed, causing DNA loops with relaxed supercoiling due to an SB to extend towards the anode, resulting in comet-like images (viewed by fluorescence microscopy), where the relative tail intensity indicates the frequency of DNA breaks (Harris et al., 2015).

The standard alkaline comet assay, as it stands, can only identify SBs and ALS (Muruzabal et al., 2021). However, numerous DNA-damaging substances cause additional types of damage, such as oxidized and alkylated bases or cross-links (Muruzabal et al., 2021). To address this limitation to some extent, modifications have been made to the comet assay by introducing a digestion step after lysis using specific DNA repair enzymes known as DNA glycosylases (Collins, 2004; Muruzabal et al., 2021). One common modification involves assessing the level of oxidized purines by incorporating a digestion process with the bacterial DNA repair enzyme called formamidopyrimidine DNA glycosylase (FPG) (Collins, 2004;

Magdolenova et al., 2012).

1.6. Cryopreservation of Stem Cells for the Long-term Storage

An essential prerequisite to the commercial and clinical deployment of stem cells is appropriate cryopreservation protocols for long-term storage (Hunt, 2011). Cell cryopreservation is a method that maintains living cells viable and functioning even at cryogenic temperatures (often between -80 ºC to -196 ºC) (Zhao & Fu, 2017; Yang et al., 2020). The fine structure of cells is preserved through the method of cryopreservation, keeping biological material preserved at cryogenic temperatures for any significant amount of time (Mazur, 1970; Sambu, 2015).

Cell-based applications, including stem cell therapy, tissue engineering, assisted human reproduction, and transfusion medicine, rely heavily on cell cryopreservation as a supporting technology (Zhao & Fu, 2017; Yang et al., 2020). Cryopreserved cells or tissues provide certain benefits for clinical uses since cryopreserved products may always be available; rigorous quality testing can be done to ascertain whether the cells or tissue are appropriate for transplantation without obtaining new samples (Ibars et al., 2016; Jang et al., 2017).

Cryopreservation of limbal suspension cultures has been shown to be advantageous since it eliminates the need for further biopsies in the event of graft failure (Kaufman et al., 2014). Moreover, if the first treatment fails, long-term cryopreservation of surplus cultivated stem cells could also permit consecutive surgeries (Mohamed-Noriega et al., 2011; Lužnik et al., 2016). Oliva et al. also demonstrated that OMECs can be stored long-term in liquid nitrogen without affecting their morphology and phenotype (Oliva et al., 2019).

Cryopreservation is the standard method for the long-term storage of cells in suspension. However, standardized freezing and thawing protocols must be developed to preserve cultured tissue's stem cell content and structural integrity (Lužnik et al., 2016). Cryoprotective agents (CPAs) are employed for the successful cryopreservation of tissue and cells by maintaining the tissue's structural and biomechanical qualities during the freezing and thawing processes (Martín-López et al., 2023).

CPAs like dimethyl sulfoxide (DMSO) or glycerol, two organic solvents, are frequently utilized in intracellular protection to minimize the damaging effects of ice formation (Yang et al., 2020). However, they are not biocompatible (Yang et al., 2020).

While DMSO use has been linked to numerous adverse effects in patients, including neurotoxicity, cardiovascular failure, respiratory arrest, arrhythmias, and others (Yang et al., 2016; Jang et al., 2017), glycerol can cause severe hemolysis and renal failure (Best, 2015; Sui et al., 2019). Therefore, throughout the cryopreservation process, its concentration should be reduced (Martín-López et al., 2023). Despite this, DMSO and glycerol have proven remarkably effective and have found widespread use in research and clinical applications. For instance, stocks of red blood cells are cryopreserved using 20 – 40 wt% glycerol, while immortalized cell lines are routinely stored in 10% (v/v) DMSO (Murray & Gibson, 2022). Additionally, cells intended for clinical transplantation, such as hematopoietic stem cells, are frequently cryopreserved in 5 – 10% DMSO, among other additives (Lysak et al., 2021).

In the present study, we assessed the effectiveness of a CPA-free solution, which is a COM containing HS, instead of the standard FBS, compared to a CPA-based solution with a low DMSO (10%) and glycerol (5% or 10%) concentration for advanced therapy medicinal products, in an attempt to minimize the potential adverse effects on patients, and also with a high concentration of glycerol (50%). Moreover, we also tested an XF storage solution and its respective CPA-based solutions with DMSO (10%), and glycerol (5% or 10%). The interest is to optimize a storage solution that contains low to no CPA and avoid using xenogeneic material, considering the risk of such materials as has been mentioned before.

1.7. Amniotic Membrane in Regenerative Medicine

AM's unique biological and mechanical properties make it highly suitable for clinical applications (Pogozhykh et al., 2018). The transparent nature of AM, along with its lack of immunogenicity, facilitates and supports wound healing and reduces pain (Koizumi et al., 2000; Svobodova et al., 2022; Vrkoslav et al., 2023). AM plays a pivotal role in minimizing fibrosis, inflammation reduction, and regulation of angiogenesis. Moreover, it exhibits antimicrobial and antiviral properties, making it an excellent choice for medical interventions (Malhotra & Jain, 2014; Jirsova & Jones, 2017).

AM has its importance for the reconstruction of the ocular surface. AM has proven to be a valuable aid in the treatment of corneal and conjunctival defects, being employed either as a scaffold or as a bandage (Dua et al., 2004). The AM acts as a short-term overlay patch to mechanically safeguard the ocular surface, stimulate normal epithelial wound healing, and prevent intermediate-term ocular cicatricial sequelae (Sharma et al., 2016). AM has particular

potential for skin regeneration (King et al., 2007; Farhadihosseinabadi et al., 2018; Kjaergaard et al., 2001; Deihim, Yazdanpanah, & Niknejad, 2016; Fairbairn, Randolph, & Redmond, 2014; Farhadihosseinabadi et al., 2018). AM also has strong adhesion to the wound's surface, preventing infection (Díaz-Prado et al., 2010). Another benefit of this close adherence is that it keeps the area hydrated, which enhances AM's ability to reduce pain (Jirsova & Jones, 2017; Vrkoslav et al., 2023).

In the context of LSCD, AM transplantation (AMT) has been combined with LESCs and OMECs transplantation (e.g., CLET or COMET) (Le & Deng, 2019). AM can be utilized as a substrate and carrier of LESCs or on its own (Díaz-Valle et al., 2007; Chugh, Jain, & Sen, 2015; Le & Deng, 2019). Cultured cells are supported and protected by AM's toughness and elasticity, which supports LECs' adhesion and migration while maintaining their *in vivo* characteristics (Meller et al., 2002; Yeh et al., 2008).

In cell-based therapies for LSCD, AM is still the most widely used substrate and carrier for LESCs or OMECs (Tsai et al., 2000; Shortt et al., 2008; Kethiri et al., 2017), although research has been done on other materials, such as fibrin gels (Rama et al., 2001; Rama et al., 2010; Fasolo et al., 2017), contact lenses (Di Girolamo et al., 2009), and nylon sheets (Daya et al., 2005). The use of AM for cell culture was detailed previously, **1.4.2 Substrates for in vitro Expansion of LESCs and OMECs**.

For this thesis work, there are two approaches. First, as mentioned in the section **1.4.2 Substrates for in vitro Expansion of LESCs and OMECs**, AM has some disadvantages as a scaffold, and to circumvent those, OMECs will be mainly cultured in fibrin gels. Secondly, to further study the properties of AM in tissue engineering in the context of skin regeneration, cryopreserved AM will be grafted for treating chronic wounds, and the healing dynamics will be evaluated. This will bring valuable insights into understanding how AM works and its inter-variability for the treatment of wounds (including ocular surface wounds).

2. Hypotheses and Aims

2.1. Hypothesis 1: Increasing the Stemness of LECs Cultures and Alternative Substrates for Cell Culture

Previous work from our group (Stadnikova et al., 2019) found that IL13 positively affected the proliferative activity and *ΔNp63α* gene expression in the conjunctival epithelium generated from limbal explants. This result suggests that IL13 may play a crucial role in maintaining stemness, which could be used in developing a new culture medium for the culture of LESCs from limbal explants. To explore this hypothesis further, we plan on conducting experiments to investigate the effects of IL13 on the proliferation and gene expression of the LESC cultures compared with those of the control group. These experiments could provide valuable insights into the mechanisms of stem cell maintenance and the development of new culture media for LESCs culture.

Based on our team's previous work (Brejchova et al., 2018), we have already demonstrated that LECs cultured on fibrin gel exhibit a high growth rate and cell proliferation with minimal fibroblast-like cell contamination. However, exploring alternative synthetic materials may reveal even more significant benefits regarding stemness, proliferation, differentiation, and fibroblast contamination. For this purpose, we are going to culture LECs on both fibrin gel and electrospun poly(L-lactide-*co*-DL-lactide) (PDLLA) nanofibrous scaffolds.

Aims:

• To determine the effect of IL13 on the stemness, differentiation, proliferation, clonogenicity, and morphology of cultured LESCs;

• To compare LECs growth and cell behavior under two different culture substrates: electrospun PDLLA nanofibrous scaffolds coated with human plasma fibronectin and fibrin gel; to analyze the differences in the gene expression of specific markers, including stem cell, proliferation, keratins, and fibroblast genes.

2.2. Hypothesis 2: Preparation of OMECs on Fibrin Gel for Grafting

Oral mucosa tissue samples contain stem/progenitor-like cells in the epithelium's basal layer, which allows the preparation of grafts containing oral mucosal epithelial stem cells. The presence of stem cell population in the cell sheet can be confirmed with markers referred to be specific to stem cells.

Bilateral LSCD is also treated with oral mucosal epithelial cell sheet grafting. The cells are typically cultivated using xenogeneic materials (FBS, 3T3 cells, and media additives of animal origin), which have the potential to spread infectious illnesses or immunological responses. Cells are cultured on various substrates, including nanofiber scaffolds, AM, and fibrin gel. We hypothesized that removing animal components would improve the safety of the transplanted cells and could enhance the culture technique, contributing to preparing a good-quality cell sheet for the treatment of bilateral LSCD. Additionally, we hypothesized that combining OMEC culture in XF culture media on fibrin gel (used as a surgical sealant) might enhance this culture technique and directly contribute to a higher percentage of stem cells in the resulting cell sheet.

Aims:

• To culture oral mucosal epithelial cells on fibrin gel and AM and compare standard complex medium and xenobiotic-free culture systems, both supplemented with pooled human serum;

• To compare the kinetics of growth, stemness maintenance, differentiation, and DNA damage between the groups;

• To prepare a stable cell sheet on fibrin gel containing viable stem cells, all while preserving genome stability. Additionally, to develop a protocol that can be readily transferred to the State Institute for Drug Control to undergo clinical approval in the Czech Republic.

2.3. Hypothesis 3: Long-term Storage of OMECs in Liquid Nitrogen

Cryopreservation is used for long-term storage at ultra-low temperatures, and CPAs are added to minimize the damaging effects of ice formation. Preserving tissues or cells for long-term storage and on-demand delivery is critical for many fields, including stem cell

research, regenerative medicine, and tissue engineering, and that also applies to LECs and OMECs for the treatment of patients suffering from LSCD.

The hypothesis of the study is that the use of CPAs in the long-term storage of cells affects the number of stem cells and the proliferation status of the following cell culture. The study aims to compare the effects of CPAs (5% glycerol, 10% glycerol, 50% glycerol or 10% DMSO) with media without cryoprotectants on the preservation of stem cells and the proliferation status of the cells for cell culture. The hypothesis is based on the premise that using cryoprotectants, such as glycerol and DMSO, can cause toxicity and damage to the cells, affecting their stemness potential and proliferation after storage. The study will investigate whether using media without cryoprotectants can preserve the number of stem cells and maintain the proliferation status of the cells for cell culture and whether this method can be used for preparing cell sheets after thawing the cells.

Aims:

• To compare different CPAs (glycerol and DMSO), including not using a CPA, for long-term storage of oral mucosal epithelial cells in suspension;

• Analyze gene expression of cultured thawed cells, including a comparison with the gene expression of samples before storage (control);

• To find the best condition for long-term storage of OMECs, which could be used for transplantation purposes.

2.4. Hypothesis 4: (A) Cryopreserved AM for the Treatment of Non-healing Wounds and (B) Inter-placental Variability in the Healing Efficiency of AM

There is a significant economic burden of chronic non-healing wounds. AM is considered an ideal biological wound dressing due to its ability to promote granulation and epithelialization, reduce exudate, relieve pain, and provide a moist environment for healing. The hypothesis is that cryopreserved AM allografts would induce wound healing, shorten wound closure time, and reduce pain compared to the standard-of-care (SOC) method.

When preparing AM for clinical use, multiple sheets are typically produced from a single placenta without keeping track of the sub-region they originated from, except in cases where a specific region is targeted. As a result, intra-placental variations are difficult to survey in clinical applications. However, the tracking of AM obtained from individual

placentas is strictly regulated by law. The hypothesis is that inter-placental variability does not affect the AM's healing efficiency (wound closure rate) when used for treating chronic non-healing wounds.

Aims:

• To evaluate the effect of cryopreserved AM from different donors on wound healing efficiency (wound closure) and to determine whether the dynamics of the wound closure can be used as a predictor for the efficacy of the AM treatment of nonhealing wounds;

• To assess the effectiveness of using cryopreserved AM grafts for treating chronic wounds and for determining if the healing process differs depending on the origin of the AM grafts (inter-placental variability);

• To determine the average percentage of wound closure achieved per one application of AM.

3. Materials and Methods

A broad spectrum of methods was used to achieve this work's aims. Individual material and methods regarding specific hypotheses are described in the appended publications or within the following paragraphs. The author managed the following steps:

3.1. Preparation of LESCs Culture and Analysis (H1)

Materials and methods for this hypothesis are explained in detail in the article in **Appendix 3: Interleukin-13 increases the stemness of limbal epithelial stem cells cultures, page 175**.

Briefly, the LECs were prepared from cadaver donor corneas, and their morphology, growth, and viability were monitored throughout the culture. The cells were also subjected to colony forming assays (CFA), immunofluorescence, and qPCR to evaluate their characteristics and expression of specific genes. The cells were cultured in a complete medium with or without IL13, and the WST-1 assay determined the proliferation activity of living cells. Statistical analysis was performed to compare the results obtained from the IL13+ and IL13- cells. The study adhered to the tenets set out in the Declaration of Helsinki and met all Czech legal requirements.

3.1.1. Culture of Limbal Explants on Nanofibrous Membranes

Nanofibrous polymer membranes by electrospinning of polymer (PDLLA, DLLA/ LLA ratio 10/90, M_w 868 270 g/mol, polydispersity index 2.3) from pyridine (9 wt%) prepared and provided by Ing. Hana Studenovská, Ph.D., and her team (Biomaterials and Bioanalogous Systems, Institute of Macromolecular Chemistry AS CR) were used as a culture substrate for the seeding of the limbal explants and compared to fibrin gels.

Before limbal explant seeding, the scaffolds underwent sterilization by soaking in 70% ethanol (Penta), followed by three washes with sterile PBS. Afterward, in a 12-well plate (Falcon®), a human fibronectin solution (Sigma-Aldrich, 600 µL, 10 µg/mL in phosphate-buffered saline (PBS)) was pipetted into each insert carrying the scaffolds. The plate was then incubated for 1 hour at 37 °C. Subsequently, the inserts were washed thrice with sterile PBS and placed upside down in a laminar flow cabinet to dry for 30 minutes. The rehydration of the nanofibrous membrane scaffold was performed by pipetting 600 µL and 600 µL of Dulbecco's modified Eagle medium (DMEM)/F12 medium supplemented with 1%

AA (Gibco) inside and outside each insert, respectively. The rehydration process was carried out for 30 minutes at 37 °C. The specifications of all materials used are detailed in **10.1 Appendix 1: List of Materials for Limbal Epithelial Cell Culture, page 167**.

3.1.2. Preparation of Fibrin Gel

The fibrin sealant (Tisseel Lyo, Baxter) was prepared according to the manufacturer's instructions: Human Fibrinogen (Sealer protein lyophilized Concentrate), Aprotinin solution, and $CaCl_2$ were preheated for about 3 minutes in a water bath at 37 ºC. Human Fibrinogen was reconstituted with the whole volume of the aprotinin solution, and the vial returned to the water bath for the complete dissolution of the lyophilized Concentrate. Then, human thrombin (Thrombin lyophilized) was reconstituted with the whole volume of $CaCl_2$ and returned to the water bath. After reconstitution, components were diluted further: 1 ml of fibrinogen was transferred to a 15-ml tube and mixed with 8 ml of phosphate-buffered saline (PBS) to achieve a final 10 mg/ml concentration. 500 µl of thrombin was mixed with 24.5 ml of PBS in a 50-ml tube to a final concentration of 10 U/ml. Equal volumes (150 µl) of each solution were gently mixed in each well of a 24-well plate by stirring using a pipette tip.

To prevent the digestion of the fibrin gel, tranexamic acid (TA) was added to the media (for cultures on fibrin); 500 mg of TA (Sepulco) was dissolved in 1 ml sterile PBS, then transferred to a 15-ml tube and diluted further with 9 ml PBS (final concentration: 50 mg/ml, 10ml PBS). TA was added to the media to a final 160 µg/ml concentration. The specifications of all materials used are detailed in **10.1 Appendix 1: List of Materials for Limbal Epithelial Cell Culture, page 167**.

3.1.3. Donors

The preparation of limbal explants is explained in detail in the appended manuscript, refer to **10.3 Appendix 3: Interleukin-13 increases the stemness of limbal epithelial stem cells cultures, page 175**. Explants from 7 donors (age 63 ± 12 years, mean ± standard deviation (SD), range 32 − 75 years) were seeded onto the fibrin gel substrate, with 5 − 6 twelfths of a corneoscleral rim considered in the observations. The same experimental setup was followed for the polymer study. Explants from 8 donors (age 53 ± 13 years, mean ± SD, range 32 − 66 years) were seeded onto the nanofibrous substrate, and 5 − 6 twelves of a corneoscleral rim were considered in the observations.

3.1.4. Explant Culture

At the seeding day (0 days post-seeding, dps), fibrin gel- and nanofibrous membrane-cultured explants were covered with 100 μL and 1100 μL of COM_L (DMEM/F12, 10% HS, 1% AA, 10 ng/mL recombinant EGF, 0.5% insulin-transferrin-selenium, 5 μg/mL hydrocortisone, 10 μg/mL adenine hydrochloride, and 10 ng/mL cholera toxin), respectively, to prevent explant detachment from the surface, and also 160 μg/ml TA added to fibrin cultures. At 1 dps, the COM_L volume was increased to 300 μL and 1200 μL, respectively, considering the explants were already firmly attached to the fibrin gel or nanofibrous membrane surface. The medium was changed thrice a week until the cells reached approximately 90 – 100 % confluency. Throughout the cultivation, the explants were observed for cell morphology, growth, confluency, and the presence of fibroblast-like cells using an inverted microscope (Olympus CKX41, Olympus, Tokyo, Japan) coupled with an EOS 250D camera (Olympus). Images were acquired using QuickPhoto Camera software (Promicra, Prague, Czech Republic). The amount of space covered by the expanding cells without unoccupied space was visually compared to estimate confluency. The specifications of all materials used are detailed in **10.1 Appendix 1: List of Materials for Limbal Epithelial Cell Culture, page 167**.

3.1.5. Reverse Transcription-Quantitative Real-Time Polymerase Chain Reaction (RT-qPCR)

The nanofibrous membrane-based cultures were lysed directly using an equal amount of the RLT Plus buffer (Qiagen), and 3 to 6 nanofibrous membranes were pooled together, utilizing a single portion of the lysis. The lysates were stored at -80 °C before the RNA extraction.

Upon reaching cell confluence (80 to 90% confluent), cells grown on fibrin gel were harvested as follows: the cells were washed twice with 500 μl of dispase II (1 U/ml, Gibco, diluted in PBS). Then, 1 ml of dispase II (1 U/ml) was added, and the fibrin gel was separated from the plastic plate using tweezers and chopped into smaller parts with surgical ophthalmic scissors. The cells were then incubated for 30 minutes at 37 ºC. Next, the solution was transferred to a 15 ml centrifuge tube and spun in the Universal 32 R centrifuge (Hettich Zentrifugen) for 10 minutes at 250 × g. The supernatant was removed, and the cell pellet was resuspended in 2 ml of TrypLE™ Express (Gibco) and incubated for 25 minutes. After that, 4

ml of media (DMEM/F12) was added to stop the enzymatic activity, and the cells were spun again for 10 minutes at $250 \times$ g. The supernatant was removed, and the resulting cell pellet was directly lysed using 350 µL of an RLT Plus buffer.

RNA extraction proceeded using the RNeasy® Micro Kit (including DNase digestion) according to the manufacturer's instructions (Qiagen). RNA was diluted into RNase-free water. RNA yield and purity (260/280, 260/230 ratios) were quantified with a spectrophotometer (Eppendorf BioPhotometer Model #6131). RNA quality was further assessed by agarose gel electrophoresis. RNA concentrations of each sample were measured and diluted accordingly to the same concentration (25 ng/µl). cDNA synthesis was done using the iScript cDNA synthesis kit (Bio-Rad).

RT-qPCR was carried out in a Hard Shell 96-well PCR plate (Bio-Rad) using SsoAdvanced Universal SYBR Green Supermix RT-qPCR Kit (Bio-Rad); 7 samples were used for each marker, and each group in 3 technical replicates. The designed primers were used for stem cell, proliferation, keratins, and fibroblast marker genes, and two housekeeping genes, Hypoxanthine phosphoribosyltransferase 1 (HPRT1) and Ribosomal protein L32 (RPL32). The results were evaluated using a Bio-Rad detection system (CFX Connect Real-Time PCR Detection System; Bio-Rad). Controls without templates were included for each primer pair to check for contaminants. As another quality control measure, melting (dissociation) curves of RT-qPCR reactions were monitored to ensure that there was only a single RT-qPCR product and no primer dimers. The specifications of all primers used are stated in **10.1 Appendix 1: List of Materials for Limbal Epithelial Cell Culture, page 167**.

3.1.6. Statistical Analysis

The statistical analyses for RT-qPCR were performed using the R software (version 4.2.3), which included the packages ggplot2 and pheatmap for visualizations, as well as Microsoft Excel. Given their non-Gaussian distribution, the relative mRNA expression values were normalized by log transformation (log.rel.mRNA). First, the expression data relative to Ribosomal protein L32 (RPL32), a housekeeping gene, were plotted in a heatmap generated using the pheatmap R package. Next, the comparisons between PDLLA and fibrin-embedded samples on gene expression changes were assessed using an unpaired t-test for each marker, following the assessment of data normality with the Shapiro test. Statistical significance was determined at $p \leq 0.05$.

3.2. Preparation of OMECs Culture and Analysis of Stem/ Progenitor Cells Specific Markers (H2)

• Review of current knowledge about the usage of COMET for the treatment of limbal stem cell deficiency (see **Appendix 4: Ex vivo cultivated oral mucosal epithelial cell transplantation for limbal stem cell deficiency: a review, page 192**)

• Preparation of *in vitro* oral mucosal epithelial cell cultures from retrieved cadaverous oral mucosa tissue and monitoring of the growth of the cells – microscopy;

• Preparation of oral mucosa for immunofluorescence analysis involved cryosectioning of the oral mucosa epithelium (whole tissue) and *in vitro* cultures using cytospin;

• Gene expression analysis of cells before culture and after confluence for both tested media conditions;

• DNA damage analysis by comet assay;

• Data analysis and statistical analysis.

3.2.1. Oral Mucosal Tissue Retrieval

The retrieval of oral mucosal donor tissue abides by the project "Experimental graft preparation for the treatment of limbal stem cell deficiency from oral mucosal cells," and local ethical approval was granted (IS, 1041/19 S-IV). The study followed the guidelines outlined in the Helsinki Declaration. The collection of donor tissue complied with all legal requirements in the Czech Republic, including that the donor not be listed on the national list of those who oppose the postmortem removal of tissues and organs. Informed consent is not necessary for using donor tissue under Czech law (Law Act No. 372/2011 Coll.) if the data are anonymized before being entered into the form.

Sixty-nine explants were collected between 2019 – 2023 from the Department of Pathology, General Teaching Hospital, and the First Faculty of Medicine, Charles University in Prague, by either of two experienced pathologists, Adam Šafanda MD, and Michaela Bártů MD Ph.D. Oral mucosal tissues were obtained from cadaver donors within 72 h after death. This thesis work is based on the results obtained from twenty-six donors. The excess was used to learn, standardize, and optimize the protocol. More details about the donors are provided in the following section. Immediately before the biopsy, the place of the collection (on the inside of the mouth, 20 mm behind the angle of the mouth) is treated with 10% iodinated povidone 10% (PVP-I, diluted in NaCl 0.9%) for 1 minute. A superficial rounded

incision is made with a disposable and sterile 6-mm biopsy punch (Kai Medical) and removed with a scalpel. Two samples were collected from each buccal mucosal side (right and left) and kept in BASE•128 (Alchimia) at 4 ºC until further processing.

3.2.2. Donors

Table 1 contains detailed information on each of the donors. For the experiments detailed in this thesis work, twenty-six samples were used. Samples specific to each type of experiment will be specified in the following sections. There were ten (38.5%) female donors, aged 66.8 ± 12.7 years (mean ± SD), and sixteen (61.5%) male donors, aged 68.0 ± 12.0 years (mean ± SD), with a post-mortem time to retrieval of 28.5 ± 13.6 hours (mean ± SD).

Specimen	Gender	Age	Cause of death	Time to retrieval of tissue (*h*)
S01	Male	60	Heart failure	39.2
S02	Male	85	Hypovolemic shock	34.4
S03	Male	44	Hemorrhagic shock	16.1
S04	Male	60	Heart failure	5.2
S05	Female	60	Pulmonary embolism	28.9
S06	Female	77	Septic shock	35.0
S07	Male	51	Intracerebral cerebral haemorrhage	40.2
S08	Female	49	Cardiorespiratory failure	26.5
S09	Male	62	Hepatic failure	17.4
S10	Male	80	Respiratory failure	6.6
S11	Female	51	Edema of the brain	44.1
S12	Male	71	Cardiorespiratory failure	25.5
S13	Male	83	Cardiorespiratory failure	30.3
S14	Female	76	Hemorrhagic shock	44.0
S15	Male	60	Septic shock	48.0
S16	Male	72	Heart failure	28.7
S17	Male	73	Cardiogenic shock	46.5
S18	Male	71	Hepatorenal failure	14.7
S19	Female	65	Septic shock	44.4
S20	Male	59	Heart failure	9.4
S21	Female	70	Septic shock	17.8
S22	Male	84	Heart failure	43.7
S23	Female	84	Heart failure	17.2

S24	Female	81	Cardiorespiratory failure	11.2
S25	Male	73	Heart failure	43.0
S26	Female	55	Septic shock	23.7

TABLE 1: Donors' characteristics – gender, age, cause of death, time to retrieve the tissue, post-mortem time to preparation of culture. *h*: hour

3.2.3. Freezing of Tissue in Cryoprotectant

Oral mucosa samples from four cadavers (S01 – S04), including a separated epithelium and submucosa tissues – were snap-frozen in liquid nitrogen and embedded in an Optimal Cutting Temperature (OCT, Penta) solution and stored at -80 ℃. Tissues were cryosectioned (Cryo-Star HM 560 Cryostat, Microm) at a thickness of 7 μm and stained with hematoxylin-eosin (HE) for morphological assessment by light microscopy. Samples were also used for immunofluorescence, detailed further (**3.2.10 Immunofluorescence, page 56**).

3.2.4. Hematoxylin and Eosin Staining

The cryo slices were stained with HE following a protocol carried out in cuvettes. After removing the cryo slices from the freezer, they were left at room temperature for 30 minutes. The cryo cuts were then placed in distilled water for one minute.

The Haematoxylin Harris solution was filtered, and the cuts were immersed in it for 3 to 10 minutes. After a brief rinse under running water, the cuts were differentiated with acid alcohol (50 mL of 96% Et-OH and 2 drops of HCl), and the slides were immersed twice. The cuts were then rinsed under running water for 5 minutes.

Subsequently, the cuts were immersed in 2% eosin (filtered) for 6 minutes. The cuts were then rinsed briefly in distilled water, allowed to dry, and installed in water media (Aquatex, Merck). To ensure the cuts were thoroughly rinsed, a weak stream of tap water was concentrated on the wall of the cuvette.

To prepare the permanent preparation, the cuts were drained and immersed in 96% Et-OH for 3 minutes. They were then immersed in 100% Et-OH for 3 to 5 minutes, carbol-xylene for 3 to 5 minutes, xylene for 5 minutes, and again xylene for 5 minutes. Finally, the cuts were immediately mounted in Solakryl (Penta), and the cuvette lids were covered with parafilm and stored in a fume hood. The hematoxylin stained the nuclei blue-violet, while the eosin stained the cytoplasm pink. For the list of materials, see **Appendix 2: List of Materials for Oral Mucosa Epithelial Cell Culture, page 171**.

3.2.5. Preparation of Cell Suspension

The donor oral mucosa samples, seen in **Figure 9A**, were washed three times in BASE•128 (Alchimia) for 10 minutes, then three times in PBS (Gibco) for three minutes each time. Then each sample was cut into half and all-together incubated in 6 ml dispase II (Gibco) solution (1 U/ml), at 37 ℃ for 1 hour. Following enzymatic treatment, samples were transferred to PBS, and with tweezers, the epithelium was separated from the submucosa. For some tissues, epithelium and submucosa were collected and stored in 1 ml RNAlater (Sigma) for further use for RT-qPCR. Epithelia were transferred to a Petri dish, treated with 1.5 ml 0.05% trypsin-EDTA (Gibco), and incubated for 15 min. Cells were harvested with a cell scraper (Corning). Trypsin-EDTA was then inactivated by diluting with 3 ml DMEM-F12 media containing 20% FBS. This cell suspension was then filtered through a 70 μm cell strainer (PluriSelect) and centrifuged for 10 minutes in the Universal 32 R centrifuge (Hettich Zentrifugen), at $250 \times g$. The supernatant was removed, and the cell pellet was resuspended in 1 ml DMEM-F12 media. Cells were counted by diluting in 1:1 with Trypan Blue dye 0.40% (Bio-Rad) using the TC20™ Automated Cell Counter (Bio-Rad). Primary cells (at least 3.0×10^5 cells) were lysed using 350 μL of an RLT Plus buffer (Qiagen, Hilden, Germany) and stored at -80 ℃ before the RT-qPCR analysis (detailed further). A schematic presentation of the cell suspension preparation is shown in **Figure 10**.
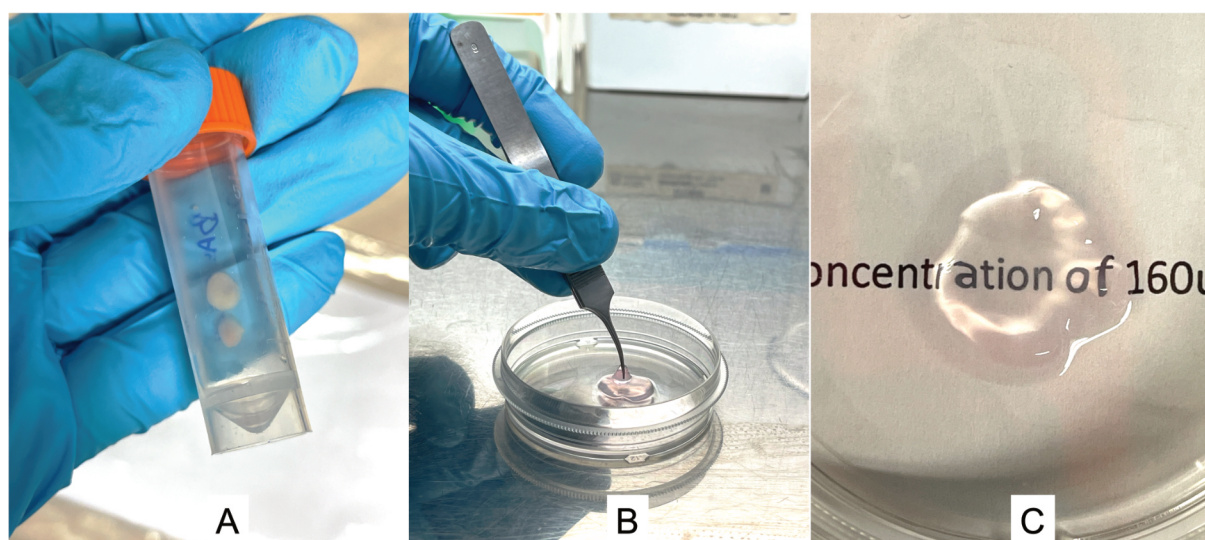
FIGURE 9: A. Oral mucosal biopsies prior to processing. B. Fibrin gel containing cultured cells on its surface. C. Same fibrin gel from Figure B. seen from above, showing its transparency. Images from the author's archive.
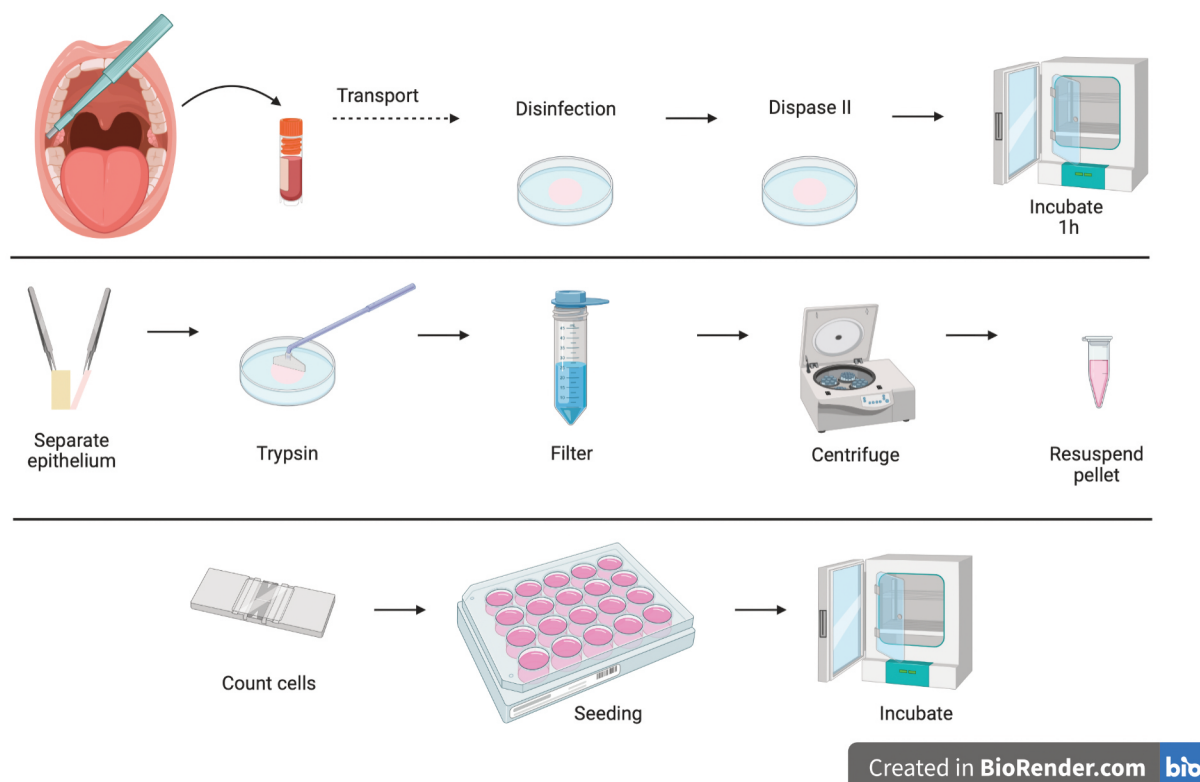
FIGURE 10: Schematic steps on the preparation of the cell culture. Dispase and trypsin are used for the preparation of the single-cell suspension and the cell scraper is used to dissociate the cells after the enzymatic treatment. Created with BioRender.com

3.2.6. Preparation of Culture Media

COM and XF media had the additives and concentrations specified in the table below, **Table 2**. For the catalog number, see **Appendix 2: List of Materials for Oral Mucosa Epithelial Cell Culture, page 171**. HS was prepared locally by collecting blood from donors. All donors were negative for hepatitis B and C, syphilis, and HIV; C-reactive protein was < 20 mg/l. First, approximately 40 ml of blood was collected from the antebrachial vein into sterile Vacutainer tubes without additives. Next, the tubes were centrifuged at 4 ºC, 3000 × g, for 15 minutes. The serum was aspirated, thoroughly pooled, aliquoted, and stored in a box at -80 ºC.

Components	Complex Media	Xenobiotic-free Media
DMEM/F12 (1:1, GlutaMAX)	1x	1x
Human Serum (HS)	10%	10%
Antibiotic-Antifungal Solution (AA)	1%	1%
Cholera Toxin	8.4 ng/ml	–

Insulin-Transferrin-Selenium (ITS)	5 µg/ml	–
Hydrocortisone	0.4 µg/ml	–
Adenine hydrochloride	24 µg/ml	–
Triiodothyronine	1.4 ng/ml	–
Epidermal growth factor (EGF)	10 ng/ml	–

TABLE 2: Formulation of complex media and xenobiotic-free media.

3.2.7. Cell Seeding and Culture

Cells were seeded on a concentration of 4.5 x 10^4 cells on the fibrin gels (see the preparation of fibrin gels in **3.1.2 Preparation of Fibrin Gel, page 47**) in a 24-well plate (VWR, United States), thus about 2.36 x 10^4 cells/cm^2. Media was changed daily in the first week, then every other day until confluence.

During the culture process, the cells were observed for cell proliferation, confluency, and morphology. The onset of the proliferation was considered when cell division was noted. Additionally, the number of days required to achieve 80 – 90% confluence was evaluated by assessing the extent of well coverage and the presence of unoccupied space within the wells due to proliferating cells. This was done using an inverted phase-contrast microscope (Olympus CKX41, Olympus, Tokyo, Japan) combined with an EOS 250D camera (Olympus). Images were captured using QuickPhoto Camera software (Promicra, Prague, Czech Republic).

3.2.8. Harvesting Cultured Cells after Cell Confluence

Upon cell confluence (80 to 90% confluent), cells were harvested for further experiments. Cells grown on fibrin gel were harvested as follows: i) two times washed with 500 µl dispase II (1 U/ml); ii) added 1 ml dispase II (1 U/ml) and fibrin gel was separated from the plastic plate by tweezers and chopped in smaller parts by surgical ophthalmic scissors, then incubated for 30 minutes at 37 ºC; iii) solution transferred to a 15ml centrifuge tube and spun in the Universal 32 R centrifuge (Hettich Zentrifugen) for 10 min at 250 × g; iv) supernatant removed and the cell pellet resuspended in 2 ml TrypLE™ Express (Gibco), and incubated for 25 minutes; v) added 4 ml media (DMEM/F12) to stop the enzymatic activity and spun again for 10 min at 250 × g; vi) supernatant removed and the cell pellet resuspended in 1 ml of media (DMEM/F12); vii) cell concentration counted in the TC20™ Automated Cell Counter (Bio-Rad), by preparing a dilution of 1:1 of the cell suspension and

trypan blue dye 0.40% (Bio-Rad).

3.2.9. Cell Viability and Cell Size

Cell viability and cell size were evaluated for primary cell suspensions (S21 – S26) and confluent cultures (COM and XF, S24 – S26) using a 1:1 dilution of the cell suspension with 0.40% trypan blue dye (Bio-Rad). For this, 20 µl of cell suspension was mixed with 20 µl of 0.40% trypan blue dye and assessed with the TC20™ Automated Cell Counter (Bio-Rad). This approach allowed for determining the absolute cell count for each analyzed cell diameter. The obtained data were plotted in an Excel sheet and analyzed to assess the distribution of cell sizes in the primary cell suspension (before seeding and culture) and the distribution of cells based on their size after reaching confluence in both media conditions (COM and XF).

Cell viability was measured manually for the remaining cultured samples, S05 – S20. Using a 1:1 dilution of the cell suspension with 0.40% trypan blue dye (Bio-Rad), 20 µl of cell suspension was mixed with 20 µl of 0.40% trypan blue dye, and both unstained live cells and stained dead cells were counted with a hemocytometer and calculated as follows: viability (%) = live cells/(live + dead cells) × 100.

3.2.10. Immunofluorescence

Immunofluorescence was performed in oral mucosa whole tissue (S01 – S04) and also for primary cells and cells after a confluent culture from donors S05, S06, S08, S09, S10, S11, S13, S14, S18, S19, and S23, for stemness (p63α, p40 (ΔNp63), and p75NTR), proliferation (Ki-67), and differentiation markers (K3, K8, K13, and K19; K19 was done only for the whole tissue).

The preparation of cryosections was already detailed in **3.2.3 Freezing of Tissue in Cryoprotectant, page 52**. The slides were defrosted at room temperature for thirty minutes, fixed with cold acetone for 10 minutes, then washed three times in PBS for 5 minutes. Then, 1h blocking at room temperature with 0.3% Triton X, 2.5% BSA, and 2.5% goat serum in PBS. Then, 1h incubation at room temperature with the primary antibody (**see Table 3**) diluted in 0.3% Triton X-0.5% bovine serum albumin. The specimens were then rinsed three times for 5 minutes in PBS and incubated for 1 h at room temperature with the corresponding secondary antibody against the species of the primary antibody (**see Table 4**). After rinsing

three times for 5 minutes in PBS, nuclear DNA was counterstained with DAPI (1:5000) for ten minutes, followed by rinsing three times in PBS. Specimens were mounted in Mowiol (Aldrich).

Following harvesting cells grown on fibrin gel (detailed in the session **3.2.8 Harvesting Cultured Cells after Cell Confluence, page 55**), 60.000 to 100.000 cells (in 100 to 120 µl) were used to prepare each cytospin slide. Cells were spun for 5 min at $180 \times g$, and slides were left to dry overnight. On the following day, cells were fixed in 300 µl 4% paraformaldehyde (Fluka Chemical) for 15 minutes at room temperature, followed by three times washing in PBS for 5 minutes each time. Then, the slides were stored in a Couplin jar with PBS at 4 ºC until further use. After fixation, the cell membranes were permeabilized for 10 minutes with 0.3% Triton X-100 (Sigma-Aldrich) diluted in PBS, followed by three times five-minutes washing in PBS, then 1h blocking at room temperature with 0.3% Triton X, 2.5% bovine serum albumin (BSA), 2.5% goat serum in PBS. Then, 1h incubation at room temperature with the primary antibody (**Table 3**) diluted in 0.3% Triton X-0.5% BSA. The cells were then rinsed three times for 5 minutes in 0.5% Tween 20 and incubated for 1 h at room temperature with the corresponding secondary antibody against the species of the primary antibody, **Table 4**. After rinsing three times in 0.5% Tween 20, nuclear DNA was counterstained with DAPI (1:5000, diluted in PBS) for ten minutes, followed by rinsing three times in PBS. Cells were mounted in Mowiol (Aldrich).

The specimens (whole tissue and cytospin slides) were examined using a Nikon Eclipse Ni-U H600L microscope at ×200 and ×400 magnifications, and images were taken using a Nikon DS-Fi3 camera (both Nikon Corporation, Tokyo, Japan). All photos were taken and analyzed in the software NIS-Elements v5.2 (Nikon Corporation, Tokyo, Japan). For the cultured cells (cytospin slides), cells were counted individually for the presence of the markers (positive cells), and at least three samples were evaluated for each condition (primary cells, COM, and XF) per marker. In each sample, at least 1000 cells were counted. An overall percentage was obtained for each marker for both conditions, COM and XF. Moreover, for the markers p63α, p40, and the colocalization of both p63α and p40, there was also a correlation with cell size for S08, S10, S18, and S19; both size and positivity were measured in the software NIS-Elements.

Antigen	Clone	Host Species	Company	Catalog Nº	Dilution used
p63α	Polyclonal	Rabbit	Cell Signaling	4892S	1:50
p40	BC28	Mouse	BioCare Medical	ACI3066C	1:50
p75NTR	Polyclonal	Rabbit	Millipore	07-476	1:100
Ki-67	MIB-1	Mouse	Agilent Dako	M7240	1:50
Keratin 3/12	AE5	Mouse	Fitzgerald	10R-C168A	1:150
Keratin 8	4.1.18	Mouse	Millipore	MAB3414	1:500
Keratin 13	EPR3671	Rabbit	abcam	ab239918	1:500
Keratin 19	EP1580Y	Rabbit	abcam	ab52625	1:500

TABLE 3: Primary antibodies for immunofluorescence.

Secondary Ab	Species	Company	Catalog Nº	Dilution
Alexa Fluor 488	Goat anti-rabbit	Invitrogen	A11008	1:400
Alexa Fluor 488	Goat anti-mouse	Invitrogen	A11029	1:400
Alexa Fluor 594	Goat anti-rabbit	Invitrogen	A11037	1:400
Alexa Fluor 594	Goat anti-mouse	Invitrogen	A11032	1:400

TABLE 4: Secondary antibodies for immunofluorescence.

3.2.11. Reverse Transcription Quantitative Real-time PCR (RT-qPCR)

Cells from the primary cell suspension and cultured cells from COM and XF groups of donors S08, S13, S14, S18, S19, S20, and S21 were lysed in the commercial Buffer RLT, and the lysates were stored at -80 °C until RNA extraction.

Methods for RT-qPCR were already detailed above; refer to **3.1.5 Reverse Transcription-Quantitative Real-Time Polymerase Chain Reaction (RT-qPCR), page 48**. The specifications of all primers used are stated in **Appendix 2: List of Materials for Oral Mucosa Epithelial Cell Culture, page 171**.

3.2.12. Comet Assay

Samples from six donors (S07, S09, S12, S13, S22, and S23) were analyzed for their DNA stability. Samples consisted of cells cultured in both COM and XF media from each donor, hence, six pairs in total. Samples were prepared according to the protocol detailed in the section **3.2.5 Preparation of Cell Suspension, page 53**. The standard comet assay procedure to measure levels of SBs was performed as described by Collins et al. and the procedure developed by Lorenzo et al., with some modifications (Collins, 2004; Lorenzo et

al., 2013).

The protocol for preparing comet assay was based on Vodenkova et al. (Vodenkova et al., 2020). In this protocol, I was responsible for preparing the comet assay slides containing the cells for analysis, and the imaging and scoring of the comets were done by RNDr. Soňa Vodenková, Ph.D., and Mgr. Kristyna Tomašová (Department of Molecular Biology of Cancer, Institute of Experimental Medicine, Czech Academy of Sciences).

Upon obtaining the cell suspension as detailed in the session **3.2.8 Harvesting Cultured Cells after Cell Confluence, page 55**, the sample was centrifuged again for 5 min, $700 \times g$, at 4 ºC and washed in 1 ml cold PBS. Samples were spun again, and the supernatant was removed; pelleted cells were embedded in the required volume of 0.7 % low melting point agarose (LMP) (dissolved in PBS) to achieve a final concentration of 2×10^5 cells/mL. From each LMP-cell suspension mixture, two 70 µL drops were transferred to each pre-coated microscope slide (the final number of cells per gel is ~14,000). Gels were covered with 22×22-mm coverslips and kept for 5 − 10 min at 4 ºC. Coverslips were removed, and the slides were transferred to the lysis solution in a Coplin jar. Cells were lysed in 2.5 M NaCl, 0.1 M EDTA-Na2, 10.0 mM Trizma base with 1% Triton X-100 (pH 10) at 4 ºC for at least 1 hour (standard time was applied in all experiments). Parallel sample slides were also prepared for each sample and incubated with the FPG enzyme. Controls for the comet assay have also been included to check for the method's performance. Samples were then transferred in an insulated box containing ice to the Institute of Experimental Medicine, where the image analysis of the slides was conducted after staining the slides with appropriate DNA stains, following the protocol detailed in Vodenkova et al. (Vodenkova et al., 2020). Data on the percentage of DNA in the tail parameter were used for the analysis.

3.2.13. Deepithelialization of Amniotic Membrane

The materials and methods for preparing AM from the placenta are described in detail in **Appendix 5: The healing dynamics of non-healing wounds using cryo-preserved amniotic membrane, page 206** and **Appendix 6: Inter-placental variability is not a major factor affecting the healing efficiency of amniotic membrane when used for treating chronic non-healing wounds, page 217**.

For the use of AM for cell culture, two AMs were further deepithelialized by incubating them with TrypLE Express (Gibco, Grand Island, NY, USA) at 37 ºC for 10

minutes. The enzymatic activity was stopped by diluting it with DMEM-F12 (Gibco). During the deepithelialization process, the AMs were gently scraped with a cell scraper (Biologix, Shandong, P.R. China) to remove amniotic epithelial cells. The deepithelialization was confirmed through staining with 0.4% trypan blue. Each dAM was then cut into smaller squares measuring 4.5 x 4.5 cm and assembled in a CellCrown™ 6-well plate insert (Scaffdex, Finland). The assembled dAM was washed three times for five minutes in BASE•128 (Alchimia, Ponte San Nicolò, Italy), followed by three additional five-minute washes in PBS. The CellCrown™ containing the dAM was inserted into a 6-well plate (VWR, United States), and culture medium (COM) was added outside (1.5 ml) and inside (1 ml) of the insert to keep the dAM moist before adding OMECs. OMECs (8×10^4 to 5×10^5) were seeded on the dAM's surface, and media was changed daily for the first week, then every other day until confluence.

3.2.14. Statistical Analysis

The data were tested for normality using the Shapiro-Wilk Test and Levene's test for the homogeneity of variance. For normal data distribution and equal variance, a parametric test was followed, either an analysis of variance (ANOVA) to test whether statistically significant differences exist between more than two samples or the unpaired t-test, which tests whether there is a difference between two samples. If the normal distribution was not assumed, or the variance was not equal across groups, nonparametric tests were used; the Mann-Whitney U Test (or Wilcoxon rank-sum test) for two independent samples and the Kruskal-Wallis test for multiple independent samples. Bonferroni post hoc test was used for the multiple pairwise comparisons. When the sample size was insufficient to assume a normal distribution, a nonparametric test, the Mann-Whitney U Test, was employed. Data were analyzed using StatPlus:mac (AnalystSoft Inc. - statistical analysis program for macOS, version v8) and Microsoft Excel for Mac (v. 16.75).

The statistical analyses for RT-qPCR were performed using the R software (version 4.2.3), which included the packages ggplot2 and pheatmap for visualizations, as well as Microsoft Excel. The gene expression (mRNA) values represent relative values to RPL32 (housekeeping gene) and are on a logarithmic scale. Initially, a heatmap was generated using the pheatmap package to illustrate the expression data in relation to RPL32. Subsequently, gene expression changes among COM, XF, and primary cell suspension samples were

evaluated using repeated measures ANOVA with a Bonferroni posthoc test for each marker. Before that, data normality was assessed using the Shapiro test. Statistical significance was determined at $p \leq 0.05$.

3.3. Long-term Storage of OMECs in Liquid Nitrogen (H3)

Cells from donors S14, S23 − S26 (see **3.2.2 Donors, page 51**) originating from the primary cell suspension or upon harvesting (**3.2.8 Harvesting Cultured Cells after Cell Confluence, page 55**) after the confluence of the first seeding were stored in different media with or without a CPA, then transferred to liquid nitrogen. **Figure 11** shows a comprehensive view of these two approaches for the long-term storage of OMECs.
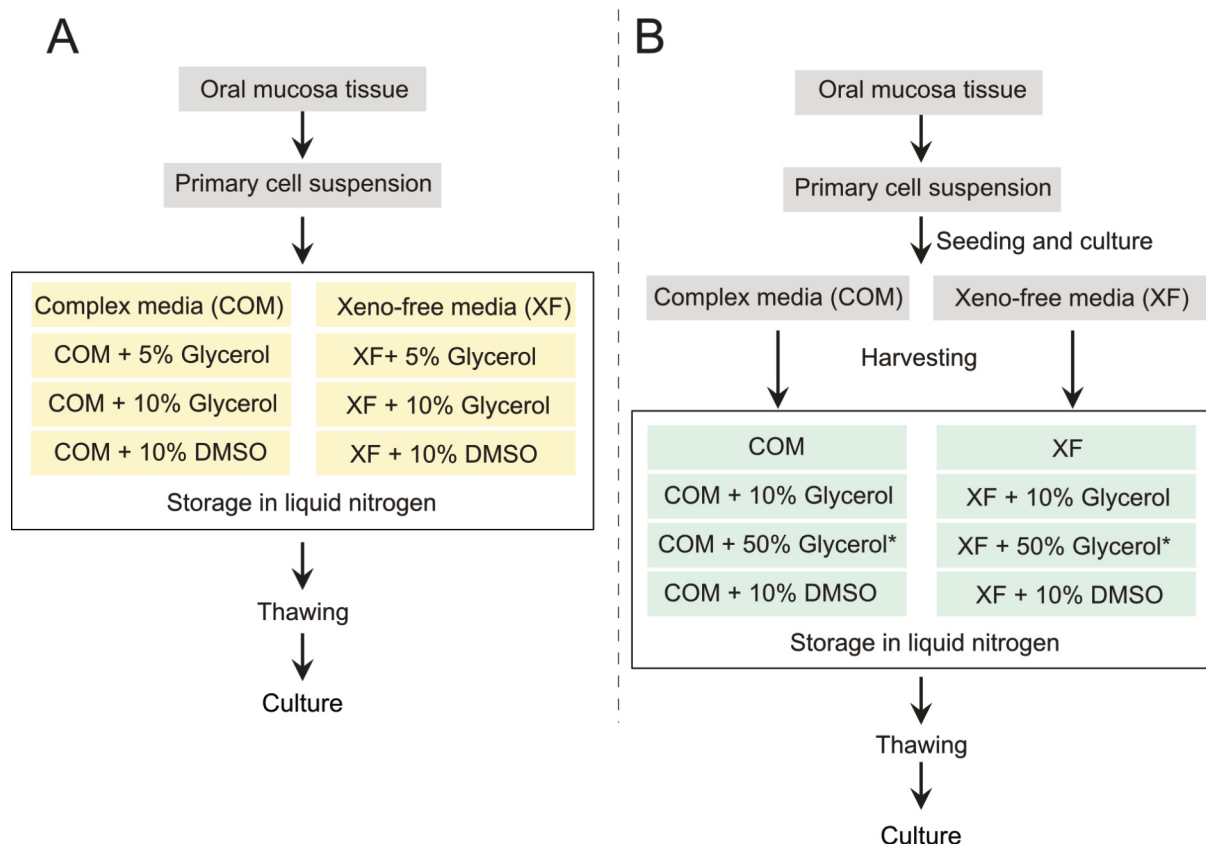
FIGURE 11: Schematic illustration of both procedures to store cells in liquid nitrogen. In A, primary cells were directly stored, whereas in B, they were first cultured in both culture media, and then upon achieving confluence, the cells were harvested and stored in liquid nitrogen. *Due to no proliferation, 50% glycerol was then replaced with 5% glycerol.

Cells were counted in an automated cell counter (TC20™, Bio-Rad), and a volume containing $1.0 - 2.0 \times 10^5$ cells was transferred to a 1.5 ml Eppendorf tube, and the medium was added to complete a magnitude of 0.5 ml. Samples were spun for 8 minutes in the

Spectrafuge mini (Labnet Intl., Inc), maximum RMP/RCF: 6,000/2,000 × g, and the cell pellet resuspended in pre-cooled freezing media to achieve a concentration of 5.0 x 10^6 cells/ ml. There were eight types of media: COM only, COM + 10% glycerol, COM + 50% glycerol, COM + 10% DMSO and the respective equivalents using XF media, XF only, XF + 10% glycerol, XF + 50% glycerol, and XF + 10% DMSO. After the first two cultures (S14 and S24), which were stored after the first passage, cells that were stored in COM + 50% glycerol or any of the XF variants did not succeed in the culture. Due to these partial results, the protocol was adapted, and instead of 50% glycerol, we replaced it with 5% glycerol. The experiments for the first passage (S25 and S26) continued only with COM storage media and its variants with CPAs. For the primary cell culture, 5% glycerol was used instead of 50% glycerol (diluted in either COM or XF), and for S23, all eight storage media variants were included, but for S26, only COM variants.

The cell suspension on freezing media was transferred to a respective cryogenic storage vial (pre-cooled), and vials were placed in an insulated box and stored in a -70 ℃ to -90 ℃ freezer for 24h – 48h. This step is important because it allows for the freezing of the cells while minimizing the formation of ice crystals, which can damage the cells. After the initial storage period, the samples were transferred to liquid nitrogen for long-term storage until further use for cell culture. This step is critical because it ensures the long-term preservation of the cells while maintaining their viability and functionality.

To begin the thawing process, the cryovials containing the frozen cells were removed from the liquid nitrogen and placed into a 37 ℃ water bath, per standard laboratory procedure. This step is done to gradually bring the cells back to their normal temperature and prevent damage to the cell membrane. Once the vials were in the water bath, they were gently swirled for less than a minute until only a small amount of ice was left in the vial. The vials were then transferred into a laminar flow hood to ensure sterility during the rest of the process.

Afterward, a pre-warmed complete growth medium was added into the centrifuge tube containing the thawed cells. The centrifugation process was then performed at approximately 200 × g for 5 – 10 minutes, which allowed the cells to be separated from any remaining debris. After the centrifugation, the supernatant was removed without disturbing the cell pellet. The cell pellet was then gently resuspended with a growth medium (either COM or XF), which helped to provide the cells with the necessary nutrients and growth

factors. Finally, the cells were seeded onto a fibrin gel support for culture (see **3.1.2 Preparation of Fibrin Gel, page 47**).

During cell culture, cell morphology was observed and properly registered. Upon confluence, cells were harvested from the fibrin gel and collected in buffer lysis for PCR. For protocols, see **3.2.8 Harvesting Cultured Cells after Cell Confluence, page 55**, and **3.2.11 Reverse Transcription Quantitative Real-time PCR (RT-qPCR), page 58**.

3.4. Amniotic Membrane Grafts for the Treatment of Non-healing Wounds (H4)

Materials and methods for this hypothesis are explained in detail in **Appendix 5: The healing dynamics of non-healing wounds using cryo-preserved amniotic membrane, page 206** and **Appendix 6: Inter-placental variability is not a major factor affecting the healing efficiency of amniotic membrane when used for treating chronic non-healing wounds, page 217**.

In the presented project, I participated in preparing AM grafts from the placenta once a week, and the detailed methods can be found in the cited appendices above. I took the lead in preparing the AMs, which were subsequently used for wound grafts in the study of wound healing and pain relief. Furthermore, I assisted in the preparation and review of the published papers.

4. Results

4.1. Influence of Interleukin-13 in LESCs (H1)

4.1.1. Limbal Epithelial Cell Growth and Morphology

The study found that LECs P0 cultures grew from limbal explants around the fifth day and achieved $90 - 100\%$ confluence after 14 days, regardless of the presence of IL13 (as shown in **Figure 12A**). Interestingly, passage (P) 1 and P2 cultures reached confluence earlier than P0 cultures, although there was no difference between cells cultured with or without IL13 (based on the data in **Figure 12D**). Notably, cell viability after passaging was similar between cultures, as demonstrated in **Figure 12E**.

However, the percentage of successful cultures decreased from P0 to P1 and P2, which could indicate that there may be some underlying factors affecting the culture conditions (see **Figure 12B**). The most significant difference was observed after P2, where only 9.7% of IL13- cultures reached confluence, compared to 42% in the IL13 group. This striking difference is also reflected in the morphology of the cells, as LECs typically exhibit cuboidal morphology with a high nucleocytoplasmic ratio in all cultures except P2 IL13- cultures, where the cells showed a more flattened or fibroblast-like morphology with a low nucleocytoplasmic ratio (as shown in **Figure 12F**).

It is important to note that fibroblast-like cell contamination was higher in the P0 group without IL13 than in the P0 group with IL13 (27.7% and 20%, respectively). Moreover, cell cultures without IL13 had a low percentage of contamination in P1 (16.2%) but increased in P2 (45.8%). Conversely, fibroblast-like cell contamination was not observed in P1 and P2 cultures with IL13, indicating that the presence of IL13 may play a role in reducing contamination (**Figure 12C**).

Overall, the study provides valuable insights into the growth and morphology of LECs cultures at different stages, highlighting the potential challenges and benefits of using IL13 in these cultures.
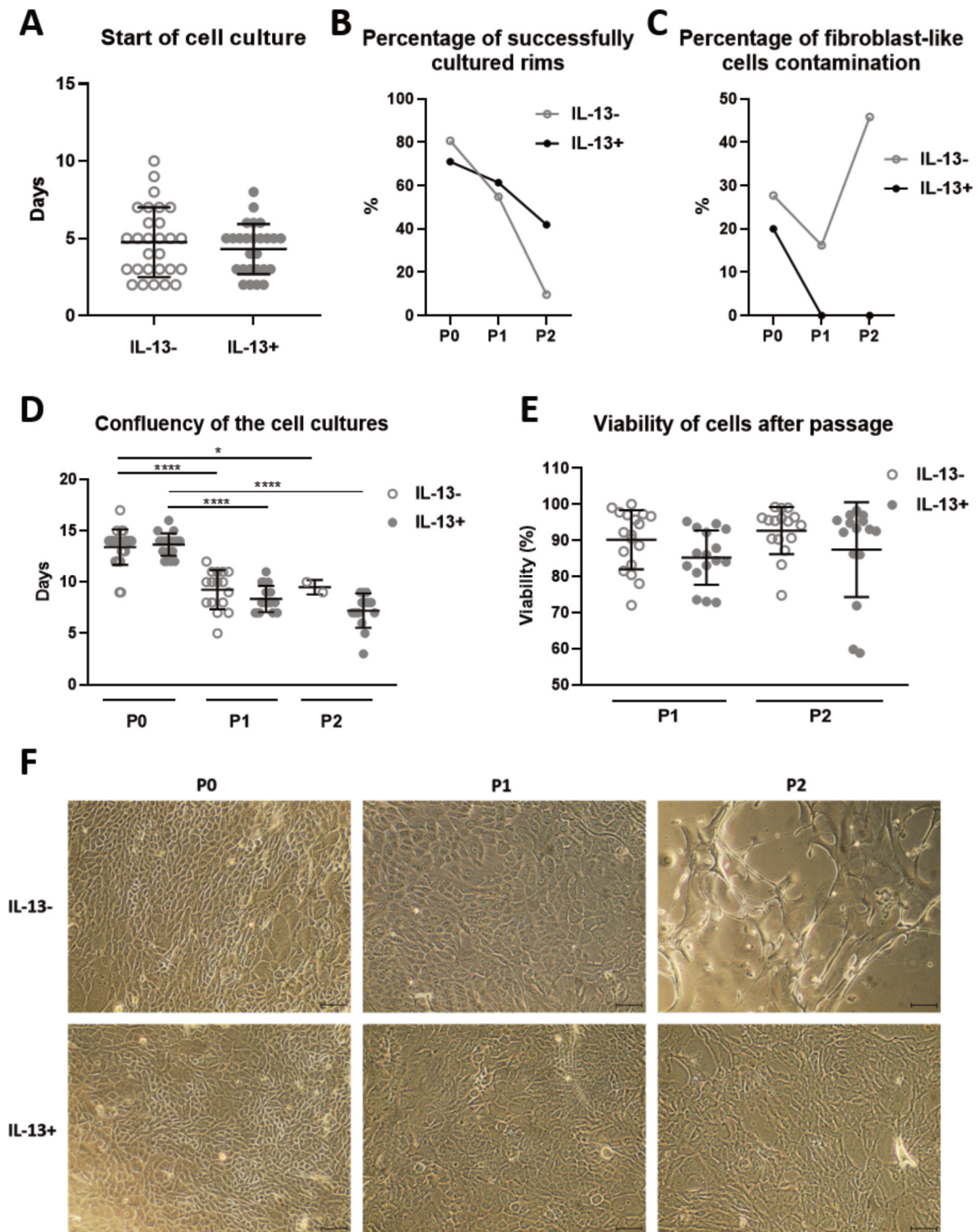
FIGURE 12: The growth and morphology of IL13- and IL13+ cell cultures. (A) The beginning of the outgrowth of LECs cultures from day 0 (D) to reaching full confluence in P0, P1, and P2 cultures. (B) The percentage of successfully cultured corneoscleral rims. (C) The percentage of fibroblast-like cells contamination in cell cultures. (E) Percentages of cell viability after the first and second passages. (F) Cell morphology was observed at the end of cultivation of P0, P1, and P2 cultures under an inverted phase-contrast microscope. Scale bars: 50 μm.

4.1.2. Colony Forming Assay

The CFA was carried out on two groups of cultures, P1 and P2, as shown in **Figure 13**. The results of the assay showed that the growth potential was significantly higher in the P1 and P2 cultures that had IL13+ (with an average of 13.79% and 8.63%, respectively) than in the P1 and P2 cultures IL13- (with an average of 4.78% and 1.19%, respectively). This difference was significant, with a *p*-value of less than 0.001 and less than 0.0001, respectively. The data also showed that the number of colonies decreased between the two passages and between the IL13+ and IL13- groups, but the decrease was more significant in the IL13- cultures than in the IL13+ cultures ($p < 0.001$ vs. $p < 0.05$). These findings suggest that the presence of IL13 protein is an important factor in the growth potential of P1 and P2 cultures.
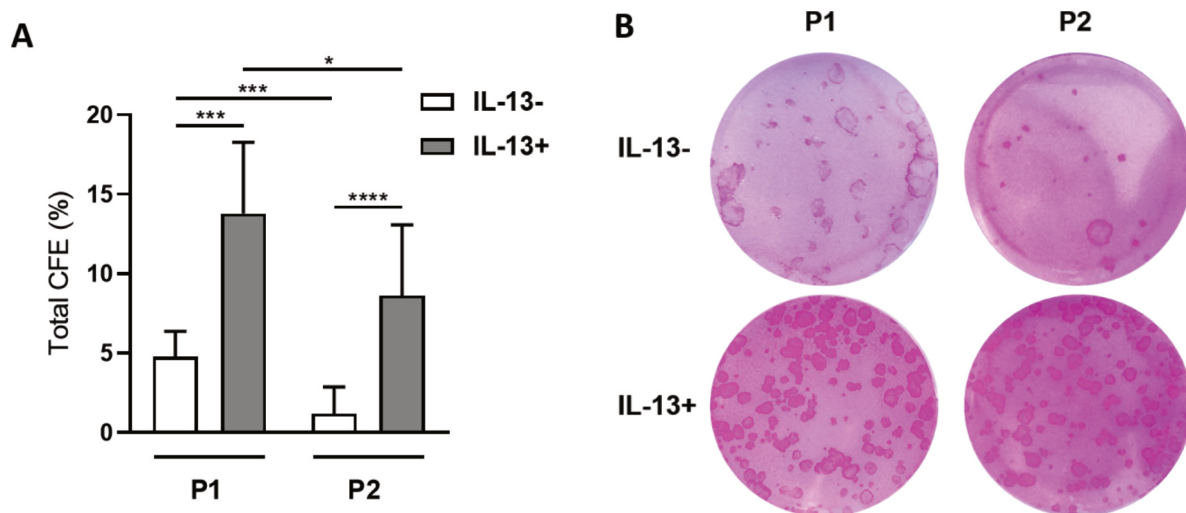
FIGURE 13: Comparison of total CFE. After the first and second passages (P1 and P2), cells were cultured with growth-arrested 3T3 mouse fibroblasts to compare their growth capacity under IL13- and IL13+ conditions. (A) Distribution of total CFE percentages of the P1 and P2 groups. Each bar represents the mean ± SD from 7 to 13 determinations. The asterisks represent a statistically significant difference between the examined groups (*$p < 0.05$, ***$p < 0.001$, ****$p < 0.0001$). (B) The colonies were stained with 2% rhodamine B.

4.1.3. Expression of Limbal Stem Cell Markers

The *ΔNp63α* gene was more expressed in cells cultured with IL13 than in cells cultured without it ($p < 0.001$). The expression consistently decreased during the LECs culture, and there was a significant difference between P0 – P1 and P1 – P2 cultures in both IL13+ and IL13- groups ($p < 0.01$). Although *BMI-1* gene expression was slightly higher in

P0 IL13+ cultures than in IL13- cells, the difference was not statistically significant. The K14 gene expression was significantly higher in IL13+ groups P0 ($p < 0.05$) and P1 ($p < 0.001$) compared to controls without IL13. The *KRT17* gene expression decreased throughout the cell culture, and there was a significant difference between the P0 IL13+ culture and the P1 and P2 IL13+ groups (both $p < 0.05$). The *KRT17* gene expression was significantly higher in P0 samples with IL13 ($p < 0.05$) compared to samples without IL13 (**Figure 14**).
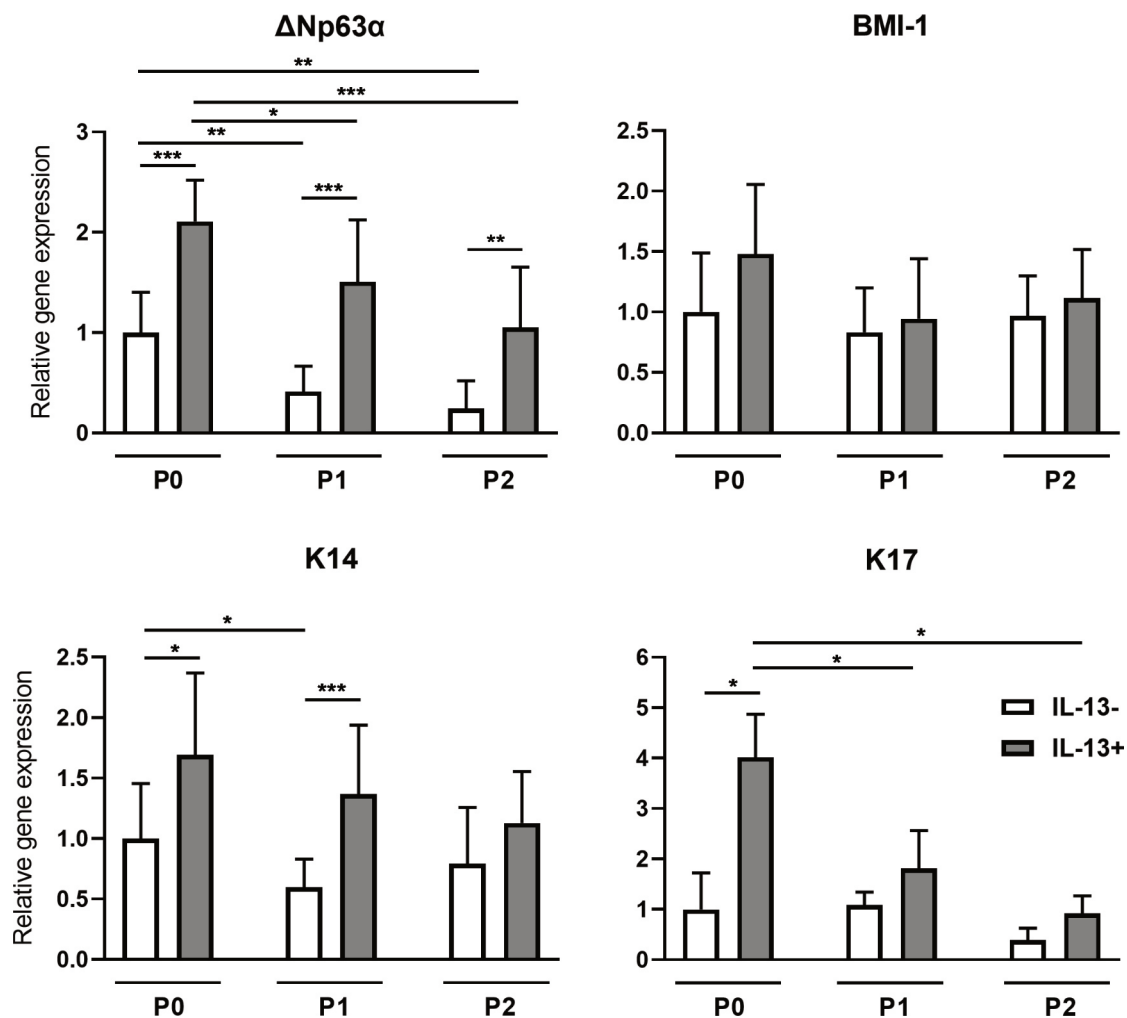
FIGURE 14: Relative gene expression of *ΔNp63α, BMI-1, KRT14*, and *KRT17* in IL13- and IL13+ cell cultures. Cells originating from limbal explants (P0) and passaged cells (P1 and P2) were analyzed at the end of the culture for *ΔNp63α, BMI-1, KRT14*, and *KRT17* gene expression by qPCR. Each bar represents the mean ± SD of three to ten determinations. The asterisks represent statistically significant difference between the examined groups (*$p < 0.05$, **$p < 0.01$, ***$p < 0.001$).

4.1.4. Immunocytochemical Staining for p63

In the study, we found that every culture and condition had cells positive for the p63, as depicted in **Figure 15A**. Interestingly, the percentage of p63-positive cells decreased significantly during cell culture without IL13. Specifically, the mean values were 94.86%, 91.65%, and 75.55% for P0, P1, and P2 cultures, respectively; $p < 0.05$. Notably, cell cultures with IL13 had a similar expression of p63 in all passages, with mean values of 96.23%, 95.54%, and 90.69% for P0, P1, and P2 cultures, respectively. Furthermore, a significantly higher percentage of p63 + cells were measured in P2 IL13+ compared to P2 IL13- culture, with $p < 0.05$, as shown in **Figure 15B**.
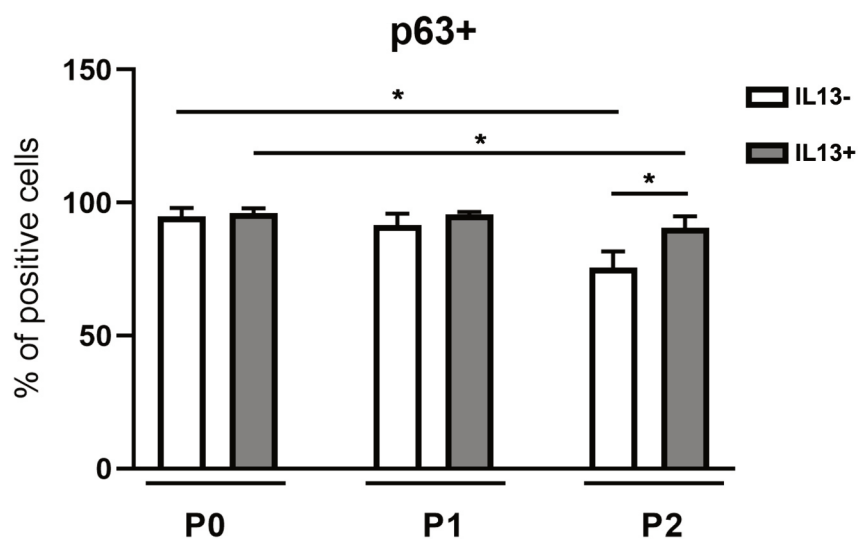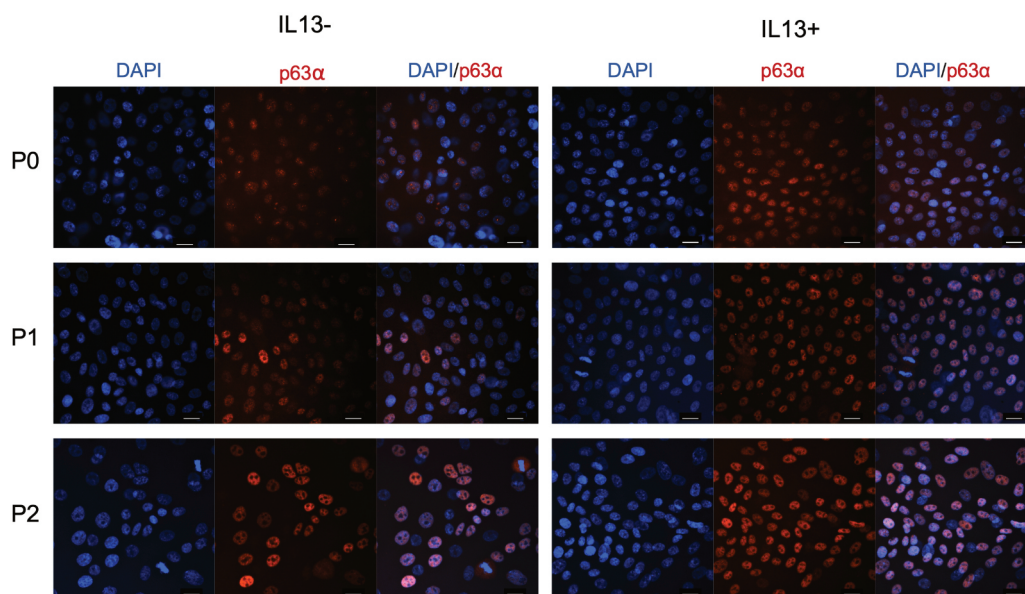
FIGURE 15: Immunostaining for the putative limbal stem cell marker p63α in IL13- and IL13+ cell cultures. (A) Cells were analyzed by immunofluorescent staining for p63α (red) at the end of P0 – P2 cultures. Nuclei were counterstained with DAPI (blue). Scale bars: 20 μm. (B) Distribution of percentages in the P0, P1, and P2 groups for p63α staining. Each bar represents the mean ± SD of three to eight determinations. The asterisks represent a statistically significant difference between the examined groups (*$p < 0.05$).

4.1.5. LECs Proliferation and Metabolic Activity

To determine the proliferation of cultured LECs, we conducted gene expression analysis of *MKI67* and utilized the WST-1 assay (as shown in **Figure 16**). While no significant differences were observed between the evaluated groups for *MKI67* gene expression, we found some interesting results when looking at the proliferation data. In P1, there was no difference between the IL13+ and IL13- groups. However, when we compared P2 IL13+ to P2 IL13-, we found a significantly higher proliferation in the former ($p < 0.01$), as determined by the WST-1 assay. Moreover, we also measured a significant decrease in proliferation activity between P1 and P2 cultures that did not include IL13 ($p < 0.01$).
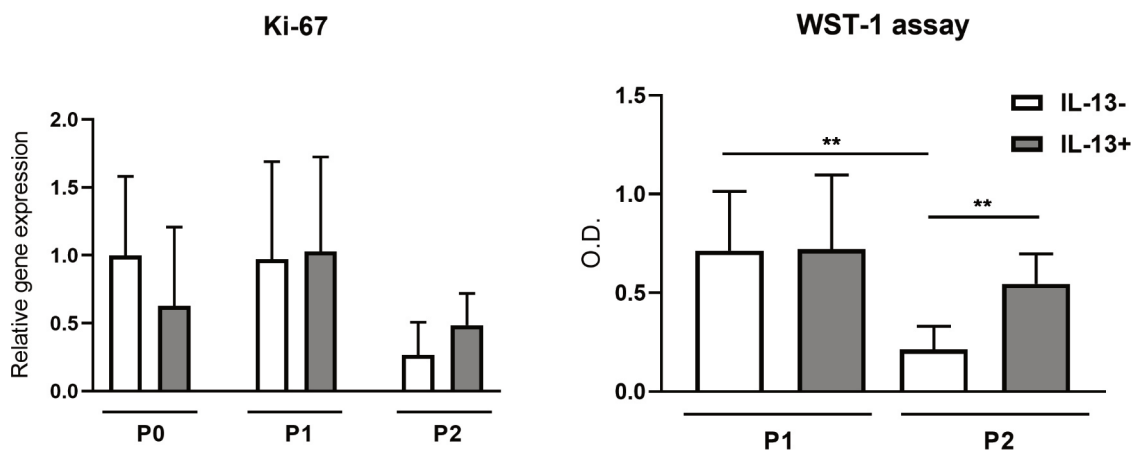
FIGURE 16: Relative gene expression of *MKI67* and WST-1 assay in IL13- and IL13+ cell cultures. (A) Cells originating from limbal explants (P0) and passaged cells (P1 and P2) at the end of culture were analyzed for *MKI67* gene expression by qPCR. Each bar represents the mean ± SD of five to ten determinations. (B) Measurement of cell proliferation after the first and second passages (P1 and P2). The WST-1 reagent was added to the cell cultures for 1 h to form formazan. The absorbance was measured at a wavelength of 450 nm via optical density. Each bar represents the mean ± SD of eight to ten determinations. The asterisks represent a statistically significant difference between the examined groups (*$p < 0.01$).

69

4.1.6. Presence of Differentiation Markers

The expression of corneal epithelium-specific *KRT3* and *KRT12* genes was consistent among all groups, although the levels were recorded to be very low. This implies that the presence or absence of IL13 did not significantly affect the expression of these genes. However, the expression of the conjunctival *KRT7* gene was noticeably higher in all IL13+ cell passages in comparison to IL13- cultures, indicating that the presence of IL13 may have a stimulatory effect on the expression of this gene. The difference was particularly significant in P0 and P1 (both $p < 0.05$). Furthermore, the study found that the *MUC4* gene was expressed in all groups, although there was a significant decrease in its expression between passages P0 and P2 and between P1 and P2 in IL13- conditions ($p < 0.05$), see **Figure 17**.
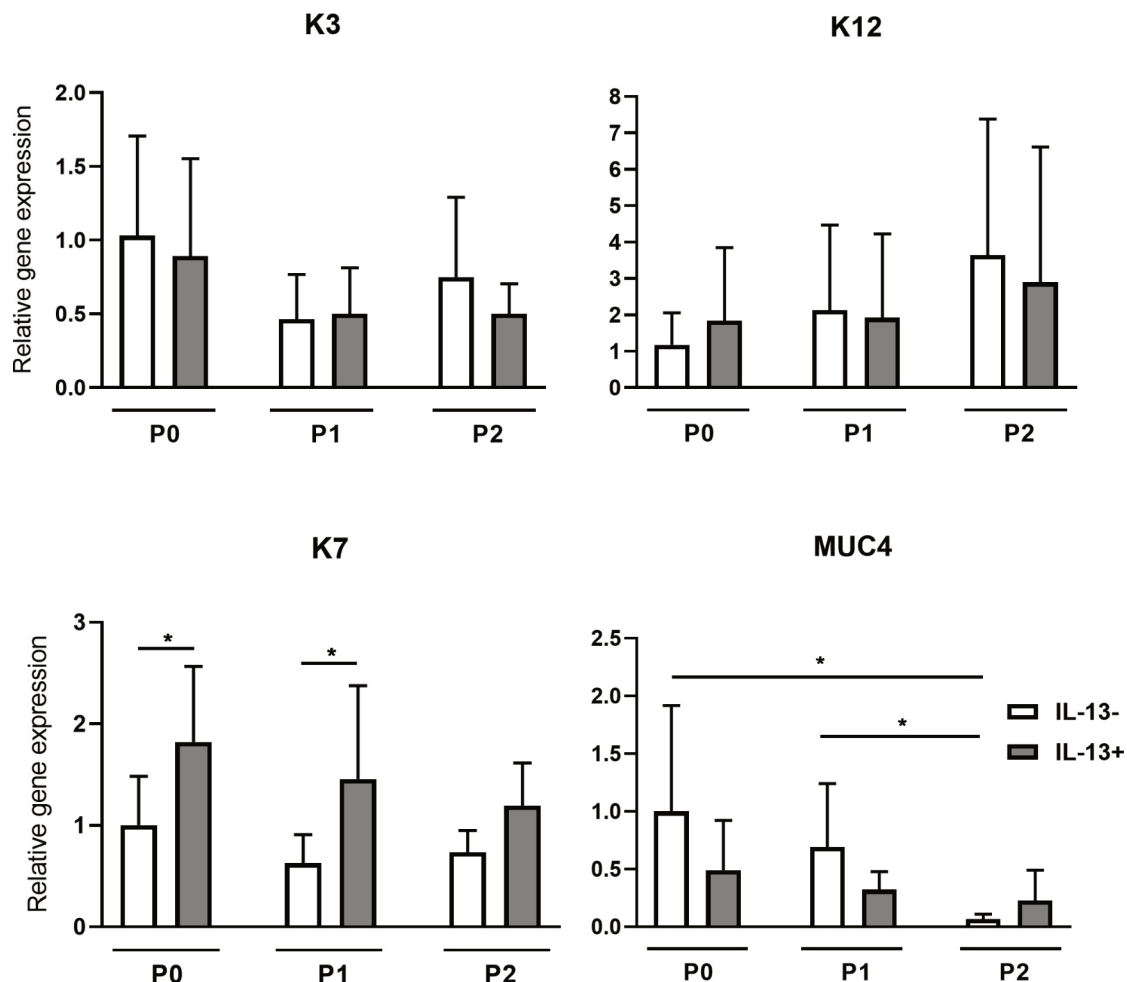
FIGURE 17: Relative gene expression of *KRT3, KRT12, KRT7,* and *MUC4* in IL13- and IL13+ cell cultures. Cells originating from limbal explants (P0) and passaged cells (P1 and P2) at the end of culture were analyzed for the expression of *KRT3, KRT12, KRT7,* and *MUC4* genes by qPCR. Each bar represents the mean ± SD of four to ten determinations. The

asterisks represent a statistically significant difference between the examined groups (*p < 0.05).

4.2. Culture of Limbal Explants on PDLLA membranes compared to Fibrin Gel (H1)

4.2.1. Growth Dynamics and Cell Morphology

At 3 – 5 dps, cell expansion commenced around the seeded explants in the fibrin gels. The expanding cells were small and displayed a typical epithelial cuboidal morphology, **Figure 18**. By 7 dps, the maximum observed percent growth was approximately 70%. The cobblestone epithelial morphology remained unchanged even at 9 – 14 dps when the confluency reached 90 – 100%. Although spindle cells were noted at the end of the cultures in 2 of the 6 donor tissues, their presence was negligible.

The growth on PDLLA nanofibrous membranes was observed at 5 – 7 dps. However, this proliferation was characterized by both cuboidal morphology and round cells, which were not observed in the case of fibrin cultures. Furthermore, from 7 – 10 dps, the cultures exhibited both epithelial and fibroblast-like cell morphology, with cells migrating across the substrate and showing multifocal growth. Multicellular cell structures, whirling patterns, and self-organizing structures were commonly observed. The cultivated cells reached 90 – 100% confluency at 16 – 21 dps, and mostly fibroblast-like cells were present at confluence, **Figure 19**.
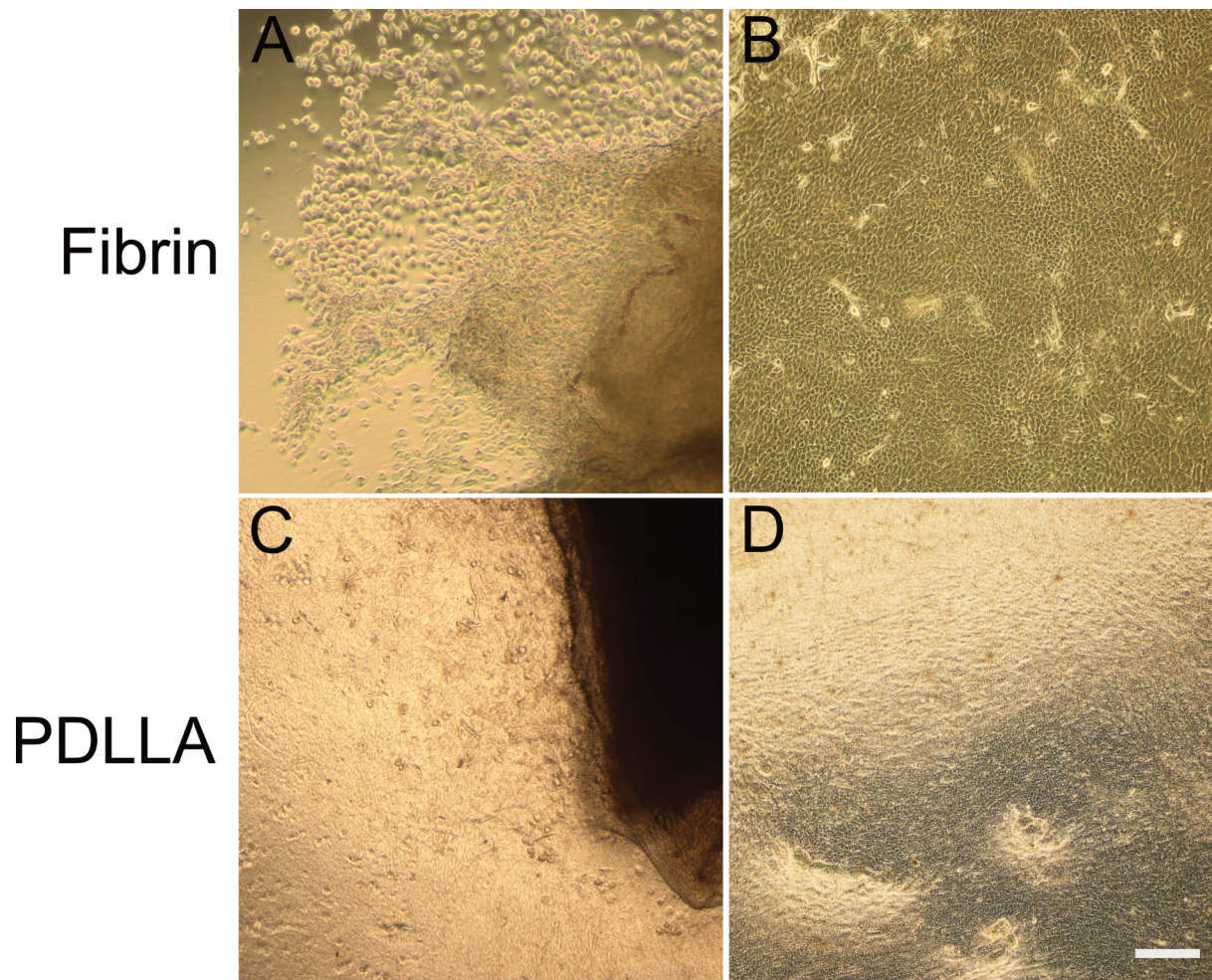
FIGURE 18: Inverted phase-contrast microscopy of limbal epithelial cell culture in fibrin gel (A and B) and PDLLA nanofibrous membranes (C and D). A and C reveal the initial stages of cell proliferation, showing rounded cells expanding from the limbal tissue (A, at 3 days post-seeding, and C at 5 days post-seeding the explant). At confluence (C, 9 days), cells on fibrin gel had a well-defined cobblestone-like uniform morphology, whereas on PDLLA membrane (D) at confluence (16 days), cells assumed a fibroblast-like morphology and self-organizing structures were also present. PDLLA: poly(L-lactide-*co*-DL-lactide) nanofibrous membrane. Scale bar: 200 µm. Images from the author's archive.
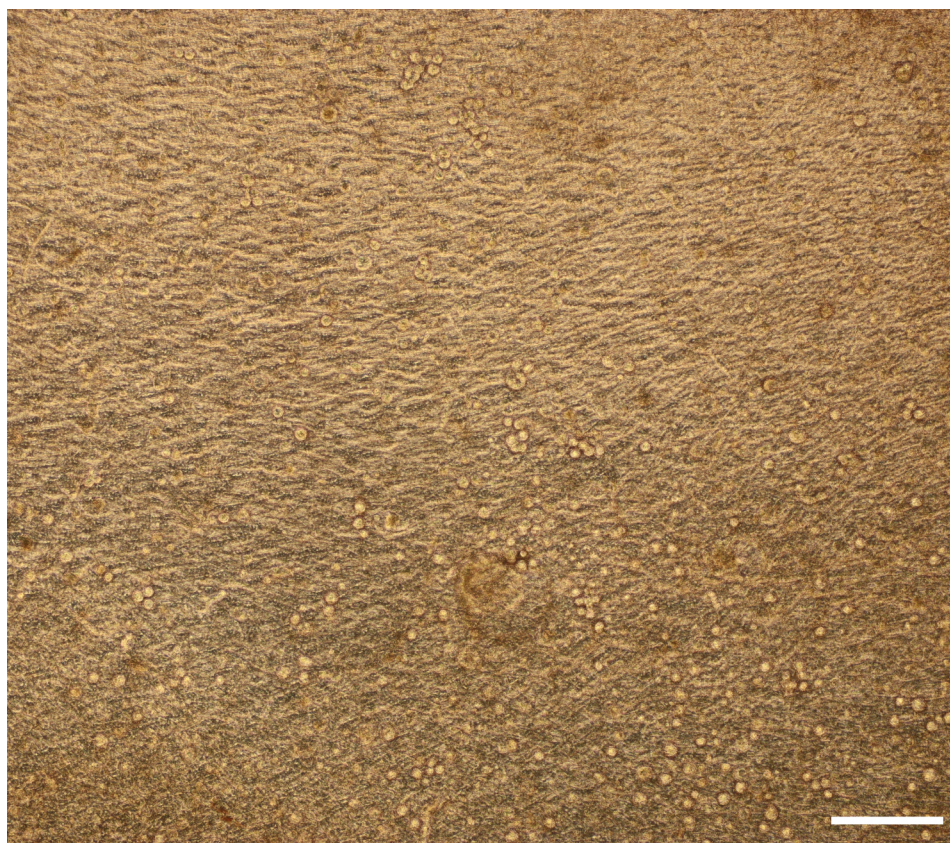
FIGURE 19: Inverted phase-contrast microscopy of limbal epithelial cell culture on poly(L-lactide-*co*-DL-lactide) (PDLLA) nanofibrous membranes. At confluence (16 days), fibroblast-like cells were visible, as well as rounded cells. Scale bar: 200 μm. Images from the author's archive.

4.2.2. Gene Expression in Cultured Cells in PDLLA Membranes and Fibrin Gel

We conducted RT-qPCR to evaluate the gene expression of stem cell, proliferation, keratin, and fibroblast markers, aiming to assess the effect of PDLLA on cell phenotype and compare it with that of fibrin gel. Bidirectional hierarchical clustering of the gene expression values revealed that the cells grown on fibrin gels tended to form a distinct group separate from cells derived from culture in PDLLA membranes, **Figure 20**. Also, based on their expression, the tested genes were classified into two groups of lower and higher expressed genes: class I, lower expression – *NGFR*, *OCT4*, *KRT12*, *ABCG2*, *VSX2*, *SOX2*, *KRT3*, *CD34*, and *ABCB5*; class II, higher expression – *KRT14*, *KRT15*, *ITGB1*, *KRT7*, *IGFBP5*, *LRIG1*, *ACTA2*, *THY1*, *FBLN1*, *CEBPD*, *MKI67*, *KLF4*, and *ΔNp63α*.

After analysis using unpaired t-tests, the progenitor and putative stem cell markers *NGFR*, *OCT4*, and ΔNp63α were significantly upregulated in fibrin compared to PDLLA

samples ($p < 0.05$), as well as the proliferation marker *KLF4* ($p < 0.01$) and the differentiation markers *KRT12* and *KRT14* ($p < 0.01$, $p < 0.05$, respectively). In contrast, explant cultivation using the PDLLA nanofibrous substrate led to a statistically significant upregulation of the fibroblast markers *ACTA2*, *FBLN1*, and *THY1* ($p < 0.05$, $p < 0.01$, and $p < 0.01$, respectively).
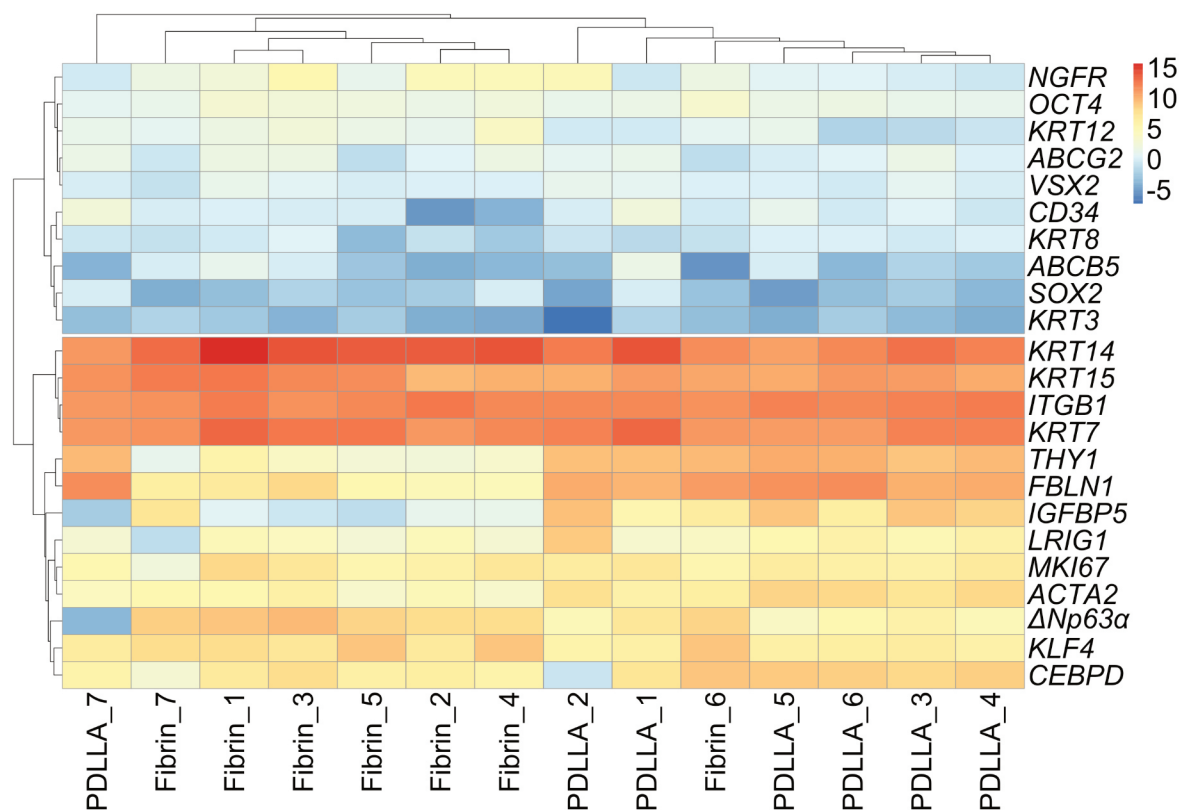
FIGURE 20: Comparisons of limbal epithelial cells (LECs) cultured in fibrin gels or nanofibrous scaffold for the gene expression of stem cell, proliferation, fibroblast and differentiation markers assessed using real-time polymerase chain reaction. A heatmap was generated to provide an overview of the relative mRNA expression (logarithmic values) for the tested genes (rows), with the samples (columns) grouped based on the substrate (fibrin or nanofibrous membrane). The color scale on the right side of the heatmap represents higher expressions in red and lower expressions in blue. PDLLA: poly(L-lactide-*co*-DL-lactide) nanofibrous membrane.

4.3. Oral Mucosal Epithelial Cells (H2)

4.3.1. Characterization of Whole Tissue

4.3.1.1. HE Staining

Oral buccal mucosa samples from four donors (S01 – S04, see **3.2.2 Donors, page 51**) were characterized by HE staining (**Figure 21**) for preliminary imaging before proceeding with further characterization through immunofluorescence, as described in **3.2.4 Hematoxylin and Eosin Staining, page 52** and **3.2.10 Immunofluorescence, page 56**. The thickness of the *stratum spinosum* varied among the samples, as well as the undulations of *rete ridges*, as some samples had a higher number of undulations (**Figure 21**, S01, S02, and S03) while also showing a flatter *stratum spinosum* (**Figure 21**, S04).
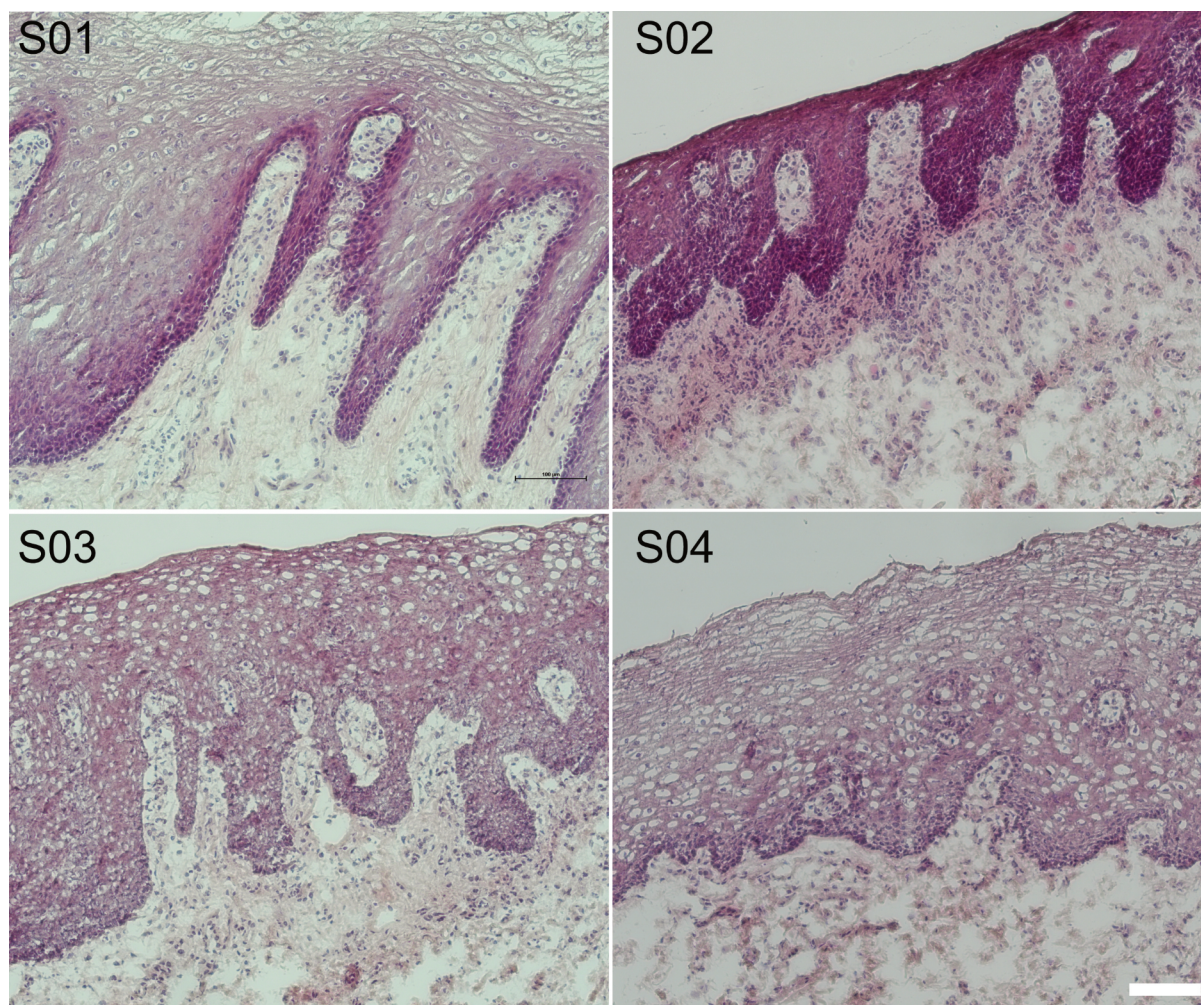
FIGURE 21: Hematoxylin and Eosin (HE) staining of a non-keratinized squamous stratified epithelium of four different buccal oral mucosa samples (donors S01 – S04). Epithelial

projections, rete ridges, are shown penetrating into the dermis or lamina propria of the oral mucosa. Scale bar = 100 μm. Images from the author's archive.

The histological staining of samples after enzymatic treatment further confirmed the effectiveness of the technique to separate the epithelium from the submucosa, **Figure 22**.
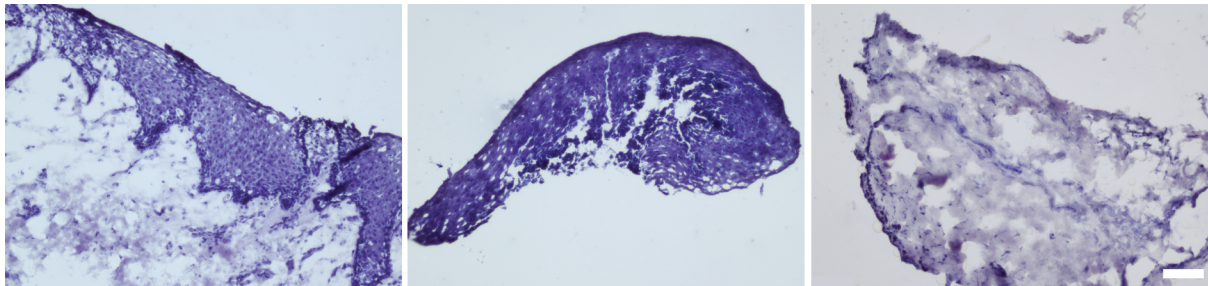
FIGURE 22: HE staining of whole tissue (oral mucosa) of S04, epithelium, and submucosa, respectively. The first image shows the whole tissue prior to enzymatic treatment, and the second and third images represent the epithelium and submucosa after successful enzymatic separation of the two layers. Only the epithelium is then used for preparing the cell suspension for cell culture. Scale bar = 100 μm. Images from the author's archive.

4.3.2. Viability and Cell size

The viability and cell size distribution measured by the automated cell counter (for details on the methods to measure the cell size, see the chapter **3.2.9 Cell Viability and Cell Size, page 56**) of the primary cell suspensions (S21 − S26) is detailed in the **Figure 23**. The viability of the primary cell suspension (S21 − S26) was 77.7% ± 18.3 % (mean ± SD); about 68.7% of the live cells were ≤ 11 μm, 25% in the range of > 11 − ≤ 18 μm, and the remaining 6.4% > 18 μm, and 96.6% of dead cells were ≤ 11 μm.
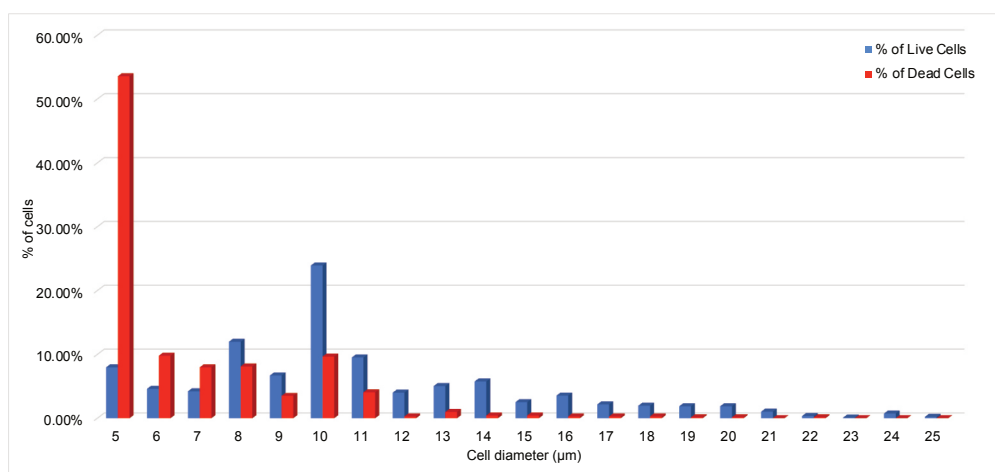
FIGURE 23: The distribution of cell diameters of the primary cell suspension in six samples (S21 − S26) using an automated cell counter. The percentage indicates the distribution of

sizes for live cells (blue) within the samples. Dead cells (red) were excluded by trypan blue staining.

The cell size of confluent cultures in COM and XF of S24 – S26 was also measured by the automated cell counter. In COM, 45.8% of the live cells were ≤ 11 μm, 47.1% in the range of > 11 – ≤ 18 μm, and the remaining 7% > 18 μm; in XF, 59% of the live cells were ≤ 11 μm, 8.4% in the range of > 11 – ≤ 18 μm, and the remaining 7% > 18 μm, **Figure 24**.
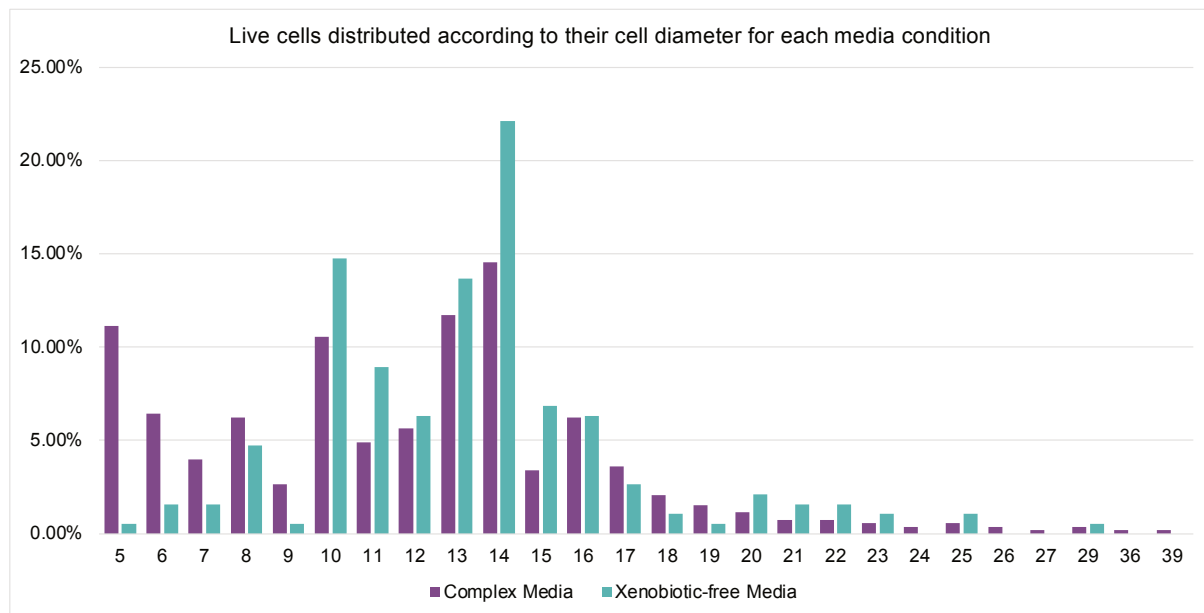
FIGURE 24: The distribution of live cells according to the cell diameter in three samples (S24 – S26) using an automated cell counter. The percentage indicates the distribution of sizes for live cells after culture and confluence in complex media and xenobiotic-free media.

4.3.2.1. Immunofluorescence

These four samples (S01 – S04) were processed for immunofluorescence characterization for stemness markers (p63α, p40, and p75NTR), proliferation marker (Ki-67), and differentiation markers (K3, K8, K13, and K19), as detailed in **3.2.10 Immunofluorescence, page 56**.

The stemness marker p63α was detected in the basal layer of all four samples, **Figure 25,** but mainly concentrated on the tips of the *rete ridges*, and the signal intensity was lower or absent in the base of the *rete ridges*; it was also weekly present in the suprabasal layer in between the epithelial projections. For the note, the bright intensity observed in the submucosa was also present in the negative control samples, in contrast to the bright signal observed in the basal layer. Similarly, p40 (ΔNp63) was also detected along the basal layer,

with a higher intensity on the tips of the *rete ridges*, and the intensity also decreased towards the base of the *rete ridges*; it was also weekly present in the suprabasal layer in between the epithelial projections. The co-localization of p63α and p40 was also evaluated, and cells were mostly positive for both markers, **Figure 26**. The marker p75NTR was also present in the basal layer of all four tissues and uniformly along the basal layer, with similar intensity in the tip and base of the *rete ridges*. Ki-67, a marker used to investigate the proliferation state of cells, is expressed unevenly in the parabasal and scarcely in the suprabasal layers of the oral mucosa epithelium, **Figure 25**.
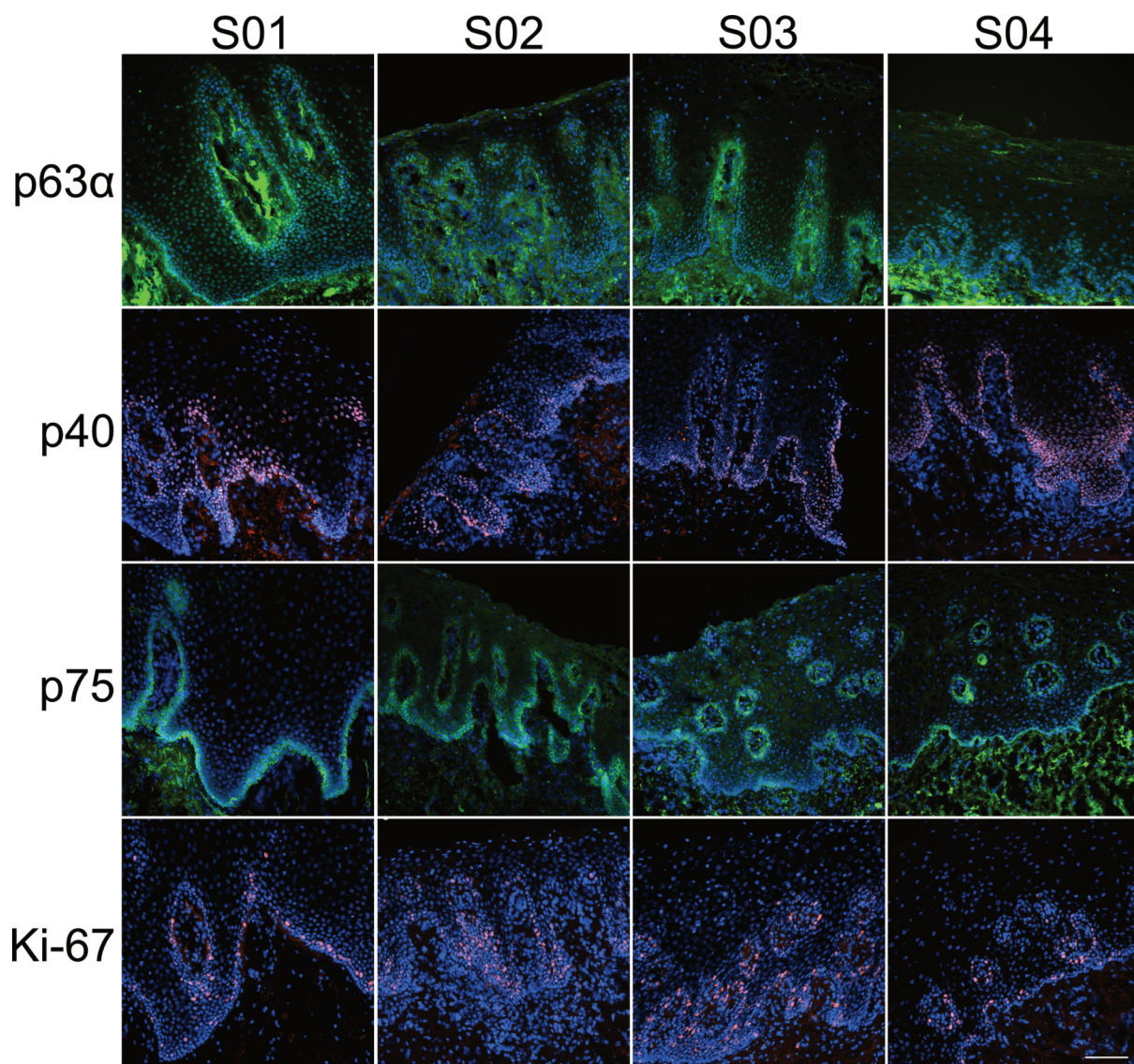
FIGURE 25: Immunofluorescence of four oral mucosa epithelia (donors S01 – S04) for the following stemness markers: p63α (green), p40 (red), p75NTR (green), and proliferation marker Ki-67 (red). Nuclei counterstained with DAPI (blue). Scale bar: 100 μm. Images from the author's archive.
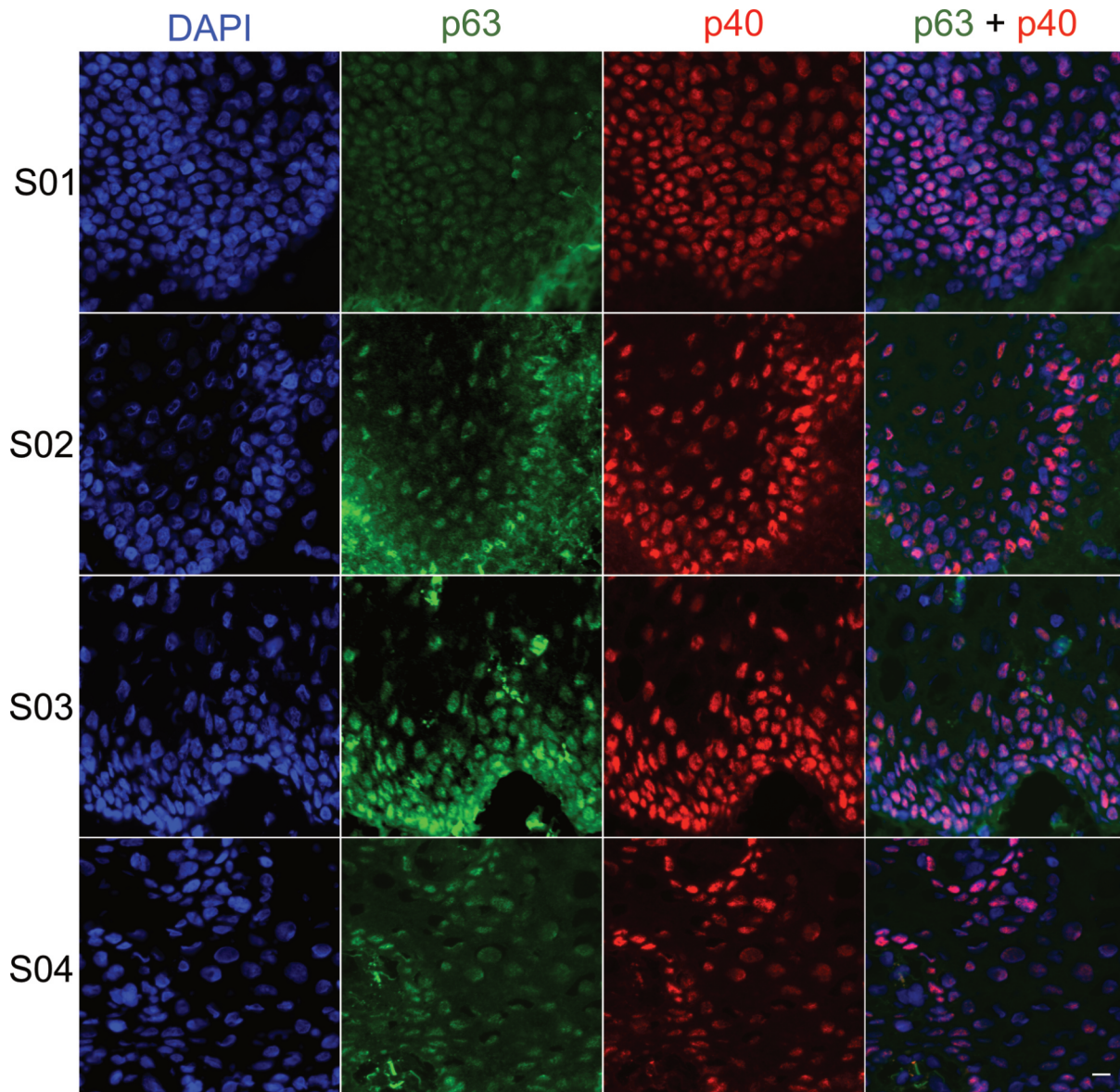
FIGURE 26: Immunofluorescence of four oral mucosa epithelia (S01 – S04) for the following stemness markers: p63α (green), p40 (red), and colocalization p63α + p40. Nuclei counterstained with DAPI (blue). Scale bar: 10 μm. Images from the author's archive.

The differentiation marker K3 was absent in one (S02) of the evaluated samples; in two of them (S03 and S04), it was minimally (< 1%) present in the suprabasal layer, and only in S01 K3 was present in the parabasal layer of a tip of a *rete ridge*, with the signal intensity decreasing upwards, and scattered in the suprabasal layer. K8 was primarily found in the basal layer, and the signal was usually more intense, particularly on the tips of the *rete ridges*, with a weaker signal spreading heterogeneously through the suprabasal-superficial layers. K13 was detected homogeneously throughout the entire suprabasal layer of all

immunostained samples and was absent in the basal layer. K19 showed much less positivity, and its distribution was heterogeneous among the samples. Still, it was concentrated in regional areas of the epithelium, with a strong signal at the tip and base of the *rete ridge* and a decrease of the signal towards the superficial layers, **Figure 27**.
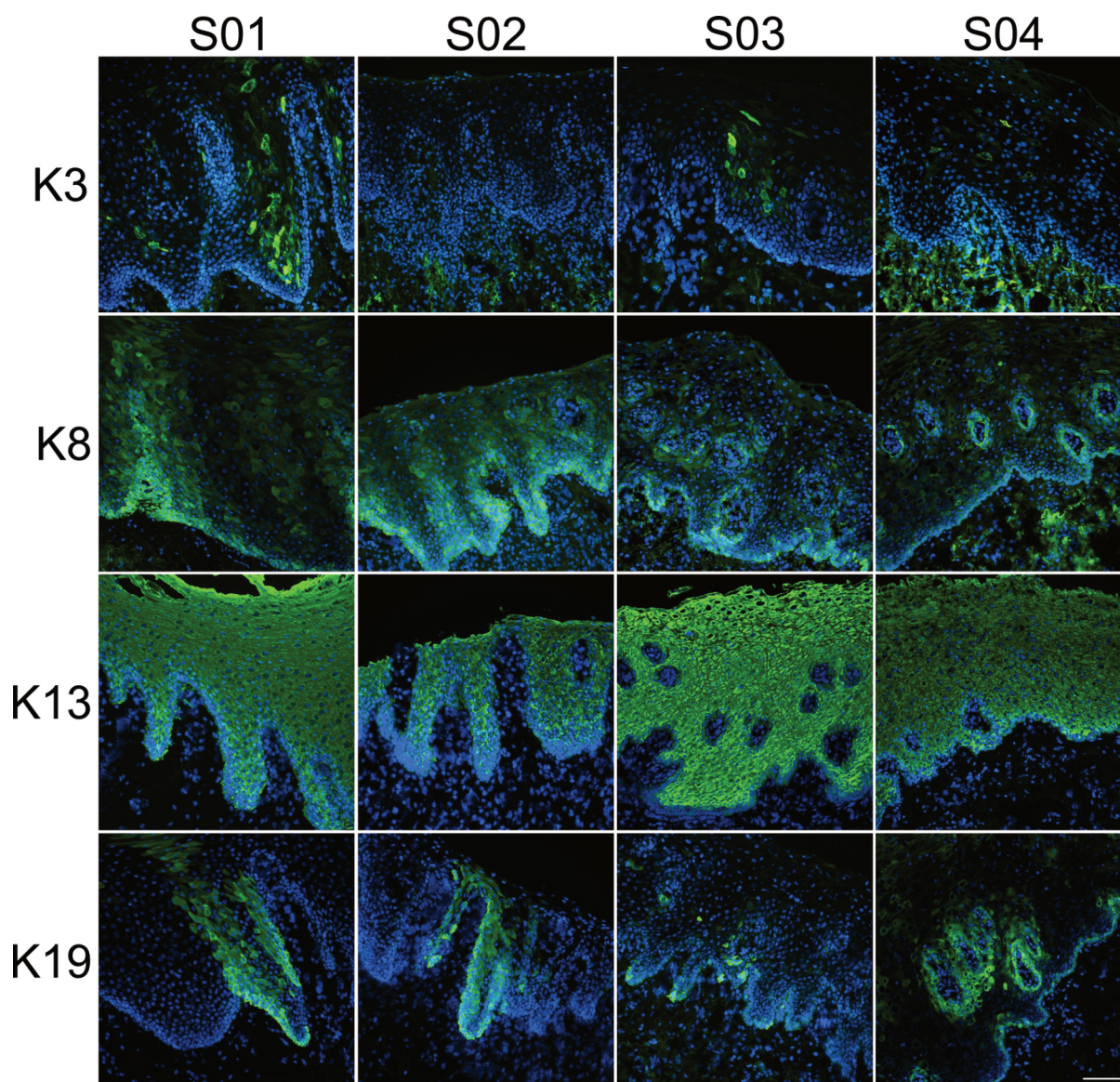
FIGURE 27: Immunofluorescence of four oral mucosa epithelia (donors S01 – S04) for the following differentiation markers: Keratin (K) 3 (green), K8 (green), K13 (green), and K19 (green). Nuclei counterstained with DAPI (blue). Scale bar: 100 μm. Images from the author's archive.

4.3.3. Oral Mucosa Cell Growth Dynamics and Cell Morphology

Among the donors whose samples were used for cell culture on COM and XF and evaluated (19 samples, S05 – S23, **Table 1, page 52**), there were eight females and eleven

male donors; for details, see **Table 5**. The average post-mortem time to tissue retrieval was 29.9 ± 13.4 h (mean ± SD), and samples were kept in Base 128 for a maximum of 24h. Cultures were prepared as described in **3.2.5 Preparation of Cell Suspension, page 53**.

Gender	*n* (%)	Age (mean ± SD)	Post-mortem time to retrieval (*h*), (mean ± SD)
Female	8 (42.1%)	66.5 ± 12.6	32.2 ± 11.4
Male	11 (57.9%)	69.6 ± 10.6	28.3 ± 15
Total	19 (100%)	68.3 ± 11.2	29.9 ± 13.4

TABLE 5: Donors' age and tissues' characteristics. *n*: absolut number; *h*: hour; SD: standard deviation.

Immediately after the seeding, the cells showed a rounded morphology. After 4 − 6 days of culture, OMECs in both culture conditions had cobblestone-like morphology, **Figure 28**. When viewed under an inverted phase-contrast microscope, the epithelial cells appeared small. They had uniform morphology, with a high nucleus-to-cytoplasm ratio, and cell-to-cell contacts were evident. When the wells were close to full confluence (90 − 100%), it was possible to observe that stratification had already initiated, causing the cells to adopt a spindle-shaped morphology towards the upper surface of the stratified layer while the cobblestone cell layer was still visible underneath, **Figure 29**. Throughout the culture period, the gel housing the cultivated OMEC sheet remained transparent.
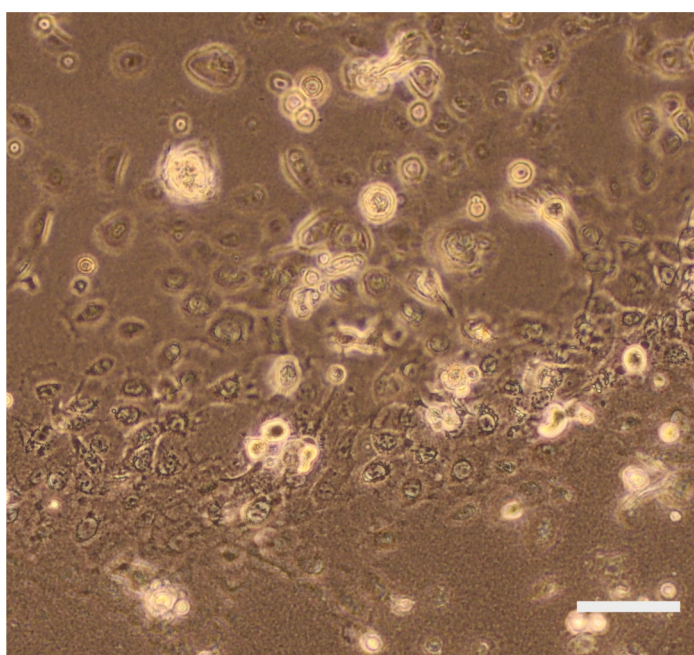
FIGURE 28: Inverted phase-contrast microscopy of oral mucosa epithelial cells on a fibrin

substrate and complex media four days after seeding the cells. The images reveal the initial stages of cell proliferation, showing clusters of cells proliferating, and some rounded cells not attached to the fibrin gel. Scale bar: 100 μm. Images from the author's archive.
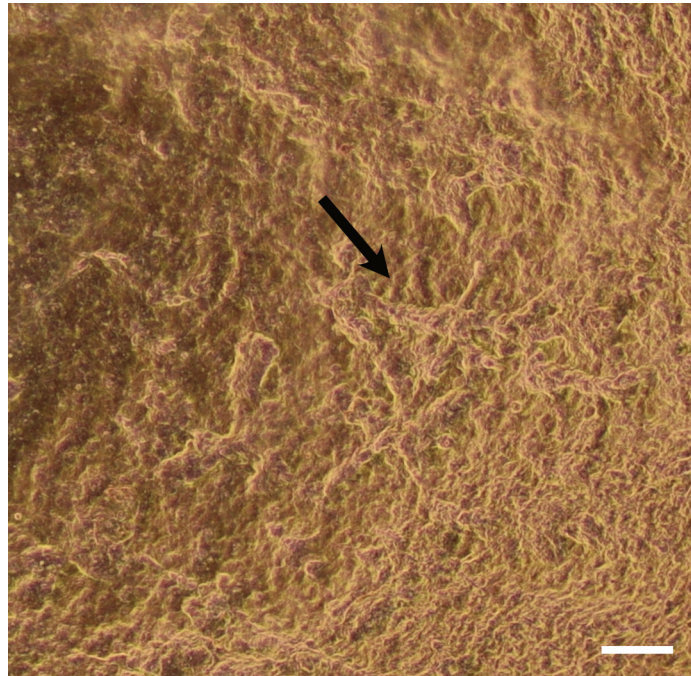
FIGURE 29: Inverted phase-contrast microscopy of oral mucosa epithelial cell culture on a fibrin gel substrate, nine days after seeding. Arrow indicates stratification near well borders at near full confluence. Scale bar: 100 μm. Images from the author's archive.

It was observed that cells grown using COM showed an earlier onset of proliferation compared to the XF group. The beginning of proliferation was determined by the number of days it took for the cells to settle on the fibrin gel and start proliferating. Based on those nineteen pairs (COM – XF, S5 – S23) of OMEC culture, the COM group took 4.7 ± 1.1 days, while the XF group took 5.4 ± 1.0 days to show proliferation. The COM group reached confluence in 11.8 ± 2.3 days, while the XF group took 12.7 ± 2.7 days, **Figure 30**. COM cultures, upon harvesting, showed a viability of $89.8\% \pm 5.1\%$ (mean $\pm$ SD), whereas XF cultures had a viability of $86.3\% \pm 7.9\%$ (mean $\pm$ SD). For details on the measurement of viability, refer to the chapter **3.2.9 Cell Viability and Cell Size, page 56**. Cell viability variances were homogeneous among the conditions (Levene's test, $p > 0.05$). Subsequently, a parametric t-test revealed no significant difference, indicating that the type of media used did not affect cell viability. **Table 6** summarizes the data on the days to the beginning of proliferation, days to reach confluence (90 – 100%), and cell viability for each media condition.

A

B
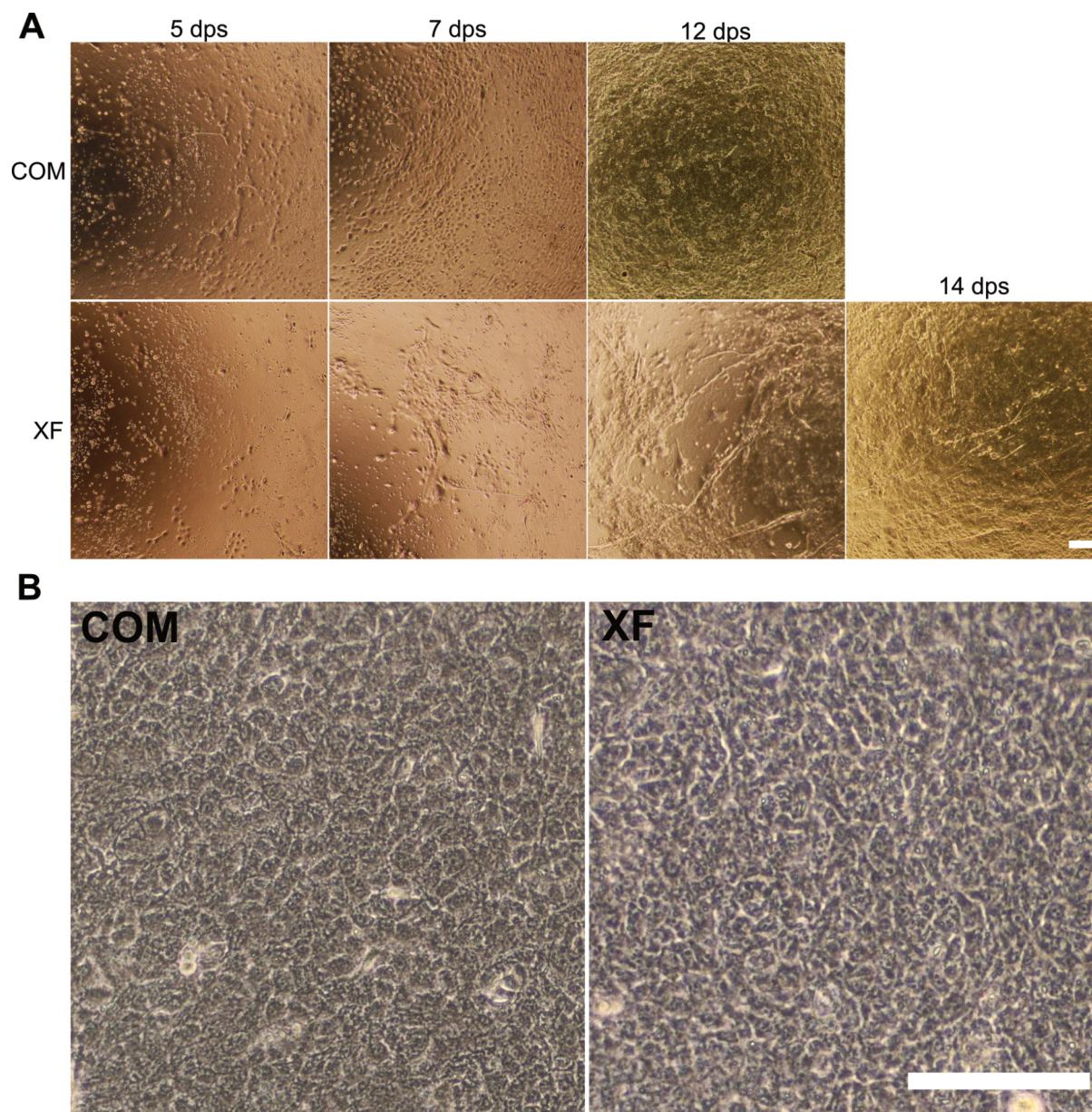
FIGURE 30: A. Inverted phase-contrast microscopy of cultures on fibrin complex media (COM) and fibrin xenobiotic-free media (XF), showing the progress of proliferation until confluence observed at 5 days post-seeding (dps), 7 dps, 12 dps, and 14 dps (XF only). B. The cobblestone-like morphology of cells in both culture media at confluence. Images from the author's archive. Scale bar: 200 μm.

Media	*n* (%)	Days lapsed to the beginning of the proliferation (mean ± SD)	Days lapsed to confluence (mean ± SD)	Viability % (mean ± SD)
Complex media	19 (50%)	4.7 ± 1.1	11.8 ± 2.3	89.8 ± 5.1
Xeno-free	19 (50%)	5.4 ± 1.0	12.7 ± 2.7	86.3 ± 7.9
Total	38 (100%)	5.0 ± 1.1	12.2 ± 2.5	88.0 ± 6.8

TABLE 6: Summary of the days to initiate proliferation, days to achieve confluence (90 – 100%), measured by the area of the well covered by a cell layer, and cell viability upon confluence for both complex media and xenobiotic-free media. n: absolut number; SD: standard deviation.

4.3.3.1. OMECs Culture on Deepithelized Amniotic Dembrane

An attempt was made to culture OMECs on dAM; however, several issues arose. Firstly, the same cell amount as seeded on the fibrin substrate (4.5×10^4 cells/well or 2.36×10^4 cells/cm^2) was insufficient for the larger area of the dAM (1.9 cm^2 on fibrin vs. 5.3 cm^2 on dAM), requiring an increased concentration. Ultimately, when 5.0×10^5 cells (9.4×10^4 cells/cm^2) were used, OMECs showed attachment and proliferation, **Figure 31**. Additionally, harvesting cells for further analysis posed a challenge. Direct application of the lysate was ineffective, and we optimized cell collection by applying Tryple Express for 30 minutes in the incubator, dilution by 2 volumes to inactivate the enzyme, followed by centrifugation of the cell suspension (10 minutes at $250 \times g$), and subsequent resuspension of cells in the lysis buffer for RT-qPCR analysis.

This study on the use of dAM is preliminary and aims to compare OMEC cultures in both fibrin gel and dAM under XF conditions.
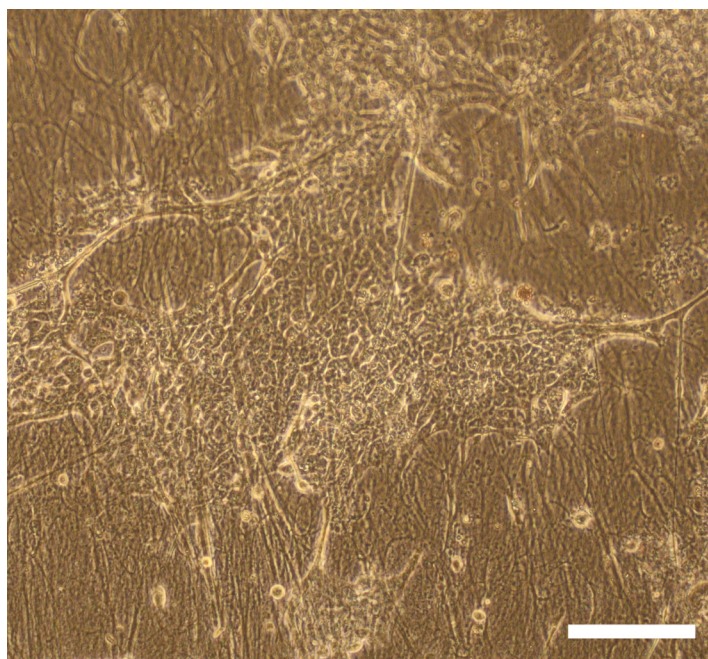
FIGURE 31: Inverted phase-contrast microscopy of oral mucosa epithelial cells proliferation on a deepithelialized amniotic membrane (dAM) four days after seeding the cells. Scale bar: 200 μm. Images from the author's archive.

4.3.4. Immunofluorescence

4.3.4.1. Cultured Cells

OMECs from S05, S06, S08, S09, S10, S11, S13, S14, S18, S19, and S23 cultured in COM and XF were immunostained for p63α, p40, p63α + p40 (ΔNp63α+), p75NTR, Ki-67, K3, K8, and K13 markers; except for p40, p75NTR and K3, primary cells were also immunostained. At least three samples per condition (primary cells, COM, and XF) were scored for each marker. For protocol on immunofluorescence and the calculation of the presence of a marker, refer to the chapter **3.2.10 Immunofluorescence, page 56**. Due to the small sample size to assume a normal distribution, a nonparametric test (Mann-Whitney U Test for two independent samples or Kruskal-Wallis for multiple independent samples) was used to compare the positivity of a marker among the groups.

Stemness markers (p63α, p40, p63α + p40, p75NTR) were detected in all samples assessed, **Figure 32**. The p63α protein was detected in cells of the primary cell suspension and from both media conditions similarly, **Figure 33**. The average presence of p63α was 68.6% ± 16.0% (mean ± SD) in the primary cell suspension, 68.8% ± 10.5% (mean ± SD) in the COM, and 64.6% ± 10.6% (mean ± SD) in the XF, not statistically significant (Kruskal-Wallis). The marker p40 (ΔNp63) was also assessed in cultured cells from both groups (COM and XF), **Figure 33**, and the presence of this marker correlates with the mean percentage of cells positive for p63α. In the COM group, 69.6% ± 8.8% (mean ± SD) were p40+, and in the XF group, 64.5% ± 6.4% (mean ± SD). The co-localization of p63α and ΔNp63 (thus, ΔNp63α+ cells) was also evaluated, **Figure 34**. In COM, there was a mean of 67% ± 11.3% (mean ± SD) positive cells for both markers simultaneously, whereas, in XF, it was co-localized in 59.6% ± 5.9% (mean ± SD) of the cells.
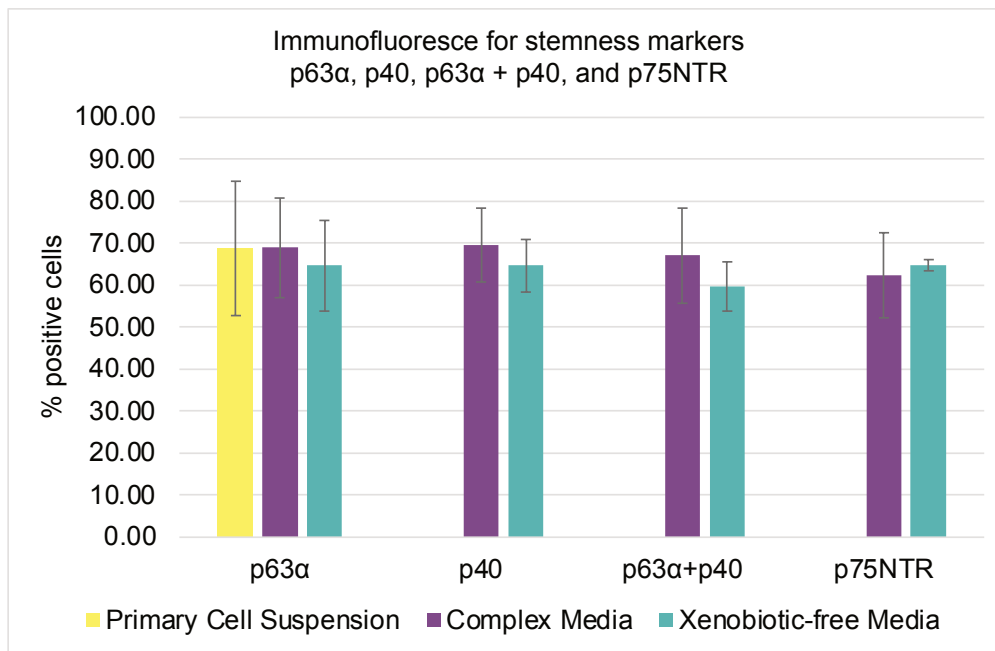
FIGURE 32: The graph illustrates the percentage of cells positive for stemness markers – p63α, p40, p63α co-localized with p40, and p75NTR. Cells from at least three different donors were assessed for each marker and condition (complex and xenobiotic-free media), and primary cells were also evaluated for p63α. The results are presented as mean ± standard deviation. No statistical significance was observed within each group (nonparametric Kruskal-Wallis test for multiple independent samples and Mann-Whitney test for two independent samples).
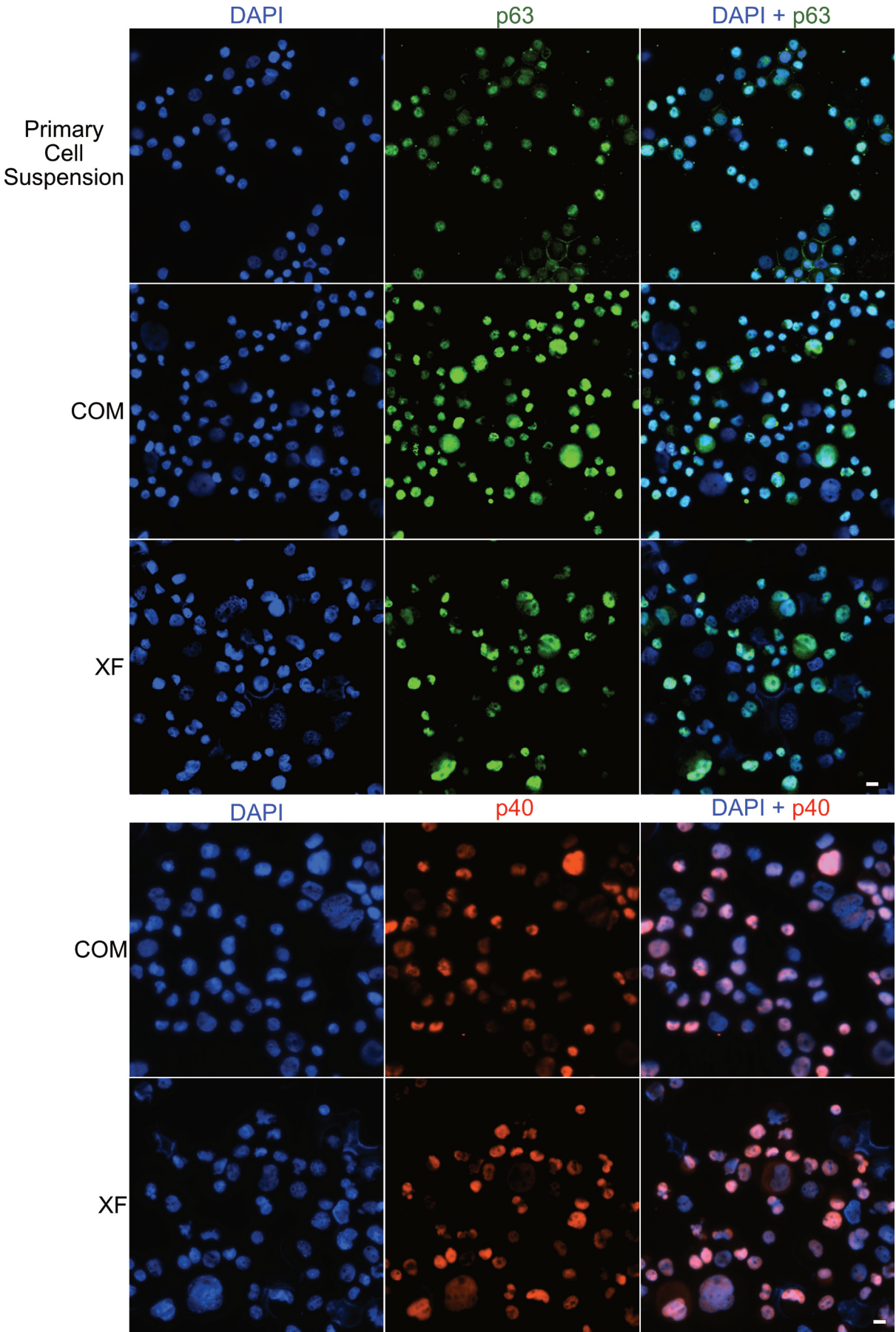
FIGURE 33: Immunofluorescence was conducted to detect the protein p63α on oral mucosa epithelial cells under three different conditions: primary cell suspension, cells cultured on complex media (COM), and xenobiotic-free media (XF). Additionally, p40 (ΔNp63) was analyzed in cultured cells (COM and XF). p63α was labeled in green, p40 in red, and the nuclei were counterstained in blue (DAPI). The scale bar represents 10 μm. The images are sourced from the author's archive.
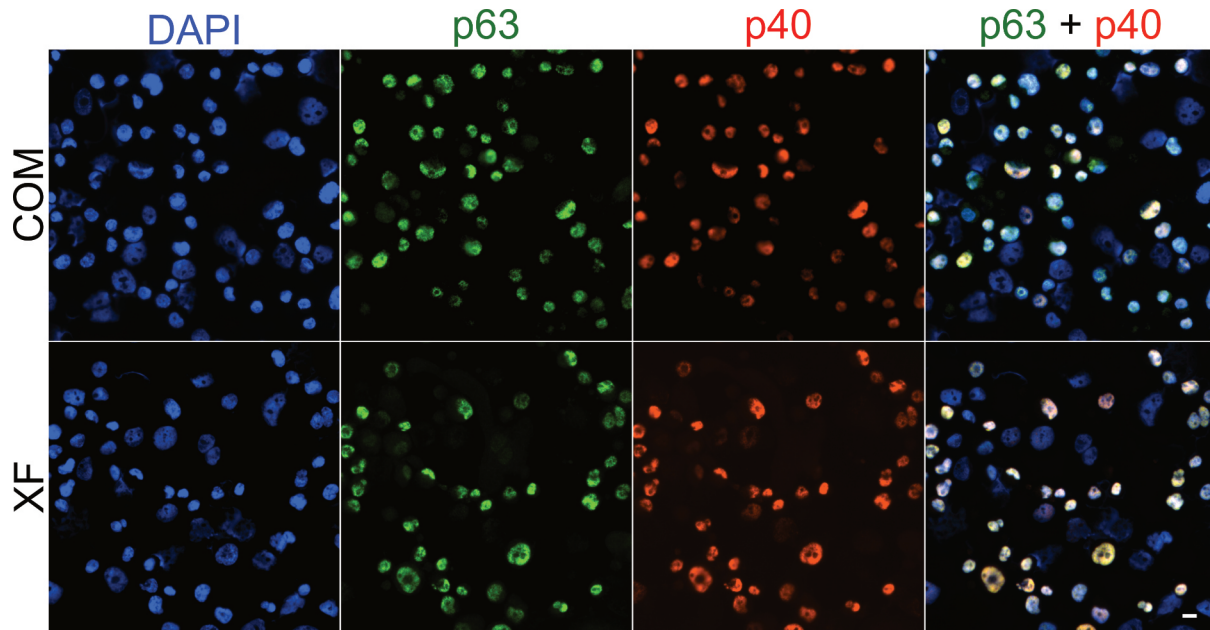
FIGURE 34: Immunofluorescence for the detection of the col-localization of the proteins p63α and p40 on oral mucosa epithelial cells cultured on complex media (COM) and xenobiotic-free media (XF). p63α in green, p40 in red, and nuclei counterstained in blue (DAPI). Scale bar: 10 μm. Images from the author's archive.

Another putative stem cell marker, the p75NTR protein, exhibited a similar pattern to p63α and p40, with detection in 62.3% ± 26.1% (mean ± SD) of cells cultured on COM and 64.7% ± 11.7% (mean ± SD) of cells cultured on XF, **Figure 35**, also not statistically significant according to the Mann-Whitney Test.
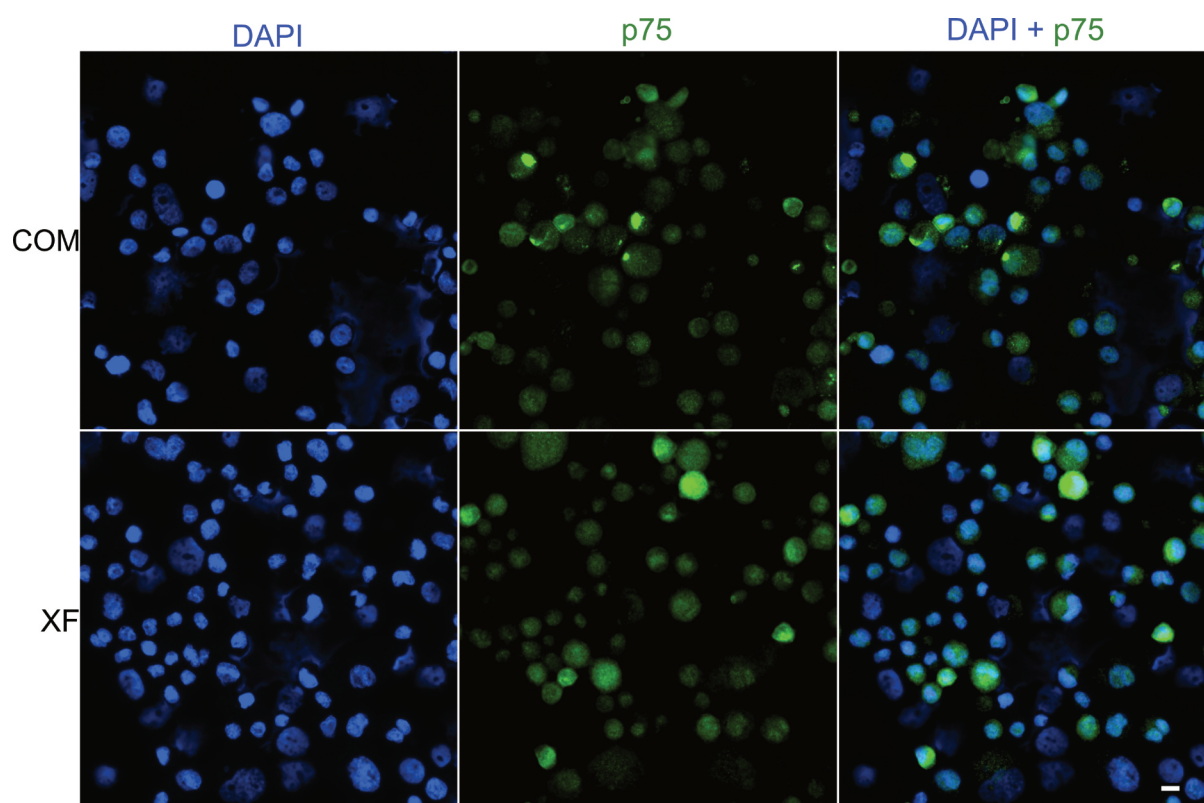
FIGURE 35: Immunofluorescence for the detection of the proteins p75NTR on oral mucosa epithelial cells cultured on complex media (COM) and xenobiotic-free media (XF). p75NTR in green and nuclei counterstained in blue (DAPI). Scale bar: 10 μm. Images from the author's archive.

The proliferation marker Ki-67 showed a higher percentage in the cultured cells (COM and XF) compared to the primary cell suspension, **Figure 36**, with approximately $35.9\% \pm 16.4\%$ (mean ± SD) of cells cultured on COM and $24.2\% \pm 21.6\%$ (mean ± SD) of cells cultured on XF, compared to the presence of Ki-67 in about $12.0\% \pm 7.1\%$ (mean ± SD) of the primary cells, **Figure 37**. Although this difference was not statistically significant (Kruskal-Willis Test).
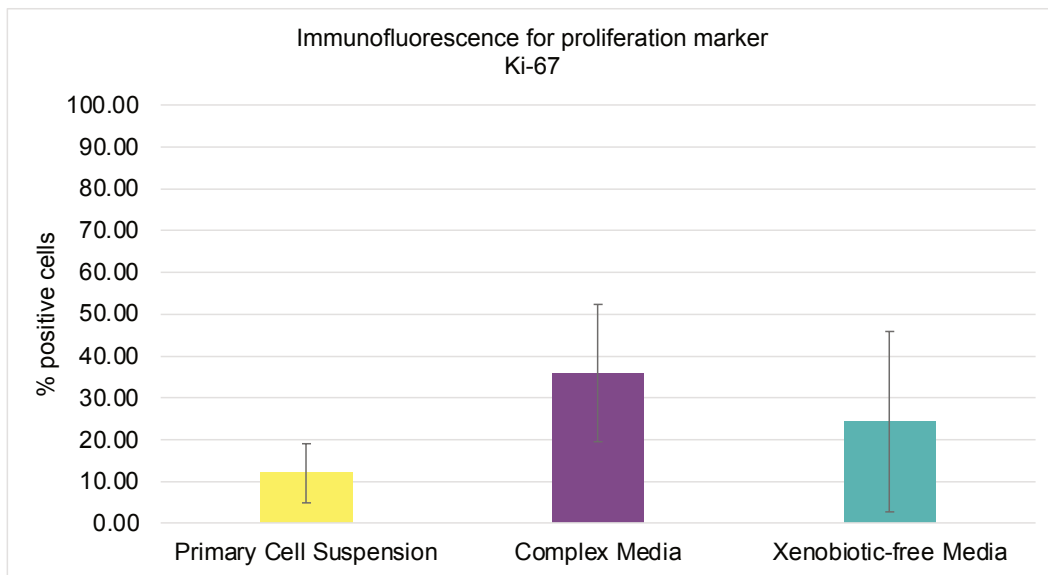
FIGURE 36: Immunostaining was performed to detect the proliferation marker Ki-67 in the primary cell suspension, complex media (COM), and xenobiotic-free media (XF). The results are presented as mean ± standard deviation. No statistical significance was observed among the groups (nonparametric Kruskal-Wallis test).
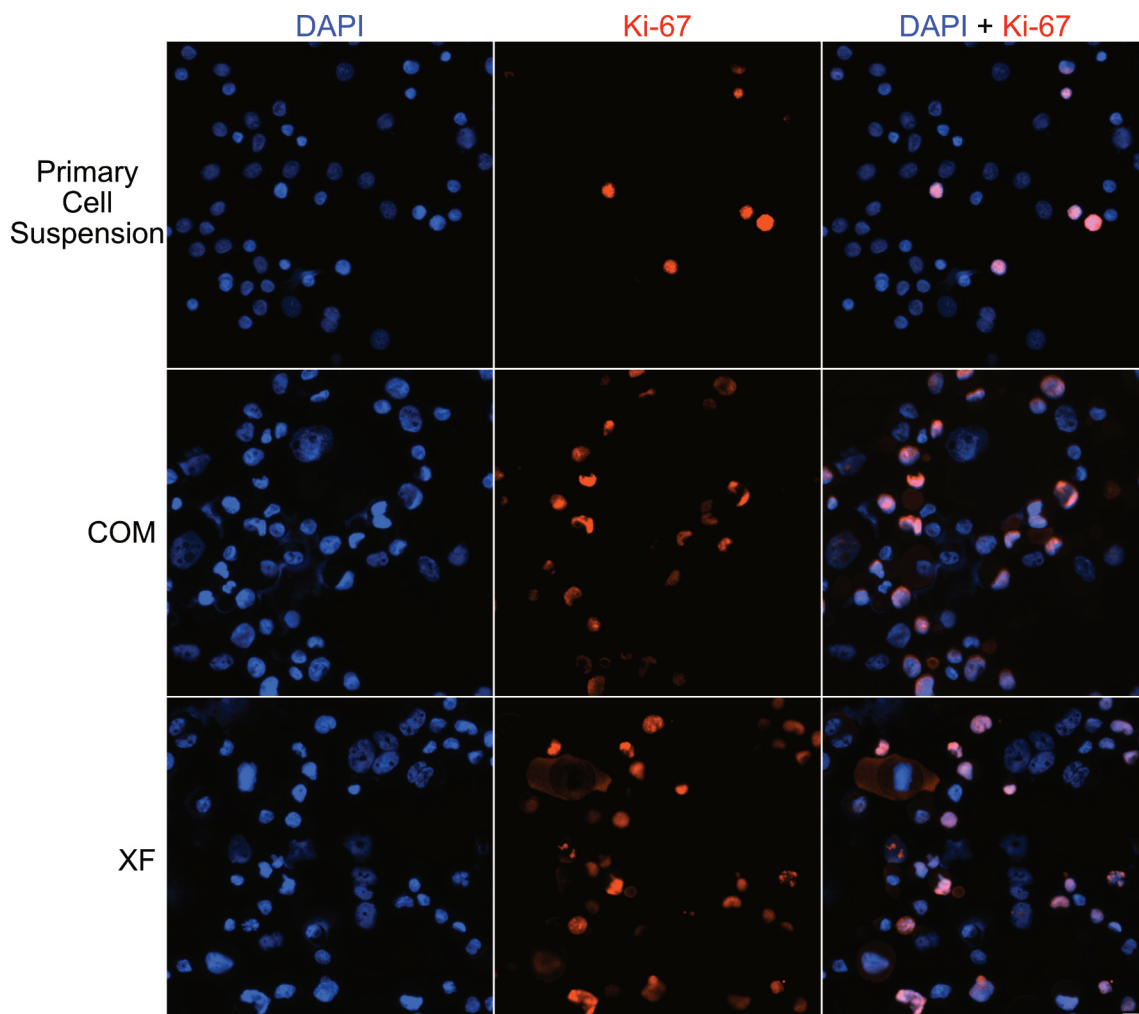
FIGURE 37: Immunofluorescence for the detection of the proliferation marker Ki-67 on oral mucosa epithelial cells in three different conditions: primary cell suspension, cells cultured on complex media (COM), and xenobiotic-free media (XF). Ki-67 in red and nuclei counterstained in blue (DAPI). Scale bar: 10 μm. Images from the author's archive.

Moreover, differentiation markers K3, K8, and K13 were also evaluated, **Figure 38**. K3 was detected in 15.1% ± 5.7% (mean ± SD) of cells in COM and, in XF, 13.3% ± 3.1% (mean ± SD), with no statistically significant difference due to small sample size. K8 was detected in 56.2% ± 9.8% (mean ± SD) of cells from the primary cell suspension, similar in COM, 53.7% ± 24.5% (mean ± SD), and lower in XF, 44.0% ± 18.8% (mean ± SD), although this difference was not statistically significant (Kruskal-Willis Test). On the other hand, K13 was detected in 68.3% ± 21.2% (mean ± SD) of cells in the primary cell suspension, whereas it was found in 17% ± 12.7% (mean ± SD) of cells cultured on COM and 26.8% ± 11.0% (mean ± SD) of cells cultured on XF. There was a statistically significant difference when comparing either culture media to the primary cell suspension ($p < 0.0001$, Kruskal-Wallis Test). Immunofluorescence images for these keratins are shown in **Figure 39** and **Figure 40**.
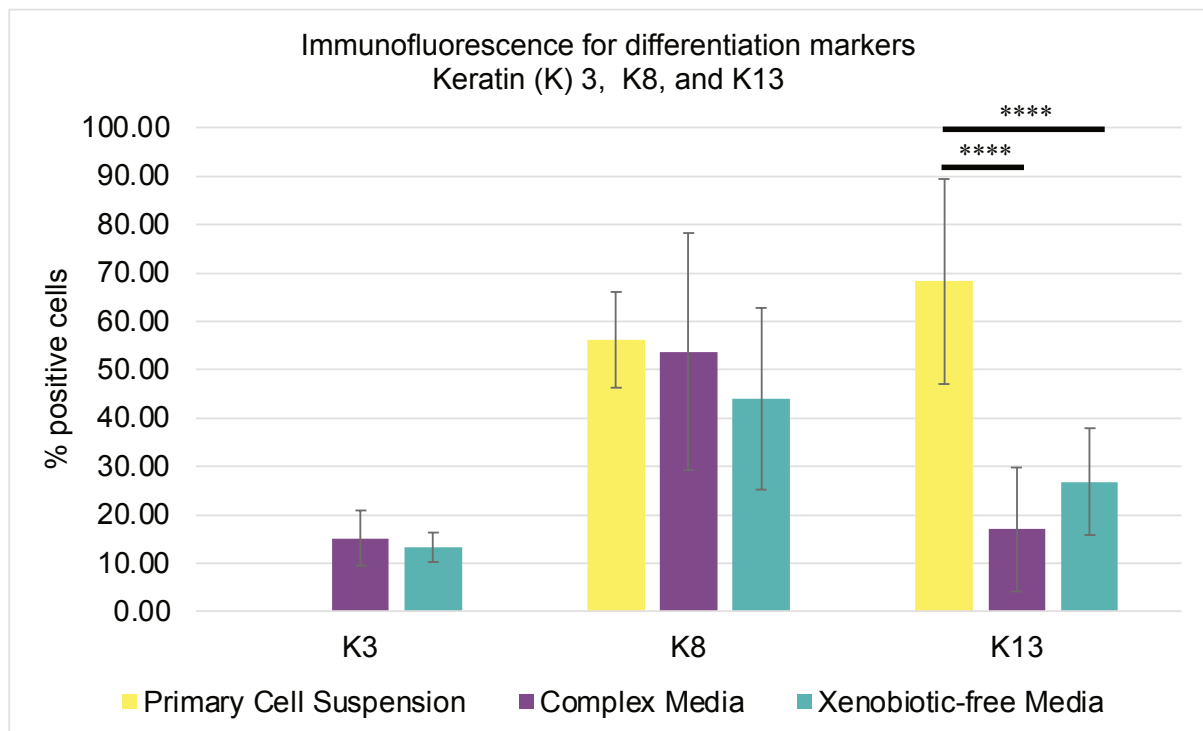
FIGURE 38: Immunostaining was performed to detect the differentiation markers keratin (K) 3, K8, and K13 in the primary cell suspension (K8 and K13), complex media (COM), and xenobiotic-free media (XF). The results are presented as mean ± standard deviation. No statistical significance was observed among the groups for K3 or K8 (nonparametric Kruskal-Wallis test). However, a statistically significant difference was found for the presence of K13

in both COM and XF compared to the primary cell suspension ($p < 0.0001$ for both cases, nonparametric Kruskal-Wallis test).
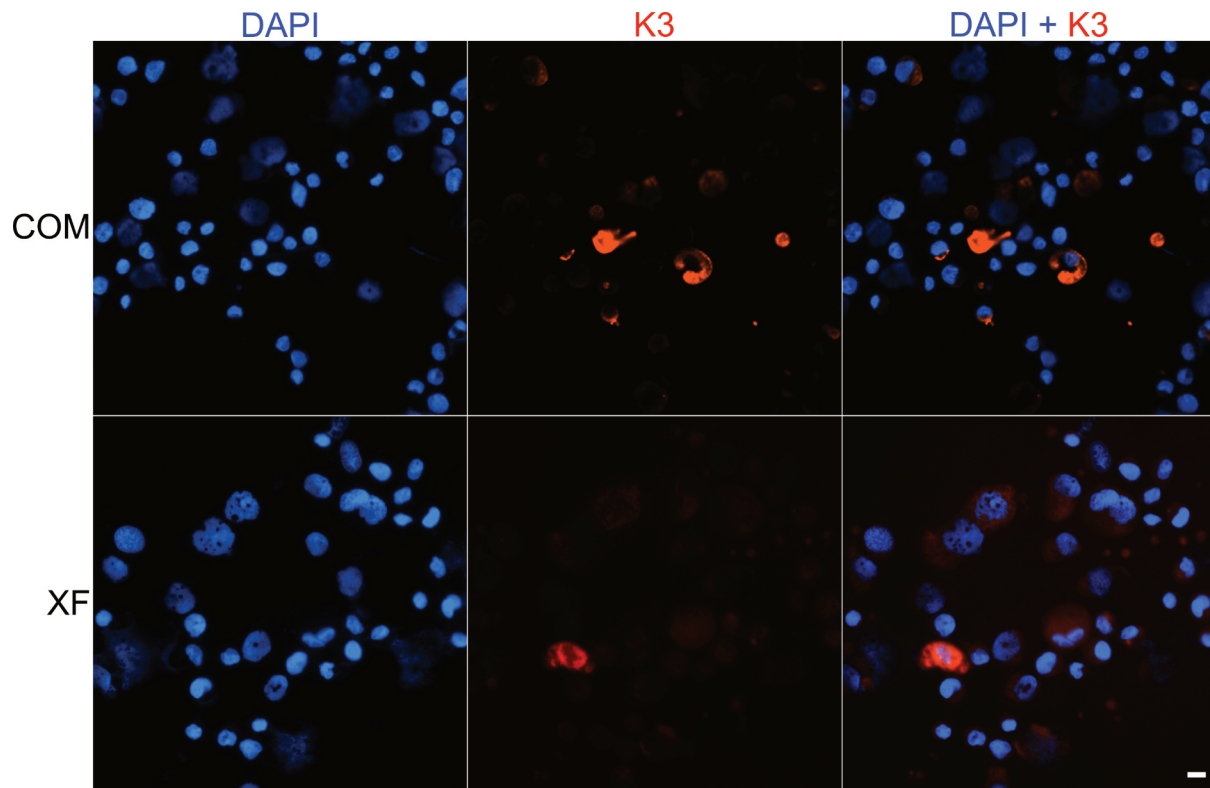
FIGURE 39: Immunofluorescence for the detection of the differentiation marker Keratin (K) 3 on oral mucosa epithelial cells in cells cultured on complex media (COM) and xenobiotic-free media (XF). K3 in red and nuclei counterstained in blue (DAPI). Scale bar: 10 μm. Images from the author's archive.
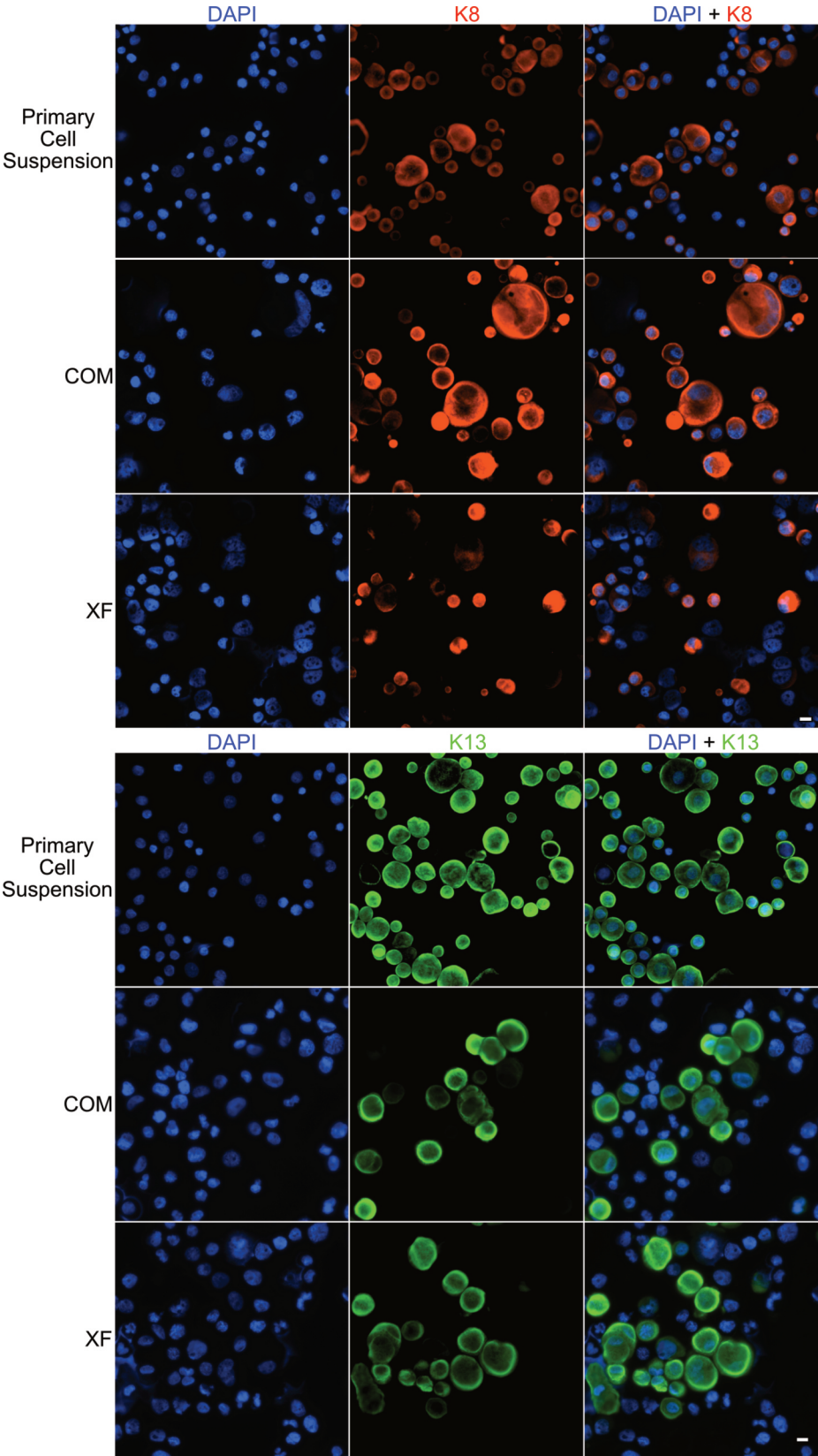
FIGURE 40: Immunofluorescence for the detection of the protein keratin (K) 8 and K13 on oral mucosa epithelial cells in three different conditions: primary cell suspension, cells cultured on complex media (COM), and xenobiotic-free media (XF). K8 in red, K13 in green,

and nuclei counterstained in blue (DAPI). Scale bar: 10 μm. Images from the author's archive.

4.3.4.2. Cell size and Stemness

Four specimens (S08, S10, S18, and S19) were also evaluated for the correlation between cell size and the presence of p63α, p40 (ΔNp63), and their co-localization (ΔNp63α+) in both conditions (COM and XF) by immunofluorescence. In COM, after culture, $4.9 \pm 5.8\%$ (mean $\pm$ SD, range $0.41 - 13\%$) of the cells had a cell diameter ≤ 11 μm, $39.6 \pm 21.8\% > 11$ and ≤ 18 μm, and $55.5 \pm 27.1\% > 18$ μm, **Figure 41**. In XF, $3.1 \pm 2.3\%$ were ≤ 11 μm, $47.0 \pm 11.0\% > 11$ and ≤ 18 μm, and $49.8 \pm 11.9\%$ larger than 18 μm.
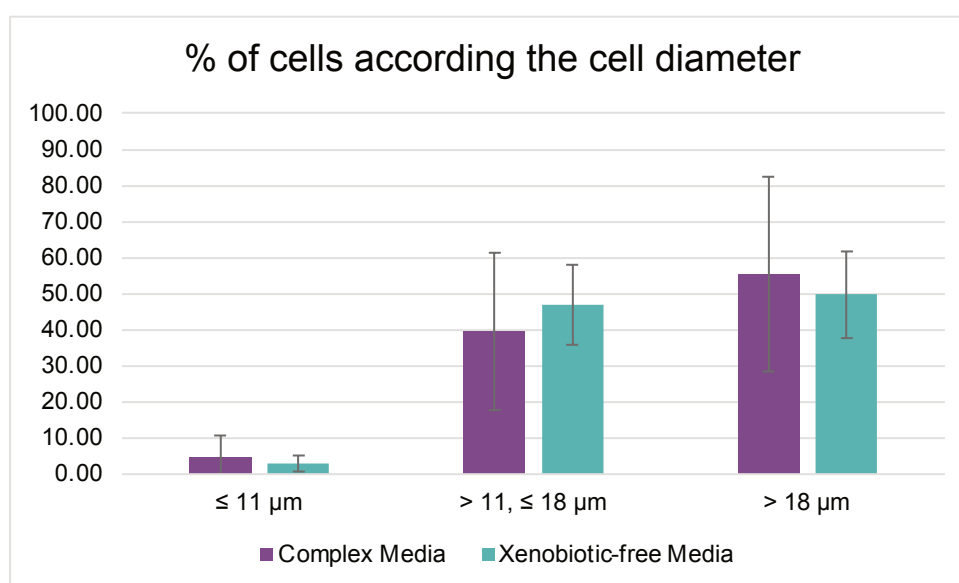
FIGURE 41: The percentage of cells falling into three different ranges of cell diameter (≤ 11 μm, $> 11 - \leq 18$ μm, and > 18 μm) was determined for both cultured conditions: complex media (COM) and xenobiotic-free media (XF).

When considering only cells ≤ 11 μm, in COM, 84.5% (4.3% when weighted for the whole amount of cells) were p63α+, 87.8% (4.5% among all cells) were p40+, and 81.8% (4.2% weighted value) were both p63α+ and p40+. Whereas in XF, 73.4% of cells ≤ 11 μm (1.9% for the whole amount) were p63α+, 72.1% (1.9% among all cells) were p40+, and 68.3% (1.8% of all cells) were positive for both p63α and p40, **Figure 42**.

Presence of stemness markers in cells ≤ 11 µm diameter
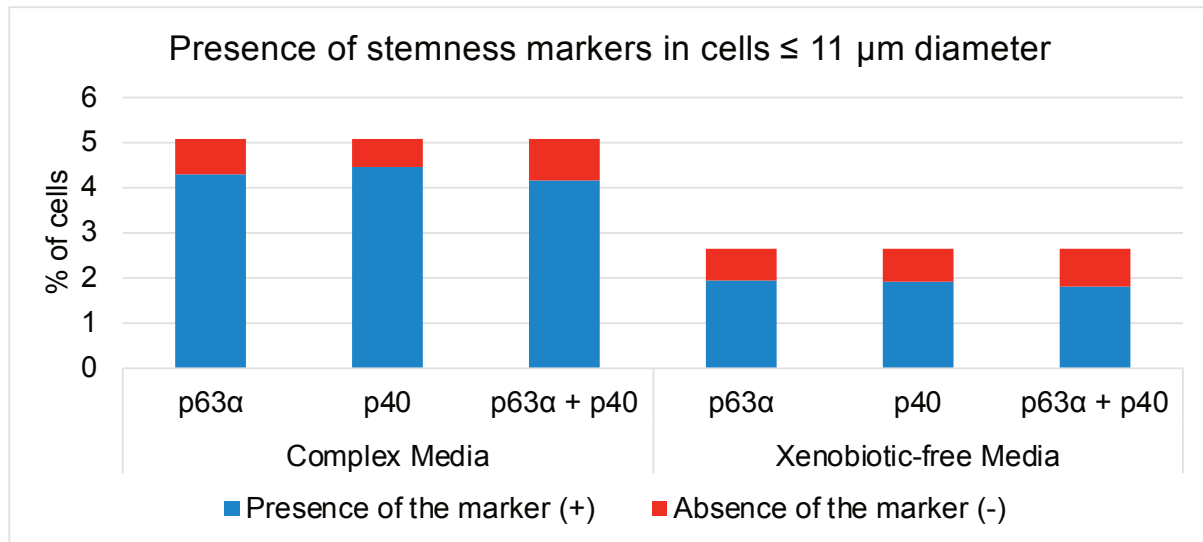
FIGURE 42: The graphs represent the correlation of cell diameter of cells ≤ 11 µm and the presence of putative stem cell markers p63α, p40, and the co-localized p63α+p40+ for both conditions − complex media (COM), and xenobiotic-free media (XF). In blue are the cells positive for the markers, and in red, negative. The overall weighted positivity of the markers was: in COM, 4.3% p63α+, 4.5% p40+, and 4.2% p63α+p40+; in XF, 1.9% p63α+, 1.9% p40+, and 1.8% p63α+p40+.

4.3.5. Reverse Transcription Quantitative Real-time PCR (RT-qPCR)

Samples from S08, S13, S14, S18, S19, S20, and S21 had their gene expression for putative stem cells, proliferation, and differentiation genes analyzed for three groups: primary cell suspension, cells cultured on COM, and cells cultured on XF. To assess the impact of media (COM or XF) on cell phenotype, we utilized RT-qPCR to evaluate the expression of such genes at the mRNA level. Through bidirectional hierarchical clustering of the log. rel.mRNA values, we observed that the control cells tended to form a distinct group separate from cells derived from culture in either medium, **Figure 43**. Also, based on their expression, the tested genes were classified into two groups of lower and higher expressed genes: class I, lower expression – *KRT3*, *NESTIN*, *KRT12*, *ABCG2*, *IGFPB5*, *PAX6*, *KRT8*, and *NANOG*; class II, higher expression – *OCT4*, *LRIG1*, *NGFR*, *ALDH3A1*, *KLF4*, *PCNA*, *ΔNp63α*, *MKI67, SOX2, KRT14, KRT13, KRT15, KRT7, KRT17, ITGB1*, and *KRT19*, **Figure 43**. The logarithmic mean values for all gene expressions for primary cells, COM, and XF are detailed in **Table 7**.
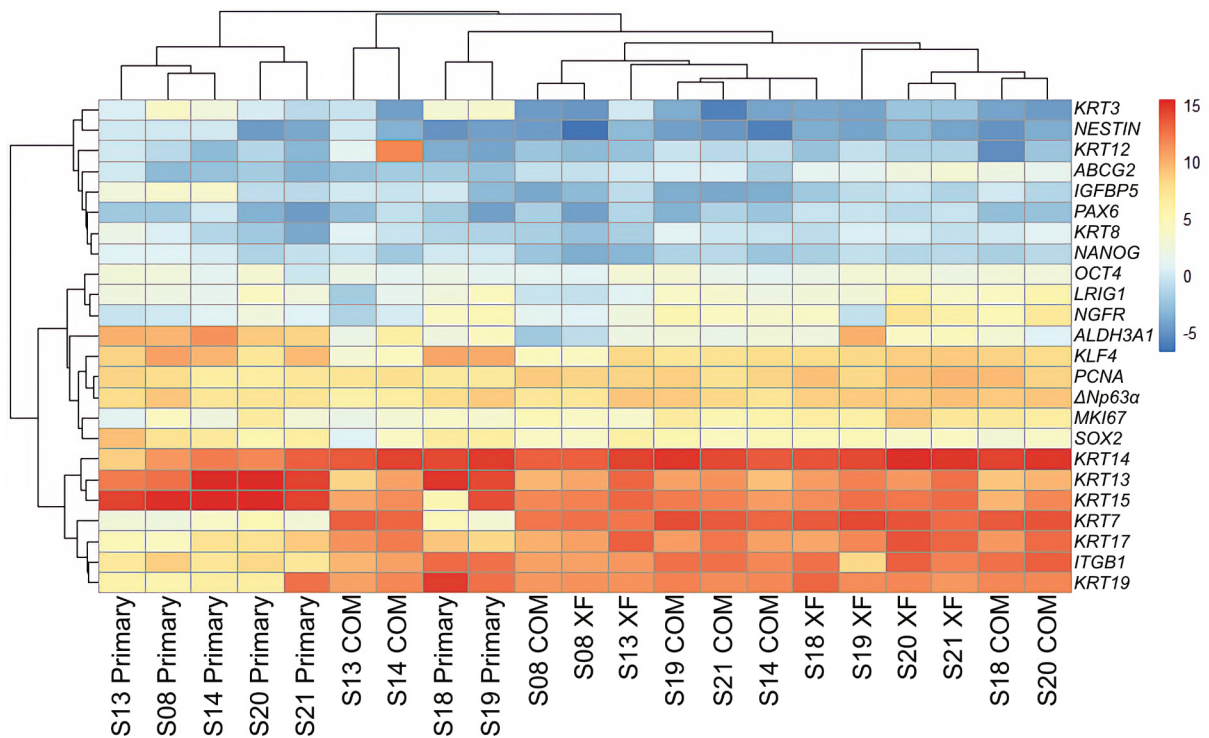
FIGURE 43: Comparisons of oral mucosa epithelial cells (OMEC) cultured in complex media (COM) or xenobiotic-free media (XF) compared to cells prior to culture (primary cells) for the gene expression of stem cell, proliferation, and differentiation markers assessed using real-time polymerase chain reaction. A heatmap was generated to provide an overview of the relative mRNA expression (logarithmic values) for the tested genes (rows), with the samples (columns) grouped based on the media used for their cultivation or control. The color scale on the right side of the heatmap represents higher expressions in red and lower expressions in blue.

Genes	Primary Cells	Complex Media	Xenobiotic-free media
Progenitor and Putative Stem Cell genes			
ΔNp63α	7.66 ± 0.97	8.08 ± 0.94	8.35 ± 1.06
KLF4	9.13 ± 1.37	6.84 ± 2.16	7.39 ± 1.95
SOX2	6.82 ± 1.20	3.72 ± 1.62	4.29 ± 1.17
NGFR	1.84 ± 2.16	3.49 ± 2.30	2.76 ± 2.74
OCT4	1.57 ± 1.11	1.92 ± 0.81	1.98 ± 0.90
LRIG1	2.72 ± 1.18	2.26 ± 2.21	2.14 ± 1.90
ABCG2	-2.55 ± 1.27	0.54 ± 1.56	1.15 ± 1.63
PAX6	-2.39 ± 1.79	-2.69 ± 1.16	-1.24 ± 1.33
NANOG	-0.22 ± 0.82	-1.68 ± 1.51	-1.38 ± 1.22
NESTIN	-2.63 ± 2.48	-3.23 ± 2.22	-3.37 ± 1.93
Proliferation genes			

ITGB1	8.71 ± 2.42	11.94 ± 1.13	10.91 ± 1.90
PCNA	7.02 ± 0.75	8.61 ± 0.67	8.85 ± 0.63
ALDH3A1	7.83 ± 3.28	1.71 ± 1.46	4.05 ± 3.05
MKI67	3.15 ± 1.96	5.66 ± 1.63	6.00 ± 1.80
IGFBP5	0.57 ± 2.52	-3.37 ± 2.29	-1.50 ± 1.40
Differentiation genes			
KRT3	2.13 ± 2.06	-3.31 ± 2.02	-3.08 ± 1.43
KRT7	3.33 ± 1.12	13.33 ± 0.83	13.15 ± 0.71
KRT8	-1.07 ± 1.70	-0.23 ± 1.42	-0.56 ± 1.12
KRT12	-2.32 ± 1.53	-1.07 ± 2.09	-0.31 ± 4.05
KRT13	14.06 ± 1.17	10.07 ± 1.09	11.78 ± 1.16
KRT14	12.00 ± 2.04	14.31 ± 0.69	14.38 ± 0.64
KRT15	13.39 ± 3.56	11.28 ± 0.92	12.34 ± 0.75
KRT17	6.77 ± 2.23	11.71 ± 0.93	12.33 ± 1.03
KRT19	9.14 ± 3.96	11.41 ± 0.48	11.79 ± 1.05

TABLE 7: Logarithmic values (mean ± SD) of all gene expressions for primary cells, complex media, and xenobiotic-free media from donors S08, S13, S14, S18, S19, S20, and S21.

4.3.5.1. Expression of Stem Cell Markers

We evaluated the gene expression of various putative stem cell genes, including *ΔNp63α, KLF4, SOX2, NGFR, OCT4, LRIG1, ABCG2, PAX6, NANOG*, and *NESTIN*. Statistical significance was observed between the groups for *SOX2* and *ABCG2*.

After analysis using repeated measures ANOVA with Bonferonni posthoc tests, *ABCG2* was significantly upregulated in the xeno-free culture relative to the control group ($p < 0.05$); on the other hand, *SOX2* was downregulated in both culture media groups in relation to the control, both significantly (COM $p < 0.05$, XF $p < 0.01$), **Figure 44**. No significant difference was observed among the groups for the remaining putative stem cell genes. However, *ΔNp63α, NGFR*, and *OCT4* showed a trend to be more expressed in both conditions compared to control (primary cells), whereas *KLF4* and *LRIG1* showed an opposite trend, with higher expression in the control samples and lower in cultured cells; again, not statistically significant. *ABCG2, PAX6, NANOG, and NESTIN* had a lower expression in general, **Table 7**.
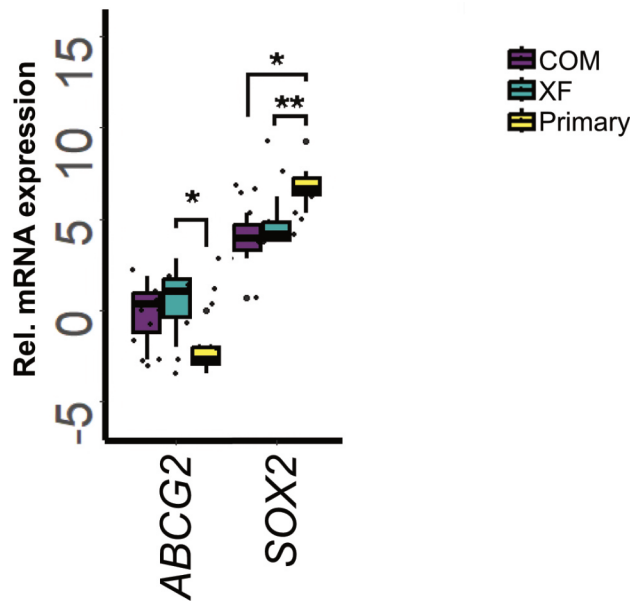
FIGURE 44: The boxplot shows the RT-qPCR results of the relative mRNA expression of specific stemness genes (*ABCG2*, and *SOX2*) from oral mucosa cells cultured in two different media, the COM (purple), XF (green), and the non-cultured samples used as control (primary cells, yellow). The asterisks indicate the level of significance (*$p < 0.05$, **$p < 0.01$, ****$p < 0.0001$, n = 7).

4.3.5.2. Expression of Proliferation Markers

We evaluated the gene expression of various proliferation genes, namely *ITGB1*, *PCNA*, *MKI67*, *ALDH3A1*, and *IGFBP5*. Statistical significance was observed between the groups for *PCNA*, *MKI67*, and *ALDH3A1*.

After analysis using repeated measures ANOVA with Bonferonni posthoc tests, the proliferation marker *PCNA* was expressed in both media groups but was significantly upregulated only in XF ($p < 0.05$). *MKI67* was upregulated in both media but with a significant difference only in the COM ($p < 0.01$). In this sense, the expression of *ALDH3A1*, a proliferation-suppressive marker, was downregulated in both media but only significantly in the COM group ($p < 0.05$), **Figure 45**. For the remaining proliferation genes, no significant difference was observed among the groups. However, *ITGB1* was highly expressed in all three conditions, with a trend of higher expression in cultured cells, whereas *IGFBP5* had low expression in all conditions and was lower in cultured cells.
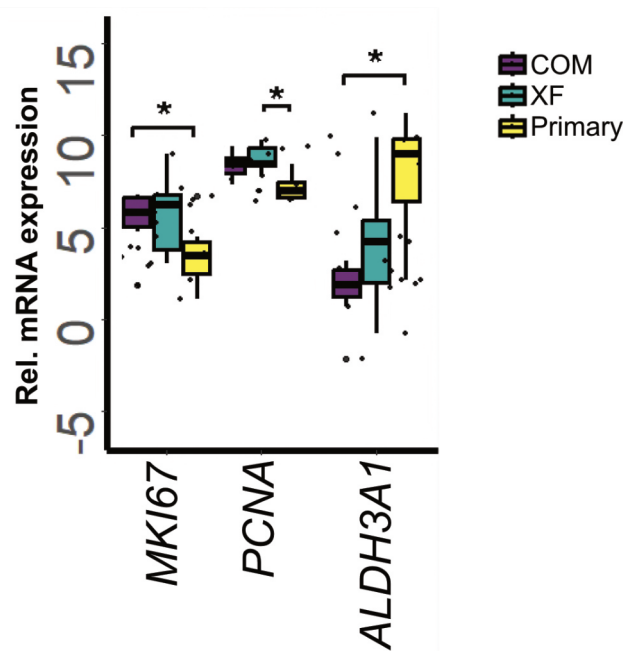
FIGURE 45: The boxplot shows the RT-qPCR results of the relative mRNA expression of specific proliferation genes (*MKI67, PCNA, ALDH3A1*) from oral mucosa cells cultured in two different media, the COM (purple), XF (green), and the non-cultured samples used as control (primary, yellow). The asterisks indicate the level of significance (*$p < 0.05$, n = 7).

4.3.5.3. Expression of Differentiation Markers

We evaluated the gene expression of various differentiation genes, namely *KRT3*, *KRT7*, *KRT8*, *KRT12*, *KRT13*, *KRT14*, *KRT15*, *KRT17*, and *KRT19*. Statistical significance was observed between the *KRT3*, *KRT7*, *KRT13*, and *KRT17* groups.

After analysis using repeated measures ANOVA with Bonferonni posthoc tests, the expression of *KRT13* was downregulated in both culture conditions (COM, $p < 0.0001$, and XF, $p < 0.05$) relative to the control group. The expression of *KRT3* followed the same trend, and it was significantly downregulated in both culture conditions (COM, $p < 0.01$, XF, $p < 0.05$). On the other hand, the expression of *KRT7* was upregulated significantly in both conditions ($p < 0.0001$). The expression of *KRT17* followed a similar trend ($p < 0.01$), **Figure 46**. No significant difference was observed among the groups for the remaining differentiation genes. *KRT14* and *KRT19* exhibited higher expression levels in both cultured conditions than primary cells. Conversely, *KRT15* showed higher expression in the primary cell suspension than COM and XF. On the other hand, *KRT8* demonstrated lower expression in all three conditions, with a slightly lower expression observed in the primary cell suspension.
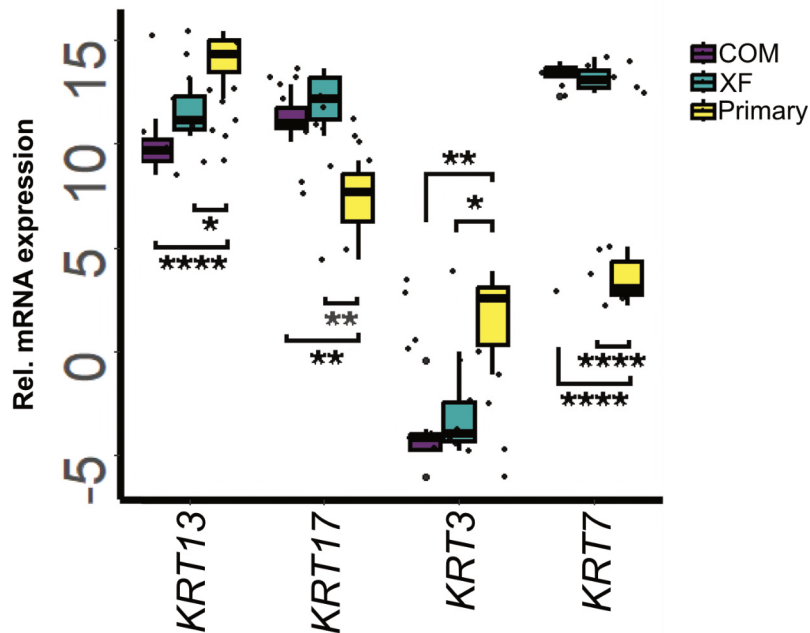
FIGURE 46: The boxplot shows the RT-qPCR results of the relative mRNA expression of specific differentiation genes (*KRT13, KRT17, KRT3*, and *KRT7*) from oral mucosa cells cultured in two different media, the COM (purple), XF (green), and the non-cultured samples used as control (primary, yellow). The asterisks indicate the level of significance (*$p < 0.05$, **$p < 0.01$, ****$p < 0.0001$, n = 7).

4.3.6. Genotoxicity Assay

The genotoxicity assay was performed in six culture pairs (COM and XF) of donors S07, S09, S12, S13, S22, and S23 (**Table 1, page 52**) within an average of 13.6 ± 1.0 (mean ± SD) dps. As shown in **Figure 47**, the OMEC cultivated in both COM and XF showed very low levels of DNA SBs + ALS after two weeks of culture. Similarly, the levels of net FPG-sensitive sites were also low under both types of cell media but lower in the xeno-free medium. In cells cultured on COM, the % tail DNA was 0.27 ± 0.19 (mean ± SD) for SBs + ALS and 4.43 ± 4.33 (mean ± SD) for net FPG-sensitive sites. On the other hand, in cells cultured on XF, the % tail DNA was 0.29 ± 0.22 (mean ± SD) for SBs + ALS and 2.80 ± 2.12 (mean ± SD) for net FPG-sensitive sites. A representative image of the comet assay for S23 is shown in **Figure 48**.

Since the sample is small to assume a normal distribution, a nonparametric test (Mann-Whitney U Test) was used. There was no statistically significant difference between SBs + ALS ($p > 0.05$) or net FPG-sensitive sites ($p > 0.05$) in COM compared to XF.
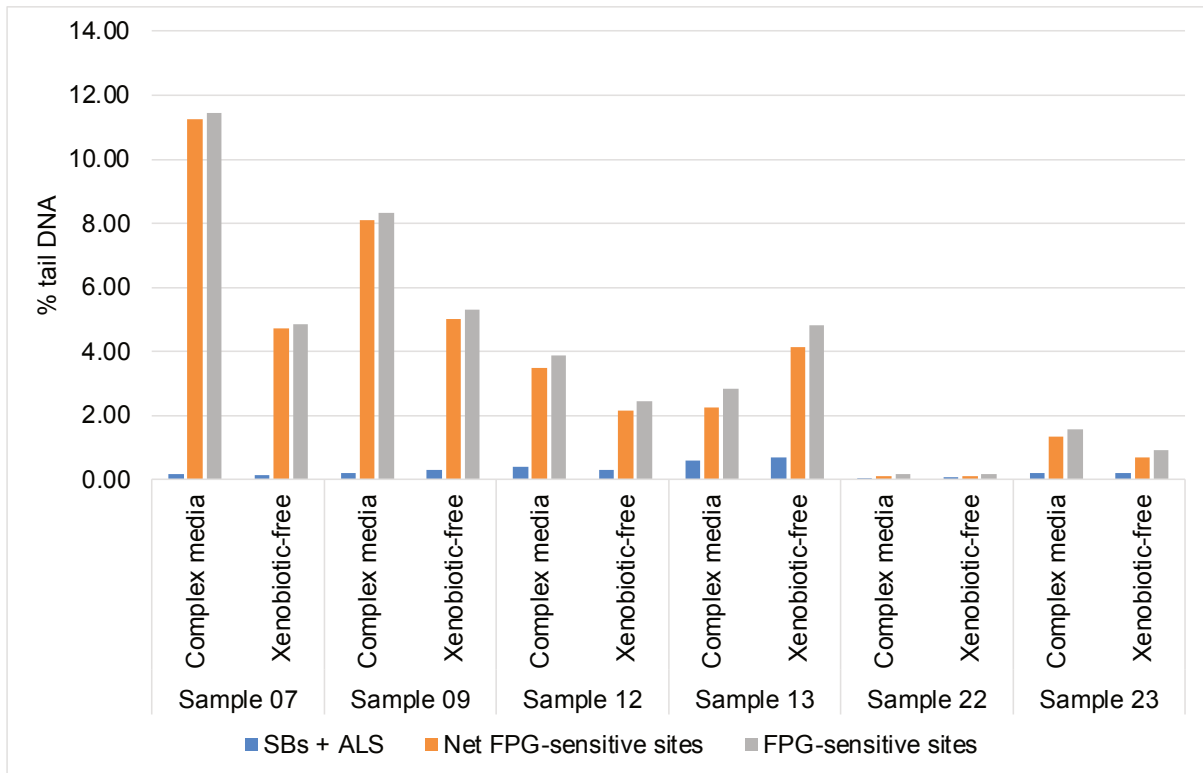
FIGURE 47: Individual data of DNA strand breaks (SBs+ALS) and net FPG-sensitive sites expressed as % tail DNA detected in six samples of oral mucosa cells expanded *ex vivo* in either complex media or xenobiotic-free media.
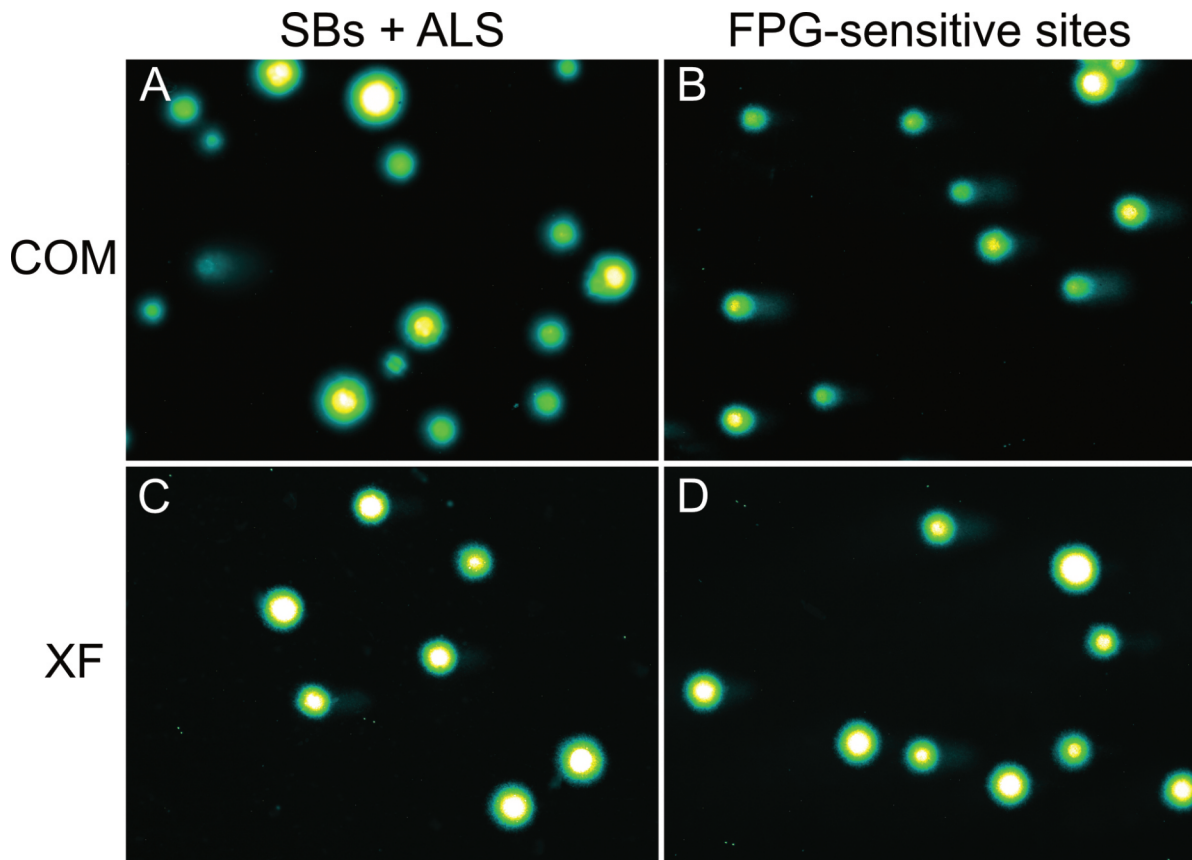
FIGURE **48**: DNA damage in oral mucosa epithelial cells (S23) cultured in either complex media (COM) or xenobiotic-free media (XF), for strand breaks (SBs), including alkali-labile sites (ALS), A and C, and oxidized purines by incorporating a digestion process with the bacterial DNA repair enzyme called formamidopyrimidine DNA glycosylase (FPG), B and D. Images kindly prepared by RNDr. Soňa Vodenková, Ph.D. (Department of Molecular Biology of Cancer, Institute of Experimental Medicine, Czech Academy of Sciences).

4.4. Long-term Storage of OMECs in Liquid Nitrogen (H3)

After preparing the primary cell suspension of cells from donors S23 and S26, cells were divided into different storage solutions for long-term storage in liquid nitrogen. For the detailed methods, refer to chapter **3.3 Long-term Storage of OMECs in Liquid Nitrogen (H3), page 61**). From S26, 5.0×10^6 cells/ml were stored in the following media: COM, COM + 5% glycerol, COM + 10% glycerol, COM + 10% DMSO; and from S23, COM, COM + 5% glycerol, COM + 10% glycerol, COM + 10% DMSO, XF, XF + 5% glycerol, XF + 10% glycerol, and XF + 10% DMSO.

Samples were stored in liquid nitrogen for an average of 21 days. Thawing of all groups from the same specimen occurred on the same day, followed by seeding of the cells on fibrin. Then, either COM or XF was added according to the storage media with which the cells were stored. Approximately 4.0×10^4 cells were seeded per well, and the culture proceeded with daily media changes, as described previously (see **3.2.7 Cell Seeding and Culture, page 55**).

Primary cells stored without CPAs (COM or XF) were not able to proliferate after thawing. All the other groups from S26 (COM + 5% glycerol, COM + 10% glycerol, and COM + 10% DMSO) were able to proliferate and reach confluence. Whereas in the second specimen (S23), cells stored in COM + 5% glycerol, COM + 10% DMSO, XF + 5% glycerol, and XF + 10% DMSO proliferated and partially reached confluence, **Figure 49** showing the growth of cells on COM and **Figure 50** the growth of cells on XF. For clarification, all descriptions of CPAs herein refer exclusively to the storage media. After storage and seeding, cells were cultured without CPAs, using only COM or XF.
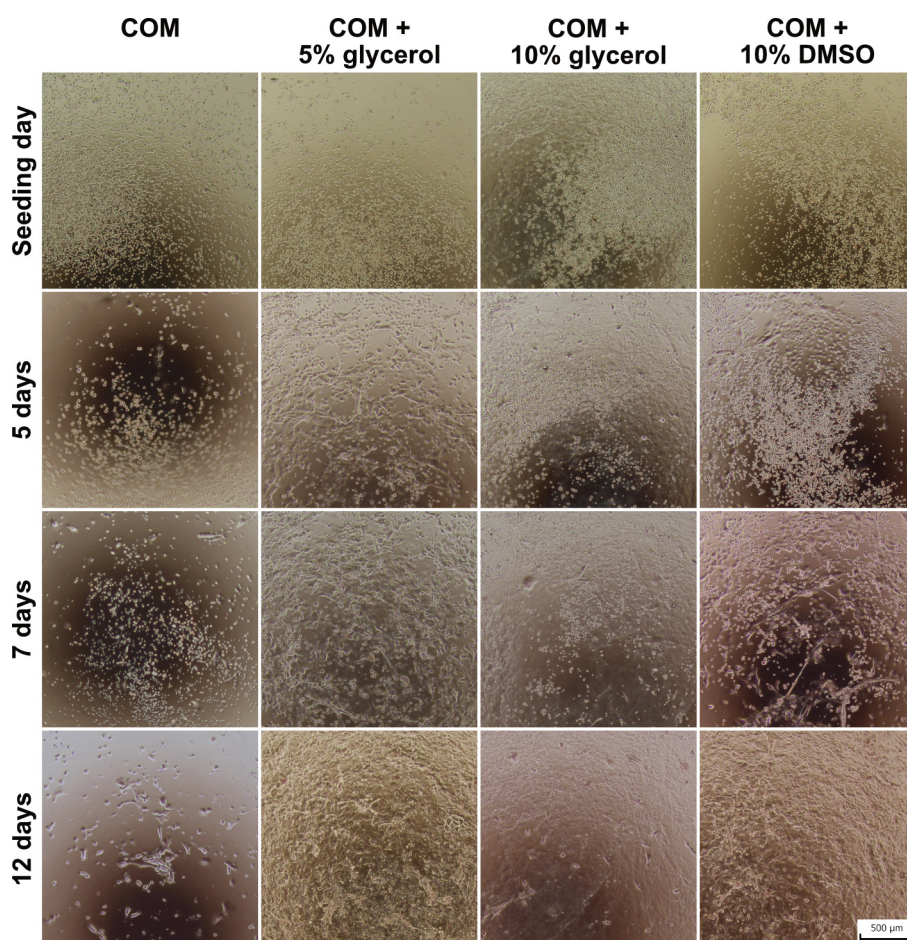
FIGURE 49: Inverted phase-contrast microscopy of cultures of oral mucosa epithelial cells (donor S23) after storage of primary cells in liquid nitrogen. Cultures on fibrin complex media (COM), COM + 5% glycerol, COM + 10% glycerol, and COM + 10% dimethyl sulfoxide (DMSO) on the seeding day, 5 days, 7 days, and 12 days after thawing and seeding the cells for culture. Cells on COM + 5% glycerol and COM + 10% DMSO grew and were able to achieve confluence. Cells on COM and COM + 10% glycerol were unable to grow. The percentage of CPAs refers to the concentration in the freezing media; after thawing, all the cells were cultured in COM. Scale bar: 500 μm. Images from the author's archive.
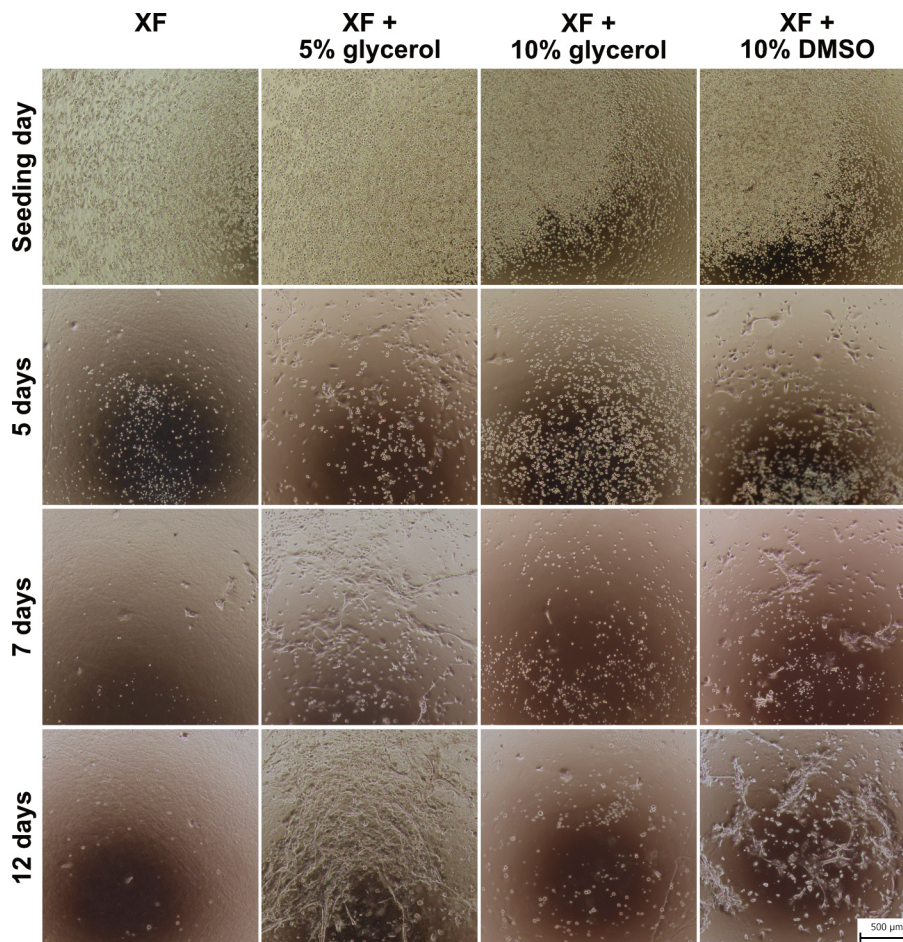
FIGURE 50: Inverted phase-contrast microscopy of cultures of oral mucosa epithelial cells (donor S23) after storage of primary cells in liquid nitrogen. Cultures on fibrin xenobiotic-free (XF), XF + 5% glycerol, XF + 10% glycerol, and XF + 10% DMSO on the seeding day, 5 days, 7 days, and 12 days after thawing and seeding the cells for culture. Cells on XF + 5% glycerol and XF + 10% DMSO grew and were able to achieve confluence; however, the growth rate was faster in XF + 5% glycerol. Cells on XF and XF + 10% glycerol were unable to grow. The percentage of CPAs refers to the concentration in the freezing media; after thawing, all the cells were cultured in XF. XF: xenobiotic-free media; DMSO: dimethyl sulfoxide. Scale bar: 500 μm. Images from the author's archive.

The cells achieved confluence on an average of 21.71 days (the average number of days required to achieve confluence per passage, regardless of the group); COM + 5% glycerol, COM + 10% DMSO, XF + 5% glycerol, and XF + 10% DMSO had a similar culture length of 20 – 21.5 days to confluence. In contrast, COM + 10% glycerol required more days to achieve confluence (27 days), and there was no growth in XF + 10% glycerol, **Figure 51**. The overall viability of cells confluent after the storage of primary cells ranged from 64.1% to 86.7%, **Figure 51**. Interestingly, both groups in XF (5% glycerol and 10% DMSO) had higher viability than COM groups (10% glycerol, 10% DMSO) and were similar

to COM + 5% glycerol.
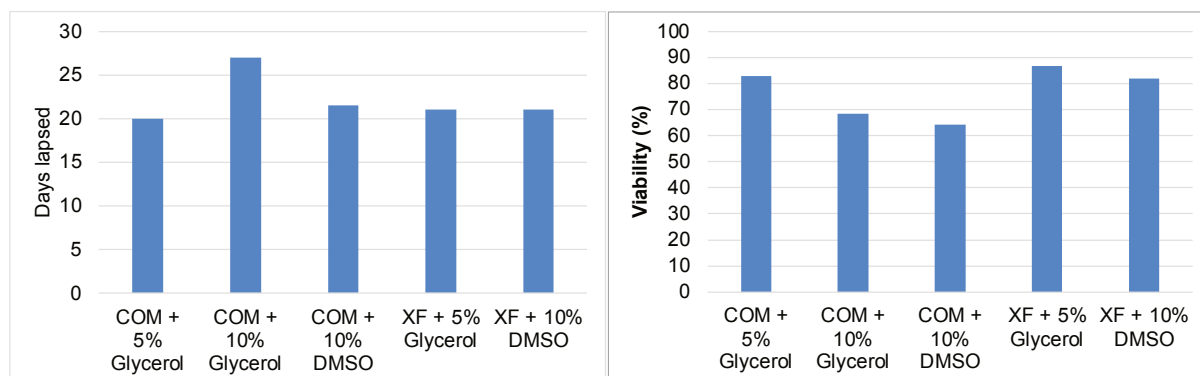
FIGURE 51: The number of days lapsed to reach confluence after storage of primary cells in liquid nitrogen and cell viability at confluence after culturing the cells following the storage (graph on the right). COM: complex media; XF: xenobiotic-free media; DMSO: dimethyl sulfoxide.

The cell size of live cells upon the confluence also varied according to the groups. Cells from COM groups (5% glycerol, 10% glycerol, and 10% DMSO) had smaller live cells (highest percentage for 5 µm cells) than cells from XF groups, 5% glycerol and 10% DMSO, in which the highest number of cells were larger, **Figure 52**.
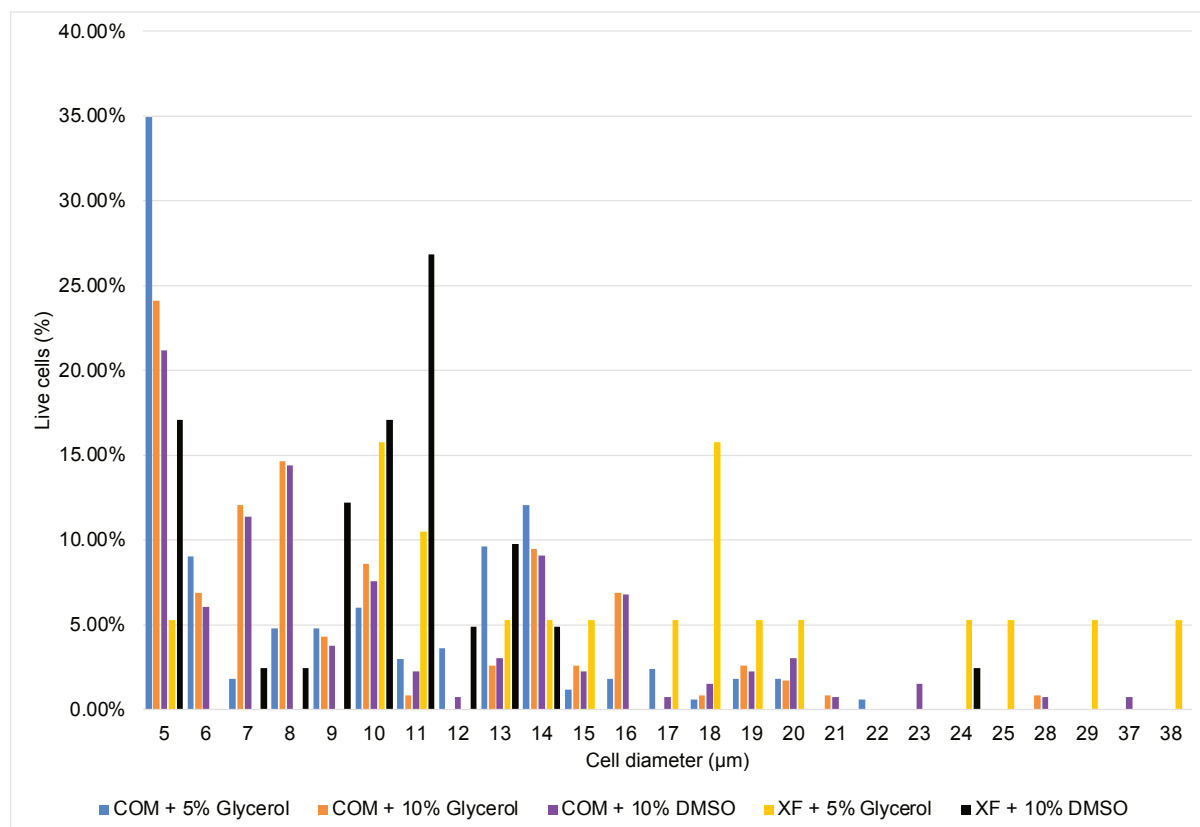
FIGURE 52: Histogram of the live cells percentage at the confluence of cultures after storage of primary cells in liquid nitrogen. The media in the horizontal axis represents the storage media, and the following culture was cultured in either complex media (COM) or xenobiotic-free condition (XF). The cell size and amount of cells were measured by an automated cell counter. DMSO: dimethyl sulfoxide.

We also considered the storage of cells after they first reached confluence (for more details, refer to **Figure 11, page 61**); then, they were passaged (herein referred to as first passage cells) and resuspended in the storage media. Upon the first two specimens (S14, S24), first passage cells were stored in COM, COM + 10% glycerol, COM + 50% glycerol, COM + 10% DMSO, XF, XF + 10% glycerol, XF + 50% glycerol, and XF + 10% DMSO. From these, cells on COM, COM + 10% glycerol, or COM + 10% DMSO were able to grow after thawing and achieved confluence. However, cells stored in COM + 50% glycerol or any XF variants did not succeed in the culture (no attachment). Because of these partial results, the protocol was adapted, and instead of 50% glycerol, we replaced it with 5% glycerol, and the experiments for the first passage continued only with COM storage media and its variants with CPAs for S25 and 26. For the note, these experiments on first passage cells happened before the experiments on the primary cells (mentioned earlier). Thus, the storage media variant with 50% glycerol was not used for the primary cells.

First passage cells of S14, S24, 25, and S26 stored in COM, COM + 5% glycerol, COM + 10% glycerol, or COM + 10% DMSO were able to achieve confluence, **Figure 53**, with an average of 11 days in the CPAs group and 14.6 days in the COM group, **Figure 54**. The overall viability of cells confluent after the storage of first passage cells was higher on average than cells from the primary cells, and interestingly, the highest was in the group without CPA, COM, 87.37%, and the lowest in COM + 5% glycerol, 71.31%, **Figure 54**.
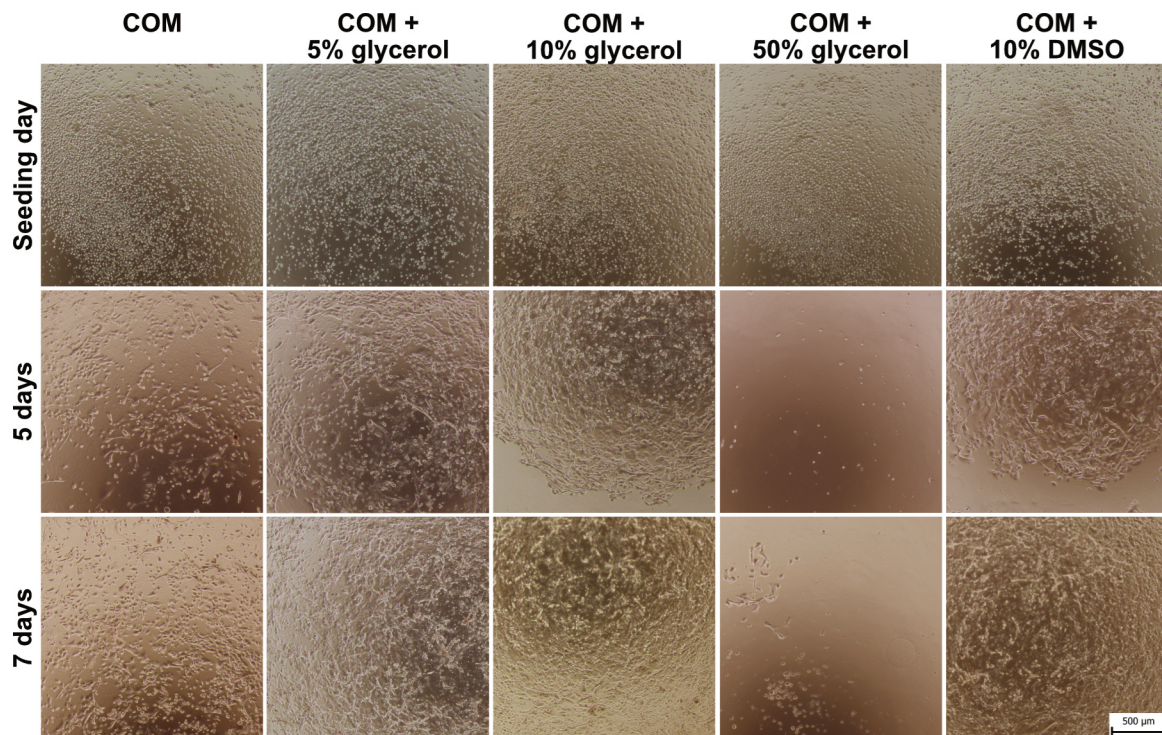
FIGURE 53: Inverted phase-contrast microscopy of cultures of oral mucosa epithelial cells after storage of cells after the first passage in liquid nitrogen. Cultures on fibrin COM (S24), COM + 5% glycerol (S25), COM + 10% glycerol (S24), COM + 50% glycerol (S24), and COM + 10% DMSO (S24) on the seeding day, 5 days, and 7 days after thawing and seeding the cells. The appearance of OMECs after storage resembles the morphology prior to storage. Cells on COM + 50% glycerol were unable to grow, while in COM the growth rate was slower than in COM + 5% glycerol, COM + 10% glycerol, or COM + 10% DMSO. The percentage of CPAs refers to the concentration in the freezing media; after thawing, all the cells were cultured in COM. COM: complex media; DMSO: dimethyl sulfoxide. Scale bar: 500 μm. Images from the author's archive.
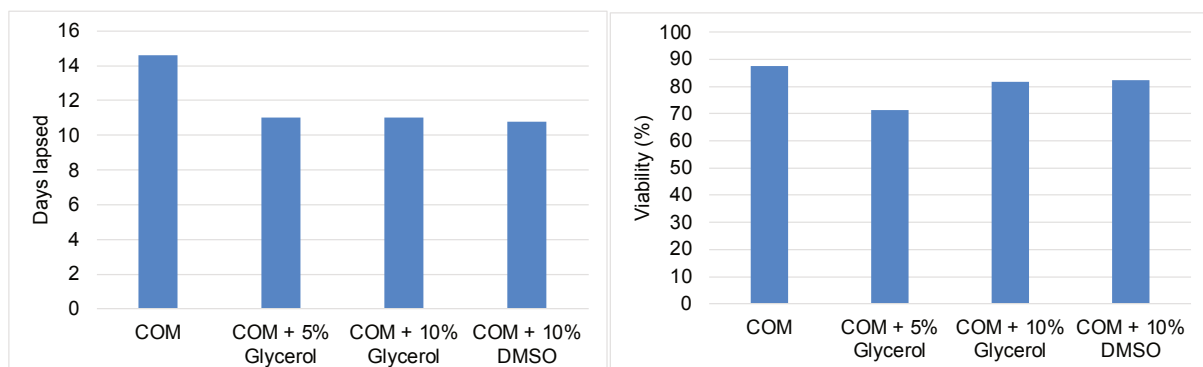
FIGURE 54: The number of days lapsed (graph on the left) to reach confluence after storage of first passage cells in liquid nitrogen and cell viability at confluence after culturing the cells following the storage (graph on the right). First passage cells indicate cells that were initially cultured in complex media (COM). Once reaching confluence, they were harvested and stored using the storage media shown in the graph. After storage, the cells were thawed and

seeded for culture, which continued in COM. DMSO: dimethyl sulfoxide.

The cell size of live cells upon the confluence also varied according to the groups. Cells from COM and COM + 5% glycerol were relatively smaller than cells from COM + 10% glycerol and COM + 10% DMSO, **Figure 55**.
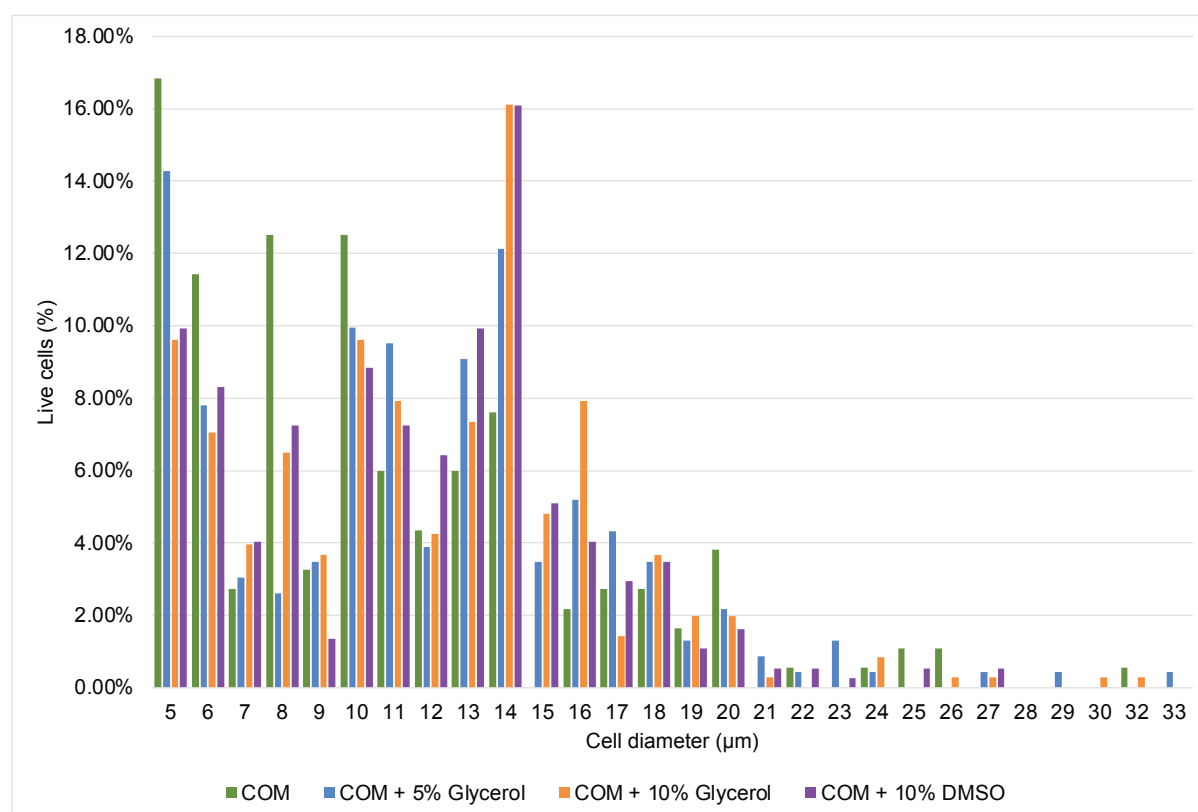
FIGURE 55: Histogram of the live cells percentage at the confluence of cultures after storage of passaged cells in liquid nitrogen. The media in the horizontal axis represents the storage media, and the following culture was cultured in complex media (COM). The cell size and amount of cells were measured by an automated cell counter. DMSO: dimethyl sulfoxide.

4.4.1. Reverse Transcription Quantitative Real-time PCR (RT-qPCR)

Samples from S14, S23, S24, S25, and S26 had their gene expression analyzed for putative stem cell, proliferation, and differentiation genes in each storage media group that cells achieved confluence after storage in liquid nitrogen. To assess the impact of storage media (COM or XF with or without CPAs – 5% glycerol, 10% glycerol, and 10% DMSO) on cell phenotype, we utilized RT-qPCR to evaluate the expression of such genes at the mRNA level. Through bidirectional hierarchical clustering of the log. rel.mRNA values, we observed that the control cells tended to form a distinct group separate from cells derived from culture

in either medium, **Figure 56**. Also, based on their expression, the tested genes were classified into two groups of lower and higher expressed genes: class I, lower expression – *KRT3*, *ABCG2*, *KRT12*, *KRT8*, *MKI67*, and *SOX2*; class II, higher expression – *KRT14*, *KRT7*, *KRT13*, *KLF4*, *ΔNp63α*, and *PCNA*.
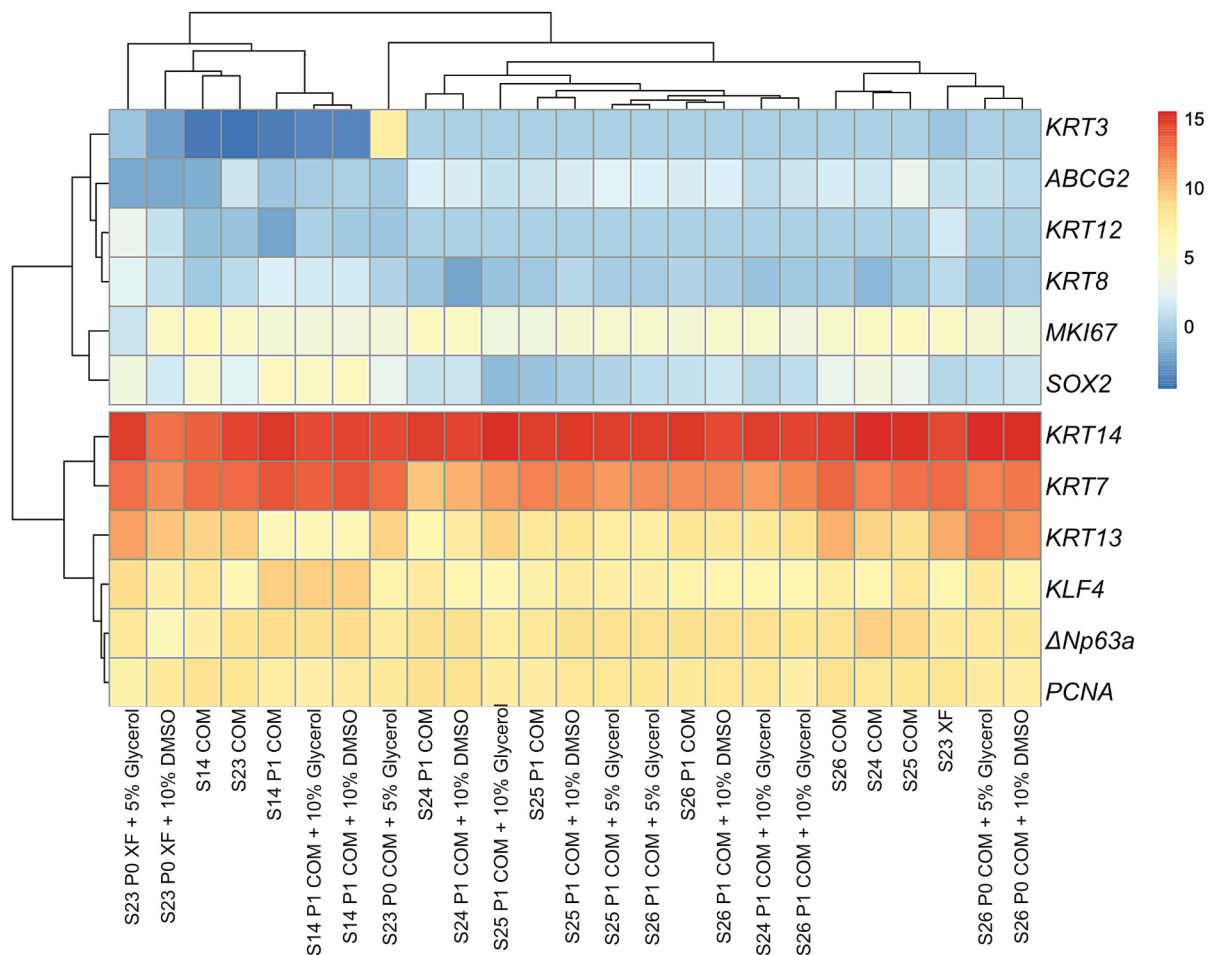
FIGURE 56: Comparisons of oral mucosa epithelial cells (OMEC) cultured in complex media (COM) or xenobiotic-free media (XF) compared to cells prior to storage (in the heatmap these are the ones named only COM or XF) for the gene expression of stem cell, proliferation, and differentiation markers assessed using real-time polymerase chain reaction. A heatmap was generated to provide an overview of the relative mRNA expression (logarithmic values) for the tested genes (rows), with the samples (columns) grouped based on the storage media used for their cultivation. The color scale on the right side of the heatmap represents higher expressions in red and lower expressions in blue. P0 refers to primary cells which were stored, then cultured; P1 designates cells that were first cultured until confluent, passaged, stored, then cultured again.

4.5. Treatment of Non-healing Wounds with Cryopreserved AM (H4, A)

We evaluated the effect of the application of cryopreserved amniotic membrane on the healing of 26 non-healing wounds (18 patients) with varying etiologies and baseline sizes (average of 15.4 cm^2), which had resisted the standard of care treatment for 6 to 456 weeks (average 88.8 weeks). Based on their average general responses to the application of cryopreserved AM, we could differentiate three wound groups. The healed group (the example of a healing wound is shown in **Figure 57A**) was characterized by complete healing (100% wound closure, maximum treatment period 38 weeks) and represented 62% of treated wounds. A wound area reduction of at least 50% was reached for all wounds in this group within the first 10 weeks of treatment, **Figure 58**. 19% of the studied wounds responded partially to the treatment (partially healed group), reaching less than 25% of closure in the first 10 weeks and 90% at maximum for an extended treatment period (up to 78 weeks),**Figure 57B**. The remaining 19% of treated wounds did not show any reaction to the AM application (unhealed defects), **Figure 57C**. The three groups have different profiles of wound area reduction, which can be used as a guideline in predicting the healing prognosis of non-healing wounds treated with a cryo-preserved amniotic membrane.

FIGURE 57: Examples of wound healing. A. Healed wound (defect 15, venous leg ulcer); B. Partially healed wound (defect 19, venous leg ulcer); C. Wound with no response (defect 25, defect after fasciotomy). W0: the wound state after 24, 456, and 100 weeks of outpatient care with SOC treatment for A, B, and C, respectively. W: number of weeks of treatment with AM.
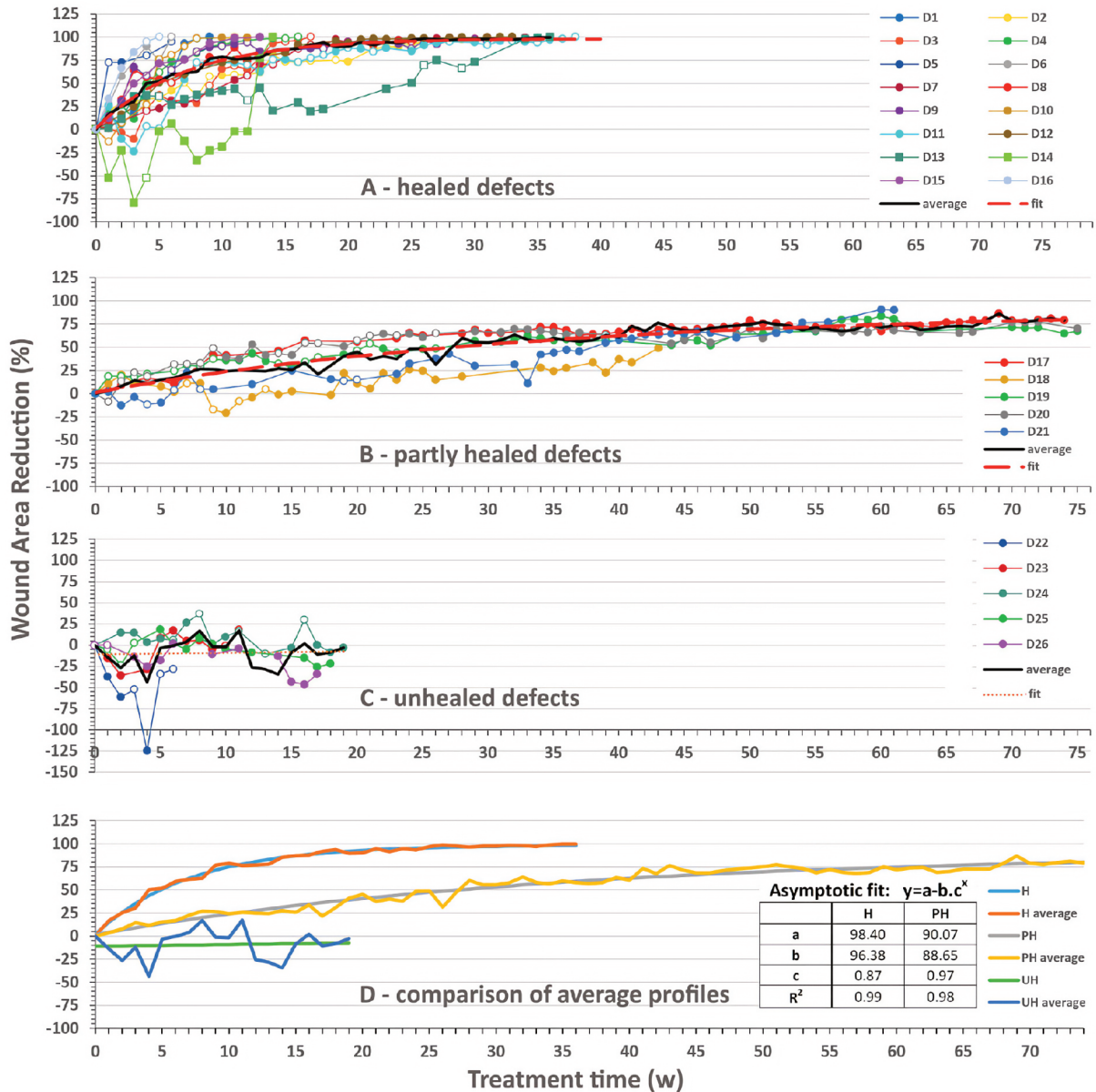
FIGURE 58: Wound closure evolution. Wound area reduction progress for healed A, partly healed B, and unhealed C, defects. D, comparison of the averages of the three groups with fitted asymptotic functions and their parameters for healed (H) and partially healed (PH) and correlation coefficients (R^2). The closed and open markers reflect visits with or without AM application for A, B, and C, respectively.

The pain level of all patients decreased even if they were not fully healed. Before the first AM treatment, the typical pain score was 3.25 out of 10 (on a scale of 0 to 10). The average pain levels were 1.95, 1.22, and 0.47 after the first, fifth, and tenth weeks of AM therapy, respectively (**Figure 59**). According to the study, there was no discernible difference in pain reduction between those who had been healed and those who had not. For more details, see **Appendix 5: The healing dynamics of non-healing wounds using cryo-**

preserved amniotic membrane, page 206.
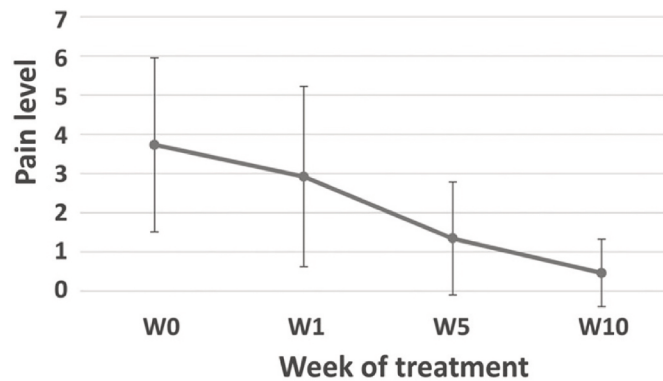
FIGURE 59: Pain level evolution during the AM treatment. Average value ± SD from all patients on a scale from 0 (no pain) to 10 (the worst pain) at week (W) 0, 1, 5, and 10 of treatment.

4.6. Inter-placental Variability in the Healing Efficiency of AM when used for Treating Chronic Non-healing Wounds (H4, B)

During the study, it was observed that the use of cryopreserved AMs resulted in complete wound closure at the end of the treatment period. To evaluate the efficiency of AM, we considered only the proliferative phase of the healing process. The average wound closure rate ranged from 5.7% to 20.99% (medians from 1.07% to 17.75%) for the studied cases 7 days after cryopreserved AM application. **Table 8** provides a summary of the values for individual placentas, and **Figure 60** presents a visual representation of the statistics.

	Average ± SD	Median	Saphiro-Wilk Test
Placenta 1	13.67 ± 12.98	17.75	0.19
Placenta 2	5.70 ± 14.47	1.07	0.18
Placenta 3	10.13 ± 8.66	10.24	0.63
Placenta 4	6.83 ± 32.75	12.29	0.60
Placenta 5	12.13 ± 17.65	9.65	0.77
Placenta 6	7.26 ± 29.11	7.02	0.33
Placenta 7	13.46 ± 14.13	11.87	0.33
Placenta 8	18.06 ± 13.07	12.87	0.01
Placenta 9	20.99 ± 17.19	16.21	0.50

TABLE 8: The average healing efficiency of the placentas is expressed as wound area

reduction in % seven days after AM application.
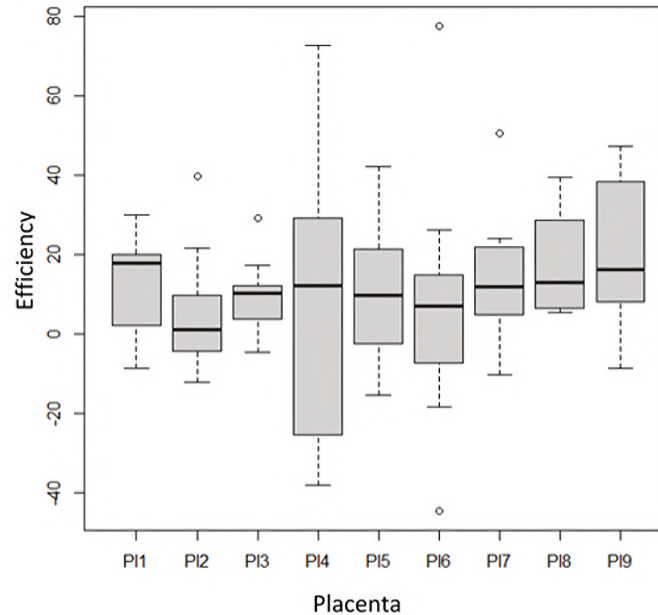
FIGURE 60: Statistical representation of the efficiencies of AMs originating from different placentas.

These findings indicate a significant improvement in the wound closure rate when using cryopreserved AM to treat non-healing wounds. It is worth noting that the wound closure rate varied in individual cases, ranging from 5.7% to 20.99%. However, the median wound closure rate was 17.75%, considerably higher than the average wound closure rate of $12.17 \pm 20.12\%$ (average ± standard deviation) 7 days after AM application. Therefore, the results of this study suggest that using cryopreserved AM for non-healing wounds can be an effective treatment option. For more details, see **Appendix 6: Inter-placental variability is not a major factor affecting the healing efficiency of amniotic membrane when used for treating chronic non-healing wounds, page 217**.

5. Discussion

The discussion will be divided into four parts. The first part focuses on LECs, as we studied the effect of IL13 to promote stemness and the study of an alternative substrate for cell culture (nanofibrous membrane). The second part delves into an in-depth analysis of the alternative use of OMECs for treating LSCD. This novel approach has been gaining attention in recent years due to its promising results, and we have cultured OMECs in fibrin gel and avoided animal products in the culture media. The third part will discuss our results on the long-term storage of OMECs, which brings advancements in cell-based therapies and tissue regeneration since LSCD could recur and require another autologous grafting. Lastly, we will explore the use of amniotic membranes to treat non-healing wounds, investigating AM's properties for wound healing. This area has seen increased interest in recent years due to its potential for improving wound healing outcomes and as a support for the culture of limbal or oral mucosal cells, potentially leading to improved treatment outcomes.

5.1. Limbal Epithelial Cell Culture

This study provides evidence that IL13 can potentially improve the properties of cultured LECs in terms of their stemness and their use for treating LSCD. Gene expression analysis revealed that adding IL13 to LECs culture upregulated the expression of the stem cell genes *KRT14*, *KRT17*, and, most significantly, *ΔNp63α*, often used to denote stemness in LESC cultures. However, according to immunofluorescence, the percentage of p63-positive cells showed a significant difference between cultures with or without IL13 only in passage 2. The discrepancy between qPCR and immunostaining findings has been previously found (López-Paniagua et al., 2013; Brejchova et al., 2018), and it can be explained by post-translational modifications or the increased dynamic range of RT-qPCR compared to immunofluorescence (Sinn et al., 2017). Another potential explanation is that mRNA levels reflect the average gene expression across the entire sample, while in immunofluorescence, it may be biased towards selected representative areas of the slide, despite our efforts to count the whole immunostained slide area (Sinn et al., 2017).

After the first passage, the clonogenic activity of LECs cultures without IL13 was around 5%, decreasing to 1% following the second passage. Adding IL13 to culture media significantly increased the clonogenic capacity (evaluated by CFA assay) of LECs cultures after both passages, correlating with the upregulation of *p63α*'s expression.

Our study indicated that IL13 did not affect the gene expression of corneal epithelial markers K3 and K12, suggesting that IL13 did not influence differentiation into the corneal epithelial phenotype. Instead, we demonstrated that IL13 promoted a more significant differentiation into the conjunctival phenotype, as evidenced by the increased K7 gene expression in all cells (passage 0 – passage 2), whereas K7 is regarded as a conjunctival epithelial marker (Jirsova et al., 2011).

It has been demonstrated previously that IL13 maintains stemness in conjunctival cell cultures from limbal explants by increasing clonal capacity and p63α expression (Stadnikova et al., 2019). A similar observation was made in intestinal stem cells, where IL13 receptor stability was increased by a circular RNA (circPan3) to activate the β-catenin pathway and maintain stemness (Zhu et al., 2019).

Based on our results, the increased gene expression of putative stem cell markers in limbal cultures supplemented with IL13 could be beneficial for preparing cell sheets grafts containing a higher amount of stem cells. As has been demonstrated, the percentage of stem cells in the transplanted epithelial graft plays a pivotal role in predicting transplantation success. Rama et al. (Rama et al., 2010) showed that limbal transplants that contain more than 3% of p63-bright cells had a significantly higher success rate (78%) in regenerating corneal epithelial tissue in eyes suffering from LSCD, as opposed to transplants with 3% or fewer p63-bright cells, which had much lesser success rates (11%). We can conclude that the presence of IL13 has a positive effect because it increases the stemness of the culture; on the other hand, it supports the conjunctival phenotype. For this reason, we are not going to include it in the standardized protocol for LECs preparation which will be transferred to the State Institute for Drug Control.

Moreover, following up with our previous study on the culture of LESCs in fibrin gels (Brejchova et al., 2018), we were also interested in investigating different scaffolds, such as electrospun nanofibers. The utilization of electrospun scaffolds constitutes a widely investigated approach in tissue engineering (Nguyen et al., 2018). These scaffolds effectively imitate 3-D extracellular matrices, exhibiting a remarkable resemblance, offering mechanical support and cell attachment points (Ortega et al., 2013).

Our findings reveal that PDLLA membranes, much like fibrin gel, effectively support the culture of LECs. However, the resulting PDLLA-based cultures exhibit distinct morphological differences compared to those grown on fibrin gel. We observed the presence

of multilayered irregular networks of cells exhibiting a heterogeneous morphological appearance after an extended cultivation period (16 – 21 days). It is plausible that longer culture time may lead to these morphological disparities. Besides that, the presence of spindle-shaped cells can be explained by mesenchymal cells, as supported by the work of Polisetti et al. (Polisetti et al., 2010). In their study, they conducted extended limbal explant cultures on deepithelized AM (dAM) in a feeder cell-free environment, resulting in spindle cells, referred to as mesenchymal cells of the limbus.

In addition to the morphological observations, gene expression analysis reveals phenotypic differences between cells cultured on PDLLA membranes and fibrin gel. Specifically, cells cultured on fibrin gels demonstrated significantly higher expression levels of stem cell genes, including *ΔNp63α*, *OCT4*, and *NGFR*. Herein, we observed upregulation of *OCT4* in both culture conditions, but the increase was notably higher in cells cultured on fibrin. We also found a significantly higher expression of *NGFR*, identified as a stem/ progenitor cell marker of ocular surface epithelium (Di Girolamo et al., 2008)*,* in cells cultured on fibrin than those on the PDLLA membrane. Lastly, the putative stem cell gene *KRT14* was also significantly upregulated in LECs cultured on fibrin gels. In summary, LECs cultured on either fibrin and PDLLA membrane express stem or progenitor cell markers, but a higher expression is found on cells cultured on fibrin. Based on this, fibrin gel seems to maintain stemness in the cultured cells, which is more beneficial for grafting purposes.

In our study, we observed that LECs cultured on fibrin gels showed a significantly higher expression of the differentiation cornea-specific gene *KRT12*. These results align with the observation of cell morphology, where cultures on fibrin clearly exhibited a uniform cobblestone morphology, characteristic of corneal epithelial cells (Sterenczak et al., 2021), whereas PDLLA cultures resembled fibroblast-like cells.

Cells on the PDLLA membrane showed significant upregulation of genes associated with mesenchymal and fibroblast cells, including *ACTA2*, *THY1*, and *FBLN1*. This aligns with the observed heterogeneity in cell morphology and the formation of self-organizing structures on PDLLA, while cells on fibrin displayed a cobblestone epithelial morphology. The higher expression of *ACTA2* on PDLLA, which is linked to endothelial-to-mesenchymal transition (Roy et al., 2015), further supports these differences. THY1, found exclusively in corneal fibroblasts and myofibroblasts, indicates cellular differentiation towards a repair phenotype in PDLLA-cultured cells (Pei, Sherry, & McDermott, 2004). *FBLN1*, an essential

component of the extracellular matrix regulating the limbal stem cell niche (Wang et al., 2020), was also elevated in PDLLA cells. It is important to note that PDLLA membranes were coated with fibronectin to enhance the limbal explant adhesion, and thus, fibronectin, as a marker of mesenchymal differentiation (Petrini et al., 2017), may have influenced the phenotype change in the PDLAA cells.

In summary, the cultures on fibrin gel retained a higher percentage of cells expressing stem cell or progenitor cell markers than the cells growing on the PDLLA membrane. On the other hand, although cells on cells cultured on the PDLLA membrane expressed stem cell markers, their morphology and phenotype did not reach the intensity of the epithelial phenotype as cells cultured in fibrin, while demonstrating upregulation of genes associated with mesenchymal cells, implying a potential transition towards a fibroblast phenotype. For the culture of LECs, fibrin gels proved a better option.

5.2. OMECs for Limbal Stem Cell Deficiency

Despite the challenges posed by current standard treatment options, using autologous OMECs for ocular surface reconstruction is a safe and effective treatment for LSCD. Using the patient's own cells in the treatment eliminates the risk of immunological rejection, a concern often associated with allogeneic transplantation. Autologous OMECs provide a therapeutic option for patients with bilateral LSCD who cannot undergo autologous CLET or SLET when there is no limbus left for collection or when invasive procedures in the normal corneal limbus should be avoided (Ghareeb et al., 2020).

5.2.1. Whole Tissue Characterization

In our study, we started with the characterization of the whole tissue to analyze the expression of stemness, proliferation, and differentiation markers in solid tissue, i.e., before cell suspension for culture was prepared, aiming to choose the best markers for cell characterization.

Our results are aligned with other studies, as all putative stemness markers were present almost exclusively in the basal layer of the epithelium. This is in accordance with previous studies, i.e., Ilmarinen et al. (Ilmarinen et al., 2013) observed that p63α staining was localized into basal and intermediate cell layers, similar to our results. Moreover, in our study, p40, which detects ΔNp63, was also present along the basal layer of the *rete ridges* and

also weekly present in the suprabasal layer in between the epithelial projections. This agrees with the observation from Chen et al. (Chen, Hsue, & Lin, 2004) where p40 was restricted to the basal and suprabasal epithelial cell layers. And we observed in the immunofluorescence of whole tissue that both markers (p63α and p40) were mainly colocalized, meaning cells were positive for both markers simultaneously.

We observed that p75NTR was present uniformly along the basal layer of the *rete ridges*, but Nakamura et al. (Nakamura et al., 2007a) identified this marker mainly in the base of the *rete ridges* and in some areas also in the tips; but similarly like in our study, not in the suprabasal or superficial layers. In fact, Nakamura et al. were the first to suggest that p75 is a potential marker of oral keratinocyte stem/progenitor cells. Similar localization was reported by Chen et al. (Chen et al., 2009), who observed that the expression of p75NTR was exclusively limited to the basal layer. In contrast to these results, Gemenetzidis et al. (Gemenetzidis et al., 2010) described a less intense expression of p75NTR in *rete ridges* tips.

We detected the presence of proliferation marker Ki-67 is expressed unevenly in the parabasal and scarcely in the suprabasal layers of the oral mucosa epithelium, mostly in agreement with the observation obtained by Ilmarinen et al. (Ilmarinen et al., 2013), that reported Ki-67-positive cells mainly were located in the suprabasal layer, and Andl et al. (Andl et al., 2016), who reported that the basal cell layer contains less than 3% Ki-67-positive cells, while approximately 20% of the para- and suprabasal cells are positive for Ki-67. Nakamura et al. (Nakamura et al., 2007a) also reported that Ki-67 was mainly expressed in the suprabasal and occasionally in the basal cell layer of the oral epithelium. On the other hand, Tra et al. (Tra et al., 2012) observed Ki-67 in the basal layer only.

Regarding differentiation markers, we observed that K3, a corneal epithelium marker (Moll et al., 2008), was present in a low percentage of the cells in the suprabasal, and one of the analyzed samples was negative for K3. Attico et al. (Attico et al., 2022) have also demonstrated that K3 is present in the oral mucosa epithelium. We also found that K8 was mainly present in the basal layer, particularly on the tips of the *rete ridges*. This is in agreement with Moll et al. (Moll et al., 2008), who stated that K8, the primary keratin of simple epithelial cells, may also be expressed focally in the basal cell layer of non-keratinizing stratified squamous epithelia and absent in differentiating keratinocytes. Still, it contrasts with the study by Hsueh et al. (Hsueh et al., 2016) in which K8 was not expressed in oral mucosal tissue. Our results are closer to Moll's findings. Due to its location/

morphological pattern, we also suggest that K8 can also be a positive marker in terms of stemness and not yet completely differentiated cells. This conclusion is also supported by a similar study on LECs (Merjava et al., 2011a), in which positive clusters of K8 cells were found in the basal layer of the limbal epithelium, and these K8-positive cells were suggested as stem cells or TACs. A similar localization was also found for K19, as it had a heterogenous distribution in the tissues, but mostly higher intensity in the basal layer and weaker signal towards the superficial layers. A similar result was observed by multiple groups (Tra et al., 2012; Gaddipati et al., 2014; Sheth et al., 2015), as all of them identified K19 on the basal layer only, but different from the study by Kolli et al. (Kolli et al., 2014), in which K19 was not expressed in the oral epithelium.

On the other hand, we localized K13 mainly in the suprabasal and superficial layers, which is in agreement with other studies as well (Tra et al., 2012; Ilmarinen et al., 2013), which considered this keratin as specific for oral mucosa; in fact, Moll et al. (Moll et al., 2008) state that in internal stratified squamous epithelia, which are primarily non-keratinizing, a highly characteristic K13 indicates the mucosal path of keratinocyte differentiation, and Groeger et al. (Groeger & Meyle, 2019) corroborates that K13 and K4 (the pair) are the mainly expressed keratins in epithelia of the buccal mucosa.

Taken together based on our results, we establish to use of p63, p40, p75NTR, Ki-67, K8, and K13 are good markers for the characterization of cultured OMECs in terms of stemness, proliferation, and differentiation, and also K3 due to its importance as a corneal-specific marker, despite its low positivity in the whole tissue.

5.2.2. Culture Substrates

Standardly, OMECs are cultured on AM (Dobrowolski et al., 2015; Prabhasawat et al., 2016; Baradaran-Rafii et al., 2017). AM possesses several properties that render it suitable for tissue engineering, including antifibrotic, anti-inflammatory, antimicrobial, anti-scarring, low immunogenicity, and useful mechanical properties (Niknejad et al., 2008). However, using AM in tissue engineering comes with particular challenges. One of these challenges is the variation in products obtained from AM preparations, both within and between placentas, which could potentially impact the resulting cultured epithelial sheet. Moreover, differences arise in the location of AM samples, some being taken from sites distal to the placental disc and others from proximal positions. Studies have indicated that proximal

human AM samples tend to be thicker and more robust, but they exhibit inferior optical properties compared to distal samples (Massie et al., 2015). To overcome these challenges, we have replaced AM with fibrin gel as a cell substrate and cell carrier. The second reason why we started with fibrin was the fact that we had its use fairly well standardized for the culture of LECs. Additionally, fibrin gel is a possible substrate to use for OMECs culture (Hirayama et al., 2012), as well as a carrier for the transfer of a cell sheet to the ocular surface (Rama et al., 2010). In fact, a higher success rate for COMET was achieved when transplanting the cells cultured on a fibrin gel compared to cells cultured on AM (Hirayama et al., 2012).

Nonetheless, we also attempted OMECs culture on denuded AM to compare with cultures on fibrin gels; however, we encountered challenges with cell attachment on dAM. Firstly, we had to increase the number of cells seeded since the surface area was larger due to the dAM being assembled in a culture insert with a 26 mm diameter. The cells took longer to attach to the dAM and start proliferating compared to the fibrin gel. Additionally, we observed that the cells formed a homogeneous and continuous cell layer in the fibrin, while in the dAM, they were dispersed in islands. Kolli et al. (Kolli et al., 2014) also reported that when trying to replace murine 3T3 feeders with AM, OMEC colonies were rather sparse and poorly defined on intact AM, and these colonies began to break down and float off the surface of the AM by 4 weeks before achieving a confluent sheet. These surface irregularities, caused by the heterogeneity of the AM surface and further deepened by fixing the AM in the culture insert, in which AM is assembled, may result in a central deepening of the AM compared to the peripheral regions due to the weight of the culture medium. This could be problematic for the following reasons: 1) cells that have to overcome unevenness or curvature in the surface during migration may react with irregularities in their morphology, causing them to stretch their shape (and the presence of long fibers) and consequently, 2) a non-uniform distribution of cells on the substrate might prolong the culture time needed to achieve a fully confluent cell layer, potentially leading to cells assuming a more differentiated status. Other studies have shown that longer culture times can result in the loss of stemness and a higher degree of differentiation (Joseph et al., 2004). Nonetheless, a direct comparison of cell features, such as the percentage of cells positive for the stemness marker, is needed to determine which substrate could be more effective regarding grafting efficacy and the number of stem cells transferred to the ocular surface.

In the cell cultures on fibrin gels, the gels remained transparent, and cells successfully proliferated and achieved confluence. As the cultured method used was cell suspension, we did not observe any issue with the cell attachment at the beginning of the culture. We cultured the cells in a 24-well plate, which has a diameter of 14.0 mm, in comparison to the cornea, which is about 11.7 mm in diameter (Rüfer, Schröder, & Erb, 2005). Thus, the resulting cell sheet would be large enough to cover the entire cornea.

5.2.3. Cell Morphology, Culture Media and Culture Growth

To optimize the clinical use of cultured OMECs for the treatment of LSCD, it is important to develop culture protocols that avoid the use of xenogeneic materials, which are commonly used in cell culture but pose a risk of transmitting infectious agents and can trigger an immune response in the patient. To address this issue, we cultured OMECs in culture media without adding animal products (herein called XF), and we replaced FBS with HS. We then compared the growth of OMECs in such conditions with the growth under standard media with additives (here referred to as COM).

To the best of my knowledge and research, this is the first report on the culture of OMECs in xenobiotic conditions without using a feeder layer (3T3 fibroblasts) and replacing FBS with HS. Other researchers have cultured OMECs in serum-free conditions (Gaddipati et al., 2014), HS as a replacement for FBS (Sotozono et al., 2014), or without a feeder layer (Kolli et al., 2014; Gaddipati et al., 2014), but not all of those conditions altogether.

In our study, OMECs exhibited a characteristic cobblestone-like morphology in both culture media, with small and uniform epithelial cells displaying a high nucleus-to-cytoplasm ratio. Such morphology was also reported by other studies, including the one by Sheth et al. (Sheth et al., 2015), in which OMECs were cultured in fibrin gel, and Kolli et al. (Kolli et al., 2014) also observed tightly packed small cells with high nucleus-to-cytoplasm ratios, consistent with stem cell or early TACs' phenotype. Notably, throughout the entire culture period in our study, the fibrin gel supporting OMECs remained transparent, and it did not interfere with the cells' growth and development. Our cultures also yielded epithelial cells from seeding to confluence, and contamination by fibroblast-like cells was not an issue. This indicates that the isolated cell suspension from the epithelial tissue was well-prepared, with minimal to no contamination by stromal cells.

Additionally, we did not observe epithelial-to-mesenchymal transition (as discussed

in the previous chapter for the culture of LECs in PDLLA membranes). Other studies on the culture of OMECs (Hirayama et al., 2012; Dobrowolski et al., 2015; Toshida et al., 2023) do not report contamination by fibroblast-like cells, so it may not be an issue with this kind of cell culture. However, a study by López et al. (López et al., 2021), reported that the OMECs showed a fibroblast-like shape, and this might have been because of a different source area of the cells, as in their study, oral mucosa was obtained from patients that required a third molar surgery, whereas in ours was from the buccal mucosa.

In our study, there were differences in the growth kinetics of OMECs between the COM and XF groups. In our research, it took about 4.7 days in COM and 5.4 days in XF for the observation of OMEC proliferation, which aligns with a study by Kolli et al. (Kolli et al., 2014), in which cell colonies, cultured on a feeder layer of murine fibroblasts, were first visible around 5.2 ± 1.3 days $(4 - 7)$ and reached confluence at 13.2 ± 0.8 days $(12 - 14)$. Similar to our findings, Sheth et al. (Sheth et al., 2015), who cultured oral mucosa explants, also achieved confluence within two weeks. However, it is important to note that, in our study, the cell viability was not significantly different between the two culture conditions (COM and XF), with $89.8\% \pm 5.1\%$ (mean $\pm$ SD) of cell viability in COM and $86.3\% \pm 7.9\%$ in XF, both higher than in the study by Hyun et al. (Hyun et al., 2017), in which viable cells grown on fibrin-coated wells and media with additives, including FBS, accounted for 70.5%.

Based on our results, the earlier onset of growth and shorter time to reach confluence in the COM group suggest that the COM may provide a more favorable environment for cell proliferation, and compared to the XF condition, the growth is somewhat faster.

5.2.4. Cell Size, Stemness

The cell size of cultured cells has been shown to play a key role in cell-based therapies for LSCD, in which the presence of stem cells in cell sheet grafts is considered. And several studies suggest that determining the level of p63 in epithelial cell sheets is essential for determining the cell sheet's quality (Baba et al., 2020). Kim et al. (Kim et al., 2004) have shown that stem cell-associated markers are preferentially present in the smaller LESCs, while differentiation markers are highly expressed in the larger LECs. Conflicting data have been shown regarding the cell size used to define small or large cultured cells, with small cells considered stem cells. For instance, De Paiva et al. (De Paiva et al., 2006) categorized cells into four ranges of size: $10 - 16$ μm, $17 - 23$ μm, $24 - 30$ μm, and ≥ 31 μm;

and the smallest cell size accounted for 11.0% ± 4.5% (mean ± SD). On the other hand, Di Iorio et al. (Di Iorio et al., 2006) categorized LECs into three ranges: 6 – 10 μm, 10 – 18 μm, and 18 – 36 μm, and the smallest size accounted for 13% of the cells. When we observe the cell size of OMECs (where much less data is available compared to LECs) and their relation to stemness, Priya et al. (Priya et al., 2011) considered small cells ranging from 9 – 11 μm, intermediate 12 – 18 μm, and large 19 – 60 μm, and Izumi et al. (Izumi, Tobita, & Feinberg, 2007) showed that cultured oral epithelial cells had a diameter of 33.9 ± 0.9 μm (mean cell diameters of 18 sorted cultured samples; no data for p63).

The data from other studies led us to consider the 11 μm cell size as a small cell, similar to Priya et al. (Priya et al., 2011), data correlated with the putative stem cell marker (p63α and p40). We obtained about 4.9% of cells ≤ 11 μm in COM and 3.1% in XF; among these, 84.5% were p63α+ in COM, and 73.4% were p63α+ in XF, resulting in 4.5% small cells-p63α+ in COM and 1.9% in XF to the total amount of cells in each condition. Pryia et al. (Priya et al., 2011) cultured OMECs on dAM and found that among cells of 9 – 11 μm, 6.2% expressed high levels of p63 and that about 2.0 ± 1.0% of stem cells were included in the *ex vivo* expanded buccal epithelium. Compared to Priya et al. (Priya et al., 2011), in our study, XF had a similar result, but COM had a higher percentage of stem cells at the end of the culture. Because of the higher number of small cells stained positive for stemness marker p63α in COM (4.3%) compared to XF (1.9%), COM is a better option for OMECs culture, also considering the established 3% of stem cells in the cell sheet for predicting transplantation success (Rama et al., 2010).

CFA was also considered to assess the growth potential for both cultured conditions (COM and XF). However, we faced an issue with such a method. The feeder layer (mitomycin C-inactivated 3T3 mouse fibroblasts) would not survive in culture when HS replaced FBS; thus, the proper analysis of the growth potential of OMECs under both conditions, including xeno-free, would not be properly assessed. Such an issue was also reported by Lužnik et al. (Lužnik et al., 2017), as none of the xeno-free media conditions allowed for the propagation or normal survival of feeder cells, including both human and murine fibroblasts. Nonetheless, CFA has been successfully used by other groups, using inactivated 3T3 fibroblasts as feeder layer and also media containing FBS (Burillon et al., 2012; Kondo et al., 2014). In fact, Kondo et al. concluded that while colony size and CFA are recognized as important criteria for forming cell sheets, the sheet-forming ability of OMECs

is hardly associated with these parameters (Kondo et al., 2014). We have then used the analysis of the cell size in combination with the presence of stemness markers, which will be discussed further, as a surrogate method to identify and characterize stem cells (Di Iorio et al., 2006).

In immunofluorescence, the ΔNp63α protein can only be detected through double staining with p63α and p40 antibodies (Hongisto et al., 2017; Vattulainen et al., 2021). In a previous study, Hongisto et al. demonstrated that 90% of the LESCs expressing either p63α or ΔNp63 are double-positive for the other marker as well (Hongisto et al., 2017), concluding that it is reasonable to assume that positivity for either of these markers indicates the presence of the specific ΔNp63α isoform. In our study, the percentage of co-localization of p63α+p40+ was similar to that reported by Hongisto et al. and consistent across both media conditions; in COM, the co-localization of p63α+p40+ was approximately 87.7%, while in XF, it was 88.0%. Moreover, the lack of significant differences in the gene expression of *ΔNp63α* among the COM and XF groups in our study suggests that the culture conditions did not affect the stemness maintenance of the OMEC. Moreover, our results on gene expression showed that Δ*Np63α* was highly expressed similarly across all conditions, including in the primary cells, and no statistical significance was found; other groups obtained similar results (Krishnan, Iyer, & Krishnakumar, 2010; Gopakumar et al., 2019).

The p75NTR protein, a marker for stem/progenitor cells of oral epithelium (Nakamura et al., 2007a; Ma et al., 2009; Nakamura et al., 2016), was detected in our study in about 62.3% of cells in COM and 64.7% in XF. Both are higher than the observed by Hsueh et al. (Hsueh et al., 2016), in which OMECs were cultured on dAM in serum-free condition and presented 32.9% of cells positive for p75NTR. The gene expression in our study also corroborates with the high expression of *p75NTR* in cultured cells, although not statistically significant compared to the primary cells, suggesting that p75NTR-positive cells were maintained in cells that proliferated from the primary cell suspension.

Similarly, the expression of *ABCG2*, another presumptive biomarker of LESC (de Paiva et al., 2005), was significantly upregulated in the XF culture group relative to the primary cell suspension. Interestingly, the expression of *ABCG2* was lower in COM cultures than in XF, and we did not find a statistically significant difference in the expression of *ABCG2* between COM and primary suspension, and it is aligned with other studies, which have shown a relatively low expression of *ABCG2* (Kolli et al., 2008; Björkblom et al.,

2016). The significant upregulation of *ABCG2* in XF indicates this media condition allows the maintenance of a side population of stem cells, as other studies have shown the presence of ABCG2 in OMECs confirmed the presence of a stem cell population (Krishnan et al., 2010; Dhamodaran et al., 2016).

We also observed in our study that *OCT4* maintained the expression level across the primary cell suspension and the cultured cells. Dhamodaran et al. (Dhamodaran et al., 2015) obtained similar results showing similar levels of *OCT4* in the control and cultured cells (from an explant tissue on AM). Also, in our study, *LRIG1* was expressed in all cultured conditions at a similar level as in the primary cell suspension. *KLF4* was highly expressed in primary and cultured cells in our study, with a slightly lower expression in cultured cells, although not statistically significant. This could also be related to the fact that the cultured cells maintained their epithelial morphology throughout the culture, as a study by Tiwari et al. (Tiwari et al., 2017) showed that KLF4 suppresses epithelial-mesenchymal transition.

The expression of stem cell marker *SOX2* was significantly downregulated in both culture media groups compared to the primary cell suspension. This result is consistent with previous studies that have shown *SOX2* downregulation in stem cells during differentiation processes (Zhang & Cui, 2014). In our study, cells were usually harvested at 80 – 90% confluence, and no visible stratification in a phase-contrast microscope was observed, and a study by Attico et al. (Attico et al., 2022), in which cells were cultured up to one week after confluence, promoting stratification up to 10 – 12 layers of cells and differentiation of the epithelial cultures, there was a significant downregulation of *SOX2*. This suggests that cell sheets containing OMECs should not be cultured longer than achieving confluence to maintain stemness factors.

On the other hand, we detected low expression levels for some stemness genes: *PAX6*, *NANOG*, and *NESTIN*. Our result on *PAX6* expression is similar to the one obtained by Attico et al. (Attico et al., 2022), in which it was absent in holoclones, meroclones, and paraclones derived from oral mucosa. Our results on the low expression of *NANOG* and *NESTIN* are aligned with Calenic et al. (Calenic et al., 2015), who reported that oral mucosa stem cells are positive for well-established stem cell markers, such as p63, OCT4 (as we demonstrated above), and K19 (also present, detailed in the next chapter), but negative for NANOG and Nestin.

In summary, the comparison between COM and XF-based cultures showed that both

media conditions maintained stemness markers in OMECs. Immunofluorescence analysis confirmed the presence of stem cell markers (p63α, p40, and p75NTR) in cultured cells, while also indicating a higher proliferative status (Ki-67). Gene expression data supported the high expression of stemness genes, with *ABCG2* being significantly higher in the XF condition. Interestingly, COM appeared to be more favorable than XF in achieving a confluent culture with smaller cells, which are considered to be stem cells. Furthermore, OMECs exhibited reduced expression of *KRT13*, a typical oral mucosa epithelium marker, suggesting a lower degree of differentiation in culture, which is beneficial for preparing grafts for ocular regeneration. Due to the combination of small cell size and expression of putative stem cell markers, OMECs cultured in COM have a higher likelihood of a positive outcome, as indicated in the study by Rama et al. (Rama et al., 2010).

5.2.5. Proliferation Markers

In our study, the proliferation marker Ki-67 had higher percentages in the cultured cells (COM 35.9%, XF 24.2%) compared to the primary cell suspension (12.0%). However, the difference was not statistically significant due to the low number of samples. The gene expression saw the same trend as *MKI67*, the gene encoding Ki-67, was upregulated in both COM and XF but with a significant difference (compared to primary cells) only in the COM group. The increased expression of Ki-67 in cultured cells is expected due to their proliferative status.

Regarding other proliferation markers, *PCNA* was expressed in both media groups but was significantly upregulated only in the XF. *PCNA* expression is associated with cells that are actively proliferating and remain in the G1/S phase for a longer time (Bologna-Molina et al., 2013). The expression of *ALDH3A1*, a proliferation-suppressive marker (Pappa et al., 2005), was downregulated in both culture media groups but only significantly in COM. This result shows that there is a high expression of proliferation genes in both cultured conditions. Still, the combination of upregulation of *MKI67* and downregulation of *ALDH3A1* in COM may have a cumulative effect on the proliferative status of the cultured cells. This is supported by the observation that cells grown on COM reached confluence slightly earlier (11.8 days) than those grown on XF (12.7 days). The earlier confluence of cells in the COM group suggests a higher rate of cell proliferation in this medium.

5.2.6. Differentiation Markers

Concerning the presence of K13, the specific oral mucosa epithelial marker, which was uniformly and highly present in the whole suprabasal and superficial layer detected in the immunofluorescence of the whole tissue as described earlier, we found a significant decrease in the number of K13-positive cells in both cultured conditions (COM and XF) compared to the primary cell suspension. The same significant difference was matched by the gene expression (*KRT13* downregulated in cultured cells), which corroborates that the cultured cells have a lesser degree of differentiation. As a marker of differentiation and stratification, it is expected that *KRT13* expression decreased in the resulting cultured sheet of our study. In fact, the study by Attico et al. (Attico et al., 2022) mentioned earlier, which allowed for the stratification of the cultured cells after confluence, noted that the expression of *KRT13* increased with stratification. So, from the perspective of ocular regeneration, it is less desirable to culture OMECs beyond confluence to maintain a less differentiated state.

We observed that *KRT7* was significantly upregulated in cultured cells in both conditions (COM and XF) compared to primary cells. This could be explained by the fact that K7 is a secondary keratin of simple epithelia (Pekny & Lane, 2007), meaning that K7 is produced in addition to or instead of primary keratins (Bragulla & Homberger, 2009). Although the oral mucosa is not a simple epithelium, the resulting cultured sheet is not stratified (based on the previously mentioned result on K13), and thus the higher expression of *KRT7* could be related to this. Nonetheless, K7 has been suggested as a marker of corneal conjunctivalization (Jirsova et al., 2011), as K7 is present in the conjunctival surface epithelium but not in corneal epithelial cells. This also raises the concern that OMECs presenting a higher expression of *KRT7* are shifting toward a conjunctival phenotype; however, the keratin panel we obtained, along with the presence and expression of stemness markers, point to the high content of progenitor cells and lesser differentiated cells. In fact, K13 has also been linked as a marker for conjunctival cells (Poli et al., 2015), and as we mentioned above, *KRT13* was downregulated after culture.

The low expression of *KRT3* and *KRT12* was already expected as these two are cornea-specific markers, and it is also aligned with the low expression we found in the whole tissue (as described earlier) and immunofluorescence of cultured cells (about 15% in both media conditions); moreover, we also noted a statistically significant downregulation of *KRT3* in cultured cells (COM and XF) compared to primary cells. Other studies have

reported the presence of K3 in the oral mucosa and the absence of K12 (Chen et al., 2009; Toshida et al., 2023). A similar result was obtained by Krishnan et al. (Krishnan et al., 2010), who cultured oral mucosa explants directly on the well (plastic), in which OMECs expressed *KRT3*, whereas *KRT12* was not expressed. In the study by Kolli et al. (Kolli et al., 2014), OMECs also expressed *KRT3* but not *KRT12*. On the other hand, in a study by Dhamodaran et al. (Dhamodaran et al., 2015), cultured OMECs on AM did not express *KRT3*, and K3 was also not detected by immunohistochemistry.

On immunofluorescence of primary and cultured cells, we observed *KRT8* expression in a similar manner in all three conditions. However, this observation did not correspond to the detected gene expression of *KRT8*, which showed low expression in all conditions. The gene expression data also differed from the earlier observation of K8 presence in the whole tissue. As explained in the previous chapter on limbal cells, this discrepancy in the presence of the marker by immunofluorescence and the gene expression results could be attributed to different post-transcription modifications or variations in the range of RT-qPCR (Osorio et al., 2011; Vélez-Bermúdez & Schmidt, 2014). Nonetheless, our lack of *KRT8* expression is aligned with another study that also reported that OMECs do not express *KRT8* (Ma et al., 2021).

We also showed the increased expression of keratins which are usually detected in the basal layer and, thus, have a relation to progenitor cells. The high expression of *KRT14*, *KRT15*, *KRT17*, and *KRT19* could be related to the number of stem cells present, and this is more relevant by noting that along these, other putative stem cell markers were also highly expressed (e.g., Δ*Np63α*, *NGFR*, and *ABCG2*). In Zsebik et al. (Zsebik et al., 2017), they showed that OMECs cultured on contact lenses express *KRT14*, and they also evaluated OMECs by immunofluorescence and detected that most K14-containing cells are also positive for p63α. In Dhamodaran et al. (Dhamodaran et al., 2015), cultured OMECs on AM also expressed *KRT15*. Regarding the expression of *KRT17*, which showed a significant upregulation in cultured cells (COM and XF), there is limited data from other studies on its expression in cultured OMECs. However, K17 has been associated with limbal basal cells (Saghizadeh et al., 2011), indicating a relation to LESCs. Therefore, the higher expression of *KRT17* in our cultures is considered favorable for grafting purposes, as it suggests a higher content of stem cells, as indicated by markers also present in LESCs. Similarly, the same study by Saghizadeh et al. (Saghizadeh et al., 2011), also demonstrated the presence of

KRT19 in a similar manner as *KRT17* in the basal limbal cells. *KRT19* also had a higher expression in cultured cells, although not statistically significant, and it has been shown to be expressed in cultured OMECs by other groups (Sheth et al., 2015; Kim et al., 2016).

Besides, it is also worth discussing whether grafting less differentiated cells with a high content of progenitor cells, and reestablishing conditions for maintenance of the limbal niche is a better approach than transplanting already differentiated (corneal phenotype) to the ocular surface. Research has demonstrated that the optimal functioning of LESCs relies on a specific microenvironment called the limbal stem cell niche (Soleimani et al., 2023). This niche is crucial in providing specific physical, autocrine, and paracrine functions (Soleimani et al., 2023). Attico et al. (Attico et al., 2022) have suggested that the transplantation of oral mucosa graft onto the ocular surface of patients could potentially offer paracrine stimulation to some recipients' remaining autologous corneal cells.

Based on this keratin panel, we observed no statistically significant difference between the two cultured conditions (COM and XF). All the significant differences were found when comparing the cultured conditions to the primary cells; therefore, cells in both cultured conditions exhibited similar gene expression. A similar pattern in both cultured conditions was observed for the presence of the markers by immunofluorescence. Considering the ultimate goal of using the cell sheet for ocular surface transplantation, it is beneficial that there is a high expression of stemness markers (including keratins related to stemness, i.g., K8, K14, K15, K17, and K19), even though there is a low expression of corneal markers (*KRT3* and *KRT12*), as, after grafting, OMECs have been shown to acquire some of the corneal phenotype characteristics, expressing *KRT3* and *KRT12* (Chen et al., 2009; Kim et al., 2018). In summary, the phenotype and gene expression of the cultured cells are consistent with their use for transplantation purposes**.**

5.2.7. Genotoxicity

In the context of ocular surface transplantation, the analysis of DNA damage in cultured cells is crucial for ensuring the safety and efficacy of the procedure. The long-term renewal of the epithelium following transplant surgery relies heavily on the presence of a functional pool of stem cells (Lorenzo et al., 2018). However, when utilizing *ex vivo* systems, which create a foreign microenvironment, the cellular function can be temporarily or permanently altered due to oxidative reactions and other stressors. These alterations can

disrupt the integrity of cellular molecules, leading to potential damage (Pathak et al., 2016), and thus we were interested in levels of potential DNA damage in our cultured cells.

In our study, there was no statistically significant difference between SBs + ALS or net FPG-sensitive site damages in cells cultured in COM or XF; however, net FPG-sensitive sites were consistently lower in the XF group, except for one sample. These differences suggest that COM and XF may have slightly different effects on DNA stability in OMECs, and further studies are needed to understand the underlying mechanisms. Our results are in agreement with the results reported by Baričević et al. (Baričević et al., 2012), who showed in an alkaline comet assay that buccal cells from control samples had a range of % tail DNA of 0.36 ± 1.19 (mean $\pm$ SD), and in our study, cultured cells in COM had % tail DNA of 0.27 ± 0.19 (mean $\pm$ SD) for SBs + ALS and in XF 0.29 ± 0.22 (mean $\pm$ SD), meaning that our cultured cells do not contain higher DNA damage compared to non-cultured cells. In their study, however, they did not assess FPG-sensitive site damages. On the other hand, our results for OMECs are relatively contrary to the results of a study by Lorenzo et al. (Lorenzo et al., 2018), where they compared LECs expanded in complex media and media with only HS as an additive and showed that levels of SBs were substantial. In contrast, levels of net FPG-sensitive sites were relatively low in LECs engineered in either media. Nonetheless, in our and their study, both types of damage were still relatively low, and despite the relative lack of complexity of the XF, we did not observe any increase in DNA base oxidation damage (Lorenzo et al., 2018). Previous studies suggest that cells cultured in a medium supplemented with HS may exhibit enhanced genome stability and the ability to maintain an unmethylated state when compared to a medium supplemented with FBS (Shahdadfar et al., 2005; Dahl et al., 2008).

The results confirm that OMECs can be effectively cultivated in both COM and XF media without inducing significant DNA damage. This is an important finding since XF media are often preferred in clinical settings due to their reduced risk of contamination and transmission of animal-derived pathogens.

5.3. Long-term Storage of OMECs

In the context of cell-based therapy, as we have so far discussed, LSCD patients often require regrafting, considering the average 70% success rate with COMET (Cabral et al., 2020). Thus, cryopreservation allows for the long-term preservation of stem cells, ensuring

their availability for future treatments (Jaiswal & Vagga, 2022). This approach enables multiple treatments from a single donation, reducing the need for repeated donations, which can be burdensome for donors. Furthermore, cryopreservation extends the shelf life of stem cells, maintaining their potency for years (Erol et al., 2021). Considering our goal of using stored cells for grafting, we were interested in analyzing how cells stored in media without CPAs would behave after thawing. If this approach proves successful, it could provide an important alternative to the use of CPAs, which are known to be toxic (Best, 2015).

Our results indicate that cells first cultured and then stored after reaching confluence achieved better growth rates and viability compared to cells stored directly from the primary cell suspension. Primary cells took more days to reach confluence after thawing and seeding (average 21.7 days, ranging from 20 – 27 days). Only cells stored in media (COM or XF) with 5% glycerol or 10% DMSO were able to proliferate, with viability ranging from 64% (COM + 10% DMSO) to the highest 87% (XF + 5% glycerol) once the cells were confluent (after storage). However, it should be noted that limited data is available in our work, as only two samples were prepared for COM storage media with CPAs variants, and only one sample of XF variants was included.

In contrast to primary cells, first passage cells that were stored after reaching confluence required an average of 11 days for groups with CPAs and 14.6 days for cells stored in COM-only, with viability of 71% (COM + 5% glycerol) to 87% (COM). Interestingly, the highest viability was observed in cells stored in COM without CPA. However, cultures in COM also required more days to reach confluence (14 days) compared to 11 days for the other groups, and then the longer time to reach confluence might lead cells to a differentiated phenotype, diminishing the number of stem cells, which is undesirable.

Furthermore, regarding cell size upon confluence after thawing and culture, primary cells stored in COM (5% glycerol, 10% glycerol, and 10% DMSO) were generally smaller on average than cells from XF groups (5% glycerol and 10% DMSO). When considering first passage cells, cells stored in COM or COM + 5% glycerol were relatively smaller than cells from COM + 10% glycerol and COM + 10% DMSO groups. These findings suggest that COM + 5% glycerol yielded a more consistent result across both scenarios (storage of primary or first passage cells). As previously discussed, smaller cells are considered stem cells; thus, COM + 5% glycerol emerges as a preferable storage medium for maintaining stemness in both cell storage stages, while achieving an earlier confluence compared to the

COM-only option.

We have demonstrated that first passage OMECs stored in COM (and CPAs variants) could successfully proliferate and form a cell sheet after being thawed and seeded again. On the other hand, although it requires more samples to draw any conclusion, first passage OMECs stored in XF (and CPAs variants) were unable to attach and proliferate after storage. It needs further investigation of the role of the additives in COM to maintain the proliferative status of the cells after storage. However, it could be related to a specific sample, as primary OMECs stored in XF (+ 5% glycerol or 10% DMSO) also proliferated, and, interestingly, they had higher viability compared to primary OMECs stored in COM with 10% glycerol or 10% DMSO, although the sample size is small to draw any significance.

Successful preparation of a cell sheet after cryopreservation of OMECs was also obtained by Morino et al. (Morino et al., 2019), who cryopreserved first passage OMECs after culture for two weeks and stored 3 x 10^6 cells in 1 ml of CELLBANKER1 (ready-to-use cell cryopreservation medium with serum containing formulation). In their study, after cryopreservation for 3 months at -80 ºC, cells were thawed and seeded on temperature-responsive cell culture inserts, and proliferating cells showed a typical polygonal cobblestone-like appearance, and then cell sheets were successfully fabricated.

Oliva et al. (Oliva et al., 2019) attempted to cryopreserve cell sheets containing rabbit OMECs and reported a loss of *ΔNp63* expression when the storage solution was composed of ethylene glycol and DMSO (cell sheets were immersed for 1 min in a solution containing 10% of both CPAs, then for 25 seconds in a solution containing 20% of both CPAs, then immersed in liquid nitrogen). Although we studied human OMECs, we did not observe the loss of *ΔNp63* in any of the groups that achieved confluence after thawing and culturing, including the groups which were stored in media containing 10% DMSO.

Regarding other genes expression, we observed a consistent pattern of expression for stemness, proliferation, and differentiation, as detailed earlier (**5.2.4 Cell Size, Stemness**, **5.2.5 Proliferation Markers**, and **5.2.6 Differentiation Markers**), with one exception, *SOX2*. The heatmap displays a relatively uniform color distribution (gene expression) across the different samples, except for *SOX2*, where a visible difference in expression is observed between the cells before storage and after storage, with lower expression in the latter. Although the small sample size does not allow for statistical significance, we observe a trend that suggests cryopreservation may influence the expression of *SOX2*. Finally, some studies

have shown that CPAs can influence gene expression (Sumida et al., 2011; Cordeiro et al., 2015); particularly, it was shown that DMSO could affect the expression of pluripotency genes in human embryonic stem cells, leading to a decrease in stem cell markers (Czysz, Minger, & Thomas, 2015). To our knowledge, storage of OMECs in such different kinds of storage media, including those without CPAs and xenobiotic-free media, has not been performed previously. This lack of prior research makes direct comparisons impossible.

These findings suggest that storing cells after the first passage improves their viability and growth potential, and it can also be carried out without the use of CPAs. However, the study did not explore the long-term effects of cryopreservation on cell functionality and genetic stability, which is a limitation of the presented results. Based on the previous discussion on OMECs culture, a recommended approach would be to first culture OMECs in COM, considering the cell sheet grafting. Simultaneously, if needed, a secondary parallel culture would be harvested (first passage cells) and stored for further use. According to the data on long-term storage, either COM or COM + 5% glycerol would preserve stemness, the difference being in terms of culture length (shorter for 5% glycerol) and viability (slightly higher in COM).

5.4. Cryopreserved AM for the Treatment of Non-healing Wounds and Inter-placental Variability in the Healing Efficiency of AM

Our study on NHW found a healing rate after the application of cryopreserved AM of 62%, consistent with similar studies. Lavery et al. also found a success rate of 62% (100% reepithelialization at 12 weeks) for cryopreserved AM in a clinical trial, compared to 21.3% for SOC (Lavery et al., 2014), Farivar et al. (Farivar et al., 2019) found that NHW using cryopreserved AM had a healing rate of 53% in a trial limited to 12 weeks and venous leg ulcers. Another multicenter trial reported a success rate of 48.4% for viable cryopreserved placental membranes (Ananian et al., 2018).

Studies show that healing efficiency depends on the baseline wound size (Abdo, 2016; Raspovic et al., 2018; Ananian et al., 2018). In our study, we could not prove statistical significance despite the larger baseline size in the unhealed group versus the healed group. Moreover, our average wound size before starting AM therapy (15.4 cm^2) was larger than in other studies using cryopreserved AM (Lavery et al., 2014; Valiente et al., 2018; Ananian et

al., 2018; Johnson et al., 2021). AM treatment frequency in similar studies varies from 2 to 3 days up to more scarce (Mermet et al., 2007; Dehghani et al., 2017). We started with weekly applications and later changed to every two weeks after 4 to 8 weeks of treatment. We then adjusted the frequency based on the wound's response and healing progress.

When treating wounds with AM, it's important to have a way to predict whether the treatment will be effective. We found that wounds can be divided into three categories: healed, partially healed, and unhealed, which respond differently to the treatment. The wounds in the healed group showed good progress, reaching 70% closure after 10 weeks and 50% after 5 weeks, which is similar to another study (Valiente et al., 2018). All wounds in this group eventually reached 50% closure. These values can be used as predictors of successful treatment.

AM not only promotes healing, but it also has an analgesic effect. All patients reported pain relief after the first application of AM, regardless of their wound's healing progress. Recently we have detected and analyzed the levels of endogenous analgesic and anti-inflammatory of lipid molecules N-acylethanolamides, particularly palmitoylethanolamide, oleoylethanolamide, and anandamide in various placental tissues, including AM We suggested that these compounds are responsible for pain relief expressed by AM (Svobodova et al., 2023; Vrkoslav et al., 2023). Regarding inter-placental variability in the healing efficiency of AM, we did not observe a significant difference in healing capacity between the individual placentas. The data suggest that if there are intra- and inter-placental differences in AM sheets' healing efficacy, they are overridden by the actual health status of the subject or even the status of its individual wounds (Horvath et al., 2023).

6. Conclusion and Future Perspectives

6.1. Conclusion 1: Increasing the Stemness of Limbal Epithelial Cell Cultures and Alternative Substrates for Cell Culture

IL13 was established as a culture supplement that improves the stemness of LECs by increasing their clonogenicity and expression of stem cell markers while maintaining their morphology (Trosan et al., 2022). Although, a drawback is that this compound is not xenobiotic-free, which should be avoided in advanced cell-based therapy. While IL13 enhances stemness, it also increases the expression of conjunctival markers in LECs. This outcome is undesired, particularly considering that one of the major issues in LSCD is the proliferation of conjunctival cells onto the cornea. Therefore, supplementing the culture media with IL13 could potentially lead to this undesirable outcome.

Additionally, we have also shown that LECs cultured on PDLLA tended to noticeable transdifferentiation toward mesenchymal morphology and also in terms of gene expression. Future research should focus on replacing or removing fibronectin as a coating for the PDLLA membranes, as it can boost its pro-mesenchymal features. Taken together, we can conclude that the culture on the PDLLA membrane was clearly suboptimal. Given the pathophysiology of LSCD, epithelial cells (including stem cells and later differentiated corneal epithelial cells) are deficient, not stromal. In contrast, fibrin gels sustained the standard cobblestone corneal morphology with a high expression of stemness markers. In terms of LECs grafting, fibrin gels posed as a better substrate alternative, and we are going to transfer this method to clinical practice.

6.2. Conclusion 2: Preparation of Oral Mucosal Epithelial Cells on Fibrin Gel for Grafting

This study aimed to optimize the culture technique for OMECs by comparing the use of COM and XF on fibrin gel. Our findings provide significant advancements in ocular surface reconstruction and cell-based therapies. We demonstrated that OMECs can be cultured on fibrin gel without the need for xenogeneic additives or feeder layers while maintaining an undifferentiated state and a sufficient pool of stem cells. This achievement is crucial for developing safer and more effective culture protocols for the clinical use of

OMECs in treating bilateral LSCD. By eliminating animal components and utilizing human-derived materials, the risk of infectious illnesses and immunological responses can be minimized. The drawback is that we observed a higher proliferation state in terms of time to reach confluence and the expression of proliferation genes in the media containing animal products (COM). Thus, although our initial intention was to demonstrate that XF would be at least equivalent to COM, COM seems to support a better cell sheet containing OMECs. Efforts should be made to prepare a COM-equivalent by substituting each additive with its non-xenogeneic equivalent.

We confirmed the presence of crucial stemness markers, such as p63α, NGFR, and ABCG2, in OMECs cultured in both COM and XF conditions. These markers play a vital role in the maintenance and function of the niche after grafting. Nonetheless, we observed a higher percentage of the combination of small cell size and the presence of p63α in OMECs cultured in COM, which makes COM a better option in terms of the number of stem cells in the cell sheet. We also analyzed the expression of differentiation markers, including K3, K7, K8, K13, K14, K15, K17, and K19, which provides insights into the potential differentiation capacity of OMECs towards corneal or conjunctival phenotypes, as well as the maintenance of oral phenotype. Understanding the expression patterns of these markers is crucial for the successful transplantation of cultured OMECs and corneal tissue regeneration (Cabral et al., 2020).

Additionally, our results indicated low levels of DNA damage in OMECs cultured in xenobiotic-free conditions, further supporting the safety and viability of this culture technique.

These insights contribute to developing improved protocols for the clinical application of OMECs and understanding their regenerative potential. This study paves the way for further advancements in cell-based therapies for ocular diseases by advancing the knowledge and techniques in ocular surface reconstruction. Based on the obtained results, several future perspectives and directions for further research can be suggested:

• Optimization of culture protocols: Although this study successfully cultivated OMECs in both COM and XF media, further optimization of culture protocols is necessary. Even though this work did not initially focus on the comparison involving cholera toxin, it serves as a surrogate possibility and can be considered as an interim solution. Animal components (e.g., cholera toxin) can be removed from the media and compared to the original complex

media containing such additives.

• Comparative studies with other cell sources: It would be valuable to compare the characteristics and functionality of OMECs with other cell sources used to treat LSCD, such as LESCs and hair follicle bulge stem cells.

In summary, the results of this study provide a solid foundation for future research on OMECs for treating LSCD. As the field of OMEC-based therapies progresses, our efforts will be directed toward translating these research findings into clinical applications. We are already preparing the documentation for the State Institute for Drug Control in the Czech Republic to obtain approval for the commencement of clinical studies using the OMECs prepared as described in this work and later introducing this OMEC-based therapy in the Czech Republic.

6.3. Conclusion 3: Long-term Storage of Oral Mucosal Epithelial Cells in Liquid Nitrogen

In conclusion, this study demonstrates the importance of CPAs in the cryogenic preservation of OMECs. The choice of storage media and the presence of CPAs significantly affect the viability, proliferation capacity, and cell size of OMECs after cryopreservation. Cells stored directly from the primary cell suspension require an appropriate CPA, such as 5% glycerol or 10% DMSO, to ensure successful attachment, proliferation, and confluence after thawing. However, cells stored after the first passage can achieve confluence without using CPAs, but when stored in COM, not XF.

The findings suggest that storing cells after the first passage improves their viability and proliferation potential, which is an important consideration for optimizing cryopreservation protocols. However, further investigation is required to evaluate the long-term effects of cryopreservation on cell functionality and genetic stability. Nevertheless, the results provide valuable insights into the selection of CPAs and storage media for the successful cryogenic preservation of OMECs, thereby contributing to the development of improved techniques for their storage and future applications in clinical practice, including regenerative medicine and tissue engineering applications.

Suggestions for future studies:

• To investigate the long-term effects of cryopreservation on the functionality and genetic stability of OMECs.

• To explore different thawing protocols to optimize cell viability and functionality after cryopreservation.

In conclusion, it can be summarized that after repeating the experiments and confirming the results, the protocol will be optimized, according to which it will be possible to store OMEC for the treatment of LSCD in the long term.

6.4. Conclusion 4: (A) Cryopreserved Amniotic Membrane for the Treatment of Non-healing Wounds and (B) Inter-placental Variability in the Healing Efficiency of Amniotic Membrane

My work on this project resulted in preparing hundreds of AM grafts for wound treatment. It was essential to prepare in clean rooms of tissue bank high-quality AM for clinical studies. Additionally, these AM grafts also served as a cell culture substrate.

Our study (Svobodova et al., 2022) found that cryopreserved amniotic membrane as a treatment for NHWs was safe and effective, with 62% of wounds completely healed. The study also identified three distinct groups of NHWs with different healing characteristics, which can be used to predict treatment outcomes. Moreover, no significant difference in healing capacity was observed between the individual placentas (Horvath et al., 2023).

AM is a very effective biomaterial not only for its healing effects but also as a suitable substrate for cell cultivation. The properties of AM need to be further investigated and used in clinical practice.

7. Souhrn a další směrování projektu

7.1. Závěr 1: Zvyšování kmenovosti kultur buněk limbálního epitelu a alternativní substráty pro kultivaci buněk

IL13, jako aditivum v kultivačním médiu zlepšuje kmenovost LECs tím, že zvyšuje expresi markerů kmenových buněk při zachování jejich morfologie (Trosan et al., 2022). Nevýhodou je, že se jedná o xenogenní látku, jejímuž použití bychom se v moderní buněčné terapii chtěli vyhnout. Kromě kmenovosti zvyšuje IL13 také expresi spojivkových markerů v LECs. Tento výsledek je nežádoucí, zvláště vezmeme-li v úvahu, že jedním z hlavních problémů u LSCD je přerůstání spojivkových buněk přes rohovku. Proto by doplnění kultivačního média IL13 mohlo potenciálně vést (kromě podpory kmenovosti) k tomuto nežádoucímu jevu.

Dále jsme ukázali, že LEC kultivované na PDLLA měly tendenci k patrné transdiferenciaci směrem k fenotypu typickému pro mezenchymální buňky (morfologie, zesílení exprese mesenchymálních genů). Budoucí výzkum by se měl zaměřit na nahrazení mezenchymální vlastnosti podporujícího fibronektinu, kterým musely být PDLLA membrány pro zvýšení adhezivity povrchu potaženy.

Závěrem můžeme shrnout, že výsledky kultivace na nanovláknech PDLLA nebyly zcela optimální, a to i v možné souvislosti s léčbou LSCD, kdy je nízký počet kmenových buněk pro epitel rohovky vážným nedostatkem úspěšného převedení tohoto postupu do klinické praxe. Na rozdíl od PDLLA si fibrinové gely udržely standardní morfologii epitelu s vysokou expresí kmenových markerů. Pokud jde o použití buněčného štěpu LEC k aplikaci u LSCD, představují fibrinové gely vhodnější alternativu substrátu, kterou budeme převádět i do klinické praxe.

7.2. Závěr 2: Příprava buněk ústní sliznice kultivovaných na fibrinovém gelu

Cílem této studie bylo optimalizovat techniku kultivace OMEC porovnáním použití COM a XF na fibrinovém gelu. Naše zjištění přinášejí významný pokrok v oblasti rekonstrukce povrchu oka a buněčných terapií. Prokázali jsme, že OMEC lze kultivovat na fibrinovém gelu v nediferencovaném stavu a s dostatečným množstvím kmenových buněk

bez použití xenogenní látek nebo vrstvy podpůrných buněk coby kultivačního povrchu. Tento výsledek má zásadní význam pro přípravu bezpečnějších a účinnějších metod pro klinické využití OMEC při léčbě bilaterální LSCD. Vyloučením xenogenních složek a využitím materiálů lidského původu lze minimalizovat riziko infekčních onemocnění a imunologických reakcí. Výsledky však ukazují vyšší míru proliferace vzhledem k dosažení konfluence a exprese proliferačních genů v buňkách kultivovaných v komplexním médiu (COM) obsahujícím cizorodé produkty. Ačkoli tedy bylo naším původním záměrem prokázat, že XF bude rovnocenným kultivačním postupem, zjistili jsme, že použití komplexního média lépe podporuje žádoucí vlastnosti OMEC. V obou kultivačních podmínkách OMEC byla nízká hladina poškození DNA, což podporuje životaschopnost této kultivační techniky.

Potvrdili jsme přítomnost klíčových markerů kmenovosti, jako jsou p63α, NGFR a ABCG2, u OMEC kultivovaných v podmínkách COM i XF. Nicméně vyšší procento kombinace malé velikosti buněk a přítomnosti p63α typické pro kmenové buňky jsme získali v OMEC kultivovaných v COM. Kromě toho jsme analyzovali expresi diferenciačních markerů epitelu, včetně K3, K7, K8, K13, K14, K15, K17 a K19, které umožňují definovat potenciální schopnosti diferenciace OMEC směrem k rohovkovému nebo spojivkovému fenotypu, stejně jako přetrvání fenotypu původního. Objasnění a pochopení exprese jednotlivých márkrů a jejich kombinace je zásadní pro úspěšnou transplantaci kultivovaných OMEC a regeneraci rohovkové tkáně (Cabral et al., 2020).

Na základě výsledků získaných v této studii lze navrhnout několik směrů dalšího výzkumu:

- Optimalizace kultivačních protokolů: Přestože v této studii byly OMEC úspěšně kultivovány v médiích COM i XF, je nutná další optimalizace kultivačních protokolů. Přesné vyladění složení XF médií, například vynechání cholera toxinu či snížení koncentrace specifických růstových faktorů by mohlo zajistit růst, diferenciaci a regenerační potenciál OMEC při snížení potenciálních nežádoucích účinků.

- Srovnávací studie s jinými buněčnými zdroji: Bylo by vhodné porovnat vlastnosti a funkčnost OMEC s dalšími buněčnými typy, například s buňkami vlasových folikulů. Srovnávací studie by mohly poskytnout poznatky o výhodách a nevýhodách jednotlivých buněčných typů, což by umožnilo zvolit nejvhodnější přístup k léčbě DLKB.

Závěrem můžeme shrnout, že výsledky této studie poskytují dobrý základ pro budoucí

výzkum i praktické využití OMEC pro léčbu LSCD. V současné době připravujeme dokumentaci pro Státní ústav pro kontrolu léčiv pro získání souhlasu se zahájením klinických studií s použitím OMEC připravených tak, jak je popsáno v této práci.

7.3. Závěr 3: Dlouhodobé skladování buněk bukální sliznice v tekutém dusíku

Tato studie prokázala výhody použití CPA při kryogenním uchovávání OMEC. Volba skladovacího média a přítomnost CPA významně ovlivňují životaschopnost, proliferační schopnost a velikost buněk OMEC po kryokonzervaci. Primární buněčné suspenze byly vzhledem k jejich růstu po rozmražení výhodněji uchovány v 5% glycerolu nebo 10% DMSO. Naopak, buňky skladované po první pasáži mohou dosáhnout po rozmražení konfluence bez použití CPA, ale pouze při skladování v komplexním médiu, nikoliv v XF médiu.

Tato zjištění naznačují, že skladování buněk po první pasáži zlepšuje jejich životaschopnost a proliferační potenciál, což je důležitý faktor pro optimalizaci protokolů kryokonzervace. Je zapotřebí provést další experimenty, a vyhodnotit dlouhodobé účinky skladování na funkčnost a genetickou stabilitu buněk. Výsledky nicméně poskytují cenné poznatky o výběru CPA a skladovacích médií pro úspěšnou kryogenní konzervaci OMEC, čímž přispívají k vývoji lepších technik jejich skladování a budoucímu využití v klinické praxi, včetně aplikací v regenerativní medicíně a tkáňovém inženýrství. V dalších plánovaných experimentech bude třeba:

• Vyhodnotit dlouhodobé účinky kryokonzervace na funkčnost a genetickou stabilitu OMEC.

• Porovnat různé protokoly rozmrazování pro optimalizaci životaschopnosti a funkčnosti buněk po kryokonzervaci.

Závěrem lze shrnout, že po zopakování experimentů a potvrzení výsledků bude optimalizován protokol, podle kterého bude možné dlouhodobě skladovat OMEC pro léčbu LSCD.

7.4. Závěr 4: Kryokonzervovaná amniová membrána pro léčbu nehojících se ran a vliv inter-placentární variability na hojení pomocí štěpu amniové membrány

Výsledkem mé práce na tomto projektu byla příprava stovek štěpů AM pro léčbu ran. V čistých prostorách tkáňové banky bylo nezbytné připravit vysoce kvalitní AM pro použití v klinických studiích. Část štěpů AM byla také použita jako substrát pro buněčné kultury (OMEC). Výsledky naší klinické studie prokázaly (Svobodova et al., 2022), že kryokonzervovaná AM je pro léčbu NHW bezpečná a účinná, přičemž zcela vyléčeno bylo 62 % ran různých typů, které nebyly dlouhodobě zhojeny pomocí standardních postupů. Studie rovněž identifikovala tři odlišné skupiny NHW s různými charakteristikami (kinetikami) hojení, které lze využít k předpovědi výsledků léčby. Další studie (Horvath et al., 2023) prokázala, že mezi AM získaných z různých placent nebyl pozorován žádný významný rozdíl ve schopnosti hojení.

AM je velmi efektivním biomateriálem nejen pro své hojivé účinky, ale také vhodným substrátem pro kultivaci buněk. Vlastnosti AM je třeba dále zkoumat a využívat v klinické praxi.

8. List of Publications Related to the Thesis

1. Trosan, P., **Cabral[1], J. V.**, Smeringaiova, I., Studeny, P., & Jirsova, K. (2022). Interleukin-13 increases the stemness of limbal epithelial stem cells cultures. PLoS One, 17(8), e0272081. https://doi.org/10.1371/journal.pone.0272081 **Impact Factor: 3.7** (Appendix 3: Interleukin-13 increases the stemness of limbal epithelial stem cells cultures, page 175);

2. **Cabral, J. V.**, Jackson, C. J., Utheim, T. P., & Jirsova, K. (2020). Ex vivo cultivated oral mucosal epithelial cell transplantation for limbal stem cell deficiency: a review. Stem Cell Res Ther, 11(1), 301. https://doi.org/10.1186/s13287-020-01783-8 **Impact Factor: 7.5** (Appendix 4: Ex vivo cultivated oral mucosal epithelial cell transplantation for limbal stem cell deficiency: a review, page 192);

3. Svobodova, A., Horvath, V., Smeringaiova, I., **Cabral, J. V**., Zemlickova, M., Fiala, R., Burkert, J., Nemetova, D., Stadler, P., Lindner, J., Bednar, J., & Jirsova, K. (2022). The healing dynamics of non-healing wounds using cryo-preserved amniotic membrane. Int Wound J, 19(5), 1243-1252. https://doi.org/10.1111/iwj.13719 **Impact Factor: 3.1** (Appendix 5: The healing dynamics of non-healing wounds using cryo-preserved amniotic membrane, page 206);

4. Horvath, V., Svobodova, A., **Cabral, J. V.**, Fiala, R., Burkert, J., Stadler, P., Lindner, J., Bednar, J., Zemlickova, M., & Jirsova, K. (2023). Inter-placental variability is not a major factor affecting the healing efficiency of amniotic membrane when used for treating chronic non-healing wounds. Cell Tissue Bank. https://doi.org/10.1007/s10561-023-10096-y **Impact Factor: 1.5** (Appendix 6: Inter-placental variability is not a major factor affecting the healing efficiency of amniotic membrane when used for treating chronic non-healing wounds, page 217);

5. Smirnov, E., Trosan, P., **Cabral, J. V.**, Studeny, P., Kereïche, S., Jirsova, K., & Cmarko, D. (2020). Discontinuous transcription of ribosomal DNA in human cells. PLoS One, 15(3), e0223030. https://doi.org/10.1371/journal.pone.0223030 **Impact Factor: 3.7** (Appendix 7: Discontinuous transcription of ribosomal DNA in human cells, page 228).

---

[1] Equivalent to the first author.

In progress or submitted:

• Electrospun poly(L-lactide-*co*-DL-lactide) nanofibrous scaffold for ex vivo limbal epithelial cell cultivation and its comparison with fibrin gel. Trousil, J., **Cabral[1], J.V.**, Voukali, E., Pop-Georgievski, O., Fenclová, T., Vacík, T., Nováčková, J., Studenovská, H., Jirsová, K. (Journal for submission: Nanomedicine: Nanotechnology, Biology and Medicine, **Impact Factor 5.4**).

• Cultivation and characterization of oral mucosal epithelial cells on fibrin gel in a xeno-free medium for the treatment of Limbal Stem Cell Deficiency. **Cabral, J.V.**, Voukali, E., Šafanda, A., Studeny, P., Jirsová, K. (Journal for submission: Experimental Eye Research, **Impact Factor 3.4**).

• DNA damage in oral mucosal epithelial cells cultured in complex and xeno-free media: A comparison. **Cabral, J.V.**, El Yamani, N., Pran, E.R., Vodenková, S., Tomašová, K., Vodička, P., Dusinska, M., Nekutová, M., Jirsová, K. (Journal for submission: Cell Biology and Toxicology, **Impact Factor 6.1**).

---

[1] Equivalent to the first author.

9. References

1.   Abdo, R.J. (2016). Treatment of diabetic foot ulcers with dehydrated amniotic membrane allograft: a prospective case series. *J Wound Care*, *25*(Sup7), S4-S9.
2.   Abdulmajeed, A.A., Dalley, A.J., & Farah, C.S. (2013). Putative cancer stem cell marker expression in oral epithelial dysplasia and squamous cell carcinoma. *J Oral Pathol Med*, *42*(10), 755-760.
3.   Ahmad, S. (2012). Concise review: limbal stem cell deficiency, dysfunction, and distress. *Stem Cells Transl Med*, *1*(2), 110-115.
4.   Ali, S., Farooq, I., & Mohammed, F. (2021). Oral Mucosa., 123-145.
5.   Allen-Hoffmann, B.L., & Rheinwald, J.G. (1984). Polycyclic aromatic hydrocarbon mutagenesis of human epidermal keratinocytes in culture. *Proc Natl Acad Sci U S A*, *81*(24), 7802-7806.
6.   Ananian, C.E., Dhillon, Y.S., Van Gils, C.C., Lindsey, D.C., Otto, R.J., Dove, C.R., Pierce, J.T., & Saunders, M.C. (2018). A multicenter, randomized, single-blind trial comparing the efficacy of viable cryopreserved placental membrane to human fibroblast-derived dermal substitute for the treatment of chronic diabetic foot ulcers. *Wound Repair Regen*, *26*(3), 274-283.
7.   Andl, C.D., Le Bras, G.F., Loomans, H., Kim, A.S., Zhou, L., Zhang, Y., & Andl, T. (2016). Association of TGFβ signaling with the maintenance of a quiescent stem cell niche in human oral mucosa. *Histochem Cell Biol*, *146*(5), 539-555.
8.   Attico, E., Galaverni, G., Bianchi, E., Losi, L., Manfredini, R., Lambiase, A., Rama, P., & Pellegrini, G. (2022). SOX2 Is a Univocal Marker for Human Oral Mucosa Epithelium Useful in Post-COMET Patient Characterization. *Int J Mol Sci*, *23*(10), 5785.
9.   Attico, E., Galaverni, G., & Pellegrini, G. (2021). Clinical Studies of COMET for Total LSCD: a Review of the Methods and Molecular Markers for Follow-Up Characterizations. *Current Ophthalmology Reports*, *9*(1), 25-37.
10. Baba, K., Sasaki, K., Morita, M., Tanaka, T., Teranishi, Y., Ogasawara, T., Oie, Y., Kusumi, I., Inoie, M., Hata, K.I., Quantock, A.J., Kino-Oka, M., & Nishida, K. (2020). Cell jamming, stratification and p63 expression in cultivated human corneal epithelial cell sheets. *Sci Rep*, *10*(1), 9282.
11. Baradaran-Rafii, A., Delfazayebaher, S., Aghdami, N., Taghiabadi, E., Bamdad, S., & Roshandel, D. (2017). Midterm outcomes of penetrating keratoplasty after cultivated oral mucosal epithelial transplantation in chemical burn. *Ocul Surf*, *15*(4), 789-794.
12. Barbaro, V., Testa, A., Di Iorio, E., Mavilio, F., Pellegrini, G., & De Luca, M. (2007). C/EBPdelta regulates cell cycle and self-renewal of human limbal stem cells. *J Cell Biol*, *177*(6), 1037-1049.
13. Baričević, M., Ratkaj, I., Mladinić, M., Zeljezić, D., Kraljević, S.P., Lončar, B., & Stipetić, M.M. (2012). In vivo assessment of DNA damage induced in oral mucosa cells by fixed and removable metal prosthodontic appliances. *Clin Oral Investig*, *16*(1), 325-331.
14. Beebe, D.C., & Masters, B.R. (1996). Cell lineage and the differentiation of corneal epithelial cells. *Invest Ophthalmol Vis Sci*, *37*(9), 1815-1825.
15. Best, B.P. (2015). Cryoprotectant Toxicity: Facts, Issues, and Questions. *Rejuvenation Res*, *18*(5), 422-436.
16. Bizheva, K., Tan, B., MacLellan, B., Hosseinaee, Z., Mason, E., Hileeto, D., & Sorbara,

L. (2017). In-vivo imaging of the palisades of Vogt and the limbal crypts with sub-micrometer axial resolution optical coherence tomography. *Biomed Opt Express*, *8*(9), 4141-4151.

17. Björkblom, B., Eidet, J.R., Utheim, T.P., Ulltveit-Moe, H.F., & Raeder, S. (2016). Xenobiotic- and Serum-Free Culture of Oral Mucosal Epithelial Cells on Contact Lenses. *Curr Eye Res*, *41*(1), 20-27.

18. Bologna-Molina, R., Mosqueda-Taylor, A., Molina-Frechero, N., Mori-Estevez, A.D., & Sánchez-Acuña, G. (2013). Comparison of the value of PCNA and Ki-67 as markers of cell proliferation in ameloblastic tumors. *Med Oral Patol Oral Cir Bucal*, *18*(2), e174-9.

19. Bonnet, C., Roberts, J.S., & Deng, S.X. (2021). Limbal stem cell diseases. *Exp Eye Res*, *205*, 108437.

20. Bragulla, H.H., & Homberger, D.G. (2009). Structure and functions of keratin proteins in simple, stratified, keratinized and cornified epithelia. *J Anat*, *214*(4), 516-559.

21. Brejchova, K., Trosan, P., Studeny, P., Skalicka, P., Utheim, T.P., Bednar, J., & Jirsova, K. (2018). Characterization and comparison of human limbal explant cultures grown under defined and xeno-free conditions. *Exp Eye Res*, *176*, 20-28.

22. Brizuela, M., & Winters, R. (2022). Histology, Oral Mucosa. In *StatPearls*. Treasure Island (FL): StatPearls Publishing.

23. Burillon, C., Huot, L., Justin, V., Nataf, S., Chapuis, F., Decullier, E., & Damour, O. (2012). Cultured autologous oral mucosal epithelial cell sheet (CAOMECS) transplantation for the treatment of corneal limbal epithelial stem cell deficiency. *Invest Ophthalmol Vis Sci*, *53*(3), 1325-1331.

24. Cabral, J.V., Jackson, C.J., Utheim, T.P., & Jirsova, K. (2020). Ex vivo cultivated oral mucosal epithelial cell transplantation for limbal stem cell deficiency: a review. *Stem Cell Res Ther*, *11*(1), 301.

25. Calenic, B., Greabu, M., Caruntu, C., Tanase, C., & Battino, M. (2015). Oral keratinocyte stem/progenitor cells: specific markers, molecular signaling pathways and potential uses. *Periodontol 2000*, *69*(1), 68-82.

26. Calonge, M., Nieto-Miguel, T., de la Mata, A., Galindo, S., Herreras, J.M., & López-Paniagua, M. (2021). Goals and Challenges of Stem Cell-Based Therapy for Corneal Blindness Due to Limbal Deficiency. *Pharmaceutics*, *13*(9), 1483.

27. Calonge, M., Pérez, I., Galindo, S., Nieto-Miguel, T., López-Paniagua, M., Fernández, I., Alberca, M., García-Sancho, J., Sánchez, A., & Herreras, J.M. (2019). A proof-of-concept clinical trial using mesenchymal stem cells for the treatment of corneal epithelial stem cell deficiency. *Transl Res*, *206*, 18-40.

28. Castro-Muñozledo, F., Meza-Aguilar, D.G., Domínguez-Castillo, R., Hernández-Zequinely, V., & Sánchez-Guzmán, E. (2017). Vimentin as a Marker of Early Differentiating, Highly Motile Corneal Epithelial Cells. *J Cell Physiol*, *232*(4), 818-830.

29. Chen, B., Mi, S., Wright, B., & Connon, C.J. (2010). Investigation of K14/K5 as a stem cell marker in the limbal region of the bovine cornea. *PLoS One*, *5*(10), e13192.

30. Chen, H.C., Chen, H.L., Lai, J.Y., Chen, C.C., Tsai, Y.J., Kuo, M.T., Chu, P.H., Sun, C.C., Chen, J.K., & Ma, D.H. (2009). Persistence of transplanted oral mucosal epithelial cells in human cornea. *Invest Ophthalmol Vis Sci*, *50*(10), 4660-4668.

31. Chen, S.Y., Han, B., Zhu, Y.T., Mahabole, M., Huang, J., Beebe, D.C., & Tseng, S.C. (2015). HC-HA/PTX3 Purified From Amniotic Membrane Promotes BMP Signaling in Limbal Niche Cells to Maintain Quiescence of Limbal Epithelial Progenitor/Stem Cells.

Stem Cells, *33*(11), 3341-3355.

32. Chen, Y.K., Hsue, S.S., & Lin, L.M. (2004). Expression of p63 (TA and deltaN isoforms) in human primary well differentiated buccal carcinomas. *Int J Oral Maxillofac Surg*, *33*(5), 493-497.

33. Chen, Z., de Paiva, C.S., Luo, L., Kretzer, F.L., Pflugfelder, S.C., & Li, D.Q. (2004). Characterization of putative stem cell phenotype in human limbal epithelia. *Stem Cells*, *22*(3), 355-366.

34. Chugh, J.P., Jain, P., & Sen, R. (2015). Comparative analysis of fresh and dry preserved amniotic membrane transplantation in partial limbal stem cell deficiency. *Int Ophthalmol*, *35*(3), 347-355.

35. Cieślar-Pobuda, A., Rafat, M., Knoflach, V., Skonieczna, M., Hudecki, A., Małecki, A., Urasińska, E., Ghavami, S., & Łos, M.J. (2016). Human induced pluripotent stem cell differentiation and direct transdifferentiation into corneal epithelial-like cells. *Oncotarget*, *7*(27), 42314-42329.

36. Collins, A.R. (2004). The comet assay for DNA damage and repair: principles, applications, and limitations. *Mol Biotechnol*, *26*(3), 249-261.

37. Collins, L.M., & Dawes, C. (1987). The surface area of the adult human mouth and thickness of the salivary film covering the teeth and oral mucosa. *J Dent Res*, *66*(8), 1300-1302.

38. Cordeiro, R.M., Stirling, S., Fahy, G.M., & de Magalhães, J.P. (2015). Insights on cryoprotectant toxicity from gene expression profiling of endothelial cells exposed to ethylene glycol. *Cryobiology*, *71*(3), 405-412.

39. Cotsarelis, G., Cheng, S.Z., Dong, G., Sun, T.T., & Lavker, R.M. (1989). Existence of slow-cycling limbal epithelial basal cells that can be preferentially stimulated to proliferate: implications on epithelial stem cells. *Cell*, *57*(2), 201-209.

40. Czysz, K., Minger, S., & Thomas, N. (2015). DMSO efficiently down regulates pluripotency genes in human embryonic stem cells during definitive endoderm derivation and increases the proficiency of hepatic differentiation. *PLoS One*, *10*(2), e0117689.

41. Dabelsteen, E. (1991). Cell adhesion molecules in oral mucosa. *Curr Opin Dent*, *1*(6), 802-808.

42. Dahl, J.A., Duggal, S., Coulston, N., Millar, D., Melki, J., Shahdadfar, A., Brinchmann, J.E., & Collas, P. (2008). Genetic and epigenetic instability of human bone marrow mesenchymal stem cells expanded in autologous serum or fetal bovine serum. *Int J Dev Biol*, *52*(8), 1033-1042.

43. Dale, B.A., Salonen, J., & Jones, A.H. (1990). New Approaches And Concepts in The Study of Differentiation of Oral Epithelia. *Critical Reviews in Oral Biology & Medicine*, *1*(3), 167-190.

44. Daya, S.M., Watson, A., Sharpe, J.R., Giledi, O., Rowe, A., Martin, R., & James, S.E. (2005). Outcomes and DNA analysis of ex vivo expanded stem cell allograft for ocular surface reconstruction. *Ophthalmology*, *112*(3), 470-477.

45. de Paiva, C.S., Chen, Z., Corrales, R.M., Pflugfelder, S.C., & Li, D.Q. (2005). ABCG2 transporter identifies a population of clonogenic human limbal epithelial cells. *Stem Cells*, *23*(1), 63-73.

46. De Paiva, C.S., Pflugfelder, S.C., & Li, D.Q. (2006). Cell size correlates with phenotype and proliferative capacity in human corneal epithelial cells. *Stem Cells*, *24*(2), 368-375.

47. de Rotth, A. (1940). Plastic repair of conjunctival defects with fetal membranes.

Archives of Ophthalmology, *23*(3), 522-525.

48. Dehghani, M., Azarpira, N., Mohammad Karimi, V., Mossayebi, H., & Esfandiari, E. (2017). Grafting with Cryopreserved Amniotic Membrane versus Conservative Wound Care in Treatment of Pressure Ulcers: A Randomized Clinical Trial. *Bull Emerg Trauma*, *5*(4), 249-258.

49. Deihim, T., Yazdanpanah, G., & Niknejad, H. (2016). Different Light Transmittance of Placental and Reflected Regions of Human Amniotic Membrane That Could Be Crucial for Corneal Tissue Engineering. *Cornea*, *35*(7), 997-1003.

50. DelMonte, D.W., & Kim, T. (2011). Anatomy and physiology of the cornea. *J Cataract Refract Surg*, *37*(3), 588-598.

51. Deng, S.X., Borderie, V., Chan, C.C., Dana, R., Figueiredo, F.C., Gomes, J.A.P., Pellegrini, G., Shimmura, S., Kruse, F.E., & and, T.I.L.S.C.D.W.G. (2019). Global Consensus on Definition, Classification, Diagnosis, and Staging of Limbal Stem Cell Deficiency. *Cornea*, *38*(3), 364-375.

52. Dhamodaran, K., Subramani, M., Jeyabalan, N., Ponnalagu, M., Chevour, P., Shetty, R., Matalia, H., Shetty, R., Prince, S.E., & Das, D. (2015). Characterization of ex vivo cultured limbal, conjunctival, and oral mucosal cells: A comparative study with implications in transplantation medicine. *Mol Vis*, *21*, 828-845.

53. Dhamodaran, K., Subramani, M., Matalia, H., Jayadev, C., Shetty, R., & Das, D. (2016). One for all: A standardized protocol for ex vivo culture of limbal, conjunctival and oral mucosal epithelial cells into corneal lineage. *Cytotherapy*, *18*(4), 546-561.

54. Di Girolamo, N., Bosch, M., Zamora, K., Coroneo, M.T., Wakefield, D., & Watson, S.L. (2009). A contact lens-based technique for expansion and transplantation of autologous epithelial progenitors for ocular surface reconstruction. *Transplantation*, *87*(10), 1571-1578.

55. Di Girolamo, N., Sarris, M., Chui, J., Cheema, H., Coroneo, M.T., & Wakefield, D. (2008). Localization of the low-affinity nerve growth factor receptor p75 in human limbal epithelial cells. *J Cell Mol Med*, *12*(6B), 2799-2811.

56. Di Iorio, E., Barbaro, V., Ferrari, S., Ortolani, C., De Luca, M., & Pellegrini, G. (2006). Q-FIHC: quantification of fluorescence immunohistochemistry to analyse p63 isoforms and cell cycle phases in human limbal stem cells. *Microsc Res Tech*, *69*(12), 983-991.

57. Di Iorio, E., Ferrari, S., Fasolo, A., Böhm, E., Ponzin, D., & Barbaro, V. (2010). Techniques for culture and assessment of limbal stem cell grafts. *Ocul Surf*, *8*(3), 146-153.

58. Díaz-Prado, S., Rendal-Vázquez, M.E., Muiños-López, E., Hermida-Gómez, T., Rodríguez-Cabarcos, M., Fuentes-Boquete, I., de Toro, F.J., & Blanco, F.J. (2010). Potential use of the human amniotic membrane as a scaffold in human articular cartilage repair. *Cell Tissue Bank*, *11*(2), 183-195.

59. Díaz-Valle, D., Santos-Bueso, E., Benítez-Del-Castillo, J.M., Méndez-Fernández, R., López-Abad, C., Martínez-de-la-Casa, J.M., & García-Sánchez, J. (2007). [Sectorial conjunctival epitheliectomy and amniotic membrane transplantation for partial limbal stem cells deficiency]. *Arch Soc Esp Oftalmol*, *82*(12), 769-772.

60. Dobrowolski, D., Orzechowska-Wylegala, B., Wowra, B., Wroblewska-Czajka, E., Grolik, M., Szczubialka, K., Nowakowska, M., Puzzolo, D., Wylegala, E.A., Micali, A., & Aragona, P. (2015). Cultivated Oral Mucosa Epithelium in Ocular Surface Reconstruction in Aniridia Patients. *Biomed Res Int*, *2015*, 281870.

61. Dua, H.S., Gomes, J.A.P., King, A.J., & Maharajan, V.S. (2004). The amniotic membrane in ophthalmology. *Survey of Ophthalmology*, *49*(1), 51-77.

62. Dua, H.S., Shanmuganathan, V.A., Powell-Richards, A.O., Tighe, P.J., & Joseph, A. (2005). Limbal epithelial crypts: a novel anatomical structure and a putative limbal stem cell niche. *Br J Ophthalmol*, *89*(5), 529-532.

63. Dvorak, H.F., Harvey, V.S., Estrella, P., Brown, L.F., McDonagh, J., & Dvorak, A.M. (1987). Fibrin containing gels induce angiogenesis. Implications for tumor stroma generation and wound healing. *Lab Invest*, *57*(6), 673-686.

64. Dziasko, M.A., Tuft, S.J., & Daniels, J.T. (2015). Limbal melanocytes support limbal epithelial stem cells in 2D and 3D microenvironments. *Exp Eye Res*, *138*, 70-79.

65. Ebrahimi, M., Taghi-Abadi, E., & Baharvand, H. (2009). Limbal stem cells in review. *J Ophthalmic Vis Res*, *4*(1), 40-58.

66. Eghrari, A.O., Riazuddin, S.A., & Gottsch, J.D. (2015). Overview of the Cornea: Structure, Function, and Development. *Prog Mol Biol Transl Sci*, *134*, 7-23.

67. Elder, M.J., Hiscott, P., & Dart, J.K. (1997). Intermediate filament expression by normal and diseased human corneal epithelium. *Hum Pathol*, *28*(12), 1348-1354.

68. Elhusseiny, A.M., Soleimani, M., Eleiwa, T.K., ElSheikh, R.H., Frank, C.R., Naderan, M., Yazdanpanah, G., Rosenblatt, M.I., & Djalilian, A.R. (2022). Current and Emerging Therapies for Limbal Stem Cell Deficiency. *Stem Cells Transl Med*, *11*(3), 259-268.

69. Erickson, G.A., Bolin, S.R., & Landgraf, J.G. (1991). Viral contamination of fetal bovine serum used for tissue culture: risks and concerns. *Dev Biol Stand*, *75*, 173-175.

70. Erol, O.D., Pervin, B., Seker, M.E., & Aerts-Kaya, F. (2021). Effects of storage media, supplements and cryopreservation methods on quality of stem cells. *World J Stem Cells*, *13*(9), 1197-1214.

71. Eslani, M., Baradaran-Rafii, A., & Ahmad, S. (2012). Cultivated limbal and oral mucosal epithelial transplantation. *Semin Ophthalmol*, *27*(3-4), 80-93.

72. Fairbairn, N.G., Randolph, M.A., & Redmond, R.W. (2014). The clinical applications of human amnion in plastic surgery. *J Plast Reconstr Aesthet Surg*, *67*(5), 662-675.

73. Farhadihosseinabadi, B., Farahani, M., Tayebi, T., Jafari, A., Biniazan, F., Modaresifar, K., Moravvej, H., Bahrami, S., Redl, H., Tayebi, L., & Niknejad, H. (2018). Amniotic membrane and its epithelial and mesenchymal stem cells as an appropriate source for skin tissue engineering and regenerative medicine. *Artif Cells Nanomed Biotechnol*, *46*(sup2), 431-440.

74. Farivar, B.S., Toursavadkohi, S., Monahan, T.S., Sharma, J., Ucuzian, A.A., Kundi, R., Sarkar, R., & Lal, B.K. (2019). Prospective study of cryopreserved placental tissue wound matrix in the management of chronic venous leg ulcers. *J Vasc Surg Venous Lymphat Disord*, *7*(2), 228-233.

75. Fasolo, A., Pedrotti, E., Passilongo, M., Marchini, G., Monterosso, C., Zampini, R., Bohm, E., Birattari, F., Franch, A., Barbaro, V., Bertolin, M., Breda, C., Di Iorio, E., Ferrari, B., Ferrari, S., Meneguzzi, M., & Ponzin, D. (2017). Safety outcomes and long-term effectiveness of ex vivo autologous cultured limbal epithelial transplantation for limbal stem cell deficiency. *Br J Ophthalmol*, *101*(5), 640-649.

76. Figueira, E.C., Di Girolamo, N., Coroneo, M.T., & Wakefield, D. (2007). The phenotype of limbal epithelial stem cells. *Invest Ophthalmol Vis Sci*, *48*(1), 144-156.

77. Flaxman, B.A., & Harper, R.A. (1975). In vitro analysis of the control of keratinocyte proliferation in human epidermis by physiologic and pharmacologic agents. *J Invest Dermatol*, *65*(1), 52-59.

78. Fuchs, E. (1995). Keratins and the skin. *Annu Rev Cell Dev Biol*, *11*, 123-153.

79. Funderburgh, J.L., Funderburgh, M.L., & Du, Y. (2016). Stem Cells in the Limbal Stroma. *Ocul Surf*, *14*(2), 113-120.

80. Gaddipati, S., Muralidhar, R., Sangwan, V.S., Mariappan, I., Vemuganti, G.K., & Balasubramanian, D. (2014). Oral epithelial cells transplanted on to corneal surface tend to adapt to the ocular phenotype. *Indian J Ophthalmol*, *62*(5), 644-648.

81. Gemenetzidis, E., Elena-Costea, D., Parkinson, E.K., Waseem, A., Wan, H., & Teh, M.T. (2010). Induction of human epithelial stem/progenitor expansion by FOXM1. *Cancer Res*, *70*(22), 9515-9526.

82. Gerdes, J., Lemke, H., Baisch, H., Wacker, H.H., Schwab, U., & Stein, H. (1984). Cell cycle analysis of a cell proliferation-associated human nuclear antigen defined by the monoclonal antibody Ki-67. *J Immunol*, *133*(4), 1710-1715.

83. Gerdes, J., Li, L., Schlueter, C., Duchrow, M., Wohlenberg, C., Gerlach, C., Stahmer, I., Kloth, S., Brandt, E., & Flad, H.D. (1991). Immunobiochemical and molecular biologic characterization of the cell proliferation-associated nuclear antigen that is defined by monoclonal antibody Ki-67. *Am J Pathol*, *138*(4), 867-873.

84. Gerdes, J., Schwab, U., Lemke, H., & Stein, H. (1983). Production of a mouse monoclonal antibody reactive with a human nuclear antigen associated with cell proliferation. *Int J Cancer*, *31*(1), 13-20.

85. Ghafar, N.A., Jalil, N.A.A., & Kamarudin, T.A. (2021). Wound healing of the corneal epithelium: a review. *Asian Biomedicine*, *15*(5), 199-212.

86. Ghareeb, A.E., Lako, M., & Figueiredo, F.C. (2020). Recent Advances in Stem Cell Therapy for Limbal Stem Cell Deficiency: A Narrative Review. *Ophthalmol Ther*, *9*(4), 809-831.

87. Goldberg, M.F., & Bron, A.J. (1982). Limbal palisades of Vogt. *Trans Am Ophthalmol Soc*, *80*, 155-171.

88. Gonzalez-Andrades, M., Argüeso, P., & Gipson, I. (2019). Corneal Anatomy. In J. L. Alió, J. L. Alió del Barrio, & F. Arnalich-Montiel (Eds.), (pp. 3-12). Springer International Publishing.

89. González, S., Chen, L., & Deng, S.X. (2017). Comparative Study of Xenobiotic-Free Media for the Cultivation of Human Limbal Epithelial Stem/Progenitor Cells. *Tissue Eng Part C Methods*, *23*(4), 219-227.

90. Gopakumar, V., Agarwal, S., Srinivasan, B., Krishnakumar, S., Krishnan, U.M., & Iyer, G. (2019). Clinical Outcome of Autologous Cultivated Oral Mucosal Epithelial Transplantation in Ocular Surface Reconstruction. *Cornea*, *38*(10), 1273-1279.

91. Groeger, S., & Meyle, J. (2019). Oral Mucosal Epithelial Cells. *Front Immunol*, *10*, 208.

92. Grueterich, M., Espana, E.M., & Tseng, S.C. (2003a). Ex vivo expansion of limbal epithelial stem cells: amniotic membrane serving as a stem cell niche. *Surv Ophthalmol*, *48*(6), 631-646.

93. Grueterich, M., Espana, E.M., & Tseng, S.C. (2003b). Modulation of keratin and connexin expression in limbal epithelium expanded on denuded amniotic membrane with and without a 3T3 fibroblast feeder layer. *Invest Ophthalmol Vis Sci*, *44*(10), 4230-4236.

94. Guérin, L.P., Le-Bel, G., Desjardins, P., Couture, C., Gillard, E., Boisselier, É., Bazin, R., Germain, L., & Guérin, S.L. (2021). The Human Tissue-Engineered Cornea (hTEC): Recent Progress. *Int J Mol Sci*, *22*(3), 1291.

95. Guo, Z.H., Zhang, W., Jia, Y.Y.S., Liu, Q.X., Li, Z.F., & Lin, J.S. (2018). An Insight into the Difficulties in the Discovery of Specific Biomarkers of Limbal Stem Cells. *Int J Mol Sci*, *19*(7), 1982.

96. Gur, G., Rubin, C., Katz, M., Amit, I., Citri, A., Nilsson, J., Amariglio, N., Henriksson,

R., Rechavi, G., Hedman, H., Wides, R., & Yarden, Y. (2004). LRIG1 restricts growth factor signaling by enhancing receptor ubiquitylation and degradation. *EMBO J*, *23*(16), 3270-3281.

97. Haagdorens, M., Van Acker, S.I., Van Gerwen, V., Ní Dhubhghaill, S., Koppen, C., Tassignon, M.J., & Zakaria, N. (2016). Limbal Stem Cell Deficiency: Current Treatment Options and Emerging Therapies. *Stem Cells Int*, *2016*, 9798374.

98. Hancox, Z., Heidari Keshel, S., Yousaf, S., Saeinasab, M., Shahbazi, M.A., & Sefat, F. (2020). The progress in corneal translational medicine. *Biomater Sci*, *8*(23), 6469-6504.

99. Harris, G., Palosaari, T., Magdolenova, Z., Mennecozzi, M., Gineste, J.M., Saavedra, L., Milcamps, A., Huk, A., Collins, A.R., Dusinska, M., & Whelan, M. (2015). Iron oxide nanoparticle toxicity testing using high-throughput analysis and high-content imaging. *Nanotoxicology*, *9 Suppl 1*, 87-94.

100. Hassell, J.R., & Birk, D.E. (2010). The molecular basis of corneal transparency. *Exp Eye Res*, *91*(3), 326-335.

101. Hata, K., Kagami, H., Ueda, M., Torii, S., & Matsuyama, M. (1995). The characteristics of cultured mucosal cell sheet as a material for grafting; comparison with cultured epidermal cell sheet. *Ann Plast Surg*, *34*(5), 530-538.

102. Haug, K., Azqueta, A., Johnsen-Soriano, S., Shahdadfar, A., Drolsum, L.K., Moe, M.C., Røger, M.T., Romero, F.J., Collins, A.R., & Nicolaissen, B. (2013). Donor cornea transfer from Optisol GS to organ culture storage: a two-step procedure to increase donor tissue lifespan. *Acta Ophthalmol*, *91*(3), 219-225.

103. Hayashi, I., Larner, J., & Sato, G. (1978). Hormonal growth control of cells in culture. *In Vitro*, *14*(1), 23-30.

104. Herndon, D.N., & Branski, L.K. (2017). Contemporary Methods Allowing for Safe and Convenient Use of Amniotic Membrane as a Biologic Wound Dressing for Burns. *Ann Plast Surg*, *78*(2 Suppl 1), S9-S10.

105. Hirayama, M., Satake, Y., Higa, K., Yamaguchi, T., & Shimazaki, J. (2012). Transplantation of cultivated oral mucosal epithelium prepared in fibrin-coated culture dishes. *Invest Ophthalmol Vis Sci*, *53*(3), 1602-1609.

106. Hongisto, H., Ilmarinen, T., Vattulainen, M., Mikhailova, A., & Skottman, H. (2017). Xeno- and feeder-free differentiation of human pluripotent stem cells to two distinct ocular epithelial cell types using simple modifications of one method. *Stem Cell Res Ther*, *8*(1), 291.

107. Horvath, V., Svobodova, A., Cabral, J.V., Fiala, R., Burkert, J., Stadler, P., Lindner, J., Bednar, J., Zemlickova, M., & Jirsova, K. (2023). Inter-placental variability is not a major factor affecting the healing efficiency of amniotic membrane when used for treating chronic non-healing wounds. *Cell Tissue Bank*.

108. Hotaling, N.A., Khristov, V., Wan, Q., Sharma, R., Jha, B.S., Lotfi, M., Maminishkis, A., Simon, C.G., & Bharti, K. (2016). Nanofiber Scaffold-Based Tissue-Engineered Retinal Pigment Epithelium to Treat Degenerative Eye Diseases. *J Ocul Pharmacol Ther*, *32*(5), 272-285.

109. Hsueh, Y.J., Huang, S.F., Lai, J.Y., Ma, S.C., Chen, H.C., Wu, S.E., Wang, T.K., Sun, C.C., Ma, K.S., Chen, J.K., Lai, C.H., & Ma, D.H. (2016). Preservation of epithelial progenitor cells from collagenase-digested oral mucosa during ex vivo cultivation. *Sci Rep*, *6*, 36266.

110. Hunt, C.J. (2011). Cryopreservation of Human Stem Cells for Clinical Application: A Review. *Transfus Med Hemother*, *38*(2), 107-123.

111. Hyun, D.W., Kim, Y.H., Koh, A.Y., Lee, H.J., Wee, W.R., Jeon, S., & Kim, M.K.

(2017). Characterization of biomaterial-free cell sheets cultured from human oral mucosal epithelial cells. *J Tissue Eng Regen Med*, *11*(3), 743-750.

112. Ibars, E.P., Cortes, M., Tolosa, L., Gómez-Lechón, M.J., López, S., Castell, J.V., & Mir, J. (2016). Hepatocyte transplantation program: Lessons learned and future strategies. *World J Gastroenterol*, *22*(2), 874-886.

113. Iglesias-Bartolome, R., Callejas-Valera, J.L., & Gutkind, J.S. (2013). Control of the epithelial stem cell epigenome: the shaping of epithelial stem cell identity. *Curr Opin Cell Biol*, *25*(2), 162-169.

114. Ilmarinen, T., Laine, J., Juuti-Uusitalo, K., Numminen, J., Seppänen-Suuronen, R., Uusitalo, H., & Skottman, H. (2013). Towards a defined, serum- and feeder-free culture of stratified human oral mucosal epithelium for ocular surface reconstruction. *Acta Ophthalmol*, *91*(8), 744-750.

115. Inatomi, T., Nakamura, T., Kojyo, M., Koizumi, N., Sotozono, C., & Kinoshita, S. (2006). Ocular surface reconstruction with combination of cultivated autologous oral mucosal epithelial transplantation and penetrating keratoplasty. *Am J Ophthalmol*, *142*(5), 757-764.

116. Islam, M.M., Sharifi, R., & Gonzalez-Andrades, M. (2019). Corneal Tissue Engineering. In J. L. Alió, J. L. Alió del Barrio, & F. Arnalich-Montiel (Eds.), (pp. 23-37). Springer International Publishing.

117. Izumi, K., Tobita, T., & Feinberg, S.E. (2007). Isolation of human oral keratinocyte progenitor/stem cells. *J Dent Res*, *86*(4), 341-346.

118. Jaiswal, A.N., & Vagga, A. (2022). Cryopreservation: A Review Article. *Cureus*, *14*(11), e31564.

119. Jang, T.H., Park, S.C., Yang, J.H., Kim, J.Y., Seok, J.H., Park, U.S., Choi, C.W., Lee, S.R., & Han, J. (2017). Cryopreservation and its clinical applications. *Integr Med Res*, *6*(1), 12-18.

120. Jirsova, K., Dudakova, L., Kalasova, S., Vesela, V., & Merjava, S. (2011). The OV-TL 12/30 clone of anti-cytokeratin 7 antibody as a new marker of corneal conjunctivalization in patients with limbal stem cell deficiency. *Invest Ophthalmol Vis Sci*, *52*(8), 5892-5898.

121. Jirsova, K., & Jones, G.L.A. (2017). Amniotic membrane in ophthalmology: properties, preparation, storage and indications for grafting-a review. *Cell Tissue Bank*, *18*(2), 193-204.

122. Johnson, E.L., Saunders, M., Thote, T., & Danilkovitch, A. (2021). Cryopreserved Placental Membranes Containing Viable Cells Result in High Closure Rate of Nonhealing Upper and Lower Extremity Wounds of Non-Diabetic and Non-Venous Pathophysiology. *Wounds*, *33*(2), 34-40.

123. Joseph, A., Powell-Richards, A.O., Shanmuganathan, V.A., & Dua, H.S. (2004). Epithelial cell characteristics of cultured human limbal explants. *Br J Ophthalmol*, *88*(3), 393-398.

124. Juhl, M., Reibel, J., & Stoltze, K. (1989). Immunohistochemical distribution of keratin proteins in clinically healthy human gingival epithelia. *Scand J Dent Res*, *97*(2), 159-170.

125. Junttila, I.S. (2018). Tuning the Cytokine Responses: An Update on Interleukin (IL)-4 and IL-13 Receptor Complexes. *Front Immunol*, *9*, 888.

126. Kaplan, N., Wang, J., Wray, B., Patel, P., Yang, W., Peng, H., & Lavker, R.M. (2019). Single-Cell RNA Transcriptome Helps Define the Limbal/Corneal Epithelial Stem/ Early Transit Amplifying Cells and How Autophagy Affects This Population. *Invest*

Ophthalmol Vis Sci, *60*(10), 3570-3583.

127. Kasai, Y., Sugiyama, H., Takagi, R., Kondo, M., Owaki, T., Namiki, H., Okano, T., Takeda, N., & Yamato, M. (2016). Brush biopsy of human oral mucosal epithelial cells as a quality control of the cell source for fabrication of transplantable epithelial cell sheets for regenerative medicine. *Regen Ther*, *4*, 71-77.

128. Kaufman, M.D., Stephen, C., Suri, M.D., & Twite, M. (2014). Recent advance in the cryopreservation of corneal limbal stem cells. *International Journal of Eye Banking*, *2*(1), 1-7.

129. Kenyon, K.R., & Tseng, S.C. (1989). Limbal autograft transplantation for ocular surface disorders. *Ophthalmology*, *96*(5), 709-22; discussion 722.

130. Kethiri, A.R., Basu, S., Shukla, S., Sangwan, V.S., & Singh, V. (2017). Optimizing the role of limbal explant size and source in determining the outcomes of limbal transplantation: An in vitro study. *PLoS One*, *12*(9), e0185623.

131. Kim, H.S., Jun Song, X., de Paiva, C.S., Chen, Z., Pflugfelder, S.C., & Li, D.Q. (2004). Phenotypic characterization of human corneal epithelial cells expanded ex vivo from limbal explant and single cell cultures. *Exp Eye Res*, *79*(1), 41-49.

132. Kim, Y.H., Kim, D.H., Shin, E.J., Lee, H.J., Wee, W.R., Jeon, S., & Kim, M.K. (2016). Comparative Analysis of Substrate-Free Cultured Oral Mucosal Epithelial Cell Sheets from Cells of Subjects with and without Stevens-Johnson Syndrome for Use in Ocular Surface Reconstruction. *PLoS One*, *11*(1), e0147548.

133. Kim, Y.J., Lee, H.J., Ryu, J.S., Kim, Y.H., Jeon, S., Oh, J.Y., Choung, H.K., Khwarg, S.I., Wee, W.R., & Kim, M.K. (2018). Prospective Clinical Trial of Corneal Reconstruction With Biomaterial-Free Cultured Oral Mucosal Epithelial Cell Sheets. *Cornea*, *37*(1), 76-83.

134. King, A.E., Paltoo, A., Kelly, R.W., Sallenave, J.M., Bocking, A.D., & Challis, J.R. (2007). Expression of natural antimicrobials by human placenta and fetal membranes. *Placenta*, *28*(2-3), 161-169.

135. Kjaergaard, N., Hein, M., Hyttel, L., Helmig, R.B., Schønheyder, H.C., Uldbjerg, N., & Madsen, H. (2001). Antibacterial properties of human amnion and chorion in vitro. *Eur J Obstet Gynecol Reprod Biol*, *94*(2), 224-229.

136. Kobayashi, A., & Sugiyama, K. (2005). In vivo corneal confocal microscopic findings of palisades of Vogt and its underlying limbal stroma. *Cornea*, *24*(4), 435-437.

137. Koizumi, N.J., Inatomi, T.J., Sotozono, C.J., Fullwood, N.J., Quantock, A.J., & Kinoshita, S. (2000). Growth factor mRNA and protein in preserved human amniotic membrane. *Curr Eye Res*, *20*(3), 173-177.

138. Kolli, S., Ahmad, S., Mudhar, H.S., Meeny, A., Lako, M., & Figueiredo, F.C. (2014). Successful application of ex vivo expanded human autologous oral mucosal epithelium for the treatment of total bilateral limbal stem cell deficiency. *Stem Cells*, *32*(8), 2135-2146.

139. Kolli, S., Lako, M., Figueiredo, F., Mudhar, H., & Ahmad, S. (2008). Loss of corneal epithelial stem cell properties in outgrowths from human limbal explants cultured on intact amniotic membrane. *Regen Med*, *3*(3), 329-342.

140. Kondo, M., Yamato, M., Takagi, R., Murakami, D., Namiki, H., & Okano, T. (2014). Significantly different proliferative potential of oral mucosal epithelial cells between six animal species. *J Biomed Mater Res A*, *102*(6), 1829-1837.

141. Koster, M.I., Kim, S., Mills, A.A., DeMayo, F.J., & Roop, D.R. (2004). p63 is the molecular switch for initiation of an epithelial stratification program. *Genes Dev*, *18*(2), 126-131.

142. Krishnan, S., Iyer, G.K., & Krishnakumar, S. (2010). Culture & characterisation of limbal epithelial cells & oral mucosal cells. *Indian J Med Res*, *131*, 422-428.

143. Kruse, F.E., & Tseng, S.C. (1992). Proliferative and differentiative response of corneal and limbal epithelium to extracellular calcium in serum-free clonal cultures. *J Cell Physiol*, *151*(2), 347-360.

144. Ksander, B.R., Kolovou, P.E., Wilson, B.J., Saab, K.R., Guo, Q., Ma, J., McGuire, S.P., Gregory, M.S., Vincent, W.J.B., Perez, V.L., Cruz-Guilloty, F., Kao, W.W.Y., Call, M.K., Tucker, B.A., Zhan, Q., Murphy, G.F., Lathrop, K.L., Alt, C., Mortensen, L.J., Lin, C.P., Zieske, J.D., Frank, M.H., & Frank, N.Y. (2014). ABCB5 is a limbal stem cell gene required for corneal development and repair. *Nature*, *511*(7509), 353-357.

145. Lachaud, C.C., Hmadcha, A., & Soria, B. (2019). Corneal Regeneration: Use of Extracorneal Stem Cells. In J. L. Alió, J. L. Alió del Barrio, & F. Arnalich-Montiel (Eds.), (pp. 123-144). Springer International Publishing.

146. Larouche, D., Hayward, C., Cuffley, K., & Germain, L. (2005). Keratin 19 as a stem cell marker in vivo and in vitro. *Methods Mol Biol*, *289*, 103-110.

147. Larouche, D., Lavoie, A., Paquet, C., Simard-Bisson, C., & Germain, L. (2010). Identification of epithelial stem cells in vivo and in vitro using keratin 19 and BrdU. *Methods Mol Biol*, *585*, 383-400.

148. Lavery, L.A., Fulmer, J., Shebetka, K.A., Regulski, M., Vayser, D., Fried, D., Kashefsky, H., Owings, T.M., Nadarajah, J., & Grafix, D.F.U.S.G. (2014). The efficacy and safety of Grafix(®) for the treatment of chronic diabetic foot ulcers: results of a multi-centre, controlled, randomised, blinded, clinical trial. *Int Wound J*, *11*(5), 554-560.

149. Lavker, R.M., & Sun, T.T. (2000). Epidermal stem cells: properties, markers, and location. *Proc Natl Acad Sci U S A*, *97*(25), 13473-13475.

150. Lavker, R.M., Tseng, S.C., & Sun, T.T. (2004). Corneal epithelial stem cells at the limbus: looking at some old problems from a new angle. *Exp Eye Res*, *78*(3), 433-446.

151. Le, Q., & Deng, S.X. (2019). The application of human amniotic membrane in the surgical management of limbal stem cell deficiency. *Ocul Surf*, *17*(2), 221-229.

152. Lehrer, M.S., Sun, T.T., & Lavker, R.M. (1998). Strategies of epithelial repair: modulation of stem cell and transit amplifying cell proliferation. *J Cell Sci*, *111*(Pt 19), 2867-2875.

153. Lekhanont, K., Choubtum, L., Chuck, R.S., Sa-ngiampornpanit, T., Chuckpaiwong, V., & Vongthongsri, A. (2009). A serum- and feeder-free technique of culturing human corneal epithelial stem cells on amniotic membrane. *Mol Vis*, *15*, 1294-1302.

154. Li, W., He, H., Kuo, C.L., Gao, Y., Kawakita, T., & Tseng, S.C. (2006). Basement membrane dissolution and reassembly by limbal corneal epithelial cells expanded on amniotic membrane. *Invest Ophthalmol Vis Sci*, *47*(6), 2381-2389.

155. Li, Y., Meng, H., Liu, Y., & Lee, B.P. (2015). Fibrin gel as an injectable biodegradable scaffold and cell carrier for tissue engineering. *ScientificWorldJournal*, *2015*, 685690.

156. Llames, S., García-Pérez, E., Meana, Á., Larcher, F., & del Río, M. (2015). Feeder Layer Cell Actions and Applications. *Tissue Eng Part B Rev*, *21*(4), 345-353.

157. López-Paniagua, M., Nieto-Miguel, T., de la Mata, A., Galindo, S., Herreras, J.M., Corrales, R.M., & Calonge, M. (2013). Consecutive expansion of limbal epithelial stem cells from a single limbal biopsy. *Curr Eye Res*, *38*(5), 537-549.

158. López, S., Hoz, L., Tenorio, E.P., Buentello, B., Magaña, F.S., Wintergerst, A., Navas, A., Garfias, Y., & Arzate, H. (2021). Can Human Oral Mucosa Stem Cells Differentiate to Corneal Epithelia. *Int J Mol Sci*, *22*(11), 5976.

159. Lorenzo, Y., Azqueta, A., Luna, L., Bonilla, F., Domínguez, G., & Collins, A.R. (2009). The carotenoid beta-cryptoxanthin stimulates the repair of DNA oxidation damage in addition to acting as an antioxidant in human cells. *Carcinogenesis*, *30*(2), 308-314.

160. Lorenzo, Y., Costa, S., Collins, A.R., & Azqueta, A. (2013). The comet assay, DNA damage, DNA repair and cytotoxicity: hedgehogs are not always dead. *Mutagenesis*, *28*(4), 427-432.

161. Lorenzo, Y., Haug Berg, K., Ringvold, A., Petrovski, G., Moe, M.C., Collins, A., & Nicolaissen, B. (2018). Levels of oxidative DNA damage are low in ex vivo engineered human limbal epithelial tissue. *Acta Ophthalmol*, *96*(8), 834-840.

162. Lužnik, Z., Bertolin, M., Breda, C., Ferrari, B., Barbaro, V., Schollmayer, P., & Ferrari, S. (2016). Preservation of Ocular Epithelial Limbal Stem Cells: The New Frontier in Regenerative Medicine. *Adv Exp Med Biol*, *951*, 179-189.

163. Lužnik, Z., Breda, C., Barbaro, V., Ferrari, S., Migliorati, A., Di Iorio, E., Ferrari, B., Griffoni, C., Grassetto, A., Elbadawy, H.M., & Bertolin, M. (2017). Towards xeno-free cultures of human limbal stem cells for ocular surface reconstruction. *Cell Tissue Bank*, *18*(4), 461-474.

164. Lysak, D., Brychtová, M., Leba, M., Čedíková, M., Georgiev, D., Jindra, P., Vlas, T., & Holubova, M. (2021). Long-Term Cryopreservation Does Not Affect Quality of Peripheral Blood Stem Cell Grafts: A Comparative Study of Native, Short-Term and Long-Term Cryopreserved Haematopoietic Stem Cells. *Cell Transplant*, *30*, 9636897211036004.

165. Ma, D.H., Hsueh, Y.J., Ma, K.S., Tsai, Y.J., Huang, S.F., Chen, H.C., Sun, C.C., Kuo, M.T., Chao, A.S., & Lai, J.Y. (2021). Long-term survival of cultivated oral mucosal epithelial cells in human cornea: generating cell sheets using an animal product-free culture protocol. *Stem Cell Res Ther*, *12*(1), 524.

166. Ma, D.H., Kuo, M.T., Tsai, Y.J., Chen, H.C., Chen, X.L., Wang, S.F., Li, L., Hsiao, C.H., & Lin, K.K. (2009). Transplantation of cultivated oral mucosal epithelial cells for severe corneal burn. *Eye (Lond)*, *23*(6), 1442-1450.

167. Ma, D.H., Wang, S.F., Su, W.Y., & Tsai, R.J. (2002). Amniotic membrane graft for the management of scleral melting and corneal perforation in recalcitrant infectious scleral and corneoscleral ulcers. *Cornea*, *21*(3), 275-283.

168. Magdolenova, Z., Lorenzo, Y., Collins, A., & Dusinska, M. (2012). Can standard genotoxicity tests be applied to nanoparticles. *J Toxicol Environ Health A*, *75*(13-15), 800-806.

169. Mainzer, C., Barrichello, C., Debret, R., Remoué, N., Sigaudo-Roussel, D., & Sommer, P. (2014). Insulin-transferrin-selenium as an alternative to foetal serum for epidermal equivalents. *Int J Cosmet Sci*, *36*(5), 427-435.

170. Malhotra, C., & Jain, A.K. (2014). Human amniotic membrane transplantation: Different modalities of its use in ophthalmology. *World J Transplant*, *4*(2), 111-121.

171. Mannello, F., & Tonti, G.A. (2007). Concise review: no breakthroughs for human mesenchymal and embryonic stem cell culture: conditioned medium, feeder layer, or feeder-free; medium with fetal calf serum, human serum, or enriched plasma; serum-free, serum replacement nonconditioned medium, or ad hoc formula? All that glitters is not gold. *Stem Cells*, *25*(7), 1603-1609.

172. Martín-López, M., Rosell-Valle, C., Arribas-Arribas, B., Fernández-Muñoz, B., Jiménez, R., Nogueras, S., García-Delgado, A.B., Campos, F., & Santos-González, M. (2023). Bioengineered tissue and cell therapy products are efficiently cryopreserved

with pathogen-inactivated human platelet lysate-based solutions. *Stem Cell Res Ther*, *14*(1), 69.

173. Martin, M.J., Muotri, A., Gage, F., & Varki, A. (2005). Human embryonic stem cells express an immunogenic nonhuman sialic acid. *Nat Med*, *11*(2), 228-232.

174. Masood, F., Chang, J.H., Akbar, A., Song, A., Hu, W.Y., Azar, D.T., & Rosenblatt, M.I. (2022). Therapeutic Strategies for Restoring Perturbed Corneal Epithelial Homeostasis in Limbal Stem Cell Deficiency: Current Trends and Future Directions. *Cells*, *11*(20), 3247.

175. Massie, I., Kureshi, A.K., Schrader, S., Shortt, A.J., & Daniels, J.T. (2015). Optimization of optical and mechanical properties of real architecture for 3-dimensional tissue equivalents: Towards treatment of limbal epithelial stem cell deficiency. *Acta Biomater*, *24*, 241-250.

176. Mazur, P. (1970). Cryobiology: the freezing of biological systems. *Science*, *168*(3934), 939-949.

177. Meller, D., Pires, R.T., & Tseng, S.C. (2002). Ex vivo preservation and expansion of human limbal epithelial stem cells on amniotic membrane cultures. *Br J Ophthalmol*, *86*(4), 463-471.

178. Merjava, S., Brejchova, K., Vernon, A., Daniels, J.T., & Jirsova, K. (2011a). Cytokeratin 8 is expressed in human corneoconjunctival epithelium, particularly in limbal epithelial cells. *Invest Ophthalmol Vis Sci*, *52*(2), 787-794.

179. Merjava, S., Neuwirth, A., Tanzerova, M., & Jirsova, K. (2011b). The spectrum of cytokeratins expressed in the adult human cornea, limbus and perilimbal conjunctiva. *Histol Histopathol*, *26*(3), 323-331.

180. Mermet, I., Pottier, N., Sainthillier, J.M., Malugani, C., Cairey-Remonnay, S., Maddens, S., Riethmuller, D., Tiberghien, P., Humbert, P., & Aubin, F. (2007). Use of amniotic membrane transplantation in the treatment of venous leg ulcers. *Wound Repair Regen*, *15*(4), 459-464.

181. Meyer-Blazejewska, E.A., Kruse, F.E., Bitterer, K., Meyer, C., Hofmann-Rummelt, C., Wünsch, P.H., & Schlötzer-Schrehardt, U. (2010). Preservation of the limbal stem cell phenotype by appropriate culture techniques. *Invest Ophthalmol Vis Sci*, *51*(2), 765-774.

182. Mimura, T., Yamagami, S., Uchida, S., Yokoo, S., Ono, K., Usui, T., & Amano, S. (2010). Isolation of adult progenitor cells with neuronal potential from rabbit corneal epithelial cells in serum- and feeder layer-free culture conditions. *Mol Vis*, *16*, 1712-1719.

183. Mohamed-Noriega, K., Toh, K.P., Poh, R., Balehosur, D., Riau, A., Htoon, H.M., Peh, G.S., Chaurasia, S.S., Tan, D.T., & Mehta, J.S. (2011). Cornea lenticule viability and structural integrity after refractive lenticule extraction (ReLEx) and cryopreservation. *Mol Vis*, *17*, 3437-3449.

184. Moll, R., Divo, M., & Langbein, L. (2008). The human keratins: biology and pathology. *Histochem Cell Biol*, *129*(6), 705-733.

185. Moll, R., Franke, W.W., Schiller, D.L., Geiger, B., & Krepler, R. (1982). The catalog of human cytokeratins: patterns of expression in normal epithelia, tumors and cultured cells. *Cell*, *31*(1), 11-24.

186. Mora, P.T., Brady, R.O., & Smith, R.W. (1970). Glycolipids in SV40 and Polyoma Virus Transformed Mouse Cell Lines. In *Blood and Tissue Antigens* (pp. 337-340). Elsevier.

187. Morino, T., Takagi, R., Yamamoto, K., Kojima, H., & Yamato, M. (2019). Explant

culture of oral mucosal epithelial cells for fabricating transplantable epithelial cell sheet. *Regen Ther*, *10*, 36-45.

188. Murray, K.A., & Gibson, M.I. (2022). Chemical approaches to cryopreservation. *Nat Rev Chem*, *6*(8), 579-593.

189. Muruzabal, D., Sanz-Serrano, J., Sauvaigo, S., Treillard, B., Olsen, A.K., López de Cerain, A., Vettorazzi, A., & Azqueta, A. (2021). Validation of the in vitro comet assay for DNA cross-links and altered bases detection. *Arch Toxicol*, *95*(8), 2825-2838.

190. Nakamura, T., Endo, K., & Kinoshita, S. (2007a). Identification of human oral keratinocyte stem/progenitor cells by neurotrophin receptor p75 and the role of neurotrophin/p75 signaling. *Stem Cells*, *25*(3), 628-638.

191. Nakamura, T., Inatomi, T., Cooper, L.J., Rigby, H., Fullwood, N.J., & Kinoshita, S. (2007b). Phenotypic investigation of human eyes with transplanted autologous cultivated oral mucosal epithelial sheets for severe ocular surface diseases. *Ophthalmology*, *114*(6), 1080-1088.

192. Nakamura, T., Inatomi, T., Sotozono, C., Amemiya, T., Kanamura, N., & Kinoshita, S. (2004). Transplantation of cultivated autologous oral mucosal epithelial cells in patients with severe ocular surface disorders. *Br J Ophthalmol*, *88*(10), 1280-1284.

193. Nakamura, T., Inatomi, T., Sotozono, C., Ang, L.P., Koizumi, N., Yokoi, N., & Kinoshita, S. (2006). Transplantation of autologous serum-derived cultivated corneal epithelial equivalents for the treatment of severe ocular surface disease. *Ophthalmology*, *113*(10), 1765-1772.

194. Nakamura, T., Yokoo, S., Bentley, A.J., Nagata, M., Fullwood, N.J., Inatomi, T., Sotozono, C., Yamagami, S., & Kinoshita, S. (2016). Development of functional human oral mucosal epithelial stem/progenitor cell sheets using a feeder-free and serum-free culture system for ocular surface reconstruction. *Sci Rep*, *6*, 37173.

195. Nguyen, K.N., Bobba, S., Richardson, A., Park, M., Watson, S.L., Wakefield, D., & Di Girolamo, N. (2018). Native and synthetic scaffolds for limbal epithelial stem cell transplantation. *Acta Biomater*, *65*, 21-35.

196. Nguyen, L.V., Vanner, R., Dirks, P., & Eaves, C.J. (2012). Cancer stem cells: an evolving concept. *Nat Rev Cancer*, *12*(2), 133-143.

197. Niknejad, H., Peirovi, H., Jorjani, M., Ahmadiani, A., Ghanavi, J., & Seifalian, A.M. (2008). Properties of the amniotic membrane for potential use in tissue engineering. *Eur Cell Mater*, *15*, 88-99.

198. Nishida, K., Yamato, M., Hayashida, Y., Watanabe, K., Maeda, N., Watanabe, H., Yamamoto, K., Nagai, S., Kikuchi, A., Tano, Y., & Okano, T. (2004a). Functional bioengineered corneal epithelial sheet grafts from corneal stem cells expanded ex vivo on a temperature-responsive cell culture surface. *Transplantation*, *77*(3), 379-385.

199. Nishida, K., Yamato, M., Hayashida, Y., Watanabe, K., Yamamoto, K., Adachi, E., Nagai, S., Kikuchi, A., Maeda, N., Watanabe, H., Okano, T., & Tano, Y. (2004b). Corneal reconstruction with tissue-engineered cell sheets composed of autologous oral mucosal epithelium. *N Engl J Med*, *351*(12), 1187-1196.

200. Nishida, T., Saika, S., & Morishige, N. (2021). Cornea and Sclera: Anatomy and Physiology. In M. J. Mannis & E. J. Holland (Eds.), *Cornea* (5th ed., pp. 1-22). Elsevier Health Sciences.

201. Nosrati, H., Alizadeh, Z., Nosrati, A., Ashrafi-Dehkordi, K., Banitalebi-Dehkordi, M., Sanami, S., & Khodaei, M. (2021). Stem cell-based therapeutic strategies for corneal epithelium regeneration. *Tissue Cell*, *68*, 101470.

202. Oda, D., & Watson, E. (1990). Human oral epithelial cell culture I. Improved conditions

for reproducible culture in serum-free medium. *In Vitro Cellular & Developmental Biology*, *26*(6), 589-595.

203. Ohta, Y., & Ichimura, K. (2000). Proliferation markers, proliferating cell nuclear antigen, Ki67, 5-bromo-2'-deoxyuridine, and cyclin D1 in mouse olfactory epithelium. *Ann Otol Rhinol Laryngol*, *109*(11), 1046-1048.

204. Okada, N., Kitano, Y., & Ichihara, K. (1982). Effects of cholera toxin on proliferation of cultured human keratinocytes in relation to intracellular cyclic AMP levels. *J Invest Dermatol*, *79*(1), 42-47.

205. Oliva, J., Florentino, A., Bardag-Gorce, F., & Niihara, Y. (2019). Vitrification and storage of oral mucosa epithelial cell sheets. *J Tissue Eng Regen Med*, *13*(7), 1153-1163.

206. Ortega, I., Ryan, A.J., Deshpande, P., MacNeil, S., & Claeyssens, F. (2013). Combined microfabrication and electrospinning to produce 3-D architectures for corneal repair. *Acta Biomater*, *9*(3), 5511-5520.

207. Osei-Bempong, C., Figueiredo, F.C., & Lako, M. (2013). The limbal epithelium of the eye--a review of limbal stem cell biology, disease and treatment. *Bioessays*, *35*(3), 211-219.

208. Øsnes-Ringen, O., Azqueta, A.O., Moe, M.C., Zetterström, C., Røger, M., Nicolaissen, B., & Collins, A.R. (2013). DNA damage in lens epithelium of cataract patients in vivo and ex vivo. *Acta Ophthalmol*, *91*(7), 652-656.

209. Osorio, S., Alba, R., Damasceno, C.M., Lopez-Casado, G., Lohse, M., Zanor, M.I., Tohge, T., Usadel, B., Rose, J.K., Fei, Z., Giovannoni, J.J., & Fernie, A.R. (2011). Systems biology of tomato fruit development: combined transcript, protein, and metabolite analysis of tomato transcription factor (nor, rin) and ethylene receptor (Nr) mutants reveals novel regulatory interactions. *Plant Physiol*, *157*(1), 405-425.

210. Papagerakis, S., Pannone, G., Zheng, L., About, I., Taqi, N., Nguyen, N.P., Matossian, M., McAlpin, B., Santoro, A., McHugh, J., Prince, M.E., & Papagerakis, P. (2014). Oral epithelial stem cells - implications in normal development and cancer metastasis. *Exp Cell Res*, *325*(2), 111-129.

211. Pappa, A., Brown, D., Koutalos, Y., DeGregori, J., White, C., & Vasiliou, V. (2005). Human aldehyde dehydrogenase 3A1 inhibits proliferation and promotes survival of human corneal epithelial cells. *J Biol Chem*, *280*(30), 27998-28006.

212. Patel, D.V., Sherwin, T., & McGhee, C.N. (2006). Laser scanning in vivo confocal microscopy of the normal human corneoscleral limbus. *Invest Ophthalmol Vis Sci*, *47*(7), 2823-2827.

213. Pathak, M., Olstad, O.K., Drolsum, L., Moe, M.C., Smorodinova, N., Kalasova, S., Jirsova, K., Nicolaissen, B., & Noer, A. (2016). The effect of culture medium and carrier on explant culture of human limbal epithelium: A comparison of ultrastructure, keratin profile and gene expression. *Exp Eye Res*, *153*, 122-132.

214. Pei, Y., Sherry, D.M., & McDermott, A.M. (2004). Thy-1 distinguishes human corneal fibroblasts and myofibroblasts from keratocytes. *Exp Eye Res*, *79*(5), 705-712.

215. Pekny, M., & Lane, E.B. (2007). Intermediate filaments and stress. *Exp Cell Res*, *313*(10), 2244-2254.

216. Pellegrini, G., Ardigò, D., Milazzo, G., Iotti, G., Guatelli, P., Pelosi, D., & De Luca, M. (2018). Navigating Market Authorization: The Path Holoclar Took to Become the First Stem Cell Product Approved in the European Union. *Stem Cells Transl Med*, *7*(1), 146-154.

217. Pellegrini, G., Dellambra, E., Golisano, O., Martinelli, E., Fantozzi, I., Bondanza, S.,

Ponzin, D., McKeon, F., & De Luca, M. (2001). p63 identifies keratinocyte stem cells. *Proc Natl Acad Sci U S A*, *98*(6), 3156-3161.

218. Pellegrini, G., Traverso, C.E., Franzi, A.T., Zingirian, M., Cancedda, R., & De Luca, M. (1997). Long-term restoration of damaged corneal surfaces with autologous cultivated corneal epithelium. *Lancet*, *349*(9057), 990-993.

219. Pellegrini, G., Golisano, O., Paterna, P., Lambiase, A., Bonini, S., Rama, P., & De Luca, M. (1999). Location and Clonal Analysis of Stem Cells and Their Differentiated Progeny in the Human Ocular Surface. *Journal of Cell Biology*, *145*(4), 769-782.

220. Petrini, I., Barachini, S., Carnicelli, V., Galimberti, S., Modeo, L., Boni, R., Sollini, M., & Erba, P.A. (2017). ED-B fibronectin expression is a marker of epithelial-mesenchymal transition in translational oncology. *Oncotarget*, *8*(3), 4914-4921.

221. Pitz, S., & Moll, R. (2002). Intermediate-filament expression in ocular tissue. *Prog Retin Eye Res*, *21*(2), 241-262.

222. Pogozhykh, O., Prokopyuk, V., Figueiredo, C., & Pogozhykh, D. (2018). Placenta and Placental Derivatives in Regenerative Therapies: Experimental Studies, History, and Prospects. *Stem Cells Int*, *2018*, 4837930.

223. Poli, M., Burillon, C., Auxenfans, C., Rovere, M.R., & Damour, O. (2015). Immunocytochemical Diagnosis of Limbal Stem Cell Deficiency: Comparative Analysis of Current Corneal and Conjunctival Biomarkers. *Cornea*, *34*(7), 817-823.

224. Poli, M., Janin, H., Justin, V., Auxenfans, C., Burillon, C., & Damour, O. (2011). Keratin 13 immunostaining in corneal impression cytology for the diagnosis of limbal stem cell deficiency. *Invest Ophthalmol Vis Sci*, *52*(13), 9411-9415.

225. Polisetti, N., Agarwal, P., Khan, I., Kondaiah, P., Sangwan, V.S., & Vemuganti, G.K. (2010). Gene expression profile of epithelial cells and mesenchymal cells derived from limbal explant culture. *Mol Vis*, *16*, 1227-1240.

226. Prabhasawat, P., Ekpo, P., Uiprasertkul, M., Chotikavanich, S., Tesavibul, N., Pornpanich, K., & Luemsamran, P. (2016). Long-term result of autologous cultivated oral mucosal epithelial transplantation for severe ocular surface disease. *Cell Tissue Bank*, *17*(3), 491-503.

227. Presland, R.B., & Jurevic, R.J. (2002). Making sense of the epithelial barrier: what molecular biology and genetics tell us about the functions of oral mucosal and epidermal tissues. *J Dent Educ*, *66*(4), 564-574.

228. Priya, C.G., Arpitha, P., Vaishali, S., Prajna, N.V., Usha, K., Sheetal, K., & Muthukkaruppan, V. (2011). Adult human buccal epithelial stem cells: identification, ex-vivo expansion, and transplantation for corneal surface reconstruction. *Eye (Lond)*, *25*(12), 1641-1649.

229. Radosevich, M., Goubran, H.I., & Burnouf, T. (1997). Fibrin sealant: scientific rationale, production methods, properties, and current clinical use. *Vox Sang*, *72*(3), 133-143.

230. Rama, P., Bonini, S., Lambiase, A., Golisano, O., Paterna, P., De Luca, M., & Pellegrini, G. (2001). Autologous fibrin-cultured limbal stem cells permanently restore the corneal surface of patients with total limbal stem cell deficiency. *Transplantation*, *72*(9), 1478-1485.

231. Rama, P., Matuska, S., Paganoni, G., Spinelli, A., De Luca, M., & Pellegrini, G. (2010). Limbal stem-cell therapy and long-term corneal regeneration. *N Engl J Med*, *363*(2), 147-155.

232. Ramachandran, C., Basu, S., Sangwan, V.S., & Balasubramanian, D. (2014). Concise review: the coming of age of stem cell treatment for corneal surface damage. *Stem Cells*

Transl Med, *3*(10), 1160-1168.

233.   Ramirez-Miranda, A., Nakatsu, M.N., Zarei-Ghanavati, S., Nguyen, C.V., & Deng, S.X. (2011). Keratin 13 is a more specific marker of conjunctival epithelium than keratin 19. *Mol Vis*, *17*, 1652-1661.

234. Ramírez, B.E., Sánchez, A., Herreras, J.M., Fernández, I., García-Sancho, J., Nieto-Miguel, T., & Calonge, M. (2015). Stem Cell Therapy for Corneal Epithelium Regeneration following Good Manufacturing and Clinical Procedures. *Biomed Res Int*, *2015*, 408495.

235. Rao, R.S., Patil, S., & Ganavi, B.S. (2014). Oral cytokeratins in health and disease. *J Contemp Dent Pract*, *15*(1), 127-136.

236. Raspovic, K.M., Wukich, D.K., Naiman, D.Q., Lavery, L.A., Kirsner, R.S., Kim, P.J., Steinberg, J.S., Attinger, C.E., & Danilkovitch, A. (2018). Effectiveness of viable cryopreserved placental membranes for management of diabetic foot ulcers in a real world setting. *Wound Repair Regen*, *26*(2), 213-220.

237. Rheinwald, J.G., & Green, H. (1975). Serial cultivation of strains of human epidermal keratinocytes: the formation of keratinizing colonies from single cells. *Cell*, *6*(3), 331-343.

238. Riau, A.K., Beuerman, R.W., Lim, L.S., & Mehta, J.S. (2010). Preservation, sterilization and de-epithelialization of human amniotic membrane for use in ocular surface reconstruction. *Biomaterials*, *31*(2), 216-225.

239. Richard, V., & Pillai, M.R. (2010). The stem cell code in oral epithelial tumorigenesis: 'the cancer stem cell shift hypothesis'. *Biochim Biophys Acta*, *1806*(2), 146-162.

240. Richardson, A., Lobo, E.P., Delic, N.C., Myerscough, M.R., Lyons, J.G., Wakefield, D., & Di Girolamo, N. (2017). Keratin-14-Positive Precursor Cells Spawn a Population of Migratory Corneal Epithelia that Maintain Tissue Mass throughout Life. *Stem Cell Reports*, *9*(4), 1081-1096.

241. Rojas, E., Lorenzo, Y., Haug, K., Nicolaissen, B., & Valverde, M. (2014). Epithelial cells as alternative human biomatrices for comet assay. *Frontiers in Genetics*, *5*.

242. Romano, A.C., Espana, E.M., Yoo, S.H., Budak, M.T., Wolosin, J.M., & Tseng, S.C. (2003). Different cell sizes in human limbal and central corneal basal epithelia measured by confocal microscopy and flow cytometry. *Invest Ophthalmol Vis Sci*, *44*(12), 5125-5129.

243.   Roy, O., Beaulieu Leclerc, V., Bourget, J.-M., Theriault, M., & Proulx, S. (2015). Understanding the Process of Corneal Endothelial Morphological Change In Vitro. *Investigative Ophthalmology & Visual Science*, *56*(2), 1228-1237.

244. Ruan, Y., Jiang, S., Musayeva, A., Pfeiffer, N., & Gericke, A. (2021). Corneal Epithelial Stem Cells-Physiology, Pathophysiology and Therapeutic Options. *Cells*, *10*(9), 2302.

245. Rüfer, F., Schröder, A., & Erb, C. (2005). White-to-white corneal diameter: normal values in healthy humans obtained with the Orbscan II topography system. *Cornea*, *24*(3), 259-261.

246.   Sabater, A.L., & Perez, V.L. (2017). Amniotic membrane use for management of corneal limbal stem cell deficiency. *Curr Opin Ophthalmol*, *28*(4), 363-369.

247. Saghizadeh, M., Dib, C.M., Brunken, W.J., & Ljubimov, A.V. (2014). Normalization of wound healing and stem cell marker patterns in organ-cultured human diabetic corneas by gene therapy of limbal cells. *Exp Eye Res*, *129*, 66-73.

248. Saghizadeh, M., Soleymani, S., Harounian, A., Bhakta, B., Troyanovsky, S.M., Brunken, W.J., Pellegrini, G., & Ljubimov, A.V. (2011). Alterations of epithelial stem

cell marker patterns in human diabetic corneas and effects of c-met gene therapy. *Mol Vis*, *17*, 2177-2190.

249.   Sambu, S. (2015). A Bayesian approach to optimizing cryopreservation protocols. *PeerJ*, *3*, e1039.

250.   Sangwan, V.S. (2001). Limbal stem cells in health and disease. *Biosci Rep*, *21*(4), 385-405.

251.   Sangwan, V.S., Basu, S., MacNeil, S., & Balasubramanian, D. (2012). Simple limbal epithelial transplantation (SLET): a novel surgical technique for the treatment of unilateral limbal stem cell deficiency. *Br J Ophthalmol*, *96*(7), 931-934.

252.   Schermer, A., Galvin, S., & Sun, T.T. (1986). Differentiation-related expression of a major 64K corneal keratin in vivo and in culture suggests limbal location of corneal epithelial stem cells. *J Cell Biol*, *103*(1), 49-62.

253.   Schlötzer-Schrehardt, U., & Kruse, F.E. (2005). Identification and characterization of limbal stem cells. *Exp Eye Res*, *81*(3), 247-264.

254.   Scholzen, T., & Gerdes, J. (2000). The Ki-67 protein: from the known and the unknown. *J Cell Physiol*, *182*(3), 311-322.

255.   Schreurs, O., Karatsaidis, A., Balta, M.G., Grung, B., Hals, E.K.B., & Schenck, K. (2020). Expression of keratins 8, 18, and 19 in epithelia of atrophic oral lichen planus. *Eur J Oral Sci*, *128*(1), 7-17.

256.   Schwab, I.R., Johnson, N.T., & Harkin, D.G. (2006). Inherent risks associated with manufacture of bioengineered ocular surface tissue. *Arch Ophthalmol*, *124*(12), 1734-1740.

257.   Schwab, I.R., Reyes, M., & Isseroff, R.R. (2000). Successful transplantation of bioengineered tissue replacements in patients with ocular surface disease. *Cornea*, *19*(4), 421-426.

258.   Secker, G.A., & Daniels, J.T. (2008). Limbal epithelial stem cells of the cornea. In *StemBook*. Cambridge (MA): Harvard Stem Cell Institute.

259.   Senoo, M., Pinto, F., Crum, C.P., & McKeon, F. (2007). p63 Is essential for the proliferative potential of stem cells in stratified epithelia. *Cell*, *129*(3), 523-536.

260.   Shahdadfar, A., Frønsdal, K., Haug, T., Reinholt, F.P., & Brinchmann, J.E. (2005). In vitro expansion of human mesenchymal stem cells: choice of serum is a determinant of cell proliferation, differentiation, gene expression, and transcriptome stability. *Stem Cells*, *23*(9), 1357-1366.

261.   Shahdadfar, A., Haug, K., Pathak, M., Drolsum, L., Olstad, O.K., Johnsen, E.O., Petrovski, G., Moe, M.C., & Nicolaissen, B. (2012). Ex vivo expanded autologous limbal epithelial cells on amniotic membrane using a culture medium with human serum as single supplement. *Exp Eye Res*, *97*(1), 1-9.

262.   Sharma, A., & Coles, W.H. (1989). Kinetics of corneal epithelial maintenance and graft loss. A population balance model. *Invest Ophthalmol Vis Sci*, *30*(9), 1962-1971.

263.   Sharma, N., Thenarasun, S.A., Kaur, M., Pushker, N., Khanna, N., Agarwal, T., & Vajpayee, R.B. (2016). Adjuvant Role of Amniotic Membrane Transplantation in Acute Ocular Stevens-Johnson Syndrome: A Randomized Control Trial. *Ophthalmology*, *123*(3), 484-491.

264.   Sharma, S.M., Fuchsluger, T., Ahmad, S., Katikireddy, K.R., Armant, M., Dana, R., & Jurkunas, U.V. (2012). Comparative analysis of human-derived feeder layers with 3T3 fibroblasts for the ex vivo expansion of human limbal and oral epithelium. *Stem Cell Rev Rep*, *8*(3), 696-705.

265.   Sheth, R., Neale, M.H., Shortt, A.J., Massie, I., Vernon, A.J., & Daniels, J.T. (2015).

Culture and Characterization of Oral Mucosal Epithelial Cells on a Fibrin Gel for Ocular Surface Reconstruction. *Curr Eye Res*, *40*(11), 1077-1087.

266. Shortt, A.J., Secker, G.A., Munro, P.M., Khaw, P.T., Tuft, S.J., & Daniels, J.T. (2007). Characterization of the limbal epithelial stem cell niche: novel imaging techniques permit in vivo observation and targeted biopsy of limbal epithelial stem cells. *Stem Cells*, *25*(6), 1402-1409.

267. Shortt, A.J., Secker, G.A., Rajan, M.S., Meligonis, G., Dart, J.K., Tuft, S.J., & Daniels, J.T. (2008). Ex vivo expansion and transplantation of limbal epithelial stem cells. *Ophthalmology*, *115*(11), 1989-1997.

268. Sinn, H.P., Schneeweiss, A., Keller, M., Schlombs, K., Laible, M., Seitz, J., Lakis, S., Veltrup, E., Altevogt, P., Eidt, S., Wirtz, R.M., & Marmé, F. (2017). Comparison of immunohistochemistry with PCR for assessment of ER, PR, and Ki-67 and prediction of pathological complete response in breast cancer. *BMC Cancer*, *17*(1), 124.

269. Soleimani, M., Cheraqpour, K., Koganti, R., Baharnoori, S.M., & Djalilian, A.R. (2023). Concise Review: Bioengineering of Limbal Stem Cell Niche. *Bioengineering (Basel)*, *10*(1), 111.

270. Sotozono, C., Inatomi, T., Nakamura, T., Koizumi, N., Yokoi, N., Ueta, M., Matsuyama, K., Kaneda, H., Fukushima, M., & Kinoshita, S. (2014). Cultivated oral mucosal epithelial transplantation for persistent epithelial defect in severe ocular surface diseases with acute inflammatory activity. *Acta Ophthalmol*, *92*(6), e447-53.

271. Spadea, L., Maraone, G., Verboschi, F., Vingolo, E.M., & Tognetto, D. (2016). Effect of corneal light scatter on vision: a review of the literature. *Int J Ophthalmol*, *9*(3), 459-464.

272. Spotnitz, W.D. (2014). Fibrin Sealant: The Only Approved Hemostat, Sealant, and Adhesive-a Laboratory and Clinical Perspective. *ISRN Surg*, *2014*, 203943.

273. Squier, C., & Brogden, K. (2011). *Human Oral Mucosa: Development, Structure and Function*. Wiley.

274. Squier, C.A., & Kremer, M.J. (2001). Biology of Oral Mucosa and Esophagus. *JNCI Monographs*, *2001*(29), 7-15.

275. Sridhar, M.S. (2018). Anatomy of cornea and ocular surface. *Indian J Ophthalmol*, *66*(2), 190-194.

276. Srinivas, S.P. (2010). Dynamic regulation of barrier integrity of the corneal endothelium. *Optom Vis Sci*, *87*(4), E239-54.

277. Stadnikova, A., Trosan, P., Skalicka, P., Utheim, T.P., & Jirsova, K. (2019). Interleukin-13 maintains the stemness of conjunctival epithelial cell cultures prepared from human limbal explants. *PLoS One*, *14*(2), e0211861.

278. Stanzel, B.V., Liu, Z., Somboonthanakij, S., Wongsawad, W., Brinken, R., Eter, N., Corneo, B., Holz, F.G., Temple, S., Stern, J.H., & Blenkinsop, T.A. (2014). Human RPE stem cells grown into polarized RPE monolayers on a polyester matrix are maintained after grafting into rabbit subretinal space. *Stem Cell Reports*, *2*(1), 64-77.

279. Sterenczak, K.A., Winter, K., Sperlich, K., Stahnke, T., Linke, S., Farrokhi, S., Klemm, M., Allgeier, S., Köhler, B., Reichert, K.M., Guthoff, R.F., Bohn, S., & Stachs, O. (2021). Morphological characterization of the human corneal epithelium by in vivo confocal laser scanning microscopy. *Quant Imaging Med Surg*, *11*(5), 1737-1750.

280. Sui, X., Wen, C., Yang, J., Guo, H., Zhao, W., Li, Q., Zhang, J., Zhu, Y., & Zhang, L. (2019). Betaine Combined with Membrane Stabilizers Enables Solvent-Free Whole Blood Cryopreservation and One-Step Cryoprotectant Removal. *ACS Biomater Sci Eng*, *5*(2), 1083-1091.

281. Sumida, K., Igarashi, Y., Toritsuka, N., Matsushita, T., Abe-Tomizawa, K., Aoki, M., Urushidani, T., Yamada, H., & Ohno, Y. (2011). Effects of DMSO on gene expression in human and rat hepatocytes. *Hum Exp Toxicol*, *30*(10), 1701-1709.

282. Sun, X., & Kaufman, P.D. (2018). Ki-67: more than a proliferation marker. *Chromosoma*, *127*(2), 175-186.

283. Svobodova, A., Horvath, V., Smeringaiova, I., Cabral, J.V., Zemlickova, M., Fiala, R., Burkert, J., Nemetova, D., Stadler, P., Lindner, J., Bednar, J., & Jirsova, K. (2022). The healing dynamics of non-healing wounds using cryo-preserved amniotic membrane. *Int Wound J*, *19*(5), 1243-1252.

284. Svobodova, A., Vrkoslav, V., Smeringaiova, I., & Jirsova, K. (2023). Distribution of an analgesic palmitoylethanolamide and other N-acylethanolamines in human placental membranes. *PLoS One*, *18*(1), e0279863.

285. Takács, L., Tóth, E., Berta, A., & Vereb, G. (2009). Stem cells of the adult cornea: From cytometric markers to therapeutic applications. *Cytometry Part A*, *75A*(1), 54-66.

286. Tekkatte, C., Gunasingh, G.P., Cherian, K.M., & Sankaranarayanan, K. (2011). "Humanized" stem cell culture techniques: the animal serum controversy. *Stem Cells Int*, *2011*, 504723.

287. Thoft, R.A., & Friend, J. (1983). The X, Y, Z hypothesis of corneal epithelial maintenance. *Invest Ophthalmol Vis Sci*, *24*(10), 1442-1443.

288. Tiwari, A., Loughner, C.L., Swamynathan, S., & Swamynathan, S.K. (2017). KLF4 Plays an Essential Role in Corneal Epithelial Homeostasis by Promoting Epithelial Cell Fate and Suppressing Epithelial-Mesenchymal Transition. *Invest Ophthalmol Vis Sci*, *58*(5), 2785-2795.

289. Torricelli, A.A., Singh, V., Santhiago, M.R., & Wilson, S.E. (2013). The corneal epithelial basement membrane: structure, function, and disease. *Invest Ophthalmol Vis Sci*, *54*(9), 6390-6400.

290. Toshida, H., Kasahara, T., Kiriyama, M., Iwasaki, Y., Sugita, J., Ichikawa, K., Ohta, T., & Miyahara, K. (2023). Early Clinical Outcomes of the First Commercialized Human Autologous Ex Vivo Cultivated Oral Mucosal Epithelial Cell Transplantation for Limbal Stem Cell Deficiency: Two Case Reports and Literature Review. *IJMS*, *24*(10), 8926.

291. Townsend, W.M. (1991). The limbal palisades of Vogt. *Trans Am Ophthalmol Soc*, *89*, 721-756.

292. Tra, W.M., van Neck, J.W., Hovius, S.E., van Osch, G.J., & Perez-Amodio, S. (2012). Characterization of a three-dimensional mucosal equivalent: similarities and differences with native oral mucosa. *Cells Tissues Organs*, *195*(3), 185-196.

293. Trosan, P., Cabral, J.V., Smeringaiova, I., Studeny, P., & Jirsova, K. (2022). Interleukin-13 increases the stemness of limbal epithelial stem cells cultures. *PLoS One*, *17*(8), e0272081.

294. Tsai, R.J., Li, L.M., & Chen, J.K. (2000). Reconstruction of damaged corneas by transplantation of autologous limbal epithelial cells. *N Engl J Med*, *343*(2), 86-93.

295. Tuan, T.L., Song, A., Chang, S., Younai, S., & Nimni, M.E. (1996). In vitro fibroplasia: matrix contraction, cell growth, and collagen production of fibroblasts cultured in fibrin gels. *Exp Cell Res*, *223*(1), 127-134.

296. Utheim, T.P. (2015). Concise review: transplantation of cultured oral mucosal epithelial cells for treating limbal stem cell deficiency-current status and future perspectives. *Stem Cells*, *33*(6), 1685-1695.

297. Utheim, T.P., Utheim, Ø.A., Khan, Q.E., & Sehic, A. (2016). Culture of Oral Mucosal

Epithelial Cells for the Purpose of Treating Limbal Stem Cell Deficiency. *J Funct Biomater*, *7*(1), 5.

298. Valiente, M.R., Nicolás, F.J., García-Hernández, A.M., Fuente Mora, C., Blanquer, M., Alcaraz, P.J., Almansa, S., Merino, G.R., Lucas, M.D.L., Algueró, M.C., Insausti, C.L., Piñero, A., Moraleda, J.M., & Castellanos, G. (2018). Cryopreserved amniotic membrane in the treatment of diabetic foot ulcers: a case series. *J Wound Care*, *27*(12), 806-815.

299. Vattulainen, M., Ilmarinen, T., Viheriälä, T., Jokinen, V., & Skottman, H. (2021). Corneal epithelial differentiation of human pluripotent stem cells generates ABCB5$^+$ and ΔNp63α^+ cells with limbal cell characteristics and high wound healing capacity. *Stem Cell Res Ther*, *12*(1), 609.

300. Vélez-Bermúdez, I.C., & Schmidt, W. (2014). The conundrum of discordant protein and mRNA expression. Are plants special. *Front Plant Sci*, *5*, 619.

301. Vodenkova, S., Azqueta, A., Collins, A., Dusinska, M., Gaivão, I., Møller, P., Opattova, A., Vodicka, P., Godschalk, R.W.L., & Langie, S.A.S. (2020). An optimized comet-based in vitro DNA repair assay to assess base and nucleotide excision repair activity. *Nat Protoc*, *15*(12), 3844-3878.

302. Vrkoslav, V., Smeringaiova, I., Smorodinova, N., Svobodova, A., Strnad, S., Jackson, C.J., Burkert, J., & Jirsova, K. (2023). Quantification of Analgesic and Anti-Inflammatory Lipid Mediators in Long-Term Cryopreserved and Freeze-Dried Preserved Human Amniotic Membrane. *Bioengineering (Basel)*, *10*(6), 740.

303. Wang, W., Li, S., Xu, L., Jiang, M., Li, X., Zhang, Y., Tighe, S., Zhu, Y., & Li, G. (2020). Differential Gene Expression between Limbal Niche Progenitors and Bone Marrow Derived Mesenchymal Stem Cells. *Int J Med Sci*, *17*(4), 549-557.

304. Weisel, J.W. (2005). Fibrinogen and fibrin. *Adv Protein Chem*, *70*, 247-299.

305. Weiskirchen, S., Schröder, S.K., Buhl, E.M., & Weiskirchen, R. (2023). A Beginner's Guide to Cell Culture: Practical Advice for Preventing Needless Problems. *Cells*, *12*(5), 682.

306. West, J.D., Dorà, N.J., & Collinson, J.M. (2015). Evaluating alternative stem cell hypotheses for adult corneal epithelial maintenance. *World J Stem Cells*, *7*(2), 281-299.

307. Winning, T.A., & Townsend, G.C. (2000). Oral mucosal embryology and histology. *Clinics in Dermatology*, *18*(5), 499-511.

308. Witzeneder, K., Lindenmair, A., Gabriel, C., Höller, K., Theiß, D., Redl, H., & Hennerbichler, S. (2013). Human-derived alternatives to fetal bovine serum in cell culture. *Transfus Med Hemother*, *40*(6), 417-423.

309. Yang, A., Kaghad, M., Wang, Y., Gillett, E., Fleming, M.D., Dötsch, V., Andrews, N.C., Caput, D., & McKeon, F. (1998). p63, a p53 homolog at 3q27-29, encodes multiple products with transactivating, death-inducing, and dominant-negative activities. *Mol Cell*, *2*(3), 305-316.

310. Yang, J., Cai, N., Zhai, H., Zhang, J., Zhu, Y., & Zhang, L. (2016). Natural zwitterionic betaine enables cells to survive ultrarapid cryopreservation. *Sci Rep*, *6*, 37458.

311. Yang, J., Gao, L., Liu, M., Sui, X., Zhu, Y., Wen, C., & Zhang, L. (2020). Advanced Biotechnology for Cell Cryopreservation. *Transactions of Tianjin University*, *26*(6), 409-423.

312. Yazdanpanah, G., Haq, Z., Kang, K., Jabbehdari, S., Rosenblatt, M.L., & Djalilian, A.R. (2019). Strategies for reconstructing the limbal stem cell niche. *Ocul Surf*, *17*(2), 230-240.

313. Yeh, H.J., Yao, C.L., Chen, H.I., Cheng, H.C., & Hwang, S.M. (2008).

Cryopreservation of human limbal stem cells ex vivo expanded on amniotic membrane. *Cornea*, *27*(3), 327-333.

314. Yin, J., & Jurkunas, U. (2018). Limbal Stem Cell Transplantation and Complications. *Semin Ophthalmol*, *33*(1), 134-141.

315. Yoon, J.J., Ismail, S., & Sherwin, T. (2014). Limbal stem cells: Central concepts of corneal epithelial homeostasis. *World J Stem Cells*, *6*(4), 391-403.

316. Yoshida, S., Shimmura, S., Kawakita, T., Miyashita, H., Den, S., Shimazaki, J., & Tsubota, K. (2006). Cytokeratin 15 can be used to identify the limbal phenotype in normal and diseased ocular surfaces. *Invest Ophthalmol Vis Sci*, *47*(11), 4780-4786.

317. Yu, M., Bojic, S., Figueiredo, G.S., Rooney, P., de Havilland, J., Dickinson, A., Figueiredo, F.C., & Lako, M. (2016). An important role for adenine, cholera toxin, hydrocortisone and triiodothyronine in the proliferation, self-renewal and differentiation of limbal stem cells in vitro. *Exp Eye Res*, *152*, 113-122.

318. Zdraveva, E., Bendelja, K., Bočkor, L., Dolenec, T., & Mijović, B. (2023). Detection of Limbal Stem Cells Adhered to Melt Electrospun Silk Fibroin and Gelatin-Modified Polylactic Acid Scaffolds. *Polymers (Basel)*, *15*(3), 777.

319. Zhang, S., & Cui, W. (2014). Sox2, a key factor in the regulation of pluripotency and neural differentiation. *World J Stem Cells*, *6*(3), 305-311.

320. Zhao, B., Allinson, S.L., Ma, A., Bentley, A.J., Martin, F.L., & Fullwood, N.J. (2008). Targeted cornea limbal stem/progenitor cell transfection in an organ culture model. *Invest Ophthalmol Vis Sci*, *49*(8), 3395-3401.

321. Zhao, G., & Fu, J. (2017). Microfluidics for cryopreservation. *Biotechnol Adv*, *35*(2), 323-336.

322. Zhu, P., Zhu, X., Wu, J., He, L., Lu, T., Wang, Y., Liu, B., Ye, B., Sun, L., Fan, D., Wang, J., Yang, L., Qin, X., Du, Y., Li, C., He, L., Ren, W., Wu, X., Tian, Y., & Fan, Z. (2019). IL-13 secreted by ILC2s promotes the self-renewal of intestinal stem cells through circular RNA circPan3. *Nat Immunol*, *20*(2), 183-194.

323. Zsebik, B., Ujlaky-Nagy, L., Losonczy, G., Vereb, G., & Takács, L. (2017). Cultivation of Human Oral Mucosal Explants on Contact Lenses. *Curr Eye Res*, *42*(8), 1094-1099.

10. Appendices

10.1. Appendix 1: List of Materials for Limbal Epithelial Cell Culture

3.1.1 Culture of Limbal Explants on Nanofibrous Membranes, page 46

Product	Company	Catalog Number
70% Ethanol	Penta	E03801
PBS pH 7.4 (10x)	Gibco	70011-036
Fibronectin	Sigma-Aldrich	10838039001
DMEM/F12 (1:1, GlutaMAX)	Gibco	31331-028
100x Antibiotic-antifungal solution	Gibco	15240-062
12 Well TC-Treated Polystyrene Permeable Support Companion Plate	Falcon	353503

3.1.2 Preparation of Fibrin Gel, page 47

		Concentration after reconstitution	Dilute in PBS	Final concentration after dilution (ready to use)
Component 1	Human Fibrinogen (Sealer protein lyophilized Concentrate)	91 mg/ml	1 ml (reconstituted sol.) + 8 ml PBS	Fibrinogen 10mg/ml
Solvent for component 1	Aprotinin solution	3000 KIU/ml		Aprotinin 333 KIU/ml
Component 2	Human thrombin (Thrombin lyophilized)	500 IU/ml	0.5 ml (reconstituted sol.) + 24.5 ml PBS	Thrombin 10 IU/ml
Solvent for component 2	$CaCl_2$	40 µmol/ml		$CaCl_2$ 0.8 µmol/ml

3.1.4 Explant Culture, page 48

Product	Company	Catalog Number
DMEM/F12 (1:1, GlutaMAX)	Gibco	31331-028
100x Antibiotic-antifungal solution	Gibco	15240-062
100nm Cholera Toxin	Sigma	C8052
Human serum	Bio&Sell	HU.SE.0500
Fetal bovine serum	Gibco	10500-064
Insulin-Transferrin-Selenium (100x)	Gibco	41400-045
Hydrocortisone	VUAB Pharma A.S., Roztoky	256084
Adenin hydrochlorid	Sigma	A9795
EGF	Gibco	PH60311L
Tranexamic Acid	Supelco	PHR1812
Well TC-Treated Polystyrene Permeable Support Companion Plate	Falcon	353503

3.1.5 Reverse Transcription-Quantitative Real-Time Polymerase Chain Reaction (RT-qPCR), page 48

Product	Company	Catalog Number
Dispase II	Gibco	17105-041
TrypLE™ Express	Gibco	12604021
Dual Chamber Cell counting slides	Bio-Rad	1450011
Trypan blue dye 0.40%	Bio-Rad	1450013
TC20™ Automated Cell Counter	Bio-Rad	1450102
Universal 32 R centrifuge	Hettich Zentrifugen	1610
RNeasy® Micro Kit	Qiagen	74004
Eppendorf Biophotometer Spectrophotometer	Eppendorf	6131
iScript cDNA synthesis kit	Bio-Rad	1708890
Hard Shell 96-well PCR plate	Bio-Rad	HSR9901
SsoAdvanced Universal SYBR Green Supermix RT-qPCR Kit	Bio-Rad	1725270
CFX Connect Real-Time PCR Detection System	Bio-Rad	1855201

3.1.5 Reverse Transcription-Quantitative Real-Time Polymerase Chain Reaction (RT-qPCR), page 48

Gene name, Gene symbol	Forward Primer	Reverse Primer	Size (bp)
Hypoxanthine phosphoribosyltransferase 1, *HPRT1*	TCTTTGCTGACCTGCTGGATTAC	GTCTGCATTGTTTTGCCAGTGTC	214
Ribosomal protein L32, *RPL32*	CTCAGACCCCTTGTGAAGCC	TTGCTTCCATAACCAATGTTGG	179
POU class 5 homeobox 1, *OCT4*	AGAAGTGGGTGGAGGAAGCTG	CCAGGTTGCCTCTCACTCG	123
SRY-box transcription factor 2, *SOX2*	GCTAGTCTCCAAGCGACGAAA	GCCTCTCCTTGAAAAATATTGGC	137
Krüppel like factor 4, *KLF4*	CCACACTTGTGATTACGCGG	GAATTTCCATCCACAGCCGT	127
Marker of proliferation Ki-67, *MKI67*	CTTTGGGTGCGACTTGACG	GTCGACCCCGCTCCTTTT	199
Tumor protein p63, *ΔNp63α*	TATCCGCATGCAGGACTCG	GAGCCAGAAGAAAGGACAGCAG	127
ATP binding cassette subfamily G member 2 (Junior blood group), *ABCG2*	GAGCCTACAACTGGCTTAGACTCAA	TGATTGTTCGTCCCTGCTTAGAC	85
ATP-binding cassette sub-family B member 5, *ABCB5*	CAGCAAGGGAAGCAAATGC	GGGTTTCGAACTAAGGCACG	139
Keratin 3, *KRT3*	GGATGTGGACAGTGCCTATATGAA	AGCACCACAGATGTGTCACTGAT	144
Keratin 7, *KRT7*	ATGGAGTGGGAGCCGTGAA	AGCCTTCAGGAGCCCAGG	146
Keratin 8, *KRT8*	CGAGATCGCCACCTACAGGA	CGAGATCGCCACCTACAGGA	116
Keratin *12, KRT12*	GGAGATCGAGCTACAGTCCCA	TCCAGGTTGCTGATGAGCTG	120
Keratin 14, *KRT14*	TCTCCTCTGGATCGCAGTCA	GCCTCAGTTCTTGGTGCGA	131
Keratin 15, *KRT15*	AGGGCCTGAATGAGGAGCTAG	CCTCATCTCTGCCAGCACAC	146
Integrin subunit beta 1, *ITGB1*	ACATTTGAGTGTGGCGCGT	CACACTGTCCGCAGACGC	163

Nerve growth factor receptor, *NGFR*	CGTATTCCGACGAGGCCA	ACCGTGTAATCCAACGGCC	138
CCAAT enhancer binding protein delta, *CEBPD*	GAGAACGAGAAGCTGCACCAG	TGAGGTATGGGTCGTTGCTG	170
Leucine rich repeats and immunoglobulin like domains 1, *LRIG1*	CCGTGGCTAATTGGCAGG	TGTCCTTGCCCACCATAGC	178
Insulin like growth factor binding protein 5, *IGFBP5*	AGCTACCGCGAGCAAGTCAA	TCGGAGATGCGGGTGTGT	125
Actin alpha 2, smooth muscle, *ACTA2*	CTTTGCTGGGGACGATGC	TCCCATTCCCACCATCACC	85
CD34 molecule, *CD34*	GGCATCTGCCTGGAGCAA	CACCTCAGACTGGGCAAGGA	153
Thy-1 cell surface antigen, *THY1*	TCCCCACCCATCTCCTCC	CGAGGTGTTCTGAGCCAGC	90
Visual system homeobox 2, *VSX2*	AAGAAACGGAAGAAGCGGC	TGGGTAGTGGGCTTCGTTG	91
Fibulin 1, *FBLN1*	CTGCGAATGCAAGACGGG	CAGCGTGTTCTCGCACTTGT	115

10.2. Appendix 2: List of Materials for Oral Mucosa Epithelial Cell Culture

3.2.1 Oral Mucosal Tissue Retrieval, page 50

Product	Company	Catalog Number
Betadine 100 mg/ml	Egis	32/389/92-S/C
NaCl 0.9% 1000 ml	B. Braun	2305960
BASE•128	Alchimia	BAS 006-00
6-mm biopsy punch	Kai Medical	BP-60F

3.2.5 Preparation of Cell Suspension, page 53

Product	Company	Catalog Number
BASE•128	Alchimia	BAS 006-00
PBS pH 7.4 (10x)	Gibco	70011-036
DMEM/F12 (1:1, GlutaMAX)	Gibco	31331-028
100x Antibiotic-antifungal solution	Gibco	15240-062
100nm Cholera Toxin	Sigma	C8052
Human serum	Bio&Sell	HU.SE.0500
Fetal bovine serum	Gibco	10500-064
Insulin-Transferrin-Selenium (100x)	Gibco	41400-045
Hydrocortisone	VUAB Pharma A.S., Roztoky	256084
Adenin hydrochlorid	Sigma	A9795
Triiodothyronine	Sigma	T6397
EGF	Gibco	PH60311L
Tranexamic Acid	Supelco	PHR1812
Dispase II	Gibco	17105-041
0.05% Trypsin-EDTA (1X)	Gibco	25300-054
RNAlater™	Sigma	R0901
Millex-GV Filter, 0.22 µm, PVDF, 13 mm	Merck Millipore	SLGVR13SL
Tissue Culture Plates 24 wells, sterile	VWR	734-2325
Petri dish 35mm, Sterile	Nunc	153066
Petri dish 60mm, Sterile	VWR	10062-890

Cell scraper (11mm blade)	Corning	C5981-100EA
pluriStrainer Mini 70 µm (Cell Strainer)	PluriSelect	43-10070-60
Dual Chamber Cell counting slides	Bio-Rad	1450011
Trypan blue dye 0.40%	Bio-Rad	1450013
TC20™ Automated Cell Counter	Bio-Rad	1450102
Universal 32 R centrifuge	Hettich Zentrifugen	1610

3.2.8 Harvesting Cultured Cells after Cell Confluence, page 55

Product	Company	Catalog Number
PBS pH 7.4 (10x)	Gibco	70011-036
Dispase II	Gibco	17105-041
DMEM/F12 (1:1, GlutaMAX)	Gibco	31331-028
TrypLE™ Express	Gibco	12604-021
Millex-GV Filter, 0.22 µm, PVDF, 13 mm	Merck Millipore	SLGVR13SL
Dual Chamber Cell counting slides	Bio-Rad	1450011
Trypan blue dye 0.40%	Bio-Rad	1450013
TC20™ Automated Cell Counter	Bio-Rad	1450102
Universal 32 R centrifuge	Hettich Zentrifugen	1610
RNeasy® Micro Kit	Qiagen	74004
Eppendorf Biophotometer Spectrophotometer	Eppendorf	6131
iScript cDNA synthesis kit	Bio-Rad	1708890
Hard Shell 96-well PCR plate	Bio-Rad	HSR9901
SsoAdvanced Universal SYBR Green Supermix RT-qPCR Kit	Bio-Rad	1725270
CFX Connect Real-Time PCR Detection System	Bio-Rad	1855201

3.2.4 Hematoxylin and Eosin Staining, page 52

Product	Company	Catalog Number
Hematoxylin Harris	Penta	14680-11000
Eosin Y	Merck	17372-87-1
Ethanol 96% p.a.	Penta	70390-11001
HCl 35%	Penta	7647-01-0
Ethanol 100%	Penta	71250-11001

Solakryl	Penta	2001280115
Xylene	Lach-ner s.r.o.	1330-20-7
Aquatex	Merck	1.08562.0050
OCT cryomount	Penta	00890-EX
Ethanol 70%	Penta	70392-11001
Carbol-xylene	Penta	180407V

3.2.10 Immunofluorescence, page 56

Product	Company	Catalog Number
Tween® 20	Sigma-Aldrich	P1379
Triton X® 100	Roth	3051.3
Normal Goat serum	Cell Signaling Technology	5425
Bovine Serum Albumin	Sigma	A9647
PBS pH 7.4 (10x)	Gibco	70011-036
DAPI	Invitrogen	
Mowiol® 4-88	Aldrich	81381
Superfrost® Plus	Thermo Scientific	J1800AMNZ
Paraformladehyde	Fluka Chemical	76240

3.2.11 Reverse Transcription Quantitative Real-time PCR (RT-qPCR), page 58

Gene name, Gene symbol	Forward Primer	Reverse Primer	Size (bp)
Hypoxanthine phosphoribosyltransferase 1, *HPRT1*	TCTTTGCTGACCTGCTGGATTAC	GTCTGCATTGTTTTGCCAGTGTC	214
Ribosomal protein L32, *RPL32*	CTCAGACCCCTTGTGAAGCC	TTGCTTCCATAACCAATGTTGG	179
POU class 5 homeobox 1, *OCT4*	AGAAGTGGGTGGAGGAAGCTG	CCAGGTTGCCTCTCACTCG	123
SRY-box transcription factor 2, *SOX2*	GCTAGTCTCCAAGCGACGAAA	GCCTCTCCTTGAAAAATATTGGC	137
Krüppel like factor 4, *KLF4*	CCACACTTGTGATTACGCGG	GAATTTCCATCCACAGCCGT	127
Nanog homeobox, *NANOG*	CAGAACTGTGTTCTCTTCCACCC	CCATTGCTATTCTTCGGCCA	198
Paired box 6, *PAX6*	GCCAGGGCAACCTACGC	TCTATTTCTTTGCAGCTTCCGC	139
Marker of proliferation Ki-67, *MKI67*	CTTTGGGTGCGACTTGACG	GTCGACCCCGCTCCTTTT	199

Proliferating cell nuclear antigen, *PCNA*	TCTGCAAGTGGAGAAC TTGGAA	TTCAGGTACCTCAGT GCAAAAGTTAG	131
Tumor protein p63, *ΔNp63α*	TATCCGCATGCAGGAC TCG	GAGCCAGAAGAAAG GACAGCAG	127
ATP binding cassette subfamily G member 2 (Junior blood group), *ABCG2*	GAGCCTACAACTGGCT TAGACTCAA	TGATTGTTCGTCCCTG CTTAGAC	85
Keratin 3, *KRT3*	GGATGTGGACAGTGCC TATATGAA	AGCACCACAGATGTG TCACTGAT	144
Keratin 7, *KRT7*	ATGGAGTGGGAGCCGT GAA	AGCCTTCAGGAGCCC AGG	146
Keratin 8, *KRT8*	CGAGATCGCCACCTAC AGGA	AGCTCAGACCACCTG CATAGC	116
Keratin *12, KRT12*	GGAGATCGAGCTACAG TCCCA	TCCAGGTTGCTGATG AGCTG	120
Keratin 13, *KRT13*	GAAGATCCGTGACTGG CACC	TCCAGGATGACCCGG TTGT	135
Keratin 14, *KRT14*	TCTCCTCTGGATCGCA GTCA	GCCTCAGTTCTTGGT GCGA	131
Keratin 17, *KRT17*	GGATGCCCACCTGACT CAGTA	GATGACCTTGCCATC CTGGA	91
Keratin 15, *KRT15*	AGGGCCTGAATGAGGA GCTAG	CCTCATCTCTGCCAG CACAC	146
Keratin 19, *KRT19*	CGAGCTAGAGGTGAAG ATCCG	TGTCGATCTGCAGGA CAATCC	152
Aldehyde dehydrogenase 3 family member A1, *ALDH3A1*	GAGATCTTCGGGCCTG TGC	CCACCCCACCACTGG ATG	160
Nestin, *NESTIN*	GGCTGCGGGCTACTGA AA	AGCGATCTGGCTCTG TAGGC	80
Integrin subunit beta 1, *ITGB1*	ACATTTGAGTGTGGCG CGT	CACACTGTCCGCAGA CGC	163
Nerve growth factor receptor, *NGFR*	CGTATTCCGACGAGGC CA	ACCGTGTAATCCAAC GGCC	138
Leucine rich repeats and immunoglobulin like domains 1, *LRIG1*	CCGTGGCTAATTGGCA GG	TGTCCTTGCCCACCA TAGC	178
Insulin like growth factor binding protein 5, *IGFBP5*	AGCTACCGCGAGCAAG TCAA	TCGGAGATGCGGGTG TGT	125

10.3. Appendix 3: Interleukin-13 increases the stemness of limbal epithelial stem cells cultures

Interleukin-13 increases the stemness of limbal epithelial stem cells cultures

Peter Trosan[1,2]☺*, **Joao Victor Cabral**[1]☺, **Ingrida Smeringaiova**[1], **Pavel Studeny**[3], **Katerina Jirsova**[1]

1 Laboratory of the Biology and Pathology of the Eye, First Faculty of Medicine, Institute of Biology and Medical Genetics, Charles University and General University Hospital in Prague, Prague, Czech Republic, **2** Department of Ophthalmology, Rostock University Medical Center, Rostock, Germany, **3** Ophthalmology Department of 3rd Medical Faculty and University Hospital Kralovske Vinohrady, Prague, Czech Republic

☺ These authors contributed equally to this work.
*peter.trosan@med.uni-rostock.de

Abstract

This study aimed to determine the effect of interleukin-13 (IL13) on the stemness, differentiation, proliferation, clonogenicity, and morphology of cultured limbal epithelial cells (LECs). Human limbal explants were used to culture LECs up to the second passage (P0-P2) with or without IL13 (IL13+ and IL13-, respectively). Cells were analyzed by qPCR (for the expression of ΔNp63α, BMI-1, keratin (K) 3, K7, K12, K14, K17, mucin 4, and MKI67) and immunofluorescence staining for p63α. The clonogenic ability was determined by colony-forming assay (CFA), and their metabolic activity was measured by WST-1 assay. The results of the CFA showed a significantly increased clonogenic ability in P1 and P2 cultures when LECs were cultured with IL13. In addition, the expression of putative stem cell markers (ΔNp63α, K14, and K17) was significantly higher in all IL13+ cultures compared to IL13-. Similarly, immunofluorescence analysis showed a significantly higher percentage of p63α positive cells in P2 cultures with IL13 than without it. LECs cultures without IL13 lost their cuboidal morphology with a high nucleocytoplasmic ratio after P1. The use of IL13 also led to significantly higher proliferation in P2, which can be reflected by a higher ability to reach confluence in P2 cultures. On the other hand, IL13 had no effect on corneal epithelial cell differentiation (K3 and K12 expression), and the expression of the conjunctival marker K7 significantly increased in all IL13+ cultures compared to the respective cell culture without IL13. This study showed that IL13 enhanced the stemness of LECs by increasing the clonogenicity and the expression of putative stem cell markers of LECs while maintaining their stem cell morphology. We established IL13 as a culture supplement for LESCs, which increases their stemness potential in culture, even after the second passage, and may lead to the greater success of LESCs transplantation in patients with LSCD.

Introduction

The corneal epithelium undergoes continuous renewal throughout life but has a limited capacity to renew itself[1]. Maintenance of the epithelium is provided by a population of limbal

epithelial stem cells (LESCs), which reside in the basal layer of the limbus, the transition zone between the cornea and the conjunctiva [2]. LESCs are slow cycling and divide asymmetrically to self-renew and differentiate to maintain the corneal epithelium [3,4]. The limbus provides a unique environment—niche, which is morphologically complex with dense innervation and vascularization [5,6]. The niche of stem cells plays a crucial role in cell division, proliferation, differentiation, migration, and maintaining their stemness. It consists of cells, the extracellular matrix, cytokines, and growth factors [7]. As already demonstrated, various growth factors could induce LESCs proliferation and migration [8–11], regulation of apoptosis [12], or differentiation [13]. Because the properties of stem cells are unique, it is challenging to mimic their environment outside the niche. Therefore, the usage of LESCs for a more prolonged culture and its possible application in treatment are limited.

It is crucial for scientific and therapeutic use to search for endogenous factors that could prolong the culture of LESCs. Supplementation of culture medium with NGF extended the life span of LESCs cultures *in vitro* and increased the expression of LESCs' putative markers *ΔNp63α* and *ABCG2* [14]. The expression of the *p63* gene is crucial for the stemness of LESCs [15]. While *TP63* transactivated isoforms (TAp63) participate in senescence and metabolism [16], the β and μ isoforms of *ΔNp63* gene play a role in epithelial differentiation during corneal regeneration, and the α variant is responsible for maintaining the stem/progenitor cells [15]. A higher percentage of the stem cell marker p63 in the sheets of transplanted limbal epithelial cells (LECs) was shown to be related to the success rate of transplantation in patients with limbal stem cell deficiency (LSCD) [17].

Our previous work found a positive effect of interleukin-13 (IL13) on proliferative activity and *ΔNp63α* gene expression in the conjunctival epithelium generated from limbal explants [18]. The effect of IL13 on increasing the expression of the *ΔNp63α* gene in conjunctival cultures leads to the idea of its role in maintaining stemness and using it as part of the medium for the culture of LESCs from limbal explants.

As a T helper 2-type cytokine, which regulates the responses of lymphocytes, myeloid cells, and nonhematopoietic cells [19], IL13 is considered one of the anti-inflammatory interleukins. The effect of IL13 on LESCs or stem cells in general is not widely studied. It is essential during early myelopoiesis when, together with the stem cell factor (SCF), it induces the proliferation of Lin-Sca-1+ progenitor cells and, together with the granulocyte-macrophage-SCF, enhances their colony formation [20]. Similarly as with IL4, IL13 can activate the STAT6 signaling pathway [19], which leads to increased clonogenic potential of prostate stem-like cells [21]. Recently, secreted IL13 was found to promote intestinal stem cell self-renewal by initiating the Foxp1 transcription factor expression, associated with the β-catenin signaling pathway responsible for maintaining their stemness [22]. Together with our observation of the role of IL13 in the stemness of conjunctival epithelial cells, it makes IL13 a promising stem cell research target. In this study, we investigated the role of IL13 in the stemness, differentiation, clonogenicity, and proliferation of LESCs.

Materials and methods

Donor corneal tissue

The study adhered to the tenets set out in the Declaration of Helsinki. Donor tissue procurement met all Czech legal requirements, including the absence of the donor in the national register of persons opposed to postmortem withdrawal of tissues and organs. On the use of the corneoscleral rim based on Czech legislation on specific health services (Law Act No. 372/2011 Coll.), informed consent is not required if the presented data are anonymized in the form. Forty corneoscleral rims were obtained from cadaver donor corneas within 24 h after death

and stored in Eusol-C preservation medium (Alchimia, Padova, Italy) until transplantation. The mean donor age ± standard deviation (SD) was 59.3 ± 9.9 (range 41–75 years).

Preparation of limbal explants and cell culture

The donor corneoscleral rims were washed three times in Dulbecco's modified Eagle's medium (DMEM)/F12 (1:1, GlutaMAX) containing 1% of 100×Antibiotic-Antimycotic (AA, Thermo Fisher Scientific, Waltham, MA, USA). Then each corneoscleral rim was cut into 12 pieces (approximately 2 ×3 mm) and washed three times in DMEM/F12 medium with 1% AA. Six explants were placed directly on the plastic bottom of the 24-well plate (one explant per well), and six pieces were placed on Thermanox plastic cell culture coverslips (Nunc, Thermo Fisher Scientific, Rochester, NY, USA) present on the bottom of the wells. Cultures grown on coverslips were used for immunostaining, and the explant grown on plastic for all other experiments. Each explant was covered with 50 µl of complete medium consisting of 1:1 DMEM/F12, 10% FBS, 1% AA, 10 ng/ml recombinant EGF, 0.5% insulin-transferrin-selenium (Thermo Fisher Scientific), 5 µg/ml hydrocortisone, 10 µg/ml adenine hydrochloride and 10 ng/ml cholera toxin (Sigma-Aldrich, Darmstadt, Germany) and maintained at 37°C in 5% CO_2. Complete medium was changed every day until cell outgrowth was seen. The tissue was then covered with 250 µl of complete medium, which was changed three times a week until the cells were 90–100% confluent. Half of the donor explants were cultured in a complete medium supplemented with 10 ng/ml recombinant human IL13 (BioLegend, San Diego, CA, USA). Similarly, after passage, cells were cultured in a complete medium with (IL13+) or without IL13 (IL13-). When primary cultures (P0) and cells after passage 1 (P1) were 90–100% conflu-ent, cells were passaged using TrypLE Express (Gibco, Thermo Fisher Scientific). After detach-ing the culture, cells were seeded again on the plastic bottom or Thermanox coverslip in 24-well plates at concentrations of 1.5×10^4 cells per well. The rest of the cells were stored in Trizol (Molecular Research Center, Cincinnati, OH, USA) for subsequent RNA isolation. All experiments were carried out on P0, P1, and P2 cells and repeated at least three times.

Morphology, cell growth, and cell viability

Expanded LECs were monitored, and the beginning of cell outgrowth, confluence, cell mor-phology, viability and contamination by fibroblast-like cells were evaluated under an inverted microscope (Olympus CX41, Olympus, Tokyo, Japan). After each passage, cell viability was defined by staining with 0.4% trypan blue (Gibco, Thermo Fisher Scientific). Both unstained live cells and stained dead cells were counted with a hemocytometer and calculated as follows: viability (%) = live cells/ (live + dead cells) ×100. The percentage of successfully cultured rims was calculated as from how many corneoscleral rims the cell culture reached confluence to the total number of rims. The percentage of fibroblast-like cells contamination was calculated as how many cultures had contamination to the overall number of cultures. Culture is taken here as cell culture from one explant. From one rim 3 explants cultures were cultured with IL13 and 3 without. If one culture had fibroblast-like cell contamination, just other two were passaged to subsequent culture.

Preparation of mouse 3T3 feeder layer

The 3T3 mouse fibroblasts were cultured in DMEM supplemented with 10% FBS and 1% AA and kept at 37°C and 5% CO_2. At 80–90% confluence, 3T3 cells were treated with 12 µg/ml mitomycin-C Kyowa (NORDIC Pharma, Prague, Czech Republic) for 2 h at 37°C under 5% CO_2 to arrest cell growth. After incubation, cells were washed with PBS three times, detached

with TrypLE Express for 2 to 4 min, and seeded in a 6-well plate at a density of 3×10^5 cells per well. Cells were used within 24 h of preparation.

Colony-forming assay (CFA)

After reaching at least 80% confluence, the cell cultures were passaged to obtain a single-cell suspension. After P1 and P2, 1000 cultured cells were seeded in 6-well plates containing growth-arrested 3T3 mouse fibroblasts. All experiments were carried out at least in triplicate for each donor and condition (i.e., IL13- and IL13+). The LECs were kept at 37 ˚C and 5% CO_2, and after 12 days of culture, colonies were fixed with cold methanol for 30 min at -20˚C. Subsequently, the cells were rehydrated with PBS and stained for 5 min at 37˚C with 2% rho-damine B (Sigma-Aldrich). After that, rhodamine B was removed, and the colonies were washed with tap water until optimal staining intensity was achieved. The plates were photo-graphed and manually computed by using Fiji image processing software (https://imagej.net/Fiji). Only bright-purple colonies were counted, small dots were excluded. The colony growth was monitored during the colony-formation phase under a microscope. The total colony-forming efficiency (CFE) (%) was calculated using the following equation:

$$CFE(\%) = \frac{number\,of\,colonies}{number\,of\,seeded\,cells} \, x\,100$$

Immunocytochemistry

The cells for immunocytochemistry (ICC) cultured on Thermanox coverslips were at 90 −100% confluency fixed in 4% paraformaldehyde for 20 min at room temperature. Immuno-cytochemical staining was performed for the p63α isotype encoded by the tumor protein P63 gene, *TP63*. After fixation, the cell membranes were permeabilized with 0.33% Triton X-100 (Sigma-Aldrich) diluted in PBS, followed by a 1 h incubation at room temperature with pri-mary p63α antibody (Cell Signalling Technology, Danvers, MA, USA; cat. No: 4892) diluted in 0.1% bovine serum albumin. The cells were then rinsed three times in 0.5% Tween 20 and incubated for 1 h at room temperature with the Alexa Fluor 594 conjugated goat anti-rabbit IgG secondary antibody (Life Technologies, Eugene, OR, USA; cat. No. A11037). After rinsing three times in 0.5% Tween 20, followed by rinsing in PBS, cells were mounted with Vecta-Shield-DAPI (4´ 6-diamidino-2-phenylindole) (Vector Laboratories, Burlingame, CA, USA) to counterstain nuclear DNA. Cell samples were examined by fluorescence microscopy (Nikon ECLIPSE Ni-U, Nikon) at ×100 and ×200 magnifications. At least 1000 cells were eval-uated to calculate the percentage of positive cells.

Quantitative real-time polymerase chain reaction (qPCR)

The expression of the *GAPDH* (glyceraldehyde-3-phosphate dehydrogenase), *ΔNp63α*, *BMI-1*, *K3*, *K7*, *K12*, *K14*, *K17*, *mucin4* (*Muc4*), and *MKI67* genes was detected by qPCR. Cells were collected after each passage (P0-P2), transferred to Eppendorf tubes containing 500 μl of TRI Reagent (Molecular Research Center, Cincinnati, OH, USA), and total RNA was extracted according to the manufacturer's instructions, followed by reverse transcription, which has been described previously [18]. Briefly, 1 μg of RNA was treated with deoxyribonuclease I (Promega, Madison, WI, USA) and used for reverse transcription (RT). First-strand comple-mentary DNA (cDNA) was synthesized using M-MLV (Moloney murine leukemia virus) reverse transcriptase and random primers (Promega) in a total reaction volume of 25 μl.

The qPCR was performed in a CFX Connect Real-Time PCR Detection System (Bio-Rad, Hercules, CA, USA). The sequences of the primers used are summarized in Table 1. The

Table 1. Primers used for quantitative real-time PCR.

Gene (human)	Sequence ($5' \to 3'$)	GenBank accession number	Product size (bp)
GAPDH	F: GAAGGGGTCATTGATGGCAAC R: GGGAAGGTGAAGGTCGGAGTC	NM_001289746.1	108
ΔNp63α	F: GAGGTTGGGCTGTTCATCAT R: GAGGAGAATTCGTGGAGCTG	NM_001114980.1	174
BMI-1	F: GCTCGCATTCATTTTCTGCT R: ACACACATCAGGTGGGGATT	NM_005180.8	163
K3	F: GGATGTGGACAGTGCCTATATG R: AGATAGCTCAGCGTCGTAGAG	NM_057088.2	106
K7	F: AGGATGTGGTGGAGGACTTC R: CTTGCTCATGTAGGCAGCAT	NM_005556.3	116
K12	F: CCAGGTGAGGTCAGCGTAGAA R: CCTCCAGGTTGCTGATGAGC	NM_005556.3	352
K14	F: TTCTGAACGAGATGCGTGAC R: GCAGCTCAATCTCCAGGTTC	NM_000526.4	189
K17	F: GCTGCTACAGCTTTGGCTCT R: GACGGGCATTGTCAATCTGT	NM_000422.2	315
MUC4	F: TCCGTGTCCTGCTGGATAACC R: GTTGCGGCTCAGGAGGACTC	NM_018406.6	104
MKI67	F: CTTTGGGTGCGACTTGACG R: GTCGACCCCGCTCCTTTT	NM_002417	199

https://doi.org/10.1371/journal.pone.0272081.t001

sequence specificity of all primers was confirmed via BLAST(http://www.ncbi.nlm.nih.gov/blast/). Conventional reverse transcription PCR was performed to confirm that only a single band was obtained. The PCR products were electrophoresed on 1% agarose gels containing GelRed Nucleic Acid Gel Stain (Biotium, Fremont, CA, USA). The qPCR parameters included initial denaturation at 95 °C for 2 min, 40 cycles of denaturation at 95 °C for 5 s, and annealing at 60 °C for 30 s. Fluorescence was monitored at 55 to 95 °C at 0.5 °C intervals for 5 s. Each experiment was carried out in triplicate. A relative quantification model was used to calculate the expression of the target gene expression compared to GAPDH, used as the endogenous control.

Determination of the proliferation activity

The proliferation activity of living cells was determined by the WST-1 assay, as described before [23]. In brief, the LECs(15×10^3 cells/ well) were cultured in a complete DMEM medium with or without IL13 in a 96-well tissue culture plate (VWR, Radnor, PA, USA) for 7 days at 37°C in an atmosphere of 5% CO_2. WST-1 reagent (Roche, Mannheim, Germany) was added to each well (10 μl/100 μl of medium), and plates were incubated for another 1 h to form formazan. A formazan-containing medium (100 μl) was transferred from each well into a new 96-well tissue culture plate. The absorbance was measured using a Tecan Infinite M200 (Tecan, Mannedorf, Switzerland) at a wavelength of 450 nm.

Statistical analysis

Statistical analysis was performed with GraphPad Prism (GraphPad Software, La Jolla, CA, USA). Descriptive statistics are reported as N (number of values), mean ±SD, or the median with quartile range. Data sets were analyzed by Mann–Whitney U nonparametric test. P-values < 0.05 were considered statistically significant.

Results

Limbal epithelial cell growth and morphology

LECs P0 cultures started to outgrow from limbal explants mostly on the fifth day, and 90–100% confluence was achieved after 14 days regardless of the presence of IL13 (Fig 1A). P1 and P2 cultures reached confluence significantly earlier than P0, but there was no difference whether the cells were cultured with or without IL13 (Fig 1D). The cell viability after passaging was comparable between the cultures (Fig 1E). The percentage of successful cultures decreased
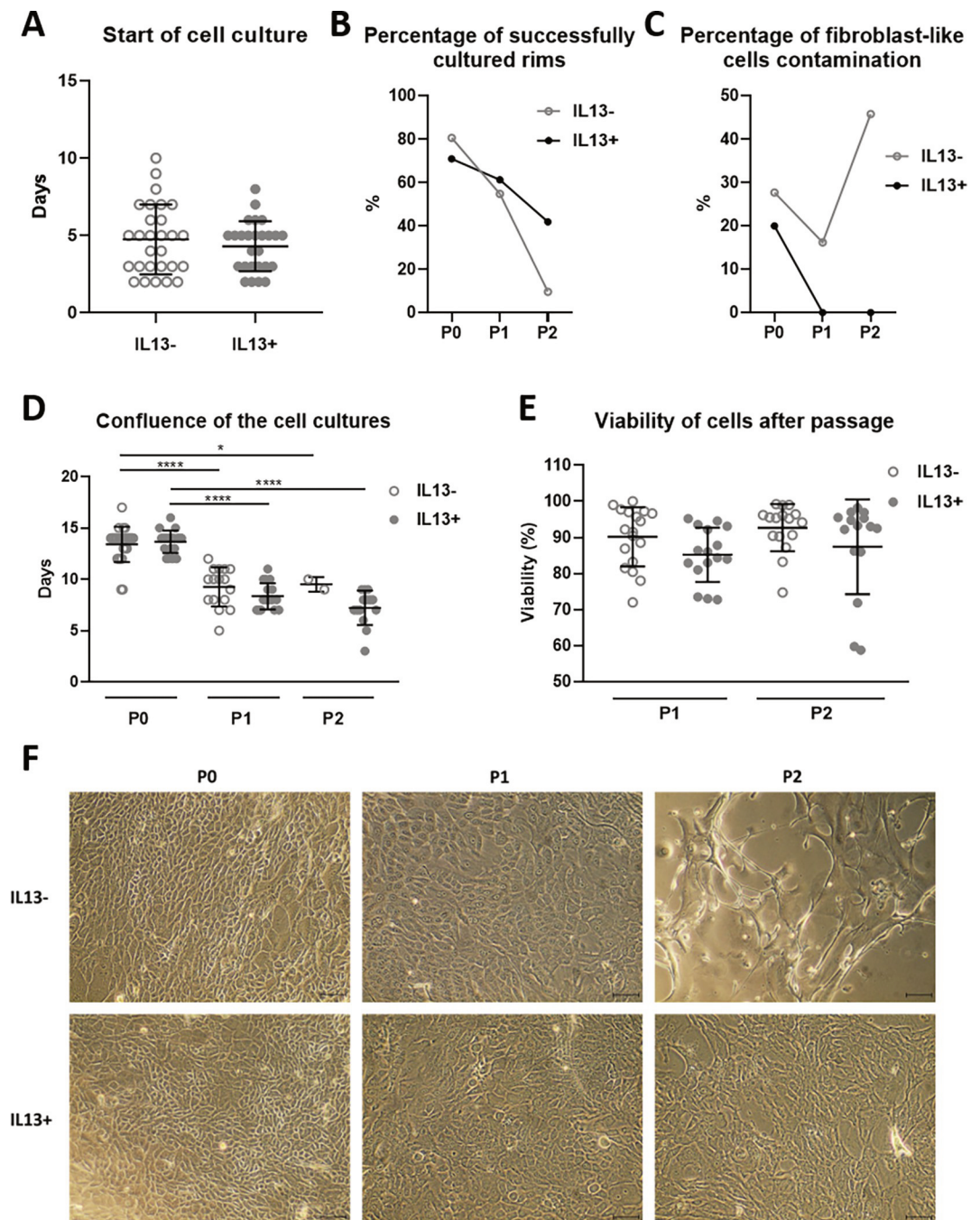
Fig 1. The growth and morphology of IL13-and IL13+cell cultures. (A) The beginning of the outgrowth of LEC cultures from day 0 (D) to reaching full confluence in P0, P1, and P2 cultures. (B) The percentage of successfully cultured corneoscleral rims. (C) The percentage of fibroblast-like cells contamination in cell cultures. (E) Percentages of cell viability after the first and second passages. (F) Cell morphology was observed at the end of cultivation of P0, P1, and P2 cultures under an inverted phase-contrast microscope. Scalebars: 50 μm.

https://doi.org/10.1371/journal.pone.0272081.g001

throughout the cell culture from P0 to P1 and P2 (Fig 1B). The most noticeable difference was after P2, where 9.7% of IL13- cultures reached confluence, compared to 42% in the IL13 + group. This fact is also reflected in the morphology of cells. Typical cuboidal morphology of
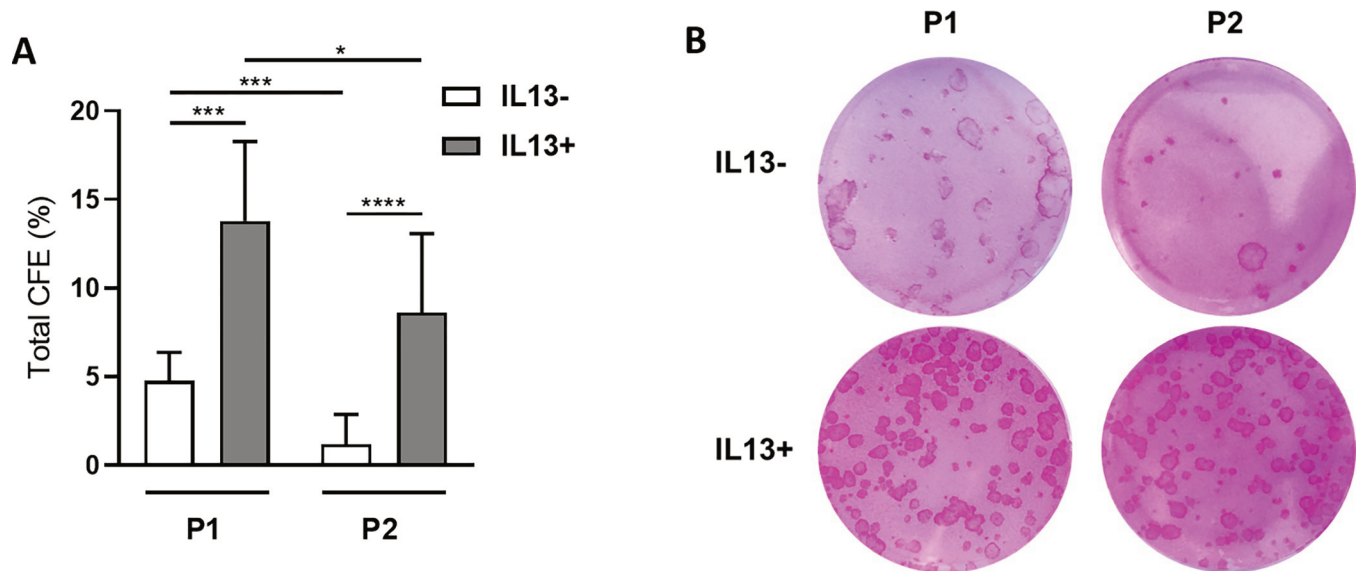
Fig 2. Comparison of total CFE. After the first and second passages (P1 and P2), cells were cultured with growth-arrested 3T3 mouse fibroblasts to compare their growth capacity under IL13- and IL13+ conditions. (A) Distribution of total CFE percentages of the P1 and P2 groups. Each bar represents the mean ±SD from 7 to 13 determinations. The asterisks represent a statistically significant difference between the examined groups (P 0.05, P 0.001, P 0.0001). (B) The colonies were stained with 2% rhodamine B.

https://doi.org/10.1371/journal.pone.0272081.g002

LECs with a high nucleocytoplasmic ratio was visible in all cultures, except P2 IL13- cultures, where cells were more flattened or fibroblast-like morphology with a low nucleocytoplasmic ratio (Fig 1F). The contamination by fibroblast-like cells was higher in the P0 group without than P0 with IL13 (27.7% and 20% respectively). Cell cultures without IL13 had a low percentage of contamination in P1 (16.2%) but increased in P2 (45.8%). On the contrary, the fibroblast-like cell contamination was not observed in P1 and P2 cultures with IL13 (Fig 1C).

CFA

The CFA was performed for P1 and P2 cultures (Fig 2). A significantly higher growth potential was observed in the P1 and P2 IL13+ groups (mean 13.79% and 8.63% respectively) than the P1 and P2 IL13- cultures (mean 4.78% and 1.19% respectively), $P<0.001$ and $P<0.0001$ respectively. The decrease of the number of colonies was between both passages and IL13 groups, more significant in IL13- than in IL13+ cultures ($P< 0.001$ vs. $P<0.05$).

Expression of limbal stem cell markers

The *ΔNp63α* gene expression was significantly higher in all cultures (P0, P1, and P2) with IL13 compared to the cells cultured without it ($P<0.001$, $P<0.001$, $P<0.01$, respectively). A consistent decrease of *ΔNp63α* gene expression was observed during the LECs culture with significance between P0-P1 and P1-P2 cultures in the IL13- (both $P<0.01$) and IL13+ ($P< 0.05$, $P<0.001$ respectively) groups. A slightly higher expression of the *BMI-1* gene was observed in P0 IL13+ cultures compared to IL13- cells with no statistical significance. The *BMI-1* expression values in P1 and P2 cultures were comparable. The gene expressions of *K14* were significantly higher in the IL13+ groups P0 ($P<0.05$) and P1 ($P<0.001$) than controls without IL13. The expression decreased significantly between P0 and P1 cultures without IL13 ($P<0,05$). A decreased *K17* gene expression tendency was found throughout the cell culture with statistical significance between the P0 IL13+ culture and the P1 and P2 IL13+ groups, respectively (both
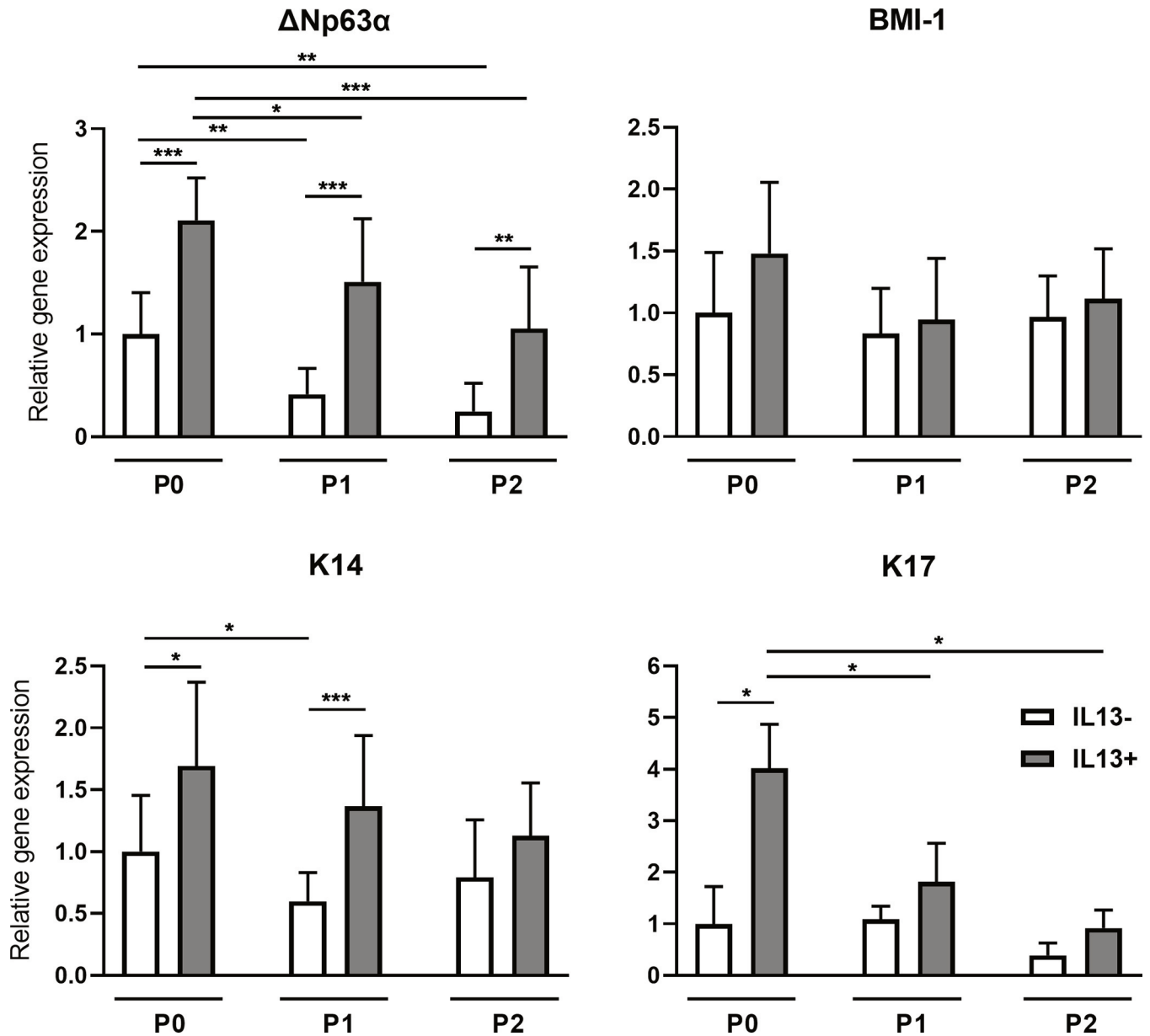
Fig 3. Relative gene expression of *ΔNp63α*, *BMI-1*, *K14*, and *K17* in IL13- and IL13+ cell cultures. Cells originating from limbal explants (P0) and passaged cells (P1 and P2) were analyzed at the end of the culture for *p63α*, *BMI-1*, *K14*, and *K17* gene expression by qPCR. Each bar represents the mean ±SD of three to ten determinations. The asterisks represent statistically significant difference between the examined groups (P < 0.05, P 0.01, P 0.001).

P<0.05). The expression of the *K17* gene was significantly higher in samples with IL13 in P0 (P<0.05) compared to samples without IL13 (Fig 3).

Immunocytochemical staining for p63

Cells positive for the p63 protein were detected in all cultures and conditions (Fig 4A). The percentage of p63 positive cells significantly decreased during cell culture without IL13 (mean values 94.86%, 91.65%, and 75.55% for P0, P1, and P2 cultures, respectively; P<0.05). Cell cultures with IL13 had a similar expression of p63 in all passages (mean values 96.23%, 95.54%,

Fig 4. Immunostaining for the putative limbal stem cell marker p63α in IL13- and IL13+ cell cultures. (A) Cells were analyzed by immunofluorescent staining for p63α (red) at the end of P0-P2 cultures. Nuclei were counterstained with DAPI (blue). Scale bars: 20 μm. (B) Distribution of percentages in the P0, P1, and P2 groups for p63α staining. Each bar represents the mean ±SD of three to eight determinations. The asterisks represent a statistically significant difference between the examined groups (P ≤ 0.05).

https://doi.org/10.1371/journal.pone.0272081.g004

A — MKI67

B — WST-1 assay

Fig 5. Relative gene expression of *MKI67* and WST-1 assay in IL13- and IL13+ cell cultures. (A) Cells originating from limbal explants (P0) and passaged cells (P1 and P2) at the end of culture were analyzed for *MKI67* gene expression by qPCR. Each bar represents the mean ±SD of five to ten determinations. (B) Measurement of cell proliferation after the first and second passages (P1 and P2). The WST-1 reagent was added to the cell cultures for 1 h to form formazan. The absorbance was measured at a wavelength of 450 nm via optical density. Each bar represents the mean ±SD of eight to ten determinations. The asterisks represent a statistically significant difference between the examined groups (P 0.01).
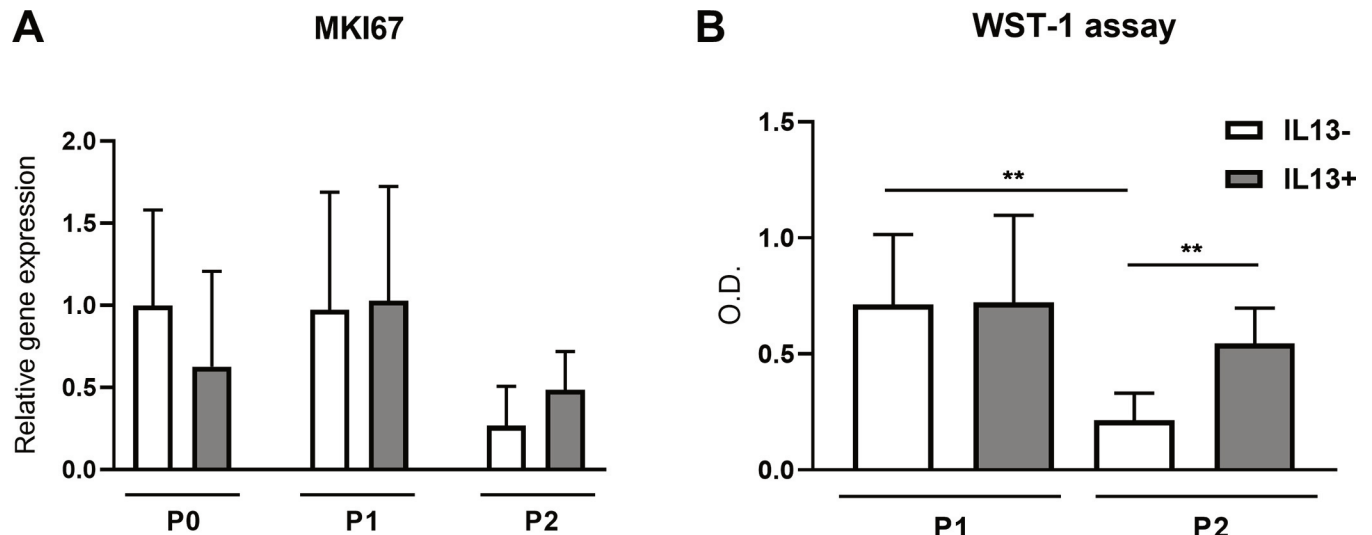
and 90.69% for P0, P1, and P2 cultures, respectively). A significantly higher percentage of p63 + cells were measured in P2 IL13+ compared to P2 IL13- culture (P<0.05) (Fig 4B).

LECs proliferation and metabolic activity

The proliferation of cultured LECs was determined by gene expression analysis of *MKI67* and WST-1 assay (Fig 5). No significant difference was observed between the evaluated groups for *MKI67* gene expression. No difference was found between IL13+ and IL13- groups in P1, but significantly higher proliferation was determined in P2 IL13+ compared to P2 IL13- (P<0.01) according to WST-1 assay. The significant decrease of the proliferation activity was measured between P1 and P2 cultures without IL13 (P<0.01).

Presence of differentiation markers

K3 and *K12* genes specific for the corneal epithelium were expressed in all groups at very low levels with no difference and significance. Conjunctival *K7* gene expression was higher in all IL13+ cell passages compared to IL13- cultures, significantly in P0 and P1 (both P<0.05). The *MUC4* gene was expressed in all groups with a significant decrease between passages P0 and P2 and between P1 and P2 in IL13- conditions (P<0.05) (Fig 6).

Discussion

In this study, we explore the potential of IL13 to improve the properties of cultured LECs, particularly in terms of their stemness and use for the treatment of LSCD. Our results showed that IL13 significantly increases stemness of LECs after P1 and P2, as shown by the CFA, by the expression of putative stem cell markers (*ΔNp63α*, *K14*, and *K17*), and by immunocytochemistry (p63α). Besides the increase in stemness, there was no change in the morphology, but cell proliferation was significantly higher after P2 cultures with IL13 compared to without IL13.
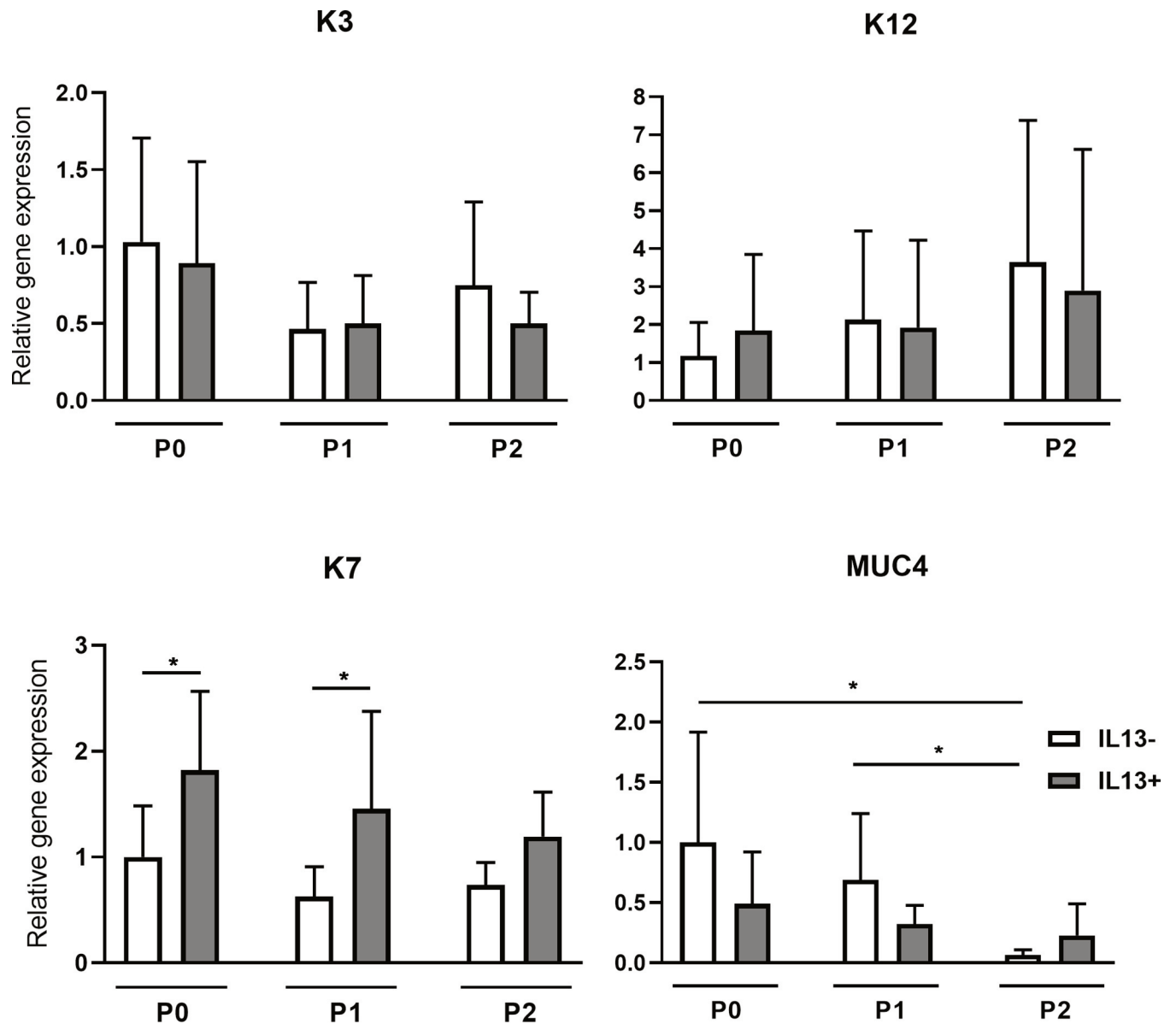
Fig 6. Relative gene expression of *K3*, *K12*, *K7*, and *MUC4* in IL13- and IL13+ cell cultures. Cells originating from limbal explants (P0) and passaged cells (P1 and P2) at the end of culture were analyzed for the expression of *K3*, *K12*, *K7*, and *MUC4* genes by qPCR. Each bar represents the mean ±SD of four to ten determinations. The asterisks represent a statistically significant difference between the examined groups (P< 0.05).

The clonogenic activity of our LESCs cultures without IL13 was about 5% after the first passage, decreasing to 1% after the second passage. This percentage was higher than the clonogenic activity in conjunctival cultures or limbal explants in previous studies [18,24]. Cultures with IL13 had significantly higher clonogenic capacity after both passages than the related passage of cultures without IL13. The higher clonogenic activity of IL13+ cultures corresponds to increased gene expression of the putative stem cell marker p63α. Previously, it was reported that coexpression of C/EBPΔ, BMI-1, and ΔNp63α identified mitotically quiescent limbal stem cells, which generate holoclones in culture [25].

Furthermore, human holoclone-forming cells have been shown to be only located in the limbus [26,27], and that more than 3% of p63 positive cells from total clonogenic cells in the

culture led to successful transplantation in patients with LSCD. Therefore, clonogenic activity is an important indicator of stem cells, as the competence for the continued proliferation of stem cells in tissues is required for normal tissues' continued integrity and function [28]. The time-dependent decrease in clonogenicity is consistent with the observation of other studies; a 4-day culture of LECs led to differentiation and loss of almost all the capacity for colony formation [14]. The loss of clonogenic properties in transient amplifying cells during culture was also found by Pellegrini et al. [26]. Moreover, a decreased number of cells with p63 stemness factor was observed during a more extended culture of LECs from limbal explants [29]. It looks like a typical stem cell process. The clonogenic activity decreased rapidly in our LECs cultures from 5% after P1 to 1% after P2. The preservation of clonogenicity and stemness due to IL13 also corresponds to the cuboidal morphology of cultured cells that had a high nucleo-cytoplasmic ratio during all cultures. On the contrary, LESCs cultures without IL13 lost their morphology after the second passage, consistent with other works [14,18]. Fibroblast-like cells contamination was lower or not present in cultures with IL13, and the epithelial phenotype was predominant compared to cultures without IL13. Still, more studies are necessary to analyze whether IL13 inhibits fibroblasts' outgrowth directly or the lower contamination is because of higher stemness in the IL13 cultures.

Our gene expression analysis showed that LECs culture with IL13 increased the expression of K14, K17, and most importantly, ΔNp63α stem cell markers, which are generally used to indicate stemness in LESCs cultures [30–33]. However, according to immunohistochemistry, the percentage of p63 positive cells showed a significant difference between cultures with or without IL13 only in P2, in which a slight increase in p63 positive cells was observed in IL13 + cells compared to IL13- culture. The discrepancy between qPCR and immunostaining findings has been previously found [34,35]. It can be explained by immunostaining analysis showing only the number of positive cells and not the amount of protein expressed. In addition, the antibody is less specific than the qPCR primers due to the six isoforms of the *p63* gene and the minor differences between them.

Generally, LESCs are slow-cycling during homeostasis and highly proliferative in case of injury [36]. Our gene expression analysis of the *MKI67* gene, which is involved in cell proliferation, showed weak expression and no difference between cultures with or without IL13 in all passages. Joyce et al. showed in the study of the expression of MKI67 in the human cornea by indirect immunofluorescence localization that most LECs did not present this marker of cell proliferation [37]. A similar observation was found in the study of limbal explant cultures, in which epithelial cells were positive for MKI67 in the first week of culture, but most expression disappeared by 3 weeks when cells migrating from explants reached confluence [29]. They hypothesized that MKI67 expression indicates the proliferative status of cells in a certain time but not the proliferation capacity of cells, as they showed a decrease in MKI67 staining in cells from confluent cultures [29]. This is in accordance with the weak gene expression of MKI67 in our cultures, as we measured the expression after the passage when cells were about to reach the confluence. Therefore, we also used another measurement of cell proliferation, the WST-1 assay, which showed no difference in cell proliferation between P1 and P2 IL13+ cultures. However, a substantially higher proliferation of IL13+ than IL13- cultures after the second passage indicates their potential to be used as a graft even after passage. This observation follows the weak potential of LECs after P2 without IL13 to reach confluence.

The gene expression of corneal epithelial markers K3 and K12 did not differ between the IL13- and IL13+ cultures. The expressions of these genes were weak, and we did not observe any changes leading to differentiation into the corneal epithelial phenotype. In contrast to our findings, some works showed 60–80% positivity of K3 and K12 in LESCs cultures [24,38]. The low expression of corneal epithelial factors can be explained as a positive effect of IL13, as the

culture cells did not differentiate into the corneal epithelial phenotype but retained their stemness. Nevertheless, it is unclear whether cells with a differentiated corneal epithelial phenotype in the graft are more important for transplant success than the presence of a niche with cells with varying degrees of differentiation [39].

Here we show that culture influenced by IL13 led to a higher differentiation into conjunctival phenotype, as we measured a higher gene expression of the *K7* gene in all cultures (P0-P2). K7 is considered a marker of the conjunctival epithelium [40]. The same differentiation potential of IL13 was observed in conjunctival cultures from limbal explants [18]. Interestingly, the expression of another conjunctival marker, MUC4, was not affected by the addition of IL13 and decreased significantly during passages. Because conjunctival cells have also been used for the successful treatment of LSCD, the presence of K7 is unlikely to adversely affect the quality of the graft. Our previous results with conjunctival epithelial cells showed that partial differentiation to the conjunctival phenotype was expected [18]. However, unlike corneal conjunctivalization, which includes a vascularized pannus that overgrows on the cornea in LSCD-affected eyes, these transplanted conjunctival epithelial cells do not have any associated fibrous or vascular tissue [41].

IL13 is essential during early myelopoiesis. However, its role in the stemness of LESCs or other cell types was unknown. The first findings were made in conjunctival cell cultures from limbal explants, where IL13 maintained the stemness of the cultures by increasing their clonal capacity and p63α expression [18]. The detailed signaling pathway for this mechanism is unclear. A similar observation of maintaining stemness via IL13–IL13R (IL13 receptor) was recently described in intestinal stem cells (ISCs) [22]. They found that the circular RNA molecule circPan3 bounds the mRNA encoding the cytokine IL13R subunit IL13Rα1 in ISCs to increase the stability of the receptor. IL13 then binds to IL13R, which initiates the expression of the transcription factor Foxp1. Foxp1 is associated with the β-catenin signaling pathway, causing activation of this pathway and maintenance of ISCs. The deletion of circPan3 in ISCs led to impaired stem cell self-renewal capacity and regeneration of the intestinal epithelium [22]. IL13 can induce through IL4Rα present in the human corneal epithelial cells the expression of various genes, such as *HAS3*, encoding hyaluronan synthases; hyaluronan in the extracellular matrix has been shown to control epithelial proliferation and regeneration [42,43]. The Wnt/β-catenin signaling is also present in the ocular surface epithelium and plays an important role in regulating LESCs proliferation [41]; further investigation of this signaling pathway would better explain the whole mechanism of IL13 in LESCs.

This study showed that IL13 enhanced the stemness of LESCs by increasing the clonogenicity and the expression of putative stem cell markers of LECs while maintaining their stem cell morphology. We established IL13 as a culture supplement for LESCs, which increases their stemness potential in culture, even after the second passage, and may lead to greater success of LECs transplantations in patients with LSCD.

Author Contributions

Conceptualization: Peter Trosan, Joao Victor Cabral, Katerina Jirsova.

Data curation: Peter Trosan, Joao Victor Cabral.

Formal analysis: Joao Victor Cabral, Katerina Jirsova.

Funding acquisition: Katerina Jirsova.

Investigation: Peter Trosan, Joao Victor Cabral, Ingrida Smeringaiova, Pavel Studeny, Katerina Jirsova.

Methodology: Peter Trosan, Joao Victor Cabral, Ingrida Smeringaiova.

Project administration: Katerina Jirsova.

Supervision: Katerina Jirsova.

Validation: Peter Trosan, Joao Victor Cabral, Pavel Studeny, Katerina Jirsova.

Visualization: Peter Trosan.

Writing – original draft: Peter Trosan, Joao Victor Cabral.

Writing – review & editing: Katerina Jirsova.

References

1. Ebato B, Friend J, Thoft RA. Comparison of limbal and peripheral human corneal epithelium in tissue culture. Invest Ophthalmol Vis Sci. 1988 Oct; 29(10):1533–1537. PMID: 3170124

2. Schermer A, Galvin S, Sun TT. Differentiation-related expression of a major 64K corneal keratin in vivo and in culture suggests limbal location of corneal epithelial stem cells. J Cell Biol. 1986 Jul; 103(1):49–62. https://doi.org/10.1083/jcb.103.1.49 PMID: 2424919

3. Cotsarelis G, Cheng SZ, Dong G, Sun TT, Lavker RM. Existence of slow-cycling limbal epithelial basal cells that can be preferentially stimulated to proliferate: implications on epithelial stem cells. Cell. 1989 Apr 21; 57(2):201–209. https://doi.org/10.1016/0092-8674(89)90958-6 PMID: 2702690

4. Castro-Muñozledo F, Gómez-Flores E. Challenges to the study of asymmetric cell division in corneal and limbal epithelia. Exp Eye Res. 2011 Jan; 92(1):4–9. https://doi.org/10.1016/j.exer.2010.11.002 PMID: 21056036

5. Van Buskirk EM. The anatomy of the limbus. Eye (Lond). 1989 Jan 1; 3 (Pt 2):101–108. https://doi.org/10.1038/eye.1989.16 PMID: 2695343

6. Meyer PA. The circulation of the human limbus. Eye (Lond). 1989; 3 (Pt 2):121–127. https://doi.org/10.1038/eye.1989.19 PMID: 2695346

7. Zhang Y, Sun H, Liu Y, Chen S, Cai S, Zhu Y, et al. The limbal epithelial progenitors in the limbal niche environment. Int J Med Sci. 2016 Oct 18; 13(11):835–840. https://doi.org/10.7150/ijms.16563 PMID: 27877075

8. Gospodarowicz D, Mescher AL, Brown KD, Birdwell CR. The role of fibroblast growth factor and epidermal growth factor in the proliferative response of the corneal and lens epithelium. Exp Eye Res. 1977 Dec; 25(6):631–649. https://doi.org/10.1016/0014-4835(77)90142-7 PMID: 304011

9. Daniels JT, Limb GA, Saarialho-Kere U, Murphy G, Khaw PT. Human corneal epithelial cells require MMP-1 for HGF-mediated migration on collagen I. Invest Ophthalmol Vis Sci. 2003 Mar; 44(3):1048–1055. https://doi.org/10.1167/iovs.02-0442 PMID: 12601028

10. Sotozono C, Inatomi T, Nakamura M, Kinoshita S. Keratinocyte growth factor accelerates corneal epithelial wound healing in vivo. Invest Ophthalmol Vis Sci. 1995 Jul; 36(8):1524–1529. PMID: 7601632

11. Lee HK, Lee JH, Kim M, Kariya Y, Miyazaki K, Kim EK. Insulin-like growth factor-1 induces migration and expression of laminin-5 in cultured human corneal epithelial cells. Invest Ophthalmol Vis Sci. 2006 Mar; 47(3):873–882. https://doi.org/10.1167/iovs.05-0826 PMID: 16505019

12. Kakazu A, Chandrasekher G, Bazan HEP. HGF protects corneal epithelial cells from apoptosis by the PI-3K/Akt-1/Bad- but not the ERK1/2-mediated signaling pathway. Invest Ophthalmol Vis Sci. 2004 Oct; 45(10):3485–3492. https://doi.org/10.1167/iovs.04-0372 PMID: 15452053

13. Trosan P, Svobodova E, Chudickova M, Krulova M, Zajicova A, Holan V. The key role of insulin-like growth factor I in limbal stem cell differentiation and the corneal wound-healing process. Stem Cells Dev. 2012 Dec 10; 21(18):3341–3350. https://doi.org/10.1089/scd.2012.0180 PMID: 22873171

14. Kolli S, Bojic S, Ghareeb AE, Kurzawa-Akanbi M, Figueiredo FC, Lako M. The Role of Nerve Growth Factor in Maintaining Proliferative Capacity, Colony-Forming Efficiency, and the Limbal Stem Cell Phenotype. Stem Cells. 2019; 37(1):139–149. https://doi.org/10.1002/stem.2921 PMID: 30599086

15. Pellegrini G, Dellambra E, Golisano O, Martinelli E, Fantozzi I, Bondanza S, et al. p63 identifies keratinocyte stem cells. Proc Natl Acad Sci USA. 2001 Mar 13; 98(6):3156–3161. https://doi.org/10.1073/pnas.061032098 PMID: 11248048

16. Di Iorio E, Barbaro V, Ruzza A, Ponzin D, Pellegrini G, De Luca M. Isoforms of DeltaNp63 and the migration of ocular limbal cells in human corneal regeneration. Proc Natl Acad Sci USA. 2005 Jul 5; 102(27):9523–9528. https://doi.org/10.1073/pnas.0503437102 PMID: 15983386

17. Rama P, Matuska S, Paganoni G, Spinelli A, De Luca M, Pellegrini G. Limbal stem-cell therapy and long-term corneal regeneration. N Engl J Med. 2010 Jul 8; 363(2):147–155. https://doi.org/10.1056/NEJMoa0905955 PMID: 20573916

18. Stadnikova A, Trosan P, Skalicka P, Utheim TP, Jirsova K. Interleukin-13 maintains the stemness of conjunctival epithelial cell cultures prepared from human limbal explants. PLoS One. 2019 Feb 11; 14 (2):e0211861. https://doi.org/10.1371/journal.pone.0211861 PMID: 30742646

19. Junttila IS. Tuning the Cytokine Responses: An Update on Interleukin (IL)-4 and IL-13 Receptor Complexes. Front Immunol. 2018 Jun 7; 9:888. https://doi.org/10.3389/fimmu.2018.00888 PMID: 29930549

20. Jacobsen SE, Okkenhaug C, Veiby OP, Caput D, Ferrara P, Minty A. Interleukin 13: novel role in direct regulation of proliferation and differentiation of primitive hematopoietic progenitor cells. J Exp Med. 1994 Jul 1; 180(1):75–82. https://doi.org/10.1084/jem.180.1.75 PMID: 7516418

21. Nappo G, Handle F, Santer FR, McNeill RV, Seed RI, Collins AT, et al. The immunosuppressive cytokine interleukin-4 increases the clonogenic potential of prostate stem-like cells by activation of STAT6 signalling. Oncogenesis. 2017 May 29; 6(5):e342. https://doi.org/10.1038/oncsis.2017.23 PMID: 28553931

22. Zhu P, Zhu X, Wu J, He L, Lu T, Wang Y, et al. IL-13 secreted by ILC2s promotes the self-renewal of intestinal stem cells through circular RNA circPan3. Nat Immunol. 2019 Jan 14; 20(2):183–194. https://doi.org/10.1038/s41590-018-0297-6 PMID: 30643264

23. Trosan P, Javorkova E, Zajicova A, Hajkova M, Hermankova B, Kossl J, et al. The Supportive Role of Insulin-like Growth Factor-I in the Differentiation of Murine Mesenchymal Stem Cells into Corneal-like Cells. Stem Cells Dev. 2016 Apr 6; 25(11):874–881. https://doi.org/10.1089/scd.2016.0030 PMID: 27050039

24. López-Paniagua M, Nieto-Miguel T, de la Mata A, Dziasko M, Galindo S, Rey E, et al. Comparison of functional limbal epithelial stem cell isolation methods. Exp Eye Res. 2016 May; 146:83–94. https://doi.org/10.1016/j.exer.2015.12.002 PMID: 26704459

25. Barbaro V, Testa A, Di Iorio E, Mavilio F, Pellegrini G, De Luca M. C/EBPdelta regulates cell cycle and self-renewal of human limbal stem cells. J Cell Biol. 2007 Jun 18; 177(6):1037–1049. https://doi.org/10.1083/jcb.200703003 PMID: 17562792

26. Pellegrini G, Golisano O, Paterna P, Lambiase A, Bonini S, Rama P, et al. Location and clonal analysis of stem cells and their differentiated progeny in the human ocular surface. J Cell Biol. 1999 May 17; 145 (4):769–782. https://doi.org/10.1083/jcb.145.4.769 PMID: 10330405

27. Majo F, Rochat A, Nicolas M, Jaoudé GA, Barrandon Y. Oligopotent stem cells are distributed throughout the mammalian ocular surface. Nature. 2008 Nov 13; 456(7219):250–254. https://doi.org/10.1038/nature07406 PMID: 18830243

28. Franken NAP, Rodermond HM, Stap J, Haveman J, van Bree C. Clonogenic assay of cells in vitro. Nat Protoc. 2006; 1(5):2315–2319. https://doi.org/10.1038/nprot.2006.339 PMID: 17406473

29. Joseph A, Powell-Richards AOR, Shanmuganathan VA, Dua HS. Epithelial cell characteristics of cultured human limbal explants. Br J Ophthalmol. 2004 Mar; 88(3):393–398. https://doi.org/10.1136/bjo.2003.018481 PMID: 14977776

30. Kramerov AA, Saghizadeh M, Maguen E, Rabinowitz YS, Ljubimov AV. Persistence of reduced expression of putative stem cell markers and slow wound healing in cultured diabetic limbal epithelial cells. Mol Vis. 2015 Dec 30; 21:1357–1367. PMID: 26788028

31. Utheim O, Islam R, Lyberg T, Roald B, Eidet JR, de la Paz MF, et al. Serum-free and xenobiotic-free preservation of cultured human limbal cells. PLoS One. 2015 Mar 3; 10(3):e0118517. https://doi.org/10.1371/journal.pone.0118517 PMID: 25734654

32. Zhao B, Allinson SL, Ma A, Bentley AJ, Martin FL, Fullwood NJ. Targeted cornea limbal stem/progenitor cell transfection in an organ culture model. Invest Ophthalmol Vis Sci. 2008 Aug; 49(8):3395–3401. https://doi.org/10.1167/iovs.07-1263 PMID: 18441310

33. Saghizadeh M, Dib CM, Brunken WJ, Ljubimov AV. Normalization of wound healing and stem cell marker patterns in organ-cultured human diabetic corneas by gene therapy of limbal cells. Exp Eye Res. 2014 Dec; 129:66–73. https://doi.org/10.1016/j.exer.2014.10.022 PMID: 25446319

34. López-Paniagua M, Nieto-Miguel T, de la Mata A, Galindo S, Herreras JM, Corrales RM, et al. Consecutive expansion of limbal epithelial stem cells from a single limbal biopsy. Curr Eye Res. 2013 May; 38 (5):537–549. https://doi.org/10.3109/02713683.2013.767350 PMID: 23405945

35. Brejchova K, Trosan P, Studeny P, Skalicka P, Utheim TP, Bednar J, et al. Characterization and comparison of human limbal explant cultures grown under defined and xeno-free conditions. Exp Eye Res. 2018 Jun 19; 176:20–28. https://doi.org/10.1016/j.exer.2018.06.019 PMID: 29928900

36. Lehrer MS, Sun TT, Lavker RM. Strategies of epithelial repair: modulation of stem cell and transit amplifying cell proliferation. J Cell Sci. 1998 Oct; 111 (Pt 19):2867–2875. https://doi.org/10.1242/jcs.111.19.2867 PMID: 9730979

37. Joyce NC, Navon SE, Roy S, Zieske JD. Expression of cell cycle-associated proteins in human and rabbit corneal endothelium in situ. Invest Ophthalmol Vis Sci. 1996 Jul; 37(8):1566–1575. PMID: 8675399

38. Li Y, Yang Y, Yang L, Zeng Y, Gao X, Xu H. Poly(ethylene glycol)-modified silk fibroin membrane as a carrier for limbal epithelial stem cell transplantation in a rabbit LSCD model. Stem Cell Res Ther. 2017 Nov 7; 8(1):256. https://doi.org/10.1186/s13287-017-0707-y PMID: 29116027

39. Calonge M, Nieto-Miguel T, de la Mata A, Galindo S, Herreras JM, López-Paniagua M. Goals and Challenges of Stem Cell-Based Therapy for Corneal Blindness Due to Limbal Deficiency. Pharmaceutics. 2021 Sep 16; 13(9). https://doi.org/10.3390/pharmaceutics13091483 PMID: 34575560

40. Jirsova K, Dudakova L, Kalasova S, Vesela V, Merjava S. The OV-TL 12/30 clone of anti-cytokeratin 7 antibody as a new marker of corneal conjunctivalization in patients with limbal stem cell deficiency. Invest Ophthalmol Vis Sci. 2011 Jul 29; 52(8):5892–5898. https://doi.org/10.1167/iovs.10-6748 PMID: 21693612

41. Ang LPK, Tanioka H, Kawasaki S, Ang LPS, Yamasaki K, Do TP, et al. Cultivated human conjunctival epithelial transplantation for total limbal stem cell deficiency. Invest Ophthalmol Vis Sci. 2010 Feb; 51(2):758–764. https://doi.org/10.1167/iovs.09-3379 PMID: 19643956

42. Kakizaki I, Itano N, Kimata K, Hanada K, Kon A, Yamaguchi M, et al. Up-regulation of hyaluronan synthase genes in cultured human epidermal keratinocytes by UVB irradiation. Arch Biochem Biophys. 2008 Mar 1; 471(1):85–93. https://doi.org/10.1016/j.abb.2007.12.004 PMID: 18158910

43. Ueta M, Sotozono C, Kinoshita S. Expression of interleukin-4 receptor α in human corneal epithelial cells. Jpn J Ophthalmol. 2011 Jul; 55(4):405–410. https://doi.org/10.1007/s10384-011-0030-6 PMID: 21617960

10.4. Appendix 4: Ex vivo cultivated oral mucosal epithelial cell transplantation for limbal stem cell deficiency: a review

Ex vivo cultivated oral mucosal epithelial cell transplantation for limbal stem cell deficiency: a review

Joao Victor Cabral[1], Catherine Joan Jackson[2,3,4], Tor Paaske Utheim[2,4,5] and Katerina Jirsova[1]*

Abstract

Destruction or dysfunction of limbal epithelial stem cells (LESCs) leads to unilateral or bilateral limbal stem cell deficiency (LSCD). Fifteen years have passed since the first transplantation of ex vivo cultivated oral mucosal epithelial cells (COMET) in humans in 2004, which represents the first use of a cultured non-limbal autologous cell type to treat bilateral LSCD. This review summarizes clinical outcomes from COMET studies published from 2004 to 2019 and reviews results with emphasis on the culture methods by which grafted cell sheets were prepared.

Keywords: Cultivated oral mucosal epithelial cell, Limbal stem cell deficiency, Oral mucosal epithelial cells, Tissue regeneration

Background

Damage to the limbus can lead to a decrease in limbal epithelial stem cells (LESCs) and dysfunctional homeostasis of the corneal epithelium. This failure, termed limbal stem cell deficiency (LSCD) [1–3], leads to disruption of the barrier function and invasion of conjunctival cells onto the corneal surface [4, 5]. Conjunctivalization is followed by vascularization, chronic inflammation, photophobia, recurrent pain, and decreased vision [4, 6–8]. LSCD is classified as partial or total and may occur unilaterally or bilaterally [9].

Conjunctival limbal autograft (CLAU) and cultivated limbal epithelium transplantation (CLET) are procedures often used in the treatment of unilateral LSCD [10, 11]. However, patients with bilateral total LSCD do not have limbal tissue available for use in either CLAU or CLET. Thus, options for a source of LESCs are limited to living-related or cadaveric donors and entail use of immunosuppression to prevent rejection [12].

In 2004, Nakamura and co-workers performed the first transplantation of autologous oral epithelial cells cultured ex vivo on human amniotic membrane (AM) to offer an alternative to use of allogenic tissue and avoid immunosuppression [13]. The treatment of LSCD using ex vivo cultivated oral mucosal epithelial cell transplantation (COMET) minimizes the risk of graft rejection and has the added advantage that it can be repeated if necessary. However, neo-angiogenesis following transplantation is a drawback associated with this procedure [13]. This review summarizes clinical outcomes from COMET case series from 2004 to 2019 and reviews the methods used in preparation of transplanted cell sheets.

General analysis of studies

The review was prepared by searching the Ovid MEDLINE database using search terms: limbus corneae, limbus, limbal stem cell deficiency, corneal epithelium, cornea, mouth mucosa, and transplantation. We found 24 studies published over the past fifteen years [13–36].

---

* Correspondence: katerina.jirsova@lf1.cuni.cz
[1]Laboratory of the Biology and Pathology of the Eye, Institute of Biology and Medical Genetics, First Faculty of Medicine, Charles University and General University Hospital in Prague, Prague, Czech Republic
Full list of author information is available at the end of the article

A case report of one patient (one eye) was excluded from this review [37].

COMET has been performed in Japan [13–19, 23–25, 27, 29, 30], Taiwan [20, 21, 28], India [22], France [26], the UK [31], Poland [32], Thailand [33], Iran [34], South Korea [35], and China [36]. In total, 343 eyes of 315 patients (64% men and 36% women) were included. The age range was from eight to 86 years, the mean age was 46.5 (± 18.6) and 50.8 (± 21.5) years for males and females, respectively. About 26% of male and 23% of female patients were younger than 30 years, while about 28% and approximately 45%, respectively, were older than 60 years.

Three hundred and twenty LSCD eyes were classified as totally deficient, eight eyes as partial [32, 33]. One study classified all 5 eyes as severe LSCD [21]. Nine studies included patients with bilateral LSCD [13–16, 19, 26, 31, 33, 34], two studies included both bilateral and unilateral cases [22, 30], and one study enrolled only patients with unilateral LSCD [25].

Patients and surgery
Etiology
The most common etiology of LSCD is corneal burn (146/343 eyes; 42.6%) resulting from chemical, thermal or unspecified causes, followed by Stevens-Johnson syndrome (SJS) (92/343 eyes; 26.8%) (Fig. 1 and Table 1). Ocular cicatricial pemphigoid (OCP) and pseudo-ocular cicatricial pemphigoid (pOCP) together composed the third most common cause of LSCD receiving COMET (44/343 eyes; 12.8%).

Diagnosis
Diagnosis of LSCD is based on the following clinical features: irregular corneal surface with loss of light reflex, corneal epithelial opacity, loss of limbal palisades of Vogt, fluorescein staining, epithelial thinning in a vortex pattern, corneal neovascularization, peripheral pannus, persistent epithelial defect (PED), corneal stroma scarring, and opacification [6, 38].

Corneal conjunctivalization can be confirmed clinically using in vivo confocal microscopy (IVCM) to define the phenotype of cells on the cornea (conjunctival epithelial cells are hyperreflective with bright nuclei and ill-defined borders, whereas corneal epithelial cells are well-defined with bright borders and dark cytoplasm) [39]. Conjunctival tissue contains goblet cells (GCs) and blood vessels, which can also be seen using IVCM [39]. Impression cytology (IC) is another method used to detect GCs on the corneal surface [4]. In case of GC absence due to severe ocular surface damage, conjunctival (but not corneal) mucins (mucin 1) [40] or keratins (keratin 7, -13, and -15) can be detected using immuno-cytochemistry [41–43]. Clinical features were used in diagnosis of LSCD in 18/24 studies [13–16, 19, 22–27, 29–33, 35, 36], five of these studies also used IC (Table 1)[19, 23, 31, 33, 36].

Pre-operative considerations
Some studies reported previous surgeries, including AM transplantation (38 eyes) [13, 15, 20–22, 28, 30, 35], and penetrating keratoplasty (PKP) (8 eyes) [14–16, 20, 21, 34, 35], or other (57 eyes) [29, 36]. Moreover, 21 eyes had previously undergone CLAU or allograft transplantation [13–15,
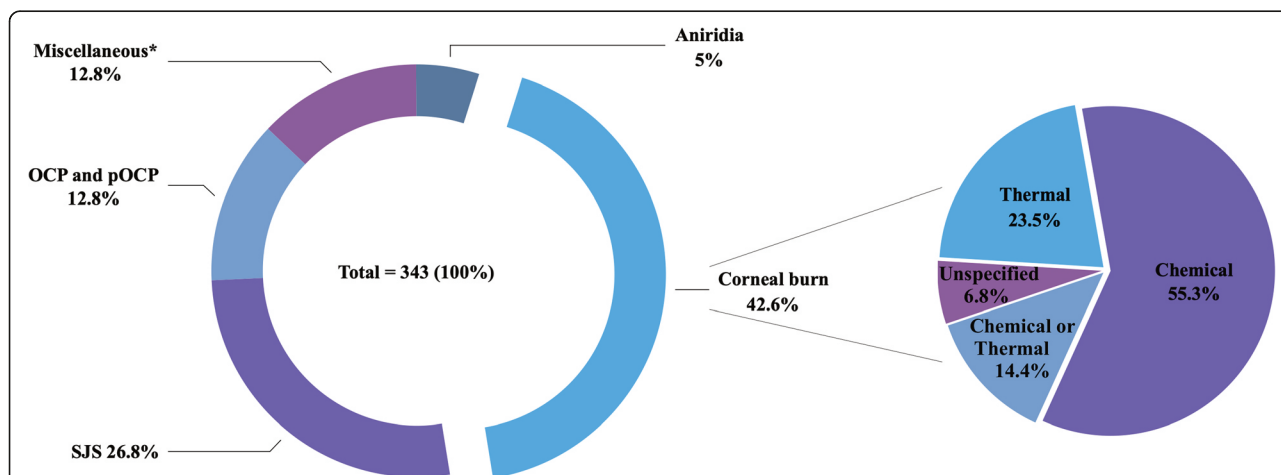
Fig. 1 Etiology of limbal stem cell deficiency (LSCD).Percentages are according to the number of eyes. OCP, ocular cicatricial pemphigoid; pOCP, pseudo-ocular cicatricial pemphigoid; SJS,Stevens-Johnson syndrome. *Miscellaneous (%):trachoma (1.45),post keratitis (1.45),idiopathic (1.2), Lyell syndrome (1.2),rosacea keratitis (0.9),congenital aniridia (0.6),contact lens hypoxia + congenital aniridia (0.6),neuroparalytic keratitis (0.6), Behcet's disease (0.6),graft-versus-host disease (0.6),squamous cell carcinoma (0.6),gelatinous drop-like dystrophy (0.3),multiple eye surgery (0.3), advanced pterygium (0.3),ocular trauma (0.3),contact lens hypoxia (0.3),cystinosis (0.3),severe Groenouw dystrophy (0.3),hepatitis C (0.3), radiation keratopathy (0.3),Salzmann's corneal degeneration (0.3),and drug toxicity (0.3)

Table 1 Summary of clinical studies

Author, year	Etiology	No. of eyes/No. of patients	Dry eye assessment pre-operatively
Nakamura et al., 2004 [13]	SJS × 3, chemical burns × 3	6/4	Yes
Nishida et al., 2004 [14]	SJS × 1, OCP × 3	4/4	Yes
Inatomi et al., 2006 a [15]	SJS × 7, chemical injury × 5, thermal injury × 1, pOCP × 1, idiopathic × 1	15/12	Yes
Inatomi et al., 2006 b [16]	SJS × 1, chemical injury × 1	2/2	Yes
Ang et al., 2006 [17]	SJS × 7, thermal injury × 1, chemical injury × 1, OCP × 1	10/10	Yes
Nakamura et al., 2007 [18]	SJS × 3, chemical injury × 3	6/5	NA
Satake et al., 2008 [19]	SJS × 2, pOCP × 2	4/4	NA
Chen et al., 2009 [20]	Chemical burn × 3, thermal burn × 1	4/4	NA
Ma et al., 2009 [21]	Chemical burn × 3, thermal burn × 2	5/5	NA
Priya et al., 2011 [22]	SJS × 1, chemical injury × 9	10/10	Yes
Satake et al., 2011 [23]	SJS × 12, chemical or thermal injury × 11, OCP × 9, pOCP × 7, gelatinous drop-like dystrophy × 1	40/36	Yes
Nakamura et al., 2011 [24]	SJS × 11, chemical or thermal injury × 1, OCP × 4, squamous cell carcinoma × 2, graft-versus-host disease × 1	19/17	Yes
Takeda et al., 2011 [25]	Chemical burn × 1, thermal burn × 2	3/3	NA
Burillon et al., 2012 [26]	Corneal burn × 9, neuroparalytic keratitis × 2, rosacea keratitis × 3, Lyell syndrome × 4, severe trachoma × 1, contact lens hypoxia × 1, congenital aniridia × 1, cystinosis × 1, severe Groenouw dystrophy × 1, hepatitis C × 1, contact lens hypoxia + congenital aniridia × 2	26/25	Unclear[a]
Hirayama et al., 2012 [27]	Chemical injury × 12, pOCP × 12 (trachoma × 4, Behcet's disease × 2, thermal burn × 1 and post keratitis × 5), SJS × 4, OCP × 4	32/32	Partially (27/32)
Chen et al., 2012 [28]	Chemical burn × 4, thermal burn × 2	6/6	NA
Sotozono et al., 2013 [29]	SJS × 21, OCP × 10, chemical or thermal injury × 7, idiopathic × 3, radiation keratopathy × 1, graft-versus-host disease × 1, congenital aniridia × 1, Salzmann's corneal degeneration × 1, drug toxicity × 1	46/40	Unclear[a]
Sotozono et al., 2014 [30]	SJS × 3, thermal injury × 3, chemical injury × 2, OCP × 2	10/9	Unclear[a]
Kolli et al., 2014 [31]	Chemical burn × 2	2/2	Partially (1/2)
Dobrowolski et al., 2015 [32]	Aniridia × 17	17/13	NA
Prabhasawat et al., 2016 [33]	SJS × 10, chemical burn × 7, multiple eye surgery × 1, advanced pterygium × 1, ocular trauma × 1	20/18	Yes
Baradaren-Rafii et al., 2017 [34]	Chemical burn × 14	14/14	Yes
Kim et al., 2018 [35]	SJS × 6, OCP × 1, chemical burn × 1	8/8	NA
Wang et al., 2019 [36]	Chemical injury × 16, thermal injury × 18	34/32	NA

LSCD limbal stem cell deficiency, NA not available, OCP ocular cicatricial pemphigoid, pOCP pseudo-ocular cicatricial pemphigoid, SJS Stevens-Johnson syndrome
[a]These studies mentioned that dry eye patients received artificial tears in the post-operative management, but it was not stated whether dry eye was assessed in all patients

18–22, 35]. In total, 148 earlier surgeries were reported. Thus, the number of eyes previously treated was 119, more than a third (34.7%)of the total number of eyes included in this review [13–16, 18–22, 28–30, 34–36].

Prognostic factors

The presence of pre-operative epithelial defects and/or poor tear production may affect successful outcome [23, 44, 45]. Thus, numerous studies included assessment of dry eye in the pre-operative evaluation (Table 1)[13–17, 22–24, 27, 31, 33, 34]. DeSousa et al. recommend that adnexal abnormalities, including the health and function of the eyelids, fornix, and tear film, be assessed and im- proved prior to surgery to ensure the best chance of epi- thelial healing [46]. Conjunctival swab has revealed the presence of pathogenic organisms, which is likely due to a poor ocular surface and absence of a tear film. There- fore, performing a conjunctival swab culture before COMET to ensure a receptive ocular surface is sug- gested [47]. A complete oral exam is also recommended as successful culture of oral mucosal epithelial cells (OMECs) sheets may be affected by poor oral hygiene and smoking [15, 34].

Surgery

Surgical technique was similar in all studies. First, the conjunctival tissue was removed from the corneal sur- face, up to 3 mm away from the limbus to expose the corneal stroma [14, 17, 26]. Dissection of symblepharon was performed where necessary, and in some cases, AM was grafted onto the bare sclera to reconstruct the con- junctival fornix [17, 29, 30, 35]. In several cases, the sub- conjunctival space was treated with Mitomycin C [13, 15–17, 19, 22, 24, 27, 33]. A cultured OMEC sheet measuring from 14 [32] to 23.4 mm [14] diameter was transferred onto the corneal surface. Most of the studies used sutures to secure the graft in place [13, 15–34, 36]. Sutures were not used if the cell sheet was carrier-free [14, 26, 27, 35]. A study also used tissue adhesive glue [33], one used fibrin glue plus temporary tarsorrhaphy [35], and another used lateral tarsorrhaphy [34].

   After surgery, AM [31] or therapeutic contact lenses (CLs) [13–36] were typically applied for 1 month [20, 29, 30] or for up to 3 months [24, 36] to protect the graft. One study reported adverse events attributed to hypoxia caused by extended use of CLs [26].

Post-operative considerations

Post-operative management varied considerably across the studies. A moist ocular surface post-COMET has been shown to be an important criterion for success [14, 24]. This was achieved by frequent application of preservative-free artificial tears [14, 19, 23, 26, 27, 32– 34, 36], autologous serum eye drops [19, 21, 23, 31–33,

35, 36], or water-retaining hyaluronic acid [19, 23, 35]. One study occluded the lacrimal punctum to increase tear retention [14]. Topical antibiotics were applied in all studies, generally from 2 weeks [32, 33] up to 6 months [22]. Post-operative inflammation was controlled by topical steroids alone [27, 31–33] or in combination with systemic steroids [13, 14, 17, 19, 21–24, 26, 29, 30, 34–36]. The length of the treatment varied from 1 week [14, 26] up to 2 months [13, 21, 34]. Two studies tapered the dose-dependent on the patient response [29, 30]. In some studies, immunosuppression in the form of cyclo- sporine [17, 24, 29, 30] or cyclophosphamide [13, 21] was used to control post-operative inflammation, and topical tacrolimus [34] was used to decrease the risk of allograft rejection following PKP.

Characteristics of the culture protocol used in clinical studies

Biopsy

The smallest tissue sample was ~ 4.7 mm^2, obtained by using a 3-mm diameter biopsy punch [31], the largest ranged from 120 to 200 mm^2 (Table 2)[35]. Fourteen studies used tissue from the buccal mucosa [14, 19, 21– 23, 26–33, 36], and two from the lip [34, 35].

Culture methods

Cell suspension was the most common culture system (23 studies), in which single OMECs were released from tissue using enzymatic treatment (Table 3)[13–30, 32– 36]. All but one [33] of the cell suspension cultures re- ported standard use of 3T3 mouse fibroblasts in cocul- ture, as a feeder layer [13–30, 32, 34–36]. The explant method was investigated in one study, where culture of the biopsy on AM demonstrated faster growth compared to culture on a feeder layer [31]. In vitro work has also shown that OMEC sheets maintain a comparable epithe- lial stem cell phenotype when cultured on autologous dermal fibroblasts compared with use of 3T3 mouse fi- broblasts [48]. Culture time was typically 2 to 3 weeks; the shortest was 1 week [32]. Good manufacturing prac- tice (GMP) regulations were followed in four studies from Japan [29, 30], South Korea [35], and the UK [31].

Medium

Dulbecco Modified Eagle's Medium with HAM F12 mix- ture (DMEM/F12) was used in more than half of the studies; in ten of these, the DMEM/F12 ratio was 1:1 [13, 15, 16, 18, 19, 22, 23, 25, 27, 34], and in three of them 3:1 (Table 3)[31, 35, 36]. Other studies used sup- plemented hormonal epithelial medium (SHEM) [20, 28], keratinocyte growth medium (KGM) [17, 24], or serum-free keratinocyte growth medium (KBM-2)[33].

   Fetal bovine serum (FBS, or FCS when referred to as "fetal calf serum") was used in nine studies [13, 16, 19–

Table 2 Size and location of oral mucosal biopsy used in COMET

Studies	Biopsy size (mm^2)	Location of biopsy
[13]	2–3	NA
[14]	9	Buccal mucosa
[15]	2–3	NA
[16]	3–5	NA
[17]	2–3	NA
[18]	NA	NA
[19]	50.24[a]	Buccal mucosa (inferior)
[20]	36	NA
[21]	36	Buccal mucosa
[22]	8	Buccal mucosa
[23]	50.24[a]	Buccal mucosa (inferior)
[24]	NA	NA
[25]	NA[c]	NA
[26]	9	Buccal mucosa (cheek)
[27]	50.24[a]	Inferior buccal mucosa
[28]	36	Buccal mucosa
[29]	9.42[b]	Buccal mucosa
[30]	9.42[b]	Buccal mucosa
[31]	4.71[c]	Buccal mucosa (cheek, 20 mm behind the angle of the mouth)
[32]	3–5	Buccal mucosa (inferior)
[33]	100	Buccal mucosa
[34]	NA	Labial mucosa (behind the lip)
[35]	120–200	Labial mucosa (inside the inferior lip)
[36]	16	Buccal mucosa (cheek)

NA not available
Area of an [a]8-, [b]6-, or [c]3-mm diameter biopsy punch

21, 28, 34–36], five used autologous serum (AS) [17, 22, 23, 27, 31], and four used FBS and AS (Table 3)[15, 29, 30, 32]. Only one was serum-free [33]. Use of AS eliminates exposure to xenogeneic compounds contained in animal serum. One study compared use of AS with FBS and found that cell sheet morphology and expression of structural proteins were similar in both groups [17]. Preliminary in vitro work has also shown that AS promotes similar expression of putative stem cells markers in cultured OMEC sheets compared to use of FBS [31]. The two patients receiving AS feeder-free cultured OMEC sheets in this study had significant improvement in corneal epithelium integrity, pain relief, and visual acuity (VA) [31].

Airlifting
Fifteen studies (258 eyes) used airlifting to promote formation of a stratified epithelium (Table 3)[13, 15–19, 23–25, 27, 29, 30, 32, 34, 36]. Airlifting produced more stratification with four to nine layers compared to two to five in non-air-lifted OMEC sheets. Stratification promotes cell-cell adhesion between superficial epithelial cells via tight junction formation, which helps to prevent loss of the transplant due to blinking [49]. On the other hand, highly differentiated air-lifted sheets have lower proliferative function, which is consistent with a decrease in p63α-expressing stem cells [50].

Substrate
AM was the most common culture substrate (Table 3). Eighteen studies used denuded AM (epithelial layer removed) [13, 15–22, 24, 26, 29, 30, 32–34, 36], and one used intact AM [31]. Of the remaining studies, two used either denuded AM or fibrin-coated culture inserts [23, 27], two used temperature-responsive cell-culture inserts [14, 26], and one study did not employ a substrate [35].

Carrier
Most studies employed AM as a culture substrate and OMECs were transferred directly on the same substrate

Table 3 Summary of culture methods used in OMEC sheet preparation

Ref.	Culture system	Substrate	Feeder layer	Nutrient	Air lifting	% SC	Medium	GMP	Carrier	Culture time (days)
[13]	S	dAM	3T3	10% FBS	Y	–	DMEM/F12 (1:1)	N	dAM	14–21
[14]	S	CellSeed[b]	3T3	NA	N	2.1 ± 0.9	NA	N	Carrier-free*	14
[15]	S	dAM	3T3	10% FBS/10% AS	Y	–	DMEM/F12 (1:1)	N	dAM	15–16
[16]	S	dAM	3T3	10% FBS[a]	Y	–	DMEM/F12 (1:1)[a]	N	dAM[a]	14
[17]	S	dAM	3T3	5% AS	Y	–	KGM	N	dAM	15–16
[18]	S[a]	dAM[a]	3T3[a]	U[d]	Y[a]	–	DMEM/F12 (1:1)[a]	N[a]	dAM	U[d]
[19]	S	dAM	3T3	10% FBS	Y	–	DMEM/F12 (1:1)[a]	N	dAM	> 14
[20]	S	dAM	3T3	5% FBS	N	–	SHEM	N	dAM	14–21[a]
[21]	S	dAM	3T3	5% FBS	N	–	U	N	dAM	14–21[a]
[22]	S	dAM	3T3	10% AS	N	2.0 ± 1.0	DMEM/F12 (1:1)	N	dAM	18–21
[23]	S	Fibrin[c]/dAM	3T3	4% AS	Y	–	DMEM/F12 (1:1)	N	U	NA
[24]	S	dAM	3T3	5% Serum	Y	–	KGM	N	dAM[a]	15–16
[25]	S[a]	dAM	3T3	U[d]	Y	–	DMEM/F12 (1:1)[a]	N	dAM	15–16
[26]	S	CellSeed[b]	3T3	NA	N	3.4 ± 2.06	NA	N	Carrier-free**	U[e]
[27]	S	Fibrin[c]/dAM	3T3	4% AS	Y	–	DMEM/F12(1:1)	N	Fibrin group: carrier-free*** AM group: denuded AM	8–16 (Fibrin)/NA (dAM)
[28]	S	dAM	3T3	5% FBS	N	–	SHEM	N	dAM	14–21[a]
[29]	S[a]	dAM[a]	3T3	10%[a] FBS/5%[b] AS	Y	–	U[d]	Y	dAM[a]	8–9
[30]	S[a]	dAM[a]	3T3	10%[a] FBS/%[c] AS	Y	–	U[d]	Y	dAM[a]	8–9
[31]	E	iAM	N	AS	U	~ 12	DMEM/F12 (3:1)	Y	iAM	21
[32]	S	dAM	3T3	10% FBS/10% AS	Y	–	DMEM/F12	N	dAM	7
[33]	S	dAM	N	Serum-free	N	–	KBM-2	N	dAM	14–21
[34]	S[a]	dAM	3T3[a]	10% FBS[a]	Y	–	DMEM/F12 (1:1)[a]	N	dAM	14–21
[35]	S	BM-free	3T3	10% FBS	N	NA	DMEM/F12 (3:1)	Y	Carrier-free****	7–12
[36]	S	dAM	3T3	5% FBS	Y	–	DMEM/F12 (3:1)	N	dAM	U[f]

AM amniotic membrane, AS autologous serum, BM-free biomaterial-free, dAM denuded amniotic membrane, iAM intact amniotic membrane, E explant, FBS fetal bovine serum, DMEM/F12 Dulbecco modified Eagle's medium (DMEM) with HAMF12 mixture, GMP good manufacturing practice, KGM keratinocyte growth medium, KBM-2 serum-free Keratinocyte Growth medium, N no, NA not available, S suspension, SHEM supplemented hormonal epithelial medium, U unclear, Y yes, 3T3 3T3 murine fibroblasts, %SC percentage of transplanted stem cells
[a] According to the referenced protocol in the paper
[b] CellSeed, temperature-responsive cell-culture inserts (CellSeed Inc., Tokyo, Japan)
[c] Fibrin-coated inserts
[d] Conflicting data among the referenced studies
[e] For at least 4 days after the confluence
[f] For at least 5 days after the confluence and then air-lifted for 1 to 2 days
*Supporter
**Polyvinylidene fluoride (PVDF) ring
***Filter paper
****Support mesh

(Table 3). Two studies using temperature-responsive cell-culture inserts transferred cells on a supporter [14] or polyvinylidene fluoride membrane rings [26], which were removed after transfer to the cornea. A filter paper ring was used to transfer cell sheets grown on a fibrin substrate [27]. A support mesh was used in one study employing substrate-free culture [35].

Phenotype of cultured cells and presence of stem cells in culture

Immunohistochemistry and RT-PCR have shown that cultured OMECs are positive for keratin (K)3, K4, and K13 [13, 14, 17, 21, 26, 31–33], the latter is not expressed in the corneal epithelium [51]. OMECs also express markers of corneal differentiation connexin 43, laminin 5 [52, 53], and putative stem cell markers ß1-integrin, p75, p63, ABCG2, C/EBPδ [52, 54]. They do not express corneal-specific K12 and transcription factor PAX6 [22, 31]. However, heterogeneous populations of progenitor cells and mature epithelial cells in oral mucosal epithelium are similar to normal in vivo corneal epithelium; thus, its feasibility as a functional ocular surface epithelium [55, 56].

It has been shown that the presence of at least 3% stem cells (defined as ΔNp63α-positive cells) is associated with clinical success in the treatment of LSCD using CLET [57]. It is likely that the percentage of stem cells in grafted OMEC sheets also influences COMET success. Nishida et al. showed p63 expression in the basal layer of OMEC cultures used in the successful treatment of four patients with LSCD (Table 3) [14]. Analysis of putative stem cell markers (ΔNp63α, ABCG2, and C/EBPδ) in transplants have shown that OMEC and limbal cells have similar expression levels [31]. Four studies employed the colony-forming efficiency (CFE) assay to show the presence of stem cells in OMEC sheets (Table 3)[14, 22, 26, 31]. To date, any correlation between stem cell content in OMEC sheets before transplantation and clinical success using COMET remains to be investigated.

Follow-up and clinical outcome

The shortest reported follow-up period was 1 month [35]; two studies had less than 1 year [26, 35], ten studies 1 to 2 years [13–17, 19, 22, 30, 32, 36], and nine studies between 2 and 3 years [20, 21, 23, 25, 27, 29, 31, 33, 34]. Only two studies had a follow-up time longer than 3 years [24, 28], in which the longest was 7.5 years (Table 4)[24].

Success rate

Clinical success was most consistently defined in terms of a stable ocular surface. Secondary objectives reported were improved VA and best-corrected VA (BCVA). Post-graft investigations rarely included IVCM [16, 21] or IC [19]. Satake et al. used IC to show that in 2/4 eyes, the oral mucosa phenotype persisted for up to 16 months post-operatively, and in some cases the assessed epithelium displayed a mixture of oral mucosal and conjunctival cells [19].

In total, 70.8% (172/243) of eyes receiving COMET achieved a stable ocular surface and were defined as successful (Table 4; see Fig. 2 for detailed results per etiology). This percentage is lower compared to transplantation of cultured limbal epithelial cells (LECs) (75%) [58]. Moreover, one study directly compared COMET to transplantation of allogeneic cultured limbal epithelial transplantation (ACLET) and reported 71.4% (30/42) eyes in the ACLET group achieved a stable ocular surface, versus 52.9% (18/34) eyes in the COMET group. The authors attributed the significantly higher success using ACLET to the lower incidence of post-operative PED, superior LEC proliferation and differentiation, and the ability of LECs to more readily form a stable corneal epithelium [36].

Visual improvement

VA improvement was reported in all but two of the studies (Fig. 2 and Table 4), and 225/331 (68.2%) eyes had some improvement. An improvement in the BCVA of at least two lines was noted in 172/271 (63.5%) eyes (data from 20 studies). The absent or incomplete description of methodology for VA/BCVA measurement prevented an accurate comparison of results between studies. VA inconsistently measured either before or after subsequent surgeries, such as PKP, was another major confounding factor.

Survival of oral mucosal epithelial cells after grafting

Nakamura et al. have shown that post-COMET specimens exhibit a decrease in the number of epithelial layers from 5 to 6 in successful grafts to 2 to 5 disorganized epithelial layers in unsuccessful grafts [18]. The phenotype of COMET grafts (assessed from corneal buttons retrieved after a secondary procedure, mostly PKP) was also investigated in order to characterize the differences between successful (four samples) and unsuccessful (two samples) graft phenotypes [18]. Successful cases showed the presence of K3, a marker common to oral and corneal epithelium, in all specimens; K12, a corneal-specific keratin, presented only occasional staining in one case. K4 and K13, markers of oral mucosal epithelium, were present in both successful and failed samples. In failed specimens, one presented occasional staining for K3, but both were negative for K12. MUC5AC, a conjunctival goblet cell marker [59], was present only in both failed cases and found absent in successful cases[18].

Other studies have also assessed the expression profile post-COMET, but only in successful cases. Results were similar to Nakamura et al., showing positive staining for K3, K4, K13 and negative staining for MUC5AC [16, 20, 31, 35]. Additionally, Kim et al. showed that the corneal-specific keratin, K12, was present in all four successful COMET specimens [35]. Two other studies have indicated occasional K12 staining, shown in 2/6 specimens [16, 20]. These results suggest that the epithelium post-

Table 4 Clinical results, complications, and follow-up

Ref.	Complications	Stable ocular surface, n/N (%)	VA improvement, n/N (%)	Improvement in at least 2 lines of BCVA, n/N (%)	Mean follow-up± SD (range) in months
[13]	Corneal epithelial defect/bacterial infection × 2	6/6 (100)	6/6 (100)	6/6 (100)	13.8 ± 2.9 (11–17)
[14]	No complications	4/4 (100)	4/4 (100)	4/4 (100)	14 (13–15)
[15]	Epithelial defect × 5	13/15 (86.7)	12/15 (80)	12/15 (80)	20 (3–34)
[16]	No complication	2/2 (100)	2/2 (100)	2/2 (100)	22.5 (19–26)
[17]	Bacterial infection × 1, epithelial defects × 4	10/10 (100)	9/10 (90)	9/10 (90)	12.6 ± 3.9 (8–19)
[18]	Bacterial infection × 1, recurrent small epithelial defects × NA	4/6 (66.7)	NA	NA	NA
[19]	Increased intraocular pressure × 1	4/4 (100)	4/4 (100)	4/4 (100)	16 (6–24)
[20]	NA	NA	4/4 (100)	4/4 (100)	31 (27–35)
[21]	Microperforation × 1, PED × 1	NA	5/5 (100)	5/5 (100)	29.6 ± 3.6 (26–34)
[22]	Corneal graft rejection × 2	5/10 (50)	5/10 (50)	3/10 (30)	18.6 (1–38)
[23]	PED × 19, stromal melting or perforation × 8, corneal infection 3 (bacterial infection × 2, recurrence of epithelial herpes simplex × 1), glaucoma × 8 (3 were new), evisceration × 2	23/40 (57.5)	23,6/40 (59)	NA [d]	25.5 (6–54.9)
[24]	PED × 7, bacterial infection × 1, ocular hypertension × 3	NA	18/19 (95)	15/19 (79)	55 ± 17 (36–90)
[25]	Recurrence of entropion × 1, epithelial defect × 1, Symblepharon 1	2/3 (66.7)[a]	NA	NA	30 (11–50)
[26]	Symblepharon × 1, Pain and graft complication × 1, inflammation × 2, corneal graft rejection × 1, keratitis × 1, increased IOP × 1, corneal perforation × 1, Meibomian cyst × 1, pain and corneal recurrence × 1	NA[b]	17/23 (73.91) [c]	16/23 (69.5)[c]	11.83 (NA)
[27]	Small epithelial defect × 1, PED × 10, ocular hypertension × 3	Substrate-free: 10/16 (62.5) AM: 6/16 (37.5) Total: 16/32 (50)	Substrate-free: 11/16 (68.8) AM: 7/16 (43.8) Total: 18/32 (56.3)	Substrate-free: 11/16 (68.8) AM: 7/16 (43.8) Total: 18/32 (56.3)	25.26 ± 10.8 (14.45–36.08) (substrate-free)[e] 33.73 ± 17 (16,68–50.79) (AM)
[28]	Glaucoma × 1	6/6 (100)	6/6 (100)	6/6 (100)	36.7 + 17 (16–56)
[29]	Hepatic dysfunction × 1, drug-induced allergy × 1, PED × 16, corneal stromal melting × 2, keratitis × 1, endophthalmitis × 1, infiltration × 3, increased IOP × 4	NA	26/46 (56.52)	25/46 (54.3)	28.7 (6.2–85.6)
[30]	Epithelial defect × 3, increased IOP × 2, bacterial infection × 1	10/10 (100)	2/10 (20)	2/10 (20)	22.79 (5.6–39.7)
[31]	Central corneal epithelial defect × 1	2/2 (100)	2/2 (100)	2/2 (100)	31 (21–41)
[32]	Stromal scarring or conjunctival vascularization or stromal vascularization × 3, epithelial defect × 4	13/17 (76.5)	15/17 (88.2)	15/17 (88.2)	16 (12–18)
[33]	PED × 1, perforation × 1	15/20 (75)	14/20 (70)[d]	NA	31.9 ± 12.1 (8–50)
[34]	Epithelial defect × 3, PED × 1, bacterial keratitis × 1, increased IOP × 2, endothelial graft rejection × 4	13/14 (92.9)	14/14 (100)	14/14 (100)	28.2 ± 8.0 (14–40)
[35]	Central epithelial defect × 1, symblepharon × 1, PED × 1, primary failure × 1, recurrence of an epithelial defect × 2	6/8 (75)	5/8 (62.5)	5/8 (62.5)	9.96 ± 4.7 (2.07–15, 8)[f]
[36]	Epithelial defect × 3, PED × 9, increased IOP × 2, stroma melting × 5	18/34 (52.94)	14/34 (41.17)	5/34 (14.7)	16.1 ± 5.8 (range NA)
	Total	172/243 (70.78)	225.6/331 (68.15)	172/271 (63.46)	

n/N number of eyes/total number of eyes, BCVA best-corrected visual acuity, IOP intraocular pressure, NA not available, PED persistent epithelial defect, VA visual acuity

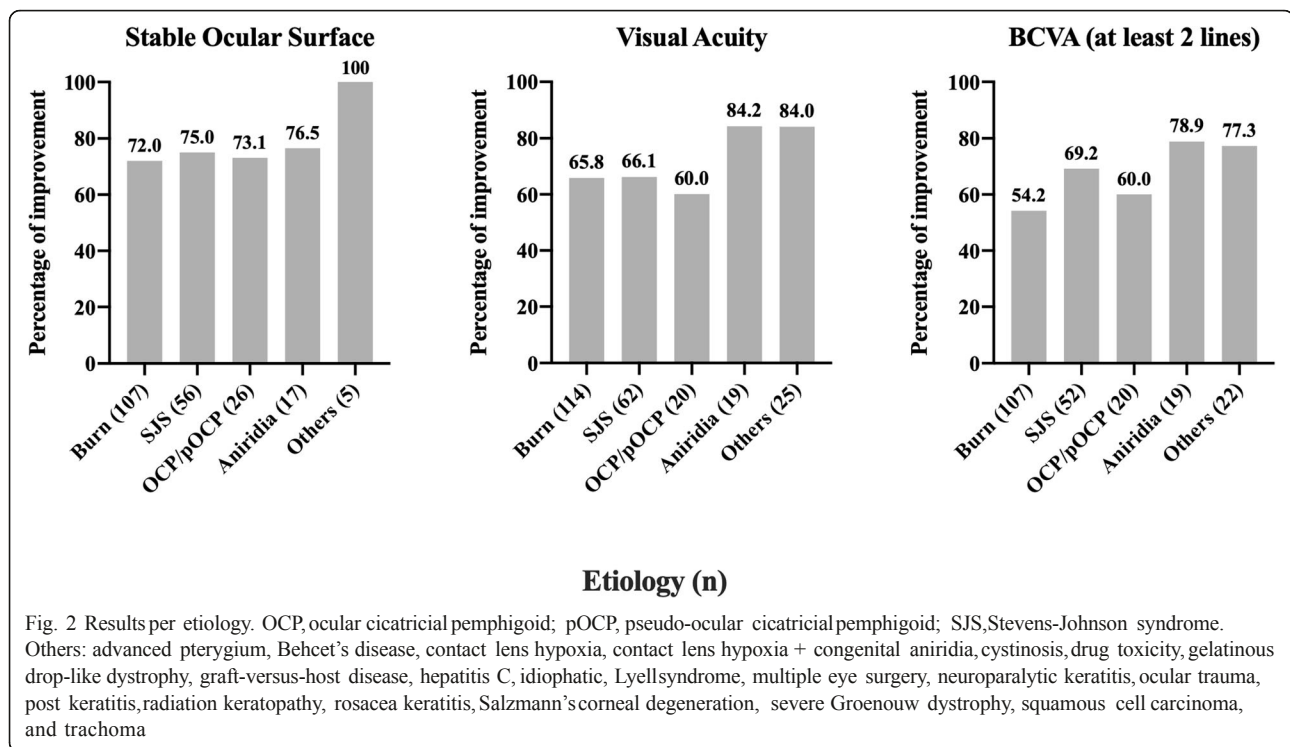[a] 100% after repeated transplantation

[b] There was a success rate of 16/25 (64%), but it is based on a composition of criteria, not on a stable ocular surface per se

[c] It excluded from the results two patients who had serious adverse events

[d] There is no mention if visual improvement was at least of two lines

[e] Follow-up was originally given in weeks as it follows: 109.8 ± 47 weeks (substrate-free) and 146.6 ± 74.1 weeks (AM)

[f] Follow-up was originally given in days as it follows: 303 ± 144 (63–482) days

Fig. 2 Results per etiology. OCP, ocular cicatricial pemphigoid; pOCP, pseudo-ocular cicatricial pemphigoid; SJS, Stevens-Johnson syndrome. Others: advanced pterygium, Behcet's disease, contact lens hypoxia, contact lens hypoxia + congenital aniridia, cystinosis, drug toxicity, gelatinous drop-like dystrophy, graft-versus-host disease, hepatitis C, idiopathic, Lyell syndrome, multiple eye surgery, neuroparalytic keratitis, ocular trauma, post keratitis, radiation keratopathy, rosacea keratitis, Salzmann's corneal degeneration, severe Groenouw dystrophy, squamous cell carcinoma, and trachoma

COMET exhibits signs of both corneal-like (K12[+]) as well as oral mucosal epithelium phenotype (K13[+]). Detection of K3[+], K4[+], K12[+], K13[+], and MUC5AC^{−} in clinically successful grafts shows that cultivated OMECs survive transplantation and continue to contribute to ocular surface integrity [18, 35].

However, without clear detection of cell origin (donor/host) [60–62] it is difficult to determine clearly whether cultivated OMECs were transdifferentiated into the corneal lineage or whether the presence of corneal epithelial cells represents expansion and migration of remaining corneal cells. In vivo study on rats has shown that transplanted oral mucosal cell sheets were able to survive and retain stem/progenitor cells for at least 8 weeks post-operatively, which results in the long-term success of transplantation of cultured OMECs in LSCD patients [63]. It has been suggested that restoration of a non-inflammatory environment post-operatively may be sufficient to allow repopulation of any remaining corneal cells to the ocular surface and/or resumption of normal homeostatic function by residual limbal stem cells [64].
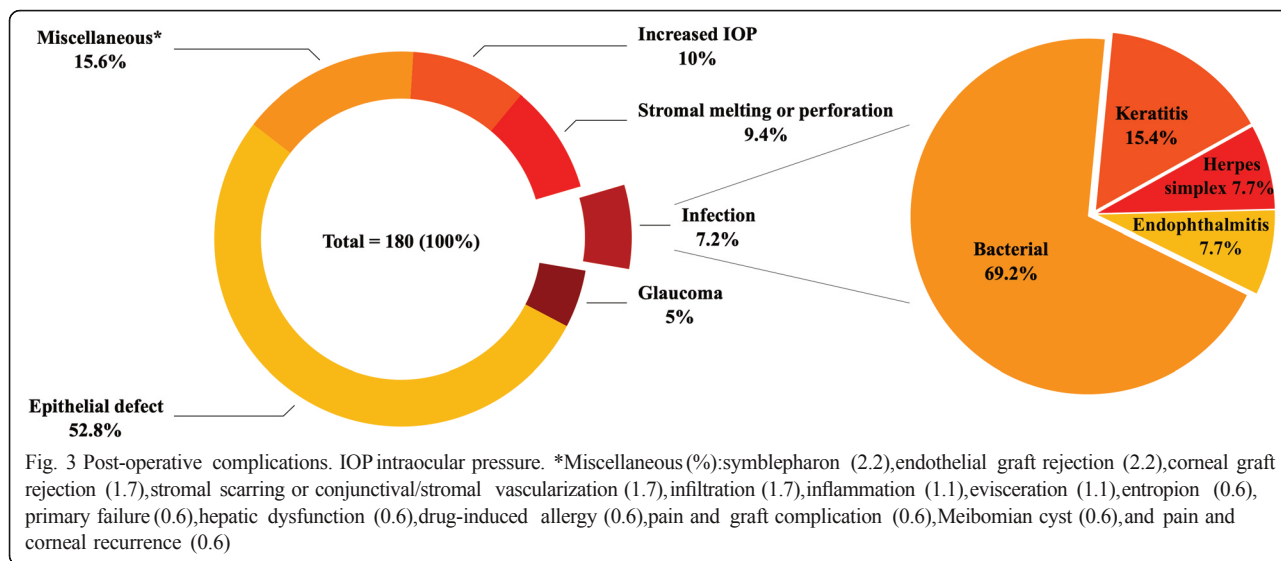
Success of stem cell transplantation and the long-term survival of the graft in ocular surface therapy not only depends on the features of transplanted cells, but also on the surrounding microenvironment, as it provides the necessary signals required for cell maintenance and growth [48, 65]. Huang et al. speculate that transplanted OMECs might be regulated by signals originating from healthy stroma and differentiate toward the corneal phenotype, while simultaneously maintaining the oral phenotype [56]. However, identification of the key factors necessary to promote transdifferentiation of OMECs to the corneal phenotype still requires further research.

Post-operative complications
The most common complications described following COMET were epithelial defects (52.8%; 36.1% PED), increased intraocular pressure or glaucoma (15%), stromal melting or perforation (9.4%), and infection (7.2%) (Fig. 3). For comparison, a review summarizing transplantation of cultured LECs (889 eyes) reported that the most common complications post-surgery were bleeding (8.7%), inflammation (7.5%), and blepharitis and epitheliopathy (4%) [58]. Epithelial defects making up more than half of the complications could reflect the often more serious nature of the bilateral LSCD diagnosis that demands an alternative treatment such as COMET.

Of note, there was no consensus on the definition of PED. For instance, Nakamura et al. considered epithelial defects to be persistent if they lasted for more than 4 weeks [24], while Hirayama et al. [27] defined PED occurring after 1 week following failure of conventional therapy. In a retrospective comparative study (76 eyes) a higher incidence of post-operative PED was reported in eyes receiving COMET (9/34 eyes) compared to those receiving ACLET (3/42 eyes) [36]. Several studies pointed to an association between incidence of post-operative with pre-operative PED [15, 23, 36]. It has also

Fig. 3 Post-operative complications. IOP intraocular pressure. *Miscellaneous (%):symblepharon (2.2),endothelial graft rejection (2.2),corneal graft rejection (1.7),stromal scarring or conjunctival/stromal vascularization (1.7),infiltration (1.7),inflammation (1.1),evisceration (1.1),entropion (0.6), primary failure (0.6),hepatic dysfunction (0.6),drug-induced allergy (0.6),pain and graft complication (0.6),Meibomian cyst (0.6),and pain and corneal recurrence (0.6)

been shown that the transplanted epithelium exhibits decreased barrier function following COMET [19].

Baradaran-Rafii et al. suggest that PKP is inevitable in most cases of LSCD involving chemical burns due to the presence of significant corneal opacification [34]. Patients receiving PKP had improved visual function and the authors recommended performing PKP several months post-COMET to achieve the best chance of success [34].

Although most studies noted neovascularization post-transplantation [13–15, 17, 20, 21, 24, 26–28, 32–34, 36], they did not define this as a complication of the procedure. Corneal peripheral neovascularization occurred slowly in most cases, during the first post-operative year [33]. However, the central corneal area was usually spared, and neovascularization usually ceased to progress after 1 year, remaining stable thereafter [14, 33] or gradually abating with time [15, 24]. In the one retrospective study comparing ACLET and COMET, the incidence of neovascularization, corneal conjunctivalization, and improvement in symblepharon was similar between the two groups [36].

Nishida et al. pointed out that stromal vascularization observed beneath COMET transplants on the periphery of the cornea should be differentiated from subepithelial neovascularization that accompanies conjunctival ingrowth, which occurs several months post-transplantation [14]. The peripheral neovascularization seen after COMET may be caused by the lack of antiangiogenic factors, such as the soluble vascular endothelial growth factor (VEGF) receptor, fms-like tyrosine kinase-1 (sFlt-1), tissue inhibitor of metalloproteinase-3 (TIMP-3) and thrombospondin-1 (TSP-1) [28, 66, 67] or by an increase in fibroblast growth factor-2 (FGF-2) [68]. Initial in vitro work suggests that OMEC sheets produced in a culture system where 3T3 fibroblast cells are replaced with limbal niche cells as a

feeder layer are less likely to induce postsurgical neovascularization [69].

Effect of preparation method on clinical success

We found that OMEC sheet preparation was relatively standardized; most studies used buccal tissue biopsy, DMEM/F12 culture medium, AM as a substrate and air lifting during culture. Several studies compared OMEC culture methods. The two elements that were directly compared were use of AS versus FBS in the culture medium [17] and use of substrate-free culture versus AM as a substrate [27]. Both AS and substrate-free culture have the advantage of minimizing patient exposure to potential contaminants. Clinical results so far suggest comparative or improved corneal epithelial integrity and VA with use of AS and substrate-free culture compared to the use of FBS and AM. However, larger defined comparative studies are necessary before conclusions can be drawn.

Hirayama et al. reported improved success (10/16; 62.5%) in patients receiving substrate-free OMEC sheets compared to those receiving OMEC cultured on AM (6/16; 37.5%) (Table 4)[27]. Improvement in BCVA was also superior in the substrate-free group with 11/16 (68.8%) showing improvement compared to 7/16 (43.8%). Both methods resulted in a stable ocular surface. However, graft survival was significantly improved in the carrier-free group. This may be attributed to direct contact of transplanted OMECs with stromal keratocytes and promotion of proliferation and differentiation of cells in the transplant [70].

Conclusions

OMECs are to date the most common choice of non-limbal autologous cells in the treatment of LSCD. COMET is a promising treatment modality for LSCD,

with a stable ocular surface reported in 70.8% (172/243) of LSCD eyes, and visual improvement achieved in 68.2% (225.6/331) based on published cases from the past 15 years (2004–2019).

Variation in methodologies (LSCD diagnosis, cell-culture protocols, transplantation technique, post-operative management, and measurement of VA) among the studies did not allow a precise comparative analysis of results. The use of unified tools for characterization of pre-operative status, as well as standardized assessment of outcomes would allow better comparison of studies.

Abbreviations
AM: Amniotic membrane; AS: Autologous serum; ACLET: Allogeneic cultured limbal epithelial transplantation; BCVA: Best-corrected visual acuity; CFE: Colony-forming efficiency; CLAU: Conjunctival limbal autograft; CLET: Cultivated limbal epithelium transplantation; CLs: Contact lenses; COMET: Ex vivo cultivated oral mucosal epithelial cell transplantation; DMEM/F12: Dulbecco Modified Eagle's Medium (DMEM) with HAMF12 mixture; FBS: Fetal bovine serum; FCS: Fetal calf serum; GCs: Goblet cells; GMP: Good manufacturing practice; KBM-2: Serum-free keratinocyte growth medium; KGM: Keratinocyte growth medium; IC: Impression cytology; IVCM: In vivo confocal microscopy; LECs: Limbal epithelial cells; LESCs: Limbal epithelial stem cells; LSCD: Limbal stem cell deficiency; OCP: Ocular cicatricial pemphigoid; OMECs: Oral mucosal epithelial cells; pOCP: Pseudo-ocular cicatricial pemphigoid; PED: Persistent epithelial defect; PKP: Penetrating keratoplasty; sFlt-1: fms-like tyrosine kinase-1; SHEM: Supplemented hormonal epithelial medium; SJS: Stevens-Johnson syndrome; TIMP-3: Tissue inhibitor of metalloproteinase-3; TSP-1: Thrombospondin-1; VA: Visual acuity; VEGF: Vascular endothelial growth factor

Author details
[1]Laboratory of the Biology and Pathology of the Eye, Institute of Biology and Medical Genetics, First Faculty of Medicine, Charles University and General University Hospital in Prague, Prague, Czech Republic. [2]Department of Medical Biochemistry, Oslo University Hospital, Oslo, Norway. [3]Department of Oral Biology, Faculty of Dentistry, University of Oslo, Oslo, Norway. [4]Department of Plastic and Reconstructive Surgery, Oslo University Hospital, Oslo, Norway. [5]Department of Ophthalmology, Sørlandet Hospital Trust Arendal, Arendal, Norway.

References
1. Schwartz GS, LoVerde L, Gomes J, Holland EJ. Classification and staging of ocular surface disease. In: Mark J. Mannis, Edward J. Holland., editors. Cornea. 4th ed. Elsevier; 2017. p. 1668–1680.
2. Chen JJ, Tseng SC. Abnormal corneal epithelial wound healing in partial-thickness removal of limbal epithelium. Invest Ophthalmol Vis Sci. 1991; 32(8):2219–33.
3. Kruse FE, Chen JJ, Tsai RJ, Tseng SC. Conjunctival transdifferentiation is due to the incomplete removal of limbal basal epithelium. Invest Ophthalmol Vis Sci. 1990;31(9):1903–13.
4. Puangsricharern V, Tseng SC. Cytologic evidence of corneal diseases with limbal stem cell deficiency. Ophthalmology. 1995;102(10):1476–85.
5. Huang AJ, Tseng SC. Corneal epithelial wound healing in the absence of limbal epithelium. Invest Ophthalmol Vis Sci. 1991;32(1):96–105.
6. Dua HS, Azuara-Blanco A. Limbal stem cells of the corneal epithelium. Surv Ophthalmol. 2000;44(5):415–25.
7. Dua HS, Joseph A, Shanmuganathan VA, Jones RE. Stem cell differentiation and the effects of deficiency. Eye (Lond). 2003;17(8):877–85.
8. Tseng SC. Staging of conjunctival squamous metaplasia by impression cytology. Ophthalmology. 1985;92(6):728–33.
9. Dua HS, Saini JS, Azuara-Blanco A, Gupta P. Limbal stem cell deficiency: concept, aetiology, clinical presentation, diagnosis and management. Indian J Ophthalmol. 2000;48(2):83–92.
10. Kenyon KR, Tseng SC. Limbal autograft transplantation for ocular surface disorders. Ophthalmology. 1989;96(5):709–22discussion 722.
11. Pellegrini G, Traverso CE, Franzi AT, Zingirian M, Cancedda R, De Luca M. Long-term restoration of damaged corneal surfaces with autologous cultivated corneal epithelium. Lancet. 1997;349(9057):990–3.
12. Zhao Y, Ma L. Systematic review and meta-analysis on transplantation of ex vivo cultivated limbal epithelial stem cell on amniotic membrane in limbal stem cell deficiency. Cornea. 2015;34(5):592–600.
13. Nakamura T, Inatomi T, Sotozono C, Amemiya T, Kanamura N, Kinoshita S. Transplantation of cultivated autologous oral mucosal epithelial cells in patients with severe ocular surface disorders. Br J Ophthalmol. 2004;88(10): 1280–4.
14. Nishida K, Yamato M, Hayashida Y, Watanabe K, Yamamoto K, Adachi E, et al. Corneal reconstruction with tissue-engineered cell sheets composed of autologous oral mucosal epithelium. N Engl J Med. 2004;351(12):1187–96.
15. Inatomi T, Nakamura T, Koizumi N, Sotozono C, Yokoi N, Kinoshita S. Midterm results on ocular surface reconstruction using cultivated autologous oral mucosal epithelial transplantation. Am J Ophthalmol. 2006; 141(2):267–75.
16. Inatomi T, Nakamura T, Kojyo M, Koizumi N, Sotozono C, Kinoshita S. Ocular surface reconstruction with combination of cultivated autologous oral mucosal epithelial transplantation and penetrating keratoplasty. Am J Ophthalmol. 2006;142(5):757–64.
17. Ang LPK, Nakamura T, Inatomi T, Sotozono C, Koizumi N, Yokoi N, et al. Autologous serum-derived cultivated oral epithelial transplants for severe ocular surface disease. Arch Ophthalmol. 2006;124(11):1543–51.
18. Nakamura T, Inatomi T, Cooper LJ, Rigby H, Fullwood NJ, Kinoshita S. Phenotypic investigation of human eyes with transplanted autologous cultivated oral mucosal epithelial sheets for severe ocular surface diseases. Ophthalmology. 2007;114(6):1080–8.
19. Satake Y, Dogru M, Yamane G-Y, Kinoshita S, Tsubota K, Shimazaki J. Barrier function and cytologic features of the ocular surface epithelium after autologous cultivated oral mucosal epithelial transplantation. Arch Ophthalmol. 2008;126(1):23–8.
20. Chen H-CJ, Chen H-L, Lai J-Y, Chen C-C, Tsai Y-J, Kuo M-T, et al. Persistence of transplanted oral mucosal epithelial cells in human cornea. Invest Ophthalmol Vis Sci. 2009;50(10):4660–8.
21. Ma DHK, Kuo MT, Tsai YJ, Chen HCJ, Chen XL, Wang SF, et al. Transplantation of cultivated oral mucosal epithelial cells for severe corneal burn. Eye (Lond). 2009;23(6):1442–50.
22. Priya CG, Arpitha P, Vaishali S, Prajna NV, Usha K, Sheetal K, et al. Adult human buccal epithelial stem cells: identification, ex-vivo expansion, and transplantation for corneal surface reconstruction. Eye (Lond). 2011;25(12): 1641–9.

23. Satake Y, Higa K, Tsubota K, Shimazaki J. Long-term outcome of cultivated oral mucosal epithelial sheet transplantation in treatment of total limbal stem cell deficiency. Ophthalmology. 2011;118(8):1524–30.

24. Nakamura T, Takeda K, Inatomi T, Sotozono C, Kinoshita S. Long-term results of autologous cultivated oral mucosal epithelial transplantation in the scar phase of severe ocular surface disorders. Br J Ophthalmol. 2011;95(7):942–6.

25. Takeda K, Nakamura T, Inatomi T, Sotozono C, Watanabe A, Kinoshita S. Ocular surface reconstruction using the combination of autologous cultivated oral mucosal epithelial transplantation and eyelid surgery for severe ocular surface disease. Am J Ophthalmol. 2011;152(2):195–201e1.

26. Burillon C, Huot L, Justin V, Nataf S, Chapuis F, Decullier E, et al. Cultured autologous oral mucosal epithelial cell sheet (CAOMECS) transplantation for the treatment of corneal limbal epithelial stem cell deficiency. Invest Ophthalmol Vis Sci. 2012;53(3):1325–31.

27. Hirayama M, Satake Y, Higa K, Yamaguchi T, Shimazaki J. Transplantation of cultivated oral mucosal epithelium prepared in fibrin-coated culture dishes. Invest Ophthalmol Vis Sci. 2012;53(3):1602–9.

28. Chen H-CJ, Yeh L-K, Tsai Y-J, Lai C-H, Chen C-C, Lai J-Y, et al. Expression of angiogenesis-related factors in human corneas after cultivated oral mucosal epithelial transplantation. Invest Ophthalmol Vis Sci. 2012;53(9):5615–23.

29. Sotozono C, Inatomi T, Nakamura T, Koizumi N, Yokoi N, Ueta M, et al. Visual improvement after cultivated oral mucosal epithelial transplantation. Ophthalmology. 2013;120(1):193–200.

30. Sotozono C, Inatomi T, Nakamura T, Koizumi N, Yokoi N, Ueta M, et al. Cultivated oral mucosal epithelial transplantation for persistent epithelial defect in severe ocular surface diseases with acute inflammatory activity. Acta Ophthalmol. 2014;92(6):e447–53.

31. Kolli S, Ahmad S, Mudhar HS, Meeny A, Lako M, Figueiredo FC. Successful application of ex vivo expanded human autologous oral mucosal epithelium for the treatment of total bilateral limbal stem cell deficiency. Stem Cells. 2014;32(8):2135–46.

32. Dobrowolski D, Orzechowska-Wylegala B, Wowra B, Wroblewska-Czajka E, Grolik M, Szczubialka K, et al. Cultivated oral mucosa epithelium in ocular surface reconstruction in aniridia patients. Biomed Res Int. 2015;2015:281870.

33. Prabhasawat P, Ekpo P, Uiprasertkul M, Chotikavanich S, Tesavibul N, Pornpanich K, et al. Long-term result of autologous cultivated oral mucosal epithelial transplantation for severe ocular surface disease. Cell Tissue Bank. 2016;17(3):491–503.

34. Baradaran-Rafii A, Delfazayebaher S, Aghdami N, Taghiabadi E, Bamdad S, Roshandel D. Midterm outcomes of penetrating keratoplasty after cultivated oral mucosal epithelial transplantation in chemical burn. Ocul Surf. 2017; 15(4):789–94.

35. Kim YJ, Lee HJ, Ryu JS, Kim YH, Jeon S, Oh JY, et al. Prospective clinical trial of corneal reconstruction with biomaterial-free cultured oral mucosal epithelial cell sheets. Cornea. 2018;37(1):76–83.

36. Wang J, Qi X, Dong Y, Cheng J, Zhai H, Zhou Q, et al. Comparison of the efficacy of different cell sources for transplantation in total limbal stem cell deficiency. Graefes Arch Clin Exp Ophthalmol. 2019;257(6):1253–63.

37. Gaddipati S, Muralidhar R, Sangwan VS, Mariappan I, Vemuganti GK, Balasubramanian D. Oral epithelial cells transplanted on to corneal surface tend to adapt to the ocular phenotype. Indian J Ophthalmol. 2014;62(5): 644–8.

38. Le Q, Xu J, Deng SX. The diagnosis of limbal stem cell deficiency. Ocul Surf. 2018;16(1):58–69.

39. Dua HS, Miri A, Alomar T, Yeung AM, Said DG. The role of limbal stem cells in corneal epithelial maintenance: testing the dogma. Ophthalmology. 2009; 116(5):856–63.

40. Barbaro V, Ferrari S, Fasolo A, Pedrotti E, Marchini G, Sbabo A, et al. Evaluation of ocular surface disorders: a new diagnostic tool based on impression cytology and confocal laser scanning microscopy. Br J Ophthalmol. 2010;94(7):926–32.

41. Jirsova K, Dudakova L, Kalasova S, Vesela V, Merjava S. The OV-TL12/30 clone of anti-cytokeratin 7 antibody as a new marker of corneal conjunctivalization in patients with limbal stem cell deficiency. Invest Ophthalmol Vis Sci. 2011;52(8):5892–8.

42. Poli M, Janin H, Justin V, Auxenfans C, Burillon C, Damour O. Keratin 13 immunostaining in corneal impression cytology for the diagnosis of limbal stem cell deficiency. Invest Ophthalmol Vis Sci. 2011;52(13):9411–5.

43. Yoshida S, Shimmura S, Kawakita T, Miyashita H, Den S, Shimazaki J, et al. Cytokeratin 15 can be used to identify the limbal phenotype in normal and diseased ocular surfaces. Invest Ophthalmol Vis Sci. 2006;47(11):4780–6.

44. Ilari L, Daya SM. Long-term outcomes of keratolimbal allograft for the treatment of severe ocular surface disorders. Ophthalmology. 2002;109(7): 1278–84.

45. Shimazaki J, Shimmura S, Fujishima H, Tsubota K. Association of preoperative tear function with surgical outcome in severe Stevens-Johnson syndrome. Ophthalmology. 2000;107(8):1518–23.

46. DeSousa J-L, Daya S, Malhotra R. Adnexal surgery in patients undergoing ocular surface stem cell transplantation. Ophthalmology. 2009;116(2):235–42.

47. Gunasekaran S, Dhiman R, Vanathi M, Mohanty S, Satpathy G, Tandon R. Ocular surface microbial flora in patients with chronic limbal stem cell deficiency undergoing cultivated oral mucosal epithelial transplantation. Middle East Afr J Ophthalmol. 2019;26(1):23–6.

48. Sharma SM, Fuchsluger T, Ahmad S, Katikireddy KR, Armant M, Dana R, et al. Comparative analysis of human-derived feeder layers with 3T3 fibroblasts for the ex vivo expansion of human limbal and oral epithelium. Stem Cell Rev Rep. 2012;8(3):696–705.

49. Kinoshita S, Koizumi N, Nakamura T. Transplantable cultivated mucosal epithelial sheet for ocular surface reconstruction. Exp Eye Res. 2004;78(3):483–91.

50. Massie I, Levis HJ, Daniels JT. Response of human limbal epithelial cells to wounding on 3D RAFT tissue equivalents: effect of airlifting and human limbal fibroblasts. Exp Eye Res. 2014;127:196–205.

51. Ramirez-Miranda A, Nakatsu MN, Zarei-Ghanavati S, Nguyen CV, Deng SX. Keratin 13 is a more specific marker of conjunctival epithelium than keratin 19. Mol Vis. 2011;17:1652–61.

52. Utheim OA, Pasovic L, Raeder S, Eidet JR, Fostad IG, Sehic A, et al. Effects of explant size on epithelial outgrowth, thickness, stratification, ultrastructure and phenotype of cultured limbal epithelial cells. PLoS One. 2019;14(3):e0212524.

53. Yamaguchi M, Ebihara N, Shima N, Kimoto M, Funaki T, Yokoo S, et al. Adhesion, migration, and proliferation of cultured human corneal endothelial cells by laminin-5. Invest Ophthalmol Vis Sci. 2011;52(2):679–84.

54. Kolli S, Bojic S, Ghareeb AE, Kurzawa-Akanbi M, Figueiredo FC, Lako M. The role of nerve growth factor in maintaining proliferative capacity, colony-forming efficiency, and the limbal stem cell phenotype. Stem Cells. 2019; 37(1):139–49.

55. Sen S, Sharma S, Gupta A, Gupta N, Singh H, Roychoudhury A, et al. Molecular characterization of explant cultured human oral mucosal epithelial cells. Invest Ophthalmol Vis Sci. 2011;52(13):9548–54.

56. Huang F, Qiu J, Xue Q, Cai R, Zhang C. Phenotypes and transdifferentiation of transplanted oral mucosal epithelial cells for limbal stem cell deficiency; 2019.

57. Rama P, Matuska S, Paganoni G, Spinelli A, De Luca M, Pellegrini G. Limbal stem-cell therapy and long-term corneal regeneration. N Engl J Med. 2010; 363(2):147–55.

58. Utheim TP. Limbal epithelial cell therapy: past, present, and future. Methods Mol Biol. 2013;1014:3–43.

59. Gipson IK, Inatomi T. Mucin genes expressed by the ocular surface epithelium. Prog Retin Eye Res. 1997;16(1):81–98.

60. Shimazaki J, Kaido M, Shinozaki N. Evidence of long-term survival of donor-derived cells after limbal allograft transplantation. … & visual science; 1999.

61. Henderson TR, Findlay I, Matthews PL, Noble BA. Identifying the origin of single corneal cells by DNA fingerprinting: part II--application to limbal allografting. Cornea. 2001;20(4):404–7.

62. Sharpe JR, Daya SM, Dimitriadi M, Martin R, James SE. Survival of cultured allogeneic limbal epithelial cells following corneal repair. Tissue Eng. 2007; 13(1):123–32.

63. Soma T, Hayashi R, Sugiyama H, Tsujikawa M, Kanayama S, Oie Y, et al. Maintenance and distribution of epithelial stem/progenitor cells after corneal reconstruction using oral mucosal epithelial cell sheets. PLoS One. 2014;9(10):e110987.

64. Liang L, Sheha H, Li J, Tseng SCG. Limbal stem cell transplantation: new progresses and challenges. Eye (Lond). 2009;23(10):1946–53.

65. Wan P-X, Wang B-W, Wang Z-C. Importance of the stem cell microenvironment for ophthalmological cell-based therapy. World J Stem Cells. 2015;7(2):448–60.

66. Kanayama S, Nishida K, Yamato M, Hayashi R, Maeda N, Okano T, et al. Analysis of soluble vascular endothelial growth factor receptor-1 secreted from cultured corneal and oral mucosal epithelial cell sheets in vitro. Br J Ophthalmol. 2009;93(2):263–7.

67. Sekiyama E, Nakamura T, Kawasaki S, Sogabe H, Kinoshita S. Different expression of angiogenesis-related factors between human cultivated corneal and oral epithelial sheets. Exp Eye Res. 2006;83(4):741–6.

68. Kanayama S, Nishida K, Yamato M, Hayashi R, Sugiyama H, Soma T, et al. Analysis of angiogenesis induced by cultured corneal and oral mucosal epithelial cell sheets in vitro. Exp Eye Res. 2007;85(6):772–81.

69. Duan C-Y, Xie H-T, Zhao X-Y, Xu W-H, Zhang M-C. Limbal niche cells can reduce the angiogenic potential of cultivated oral mucosal epithelial cells. Cell Mol Biol Lett. 2019;24:3.

70. Wilson SE, Mohan RR, Mohan RR, Ambrósio R, Hong J, Lee J. The corneal wound healing response. Prog Retin Eye Res. 2001;20(5):625–37.

Publisher's Note

10.5. Appendix 5: The healing dynamics of non-healing wounds using cryo-preserved amniotic membrane

ORIGINAL ARTICLE

IWJ WILEY

The healing dynamics of non-healing wounds using cryo-preservedamniotic membrane

Alzbeta Svobodova[1] | Vojtech Horvath[2] | Ingrida Smeringaiova[3] |
Joao Victor Cabral[3] | Martina Zemlickova[4] | Radovan Fiala[5] | Jan Burkert[5,6] |
Denisa Nemetova[6] | Petr Stadler[2] | Jaroslav Lindner[1] | Jan Bednar[3] |
Katerina Jirsova[3,6] ⓘ

[1]2nd Department of Surgery—Department of Cardiovascular Surgery, First Faculty of Medicine, Charles University and General University Hospital in Prague, Prague, Czech Republic

[2]Department of Vascular Surgery, Na Homolce Hospital, Prague, Czech Republic

[3]Laboratory of the Biology and Pathology of the Eye, Institute of Biology and Medical Genetics, First Faculty of Medicine, Charles University, Prague, Czech Republic

[4]Clinic of Dermatovenerology, General Teaching Hospital and First Faculty of Medicine, Charles University, Prague, Czech Republic

[5]Department of Cardiovascular Surgery, Motol University Hospital, Prague, Czech Republic

[6]Department of Transplantation and Tissue Bank, Motol University Hospital, Prague, Czech Republic

Correspondence
Assoc. Prof. Katerina Jirsova, Ph.D., Laboratory of the Biology and Pathology of the Eye, Institute of Biology and Medical Genetics, First Faculty of Medicine, Charles University, Albertov 4 128 00 Prague, Czech Republic.
Email: katerina.jirsova@lf1.cuni.cz

Funding information
Ministerstvo Zdravotnictví Ceské Republiky, Grant/Award Number:

Abstract

We evaluated the effect of the application of cryo-preserved amniotic membrane on the healing of 26 non-healing wounds (18 patients) with varying aetiologies and baseline sizes (average of 15.4 cm^2), which had resisted the standard of care treatment for 6 to 456 weeks (average 88.8 weeks). Based on their average general responses to the application of cryo-preserved AM, we could differentiate three wound groups. The first healed group was characterised by complete healing (100% wound closure, maximum treatment period 38 weeks) and represented 62% of treated wounds. The wound area reduction of at least 50% was reached for all wounds in this group within the first 10 weeks of treatment. Exactly 19% of the studied wounds responded partially to the treatment (partially healed group), reaching less than 25% of closure in the first 10 weeks and 90% at maximum for extended treatment period (up to 78 weeks). The remaining 19% of treated wounds did not show any reaction to the AM application (unhealed defects). The three groups have different profiles of wound area reduction, which can be used as a guideline in predicting the healing prognosis of non-healing wounds treated with a cryo-preservedamniotic membrane.

Key Messages

- we evaluated the effect of the application of cryo-preserved amniotic membrane on the healing of non-healing wounds
- twenty-six wounds (18 patients) of various aetiologies and baseline sizes with a history of long preceding resistance to standard care were treated for an extended time period (up to 78 weeks)
- we showed that the amniotic membrane application had a profitable effect promoting a complete healing of 62% of treated, previously non-healing defects

- analysis of our results also suggests that the dynamics of healing process can be used as a predictor of the outcome of the treatment

KEYWORDS
cryo-preserved amniotic membrane, healing dynamics, non-healing wounds

1 | INTRODUCTION

The general term 'chronic wounds' envelopes a heterogeneous group of wounds exhibiting specific healing process physiology different from the acute ones. They typically require a considerably long healing time and are characterised by tissue renewal by granulation.[1] The period required for a wound to be classified as chronic has been defined in the range of 4 weeks up to more than 3 months.[2] As the nomenclature 'chronic wound' is not clear, the European Wound Management Association (EWMA) proposed to use the term 'non-healing wounds' (NHWs),[3] which will be used herein. Common features of NHW include persistent infections, the formation of drug-resistant microbial biofilms, and loss of dermal/epidermal cells ability to respond to reparative stimuli.[4] NHWs are associated with numerous pathological conditions: diabetes mellitus (DM), peripheral artery disease (PAD), chronic venous insufficiency, post-traumatic wounds, or postsurgical wound dehiscence. Apart from the pathological effects, the NHWs have an important impact on the quality of life of affected subjects in the sense of elimination or discrimination from society, limited mobility, and productivity.[5]

The current standard of care (SOC) for treating NHW includes surgical debridement, infection control, appropriate dressing, and treatment of primary pathology. Despite the development of many types of wound dressings, the healing of NHW is often challenging to achieve. Using SOC, closure rates for NHW range from 21% to 35%, and the recurrence rate is high.[6] The increase in the healing efficiency and reduction of the recurrence rate, the healing time, and the costs are thus the objectives of the new approaches to NHW care. The use of different forms of biological dressings, particularly placental derivatives, has been accepted as a promising tool in regenerative medicine.[7-10] Most frequently, they are based on amniochorionic (ACM) or amniotic membrane (AM). For decades the ACM and AM have been recognised for their wound healing stimulation properties and their negligible immunogenicity, making them an attractive choice for biological wound dressing. AM application has been adapted particularly in the ocular surface healing, and in the last decade, its efficiency is broadly confirmed in other surgical procedures in dermatology, plastic surgery, genitourinary medicine, and otolaryngology.[8,11-13]

AM application promotes several effects supporting wound healing, namely anti-inflammatory, anti-fibrotic, anti-microbial, neurotrophic, and analgesic. Besides that, AM influences angiogenesis. AM grafting does not lead to immunological rejection, and there is no need for any immunosuppressive treatment.[13-16] Therefore, the AM grafts are considered a safe substrate, promoting proper granulation and epithelisation, assuring better hydration of the wound bed while suppressing excessive fibrosis. Many studies have reported the healing benefits of AM applied to NHW; improved healing rates (percentage of completely healed wounds) and significantly shortened healing times have been documented.

Systematic studies of the effect of the AM or ACM effect date back to the early 80s of the last century.[17] Often such studies report different healing success rates and wound closure progress, depending on the procedure of AM or ACM preparation (cryo-preserved, dried, or lyophilised),[18] AM application frequency,[19] type of wound treated (diabetic, venous, or arterial ulcer, surgical wound, dehiscence),[20] and the treatment and application approach selected.[7,21,22]

The complete healing rate of NHW because of AM's beneficial effect is reported to be anywhere between 20%[23] and 100%,[24] indicating the existence of non-negligible proportions of subjects who will not respond to the AM treatment. However, it is still unclear whether it is possible to identify such individuals already at the early treatment period (although some indications exist[25]). Because of the elevated cost of AM treatment, this information can be an important economic factor when opting for AM application after SOC failure.

In the present work, we studied the effect of cryo-preserved AM application on NHW of various aetiologies (venous, arterial, postoperative, diabetic) and various sizes (from 0.5 to 98 cm^2), which had previously resisted SOC for more than 6 weeks (average 88.8). By evaluating the healing progress, we aimed to determine the efficiency of the AM treatment and analyse whether the dynamics of the wound closure can be used as a predictor/estimator for the efficacy of the AM treatment of NHW.

2 | MATERIALS AND METHODS

The study followed the Ethics Committee standards of four participating institutions (1st Medical Faculty of Charles University, General University Hospital, University Hospital Motol, and Na Homolce Hospital, all in Prague) and adhered to the tenets set out in the Declaration of Helsinki.

3 | SUBJECTS

The patients for the study were selected according to the following criteria: Inclusion criteria: age ≥18 years, the presence of resistant NHW with the duration of more than 6 weeks, wound of maximum size of 150 cm^2 extending through the full thickness of the skin but not reaching to the tendon or bone. Exclusion criteria: Tendon or bone exposure in the wound, allergy to antibiotics used in solution for AM decontamination, transcutaneous oximetry value below 30 mmHg for patients with DM, known history of AIDS or HIV, ankle brachial index (ABI) <0.5, for all patients except those with DM, suspicious for cancer or history of radiation at wound site, severe (uncontrolled) systemic disease, or planned surgical intervention in the next 6 months.

Patients willing to participate in the study and complying with the criteria signed an informed consent form. Eighteen patients were enrolled in the study (13 men, 5 women) with a total of 26 wounds (multiple wounds in some patients). The average age of the patients was 62.6 years (26 to 85). The treated wound size varied between 0.5 and 98 cm^2 with an average of 15.4 ± 20.2 cm^2. The wound resistance to treatments preceding the enrolment into the study spanned from 6 to 456 weeks with an average of 88.8 weeks. The demographic data of patients are summarised in Table 1.

4 | AM GRAFTS PREPARATION

All placenta donors signed informed consent and were checked negative for hepatitis B and C, syphilis, and HIV, and C-reactive protein was < 20 mg/L. Placentas were obtained from full-term deliveries by elective caesarean section in the Motol University Hospital, Prague, and before processing visually inspected for injuries, visible pathologies, or comorbidities. Then they were immediately placed in a sterile container, overlaid with decontamination solution BASE•128 (Alchimia, Ponte San Nicolò, Italy), and stored at room temperature for 20 hours. The placentas were subsequently processed in aseptic conditions. They were repeatedly cleansed using physiological solution (0.9% NaCl), AM sheets were peeled off by blunt dissection, and blood clots were removed. AM was then overlaid with DMEM (c.n. 32 430 027, Thermo Fisher Scientific) supplemented with antibiotics (Piperacillin/Tazobactam, Amphotericin B, Vancomycin, and Gentamicin) and stored for at least 2 hours to complete the decontamination. Next, the AM sheets were rinsed in physiological solution, stretched on Sanatyl support (Tylex, Letovice, Czech Republic), and sectioned into patches of the desired size. Finally, AM pieces were placed in containers filled with storage medium (50% glycerol in DMEM) (glycerol, Dr Kulich Pharma, Czech Republic) and stored at 80 C. Tissues with negative microbiology tests and negative repeated serology examination performed after 6 months were released after 6 months for grafting.

5 | AM DRESSING APPLICATION AND THE WOUND TREATMENT PROCEDURE

All patients followed up a standard visit protocol. The study visits were scheduled every 7 days and included photodocumentation of the healing process, evaluation of subjective pain perception and completion of patients quality of life questionnaire, the treatment of the wound and surrounding skin, application of AM, and secondary fixation dressing application. The initial AM application frequency was set to weekly (every visit), but it was modulated later according to the evolution of the healing progress. Wound care procedure was standardised for all centres similarly: wound debridement, rinsing with saline, cultivation collection (each 4 weeks, or if necessary), and disinfectant solution application. After thawing, the AM was removed from the storage solution and washed with saline (2 5 minutes) in a sterile container. The AM graft was applied with at least 5 mm overlap, and complete contact with the wound surface was assured. After verifying appropriate graft adhesion, a fixation with foam cover (Mepilex XT, Mölnlycke Health, Sweden) was formed with an overlap of at least 2 cm and fixed with a bandage. In patients with venous insufficiency, a compression bandage was added. Wound dressing was left for 3 to 5 days, depending on the condition of the wound. In case of need of redressing at home, the patients were equipped with the necessary material and were eventually assisted by home care agency.

6 | HEALING PROCESS EVALUATION

The wound healing progress was regularly monitored during the scheduled visits for wound treatment and

TABLE 1   Demographic data

Patient number	Age	Sex	DM	Smoker	Comorbidities	Defect number	Location	Aetiology
P1	77	M	N	N	atrial fibrillation	D1	right calf	venous
P2	60	M	Y	N	hypertension, hyperlipidaemia, renal insufficiency, atrial fibrillation, st.p. AVR	D2	left calf	venous
						D3	left calf	venous
P3	72	M	N	N	hypertension, atrial fibrillation, renal insufficiency	D4	left calf	venous
						D5	left calf	venous
						D6	left calf	venous
						D7	left calf	venous
P4	64	M	N	N	renal insufficiency	D8	right calf	venous
						D9	right calf	venous
P5	72	M	N	N	hypertension	D10	right ankle	venous/ arterial
						D11	right ankle	venous/ arterial
P6	56	F	N	Y	hypertension, peripheral artery disease	D12	left calf	defect after fasciotomy
P7	33	M	N	Y	hypertension	D13	right lower leg	venous
P8	60	M	N	N	hypertension	D14	right leg	venous
P9	66	F	N	Y	hypertension	D15	left ankle	venous
P10	65	M	Y	N	hypertension	D16	right leg	arterial
P11	85	F	Y	N	hypertension, peripheral arterial disease, anaemia	D17	left ankle	venous
P12	26	F	N	N	hypertension, hyperlipidaemia, st.p. AVR, st.p. CABG	D18	sternum	dehiscence
P13	45	M	N	N	hypertension	D19	left ankle	venous
						D20	left ankle	venous
P14	68	F	Y	N	X	D21	right ankle	venous
P15	67	M	Y	N	hypertension, hyperlipidaemia	D22	left calf	venous
						D23	left calf	venous
P16	67	M	N	N	X	D24	right ankle	venous
P17	74	M	Y	Y	hypertension, peripheral artery disease, chronic renal failure, anaemia, st.p. CABG	D25	left calf	defect after fasciotomy
P18	69	M	N	Y	hypertension	D26	left ankle	arterial

Abbreviations: DM, diabetes mellitus; st.p. AVR, status post aortic valve replacement; st.p. CABG, status post coronary artery bypass grafting.

dressing renewal. The wound size and the state were photo-documented with a scale indicating the patient ID number, the defect number, and the visit date placed in the closest proximity of the wound to assure the image unique identifier and proper image scaling. The wound size was determined by manual tracing of the wound border on calibrated images with automatic determination of the area size using NIS-Elements software (Laboratory Imaging, The Czech Republic). Wound area reduction, WAR = 100*(Baseline size Current size)/Baseline size): the parameter was used to evaluate the healing progress, expressing the wound area's percentage at a given treatment period relative to the original size.

The wound was considered as healed (H) only when 100% reepithelialisation was achieved. Wounds with WAR between 50 and 99% were considered as partially healed (PH). Not achieving a reduction in the area by at least 50% was judged as failure to heal (unhealed defects [UH]), in accordance with the most often used criterion.[26] The average wound closure profiles for the H and PH group were fitted with asymptotic function ($y = a \cdot b.c^x$) using ORIGIN50 software. For the unhealed (UH) group, only an approximate linear fit was performed because of the scattered character of the average.

Other than the wound itself, the perception of pain related to the wound was also monitored. The pain

FIGURE 1   Examples of wound closing. A, healed (H) wound (D15, venous leg ulcer); B, partially healed (PH) wound (D19, venous leg ulcer); C, wound with no reaction (D25, defect after fasciotomy). W0: the wound state after 24, 456, and 100 weeks of outpatient care with SOC treatment for A, B, and C, respectively. W: number of weeks of treatment with AM

TABLE 2   Defects' characteristics and outcome data

Patient number	Defect number	Time from onset (w)	Baseline size (cm^2)	Treatment duration (w)	Wound closure (%)	End status	Number of visits	Number of AM applications
P1	D1	315	2.6	9	100	H	10	9
P2	D2	36	16.8	32	100	H	31	15
	D3	36	4.5	17	100	H	17	11
P3	D4	7	28.1	16	100	H	15	11
	D5	7	1.0	6	100	H	5	2
	D6	7	2.4	6	100	H	6	4
	D7	7	13.8	36	100	H	36	15
P4	D8	13	6.2	31	100	H	31	14
	D9	13	2.9	35	100	H	31	15
P5	D10	6	1.3	12	100	H	11	4
	D11	250	5.2	38	100	H	37	19
P6	D12	6	48.7	33	100	H	29	29
P7	D13	53	5.3	36	100	H	34	30
P8	D14	12	0.5	14	100	H	14	14
P9	D15	24	10.7	13	100	H	8	8
P10	D16	8	6.0	5	100	H	6	4
P11	D17	52	98.0	74	79	PH	74	69
P12	D18	20	14.4	44	50	PH	38	32
P13	D19	456	22.9	78	64	PH	67	46
	D20	456	13.9	78	74	PH	67	45
P14	D21	50	7.1	49	90	PH	39	39
P15	D22	117	30.5	6	28	UH	6	4
	D23	117	5.6	11	18	UH	11	9
P16	D24	100	5.0	19	3	UH	19	12
P17	D25	100	33.6	18	22	UH	13	9
P18	D26	40	12.7	17	34	UH	13	11

level was evaluated using the 0 to 10 scale, 0 equal none, 10—unbearable.

7 | RESULTS

Of 18 patients (26 defects), 10 responded to the AM treatment by complete healing of all wounds (H group, 16 defects, 62%). Four patients (five defects, 19%) exhibited partially positive limited response (PH group). They reached on average $71.4 \pm 13.6\%$ of WAR and never exceeded 90% wound closure despite, in some cases, significantly prolonged treatment (up to 74 weeks). They showed less than 20% improvement over the period of first 9 to 20 weeks. Four patients (five defects, 19%) did

not react to the treatment at all and were assigned to the unhealed group (UH group). In no case, an adverse secondary reaction to the AM application was observed. In cases when the defect responded well to the AM treatment, the epithelisation onset was very fast (after 2 AM applications), and the wound closure progressed rapidly towards complete healing. Typical wound healing in the course of treatment (D16) is presented in Figure 1A.

The period required for the defect's complete healing in the H group varied from 5 to 38 weeks (average 21.2 ± 12.2, median 16.5) and 2 to 30 AM applications (12.8 ± 7.9, 12.5) were needed. The WAR progress in the PH group was significantly slower, and its average showed the tendency to converge to a maximum value of approximately 88%. The data summarising outcomes for
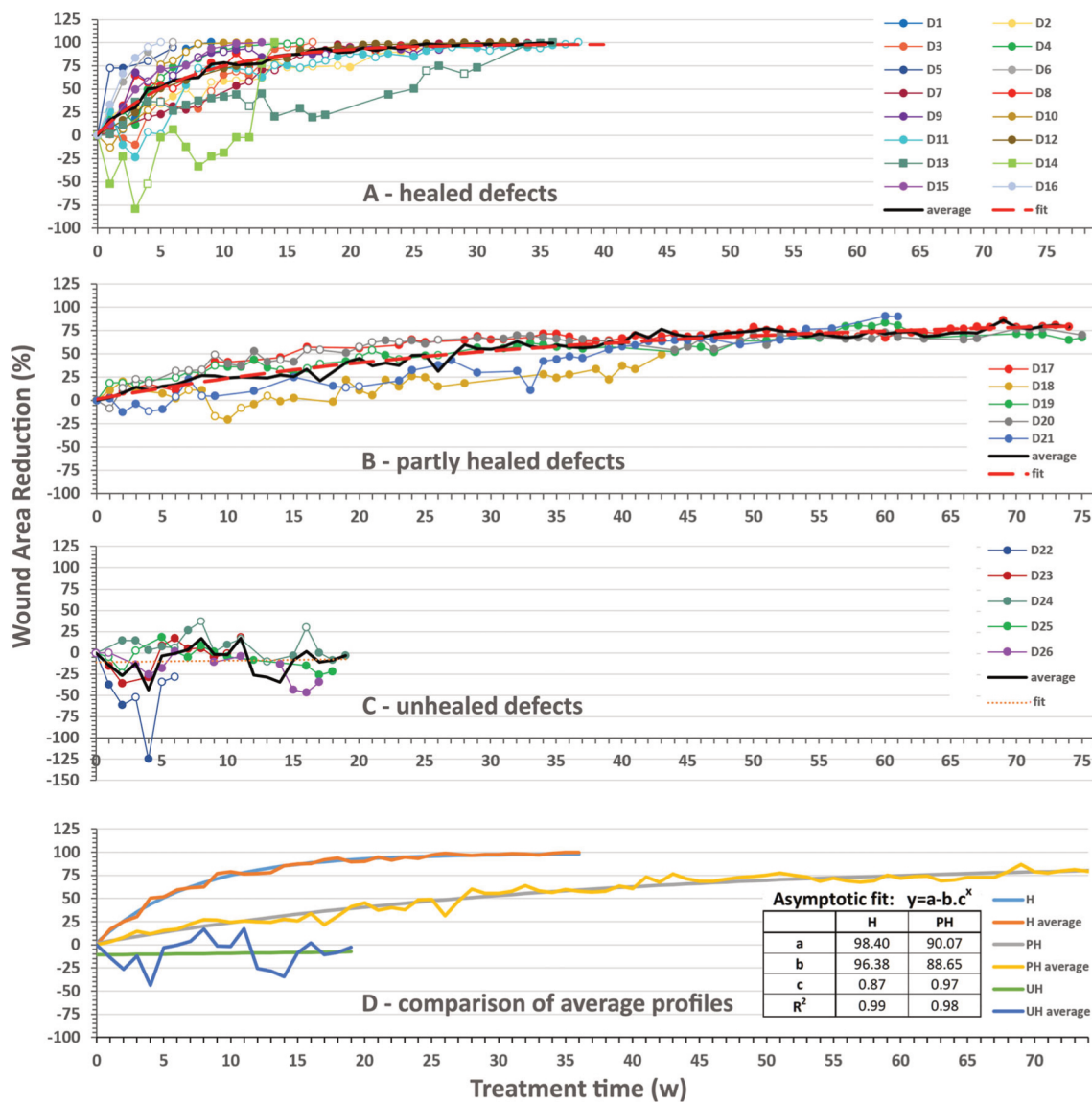
FIGURE 2 Wound closure evolution. WAR progress for healed A, partly healed B, and unhealed C, defects. D, comparison of the averages of the three groups together with fitted asymptotic functions and their parameters for H and PH and correlation coefficients (R^2). For A, B, and C, the closed and open markers reflect visits with or without AM application, respectively

individual defects are presented in Table 2. We have recorded the WAR profile for each defect and determined the average healing profiles separately for each group (H, PH, UH) (Figure 2). From the average WAR curve for healed defects (H) and its fit (regression coefficient $R^2 = 0.987$) (Figure 2A, D), we established that on average 50% of healing was achieved in 5 weeks of treatment and 70% in 10 weeks. All healed defects reached at least 50% of closure within the first 10 weeks of treatment (Figure 2A) with two exceptions: The defects D13, D14 (lines with square markers in Figure 2A) exhibited a profile significantly diverging from the rest of the defects in the group. They were characterised by delayed onset (12 and 17 weeks, respectively) of the AM stimulated healing and partial initial worsening. After this lag period, during which the healing profiles resembled those of the PH group, both defects started to progress and reached complete closure. The most prolonged healing in the H group lasted 44 weeks (defects D8 and D9).

Five defects (D17 to D21) healed partially, and despite the prolonged care period (up to 78 weeks) these defects progressed slowly without reaching the complete closure (Figure 1B, Figure 2B). The average WAR of these defects followed a different curve compared with the H group's characteristics, and approximately 27 weeks were necessary to reach 50% of closure (average). The average WAR value was 71% at the end of treatment. The course of the fitted curve is significantly flatter compared with the H group and predicts the maximum reachable WAR of approximately 90% (a = 88, Figure 2D).

Four patients (five defects, D22 to D26) did not respond to the AM treatment despite intense care, Figure 1C, Figure 2C. Their WAR values oscillated around 0, meaning that their size randomly changed around the baseline. The very approximate linear fit shows virtually no effect of the treatment on the wound size.

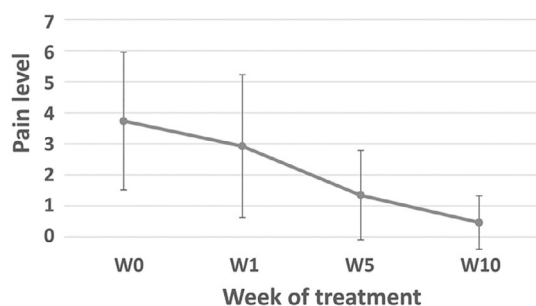The degree of pain in all patients decreased independently of the healing progress from an average of 3.25 before the first AM application to 1.95, 1.22, and 0.47 after the first, fifth, and the tenth week of AM treatment, respectively, on a scale from 0 (no pain) to 10 (the worst pain) (Figure 3). No difference in pain relief was found between healed and unhealed patients.

8 | DISCUSSION

When AM is used for the treatment of NHW, several factors may affect the outcome: the wound aetiology, baseline size, period from onset to treatment start, type of AM used (cryo-preserved, dried, lyophilised, etc.), frequency of AM application, treatment period, and the individual sensitivity to the AM effect, which can be directly related to the general health status of the subject's organism, including age, and BMI and comorbidities of the subjects. In this multicentric study, we assessed the effect of cryo-preserved AM application on the healing of NHW. Apart from evaluating the general healing effect, one of the aims of the study was to understand if there is a way to predict the outcome of the AM stimulated healing process already at the early stages of the treatment. Although the logistics (long-term storage and the delivery in frozen state) related to the use of such material is more complex than that of, for example, dried or lyophilised tissues, cryo-preserved AM should preserve the majority of the growth factors and other molecules affecting the healing process in their active form and, therefore, promote the treatment efficiency.[7,27-29] Some studies, however, indicate that the quality of lyophilised AM levels that of cryo-preserved AM in terms of preservation of active molecular components[30] and efficiency in NHW treatment.[18]

The observed healing rate of 62% in our study is concordant with values reported in similar studies. In a multicentre, controlled, randomised, blinded, clinical trial, Lavery et al observed 62% successful healing rate (100% reepithelialisation at 12 weeks) for cryo-preserved AM compared with 21.3% success rate using SOC.[31] In a retrospective study evaluating 350 NHW from WoundExpert electronic health records, the rate of closure using cryo-preserved AM was found to be 59.4%.[32] Farivar and colleagues,[33] in a trial limited to 12 weeks and venous leg ulcers, reached 53% healing with a comparable set of NHW when using cryo-preserved AM and the average healing time of 10.9 weeks, which is markedly shorter compared with 25.5 weeks in our study. It should be noted, however, that the average NHW duration period before AM treatment in our patients was 88 weeks, which is considerably higher than in Farivar's study and other comparable studies using cryo-preserved AM.[24,31,34] Interestingly, in Ref. 33, 57% of unhealed defects showed WAR >50%, which is very similar to our 50% (five defects) representing the PH group. Another

FIGURE 3 Pain level evolution during the AM treatment. Average value ± SD from all patients on a scale from 0 (no pain) to 10 (the worst pain) at week (W) 0, 1, 5, and 10 of treatment

multicentre trial reported a success rate of 48.4% (100% reepithelialisation at 8 weeks) for viable cryo-preserved placental membrane.[34]

In general, the reported in literature rate of complete wound closure using cryo-preserved AM are quite dispersed from 20%[23] through 46%,[31] 53%,[33] 84%[35] to 100%.[24] However, some studies were realised with limited AM application period reducing, thus, the potential healing completion had the treatment been continued. Time to complete closure appears to be also variable, ranging from 6 to 56 weeks.[23,24] Therefore, the extended healing period for some defects in the present work is in the range of values reported previously.

Some works report the healing efficiency's dependence on the baseline size.[32,34,36] In our study, although the average baseline size is superior in the UH group compared with H group, we could not prove its statistical significance. The average wound size before starting AM therapy (15.4 cm^2) was larger in our study than in other studies using cryo-preserved AM.[24,31,34,35]

The frequency of AM or AM-based derivatives application used in similar studies varies from frequent (2 to 3 days[37]) to scarce.[23] We set the standard application period to weekly at the beginning of treatment. In later phases (generally after 4 to 8 weeks), the AM application frequency was changed to bi-weekly and then modulated according to the wound reaction to the treatment and healing evolution.

AM treatment cost is rather high. Thus, the question at which state its application is adequate and what are the indications suggesting its efficiency is important. Existing data show that WAR of 50% after 4 weeks of SOC is a strong indicator of appropriate healing for diabetic foot ulcers.[38] WAR change in percent was reported as an indicator of a good prognosis for venous leg ulcers.[26,39] Failure to reach such rates by SOC suggests the need for initiating alternative and/or advanced treatments.[40]

When AM application is undertaken, an indicator of the probability of complete healing would be a valuable tool for deciding whether the treatment should be continued for an extended period or not. Analysis of our results allowed us to separate the wounds into three categories with different sensitivity to the AM treatment—H, PH, and UH. The wounds in the H group achieved, on average, 70% closure after 10 weeks and 50% after 5 weeks, which is similar to the values reported elsewhere.[24] All wounds in this group attained 50% closure in 10 weeks; therefore, it would seem adequate to establish these values as predictors for successful treatment. However, this criterion may exclude the cases that would have finally benefited from the AM application had the treatment not been aborted (D13, 14). The average WAR progress for NHW in PH and UH groups is different. The

wounds completely insensitive to the AM application (UH group) are readily recognisable at the early stages of treatment (10 weeks at maximum) by the flat average progression line. To distinct NHW with the potential to heal completely (H) or to be only partially reduced over prolonged treatment (PH) is, however, more complicated. We have characterised the healing progress of these two groups by parameters of the fitted asymptotic function. The determined 'a' parameter defines the maximum reachable value of wound closure and thus can be used to predict the extent to which the wound would heal. Compared with the H group, the PH group shows significantly slower evolution with the indicated limit of only ~90% ('a' value), suggesting that these wounds will never reach complete healing when using this type of treatment, and probably it is of low interest to continue with rather expensive AM application. Instead, the treatment strategy should be reconsidered. Unfortunately, the data spread is wide, and therefore such distinction at the level of an individual patient can hardly be applied with high certitude before the weeks 12 to 13 of treatment. Interestingly, this value coincides with the time limit of most studies evaluating the effect of skin substitutes (for a complete overview, see Ref. 26.

Our results also show that the repeated and persistent application can eventually trigger the healing process even in defects not responding immediately to the AM treatment and not fitting into the above-stated values for H-type wounds. That was indeed the case of defects D13 and D14, which for an extended period exhibited only a minimal response to the treatment and reached the 50% closure only after 25 and 12 weeks, respectively, but finally healed completely. The important feature of AM is, besides healing acceleration and stimulation, its analgesic effect; pain relief has been perceived after first AM applications by all patients independently of wound healing. In any case, the AM application in NHW healing will always require a highly individual approach and should reflect previous wound treatment/healing history and the patient's general health condition.

9 | CONCLUSION

From our results, we conclude that cryo-preserved AM represents a safe and useful treatment with a strongly beneficial effect for managing NHWs. In our study, the AM application led to the complete healing of 62% of wounds. We have shown that it was possible to separate the NHW into three distinct groups with different healing characteristics (H, PH, U) according to their WAR profiles. This can then be used as a guideline for the prediction of the eventual outcome of the treatment.

CONFLICT OF INTEREST

The authors declare no conflicts of interest.

DATA AVAILABILITY STATEMENT

Data available on request from the authors.

ORCID

Katerina Jirsova ⬤ https://orcid.org/0000-0002-4625-6701

REFERENCES

1. Martin P, Nunan R. Cellular and molecular mechanisms of repair in acute and chronic wound healing. Br J Dermatol. 2015;173(2):370-378.
2. Zelen CM, Serena TE, Denoziere G, Fetterolf DE. A prospective randomised comparative parallel study of amniotic membrane wound graft in the management of diabetic foot ulcers. Int Wound J. 2013;10(5):502-507.
3. Moore Z. Why is EWMA interested in implementation?. (Oral presentation). 20th Conference of the European Wound Management Association, Geneva, 2010. Frederiksberg, Denmark: EWMA; 2010.
4. Frykberg RG, Banks J. Challenges in the treatment of chronic wounds. Adv Wound Care (New Rochelle). 2015;4(9):560-582.
5. Jarbrink K, Ni G, Sonnergren H, et al. The humanistic and economic burden of chronic wounds: a protocol for a systematic review. Syst Rev. 2017;6(1):15.
6. Gibbons GW. Grafix([R]), a cryopreserved placental membrane, for the treatment of chronic/stalled wounds. Adv Wound Care (New Rochelle). 2015;4(9):534-544.
7. Johnson A, Gyurdieva A, Dhall S, Danilkovitch A, Duan-Arnold Y. Understanding the impact of preservation methods on the integrity and functionality of placental allografts. Ann Plast Surg. 2017;79(2):203-213.
8. Malhotra C, Jain AK. Human amniotic membrane transplantation: different modalities of its use in ophthalmology. World J Transplant. 2014;4(2):111-121.
9. Parolini O, Alviano F, Bagnara GP, et al. Concise review: isolation and characterization of cells from human term placenta: outcome of the first international workshop on placenta derived stem cells. Stem Cells. 2008;26(2):300-311.
10. Pathak M, Olstad OK, Drolsum L, et al. The effect of culture medium and carrier on explant culture of human limbal epithelium: a comparison of ultrastructure, keratin profile and gene expression. Exp Eye Res. 2016;153:122-132.
11. Barr SM. Dehydrated amniotic membrane allograft for treatment of chronic leg ulcers in patients with multiple comorbidities: a case series. J Am Coll Clin Wound Spec. 2014;6(3): 38-45.
12. Jirsova K, Jones GLA. Amniotic membrane in ophthalmology: properties, preparation, storage and indications for grafting—a review. Cell Tissue Bank. 2017;18(2):193-204.
13. Mamede AC, Carvalho MJ, Abrantes AM, Laranjo M, Maia CJ, Botelho MF. Amniotic membrane: from structure and functions to clinical applications. Cell Tissue Res. 2012;349(2): 447-458.
14. Dua HS, Azuara-Blanco A. Amniotic membrane transplantation. Br J Ophthalmol. 1999;83(6):748-752.
15. Litwiniuk M, Bikowska B, Niderla-Bielinska J, et al. Potential role of metalloproteinase inhibitors from radiationsterilized amnion dressings in the healing of venous leg ulcers. Mol Med Rep. 2012;6(4):723-728.
16. McQuilling JP, Vines JB, Kimmerling KA, Mowry KC. Proteomic comparison of amnion and Chorion and evaluation of the effects of processing on placental membranes. Wounds. 2017; 29(6):E36-E40.
17. Bennett JP, Matthews R, Faulk WP. Treatment of chronic ulceration of the legs with human amnion. Lancet. 1980; 1(8179):1153-1156.
18. Ananian CE, Davis RD, Johnson EL, et al. Wound closure outcomes suggest clinical equivalence between lyopreserved and cryopreserved placental membranes containing viable cells. Adv Wound Care (New Rochelle). 2019;8(11):546-554.
19. Zelen CM, Serena TE, Snyder RJ. A prospective, randomised comparative study of weekly versus biweekly application of dehydrated human amnion/chorion membrane allograft in the management of diabetic foot ulcers. Int Wound J. 2014;11(2): 122-128.
20. Suzuki K, Michael G, Tamire Y. Viable intact cryopreserved human placental membrane for a non-surgical approach to closure in complex wounds. J Wound Care. 2016;25(Sup10): S25-S31.
21. Regulski M, Jacobstein DA, Petranto RD, Migliori VJ, Nair G, Pfeiffer D. A retrospective analysis of a human cellular repair matrix for the treatment of chronic wounds. Ostomy Wound Manage. 2013;59(12):38-43.
22. Bianchi C, Cazzell S, Vayser D, et al. A multicentre randomised controlled trial evaluating the efficacy of dehydrated human amnion/chorion membrane (EpiFix([R]))allograft for the treatment of venous leg ulcers. Int Wound J. 2018;15(1):114-122.
23. Mermet I, Pottier N, Sainthillier JM, et al. Use of amniotic membrane transplantation in the treatment of venous leg ulcers. Wound Repair Regen. 2007;15(4):459-464.
24. Valiente MR, Nicolas FJ, Garcia-Hernandez AM, et al. Cryopreserved amniotic membrane in the treatment of diabetic foot ulcers: a case series. J Wound Care. 2018;27(12):806-815.
25. Serena TE, Yaakov R, DiMarco D, et al. Dehydrated human amnion/chorion membrane treatment of venous leg ulcers: correlation between 4-week and 24-week outcomes. J Wound Care. 2015;24(11):530-534.

26. Snyder D, Sullivan N, Margolis D, Schoelles K. Skin substitutes for treating chronic wounds. Technology Assessment Program—Technical Brief 2020;Project ID: WNDT0818.

27. Duan-Arnold Y, Gyurdieva A, Johnson A, Jacobstein DA, Danilkovitch A. Soluble factors released by endogenous viable cells enhance the antioxidant and chemoattractive activities of cryopreserved amniotic membrane. Adv Wound Care (New Rochelle). 2015;4(6):329-338.

28. Duan-Arnold Y, Gyurdieva A, Johnson A, Uveges TE, Jacobstein DA, Danilkovitch A. Retention of endogenous viable cells enhances the anti-inflammatory activity of cryopreserved amnion. Adv Wound Care (New Rochelle). 2015; 4(9):523-533.

29. Duan-Arnold Y, Uveges TE, Gyurdieva A, Johnson A, Danilkovitch A. Angiogenic potential of cryopreserved amniotic membrane is enhanced through retention of all tissue components in their native state. Adv Wound Care (New Rochelle). 2015;4(9):513-522.

30. Dhall S, Sathyamoorthy M, Kuang JQ, et al. Properties of viable lyopreserved amnion are equivalent to viable cryopreserved amnion with the convenience of ambient storage. PLoS One. 2018;13(10):e0204060.

31. Lavery LA, Fulmer J, Shebetka KA, et al. The efficacy and safety of Grafix([R]) for the treatment of chronic diabetic foot ulcers: results of a multi-centre, controlled, randomised, blinded, clinical trial. Int Wound J. 2014;11(5):554-560.

32. Raspovic KM, Wukich DK, Naiman DQ, et al. Effectiveness of viable cryopreserved placental membranes for management of diabetic foot ulcers in a real world setting. Wound Repair Regen. 2018;26(2):213-220.

33. Farivar BS, Toursavadkohi S, Monahan TS, et al. Prospective study of cryopreserved placental tissue wound matrix in the management of chronic venous leg ulcers. J Vasc Surg Venous Lymphat Disord. 2019;7(2):228-233.

34. Ananian CE, Dhillon YS, Van Gils CC, et al. A multicenter, randomized, single-blind trial comparing the efficacy of viable cryopreserved placental membrane to human fibroblast-derived dermal substitute for the treatment of chronic diabetic foot ulcers. Wound Repair Regen. 2018;26(3):274-283.

35. Johnson EL, Saunders M, Thote T, Danilkovitch A. Cryopreserved placental membranes containing viable cells result in high closure rate of nonhealing upper and lower extremity wounds of non-diabetic and non-venous pathophysiology. Wounds. 2021;33(2):34-40.

36. Abdo RJ. Treatment of diabetic foot ulcers with dehydrated amniotic membrane allograft: a prospective case series. J Wound Care. 2016;25(Sup7):S4-S9.

37. Dehghani M, Azarpira N, Mohammad Karimi V, Mossayebi H, Esfandiari E. Grafting with cryopreserved amniotic membrane versus conservative wound care in treatment of pressure ulcers: a randomized clinical trial. Bull Emerg Trauma. 2017;5(4): 249-258.

38. Sheehan P, Jones P, Caselli A, Giurini JM, Veves A. Percent change in wound area of diabetic foot ulcers over a 4-week period is a robust predictor of complete healing in a 12-week prospective trial. Diabetes Care. 2003;26(6):1879-1882.

39. Kantor J, Margolis DJ. A multicentre study of percentage change in venous leg ulcer area as a prognostic index of healing at 24 weeks. Br J Dermatol. 2000;142(5):960-964.

40. Kimmel HM, Robin AL. An evidence-based algorithm for treating venous leg ulcers utilizing the Cochrane database of systematic reviews. Wounds. 2013;25(9):242-250.

10.6. Appendix 6: Inter-placental variability is not a major factor affecting the healing efficiency of amniotic membrane when used for treating chronic non-healing wounds

FULL LENGTH PAPER

Inter-placental variability is not a major factor affecting the healing efficiency of amniotic membrane when used for treating chronic non-healing wounds

Vojtech Horvath · **Alzbeta Svobodova** · **Joao Victor Cabral** ·
Radovan Fiala · **Jan Burkert** · **Petr Stadler** · **Jaroslav Lindner** ·
Jan Bednar · **Martina Zemlickova** · **Katerina Jirsova**

Abstract This study aimed to evaluate the efficacy of cryopreserved amniotic membrane (AM) grafts in chronic wound healing, including the mean percentage of wound closure per one AM application, and to determine whether the healing efficiency differs between AM grafts obtained from different placentas. A retrospective study analyzing inter-placental differences in healing capacity and mean wound closure after the application of 96 AM grafts prepared from nine placentas. Only the placentas from which the AM grafts were applied to patients suffering from long-lasting non-healing wounds successfully healed by AM treatment were included. The data from the rapidly progressing wound-closure phase (p-phase) were analyzed. The mean efficiency for each placenta, expressed as an average of wound area reduction (%) seven days after the AM application (baseline, 100%), was calculated from at least 10 applications. No statistical difference between the nine placentas' efficiency was found in the progressive phase of wound healing.

V. Horvath · P. Stadler
Department of Vascular Surgery, Na Homolce Hospital, Prague, Czech Republic
e-mail: vojtech.horvath@homolka.cz

P. Stadler
e-mail: Petr.Stadler@homolka.cz

A. Svobodova · J. Lindner
2nd Department of Surgery – Department of Cardiovascular Surgery, First Faculty of Medicine, Charles University and General University Hospital in Prague, Prague, Czech Republic
e-mail: alzbeta.svobodova@nemcl.cz

J. Lindner
e-mail: Jaroslav.Lindner@vfn.cz

J. V. Cabral · J. Bednar · K. Jirsova (✉)
Laboratory of the Biology and Pathology of the Eye, Institute of Biology and Medical Genetics, First Faculty of Medicine, Charles University and General University Hospital in Prague, Albertov 4, 128 01 Prague, Czech Republic
e-mail: katerina.jirsova@lf1.cuni.cz

J. V. Cabral
e-mail: victor.cabral@lf1.cuni.cz

J. Bednar
e-mail: jan.Bednar@lf1.cuni.cz

R. Fiala · J. Burkert
Department of Cardiovascular Surgery, Motol University Hospital, Prague, Czech Republic
e-mail: Radovan.Fiala@fnmotol.cz

J. Burkert
e-mail: Jan.Burkert@fnmotol.cz

J. Burkert · K. Jirsova
Department of Transplantation and Tissue Bank, Motol University Hospital, Prague, Czech Republic

M. Zemlickova
Clinic of Dermatovenerology, General Teaching Hospital and 1st Faculty of Medicine, Charles University, Prague, Czech Republic
e-mail: Martina.Zemlickova@vfn.cz

The 7-day average wound reduction in particular placentas varied from 5.70 to 20.99% (median from 1.07 to 17.75) of the baseline. The mean percentage of wound surface reduction of all analyzed defects one week after the application of cryopreserved AM graft was $12.17 \pm 20.12\%$ (average± SD). No significant difference in healing capacity was observed between the nine placentas. The data suggest that if there are intra- and inter-placental differences in AM sheets' healing efficacy, they are overridden by the actual health status of the subject or even the status of its individual wounds.

Keywords Placenta · Amniotic membrane · Wound healing efficiency

Introduction

For years, the human amniotic membrane (AM) has become widely used as a bioactive dressing or the basic substrate for producing broadly distributed derivatives with beneficial healing properties (Fenelon et al. 2021; Nejad et al. 2021; Elkhenany et al. 2022). While AM transplantation was primarily adopted in ophthalmology for the reconstruction of the ocular surface (corneal ulcers, persistent epithelial defects, limbal stem cell deficiency, ocular neoplasia, pterygium), and for ocular surface wound healing (e.g., for chemical and thermal injuries, dry eye disease, recurrent corneal erosions or cicatrizing conjunctivitis such are Steven's Johnson syndrome, toxic epidermal necrolysis, pemphigoid or graft versus host disease) (Tsubota et al. 1996; Fuchsluger et al. 2005; Meller et al. 2011; Tabatabaei et al. 2017; Walkden 2020). Later its application has been extended to the problem of healing wounds other than that of the eye, and its use has been developing strongly over the last few decades (DiDomenico et al. 2016; Johnson et al. 2021). The primary material for AM acquisition, the placenta, is readily available and relatively abundant compared to other transplants (Jirsova and Jones 2017). AM's anti-inflammatory, anti-fibrotic, anti-microbial, neurotrophic, analgesic, anti-, and pro-angiogenic properties, along with the epithelization promotion, make it an ideal material for treating a wide variety of wounds (Wassmer and Berishvili 2020; Elkhenany et al. 2022). The rationale behind most of the mentioned effects has been characterized

(Baradaran-Rafii et al. 2013), although the presence of substances, which can be responsible for the direct analgesic effect of AM, has only recently been suggested (Svobodova et al. 2023)**.** The AM immunogenicity is very low; thus, the risk of rejection or incompatibility complication is practically non-existent (Adinolfi et al. 1982; Hori et al. 2006).

The efficiency of AM is assigned to the presence of extracellular matrix proteins, a variety of growth factors, and cytokines, the production of which can direct adhesion, migration, proliferation, and differentiation of epithelial and stromal cells, as well as the stem and progenitor cells of epithelial and mesenchymal origin (Koizumi et al. 2000a, b; Bomfim Pereira et al. 2016; Wassmer and Berishvili 2020; Ruiz-Canada et al. 2021).

However, this also suggests that the properties of the AM prepared for transplantation will be dependent on many factors that can influence the production, concentration, and activity preservation of these substances in the AM. AM quality can be influenced by factors related to the donor/placenta-specific variations (Hopkinson et al. 2006a, b; Krabcova et al. 2014; Deihim et al. 2016) and by the handling dependent/induced factors (Allen et al. 2013; Paolin et al. 2016). The formers are responsible for both donor-dependent (inter-placental) variations (Hopkinson et al. 2006a, b; Krabcova et al. 2014) and intra-placental sub-region variations of AM composition (Deihim et al. 2016; Litwiniuk et al. 2018; Moraes et al. 2021). They can be influenced by the donor's overall physiological status, genetic predisposition, the presence of pathology, or even by the week of pregnancy at which the placenta was retrieved (Skinner et al. 1981; Tossetta et al. 2014).

Studies evaluating the effect of intra- or inter-placental variations are relatively scarce. The evaluation of the properties of placental subregions was documented in several studies, describing the sub-regional differences from different aspects: the presence of stem cell markers (Lemke et al. 2017; Centurione et al. 2018; Garcia-Lopez et al. 2019), proliferation and differentiation capacity (Germain et al. 1992; Curtis et al. 1997; Farrugia et al. 2000; Han et al. 2008; Kim et al. 2011; Centurione et al. 2018), factors influencing wound healing and angiogenesis (Han et al. 2008; Gicquel et al. 2009; Lee et al. 2010; Banerjee et al. 2018; Litwiniuk et al. 2018) and other factors.

It was suggested that AM from placental and reflected sub-regions might have different potentials for tissue regeneration due to the different mitochondrial activity, which may be, in turn, crucial for clinical applications (Banerjee et al. 2015). Similarly, the study based on the evaluation of TGFβs (1,2,3) presence discovered significant differences in their concentration among individual donors proposing a potential modification of the healing effect based on the donor individuality (Hopkinson et al. 2006a, b; Han et al. 2008). Another study evaluated the placenta quality dependent on the pregnancy week retrieval (Skinner et al. 1981). Contrary, no significant difference in pluripotency markers concentration was found between the placental and reflected amnion (Garcia-Lopez et al. 2019), suggesting the homogeneous distribution of the pluripotency transcription factors, making all regions of AM equal in the regenerative processes effect. For an excellent review analyzing the data concerning the AM sub-regional differences, see Weidinger et al. (2020).

The studies evaluating the AM properties variations due to tissue processing are much more abundant as these parameters can be much better controlled. Tissue processing encapsulates the procedures employed through the AM graft preparation chain, from placenta retrieval, decontamination, AM preparation, and storage and treatment until the moment of transplantation (Aykut et al. 2015; Jirsova and Jones 2017). As the influence of these factors can be rather straightforwardly and rigorously evaluated, numerous studies were devoted to elucidating the effect of AM decontamination/sterilization procedure (Singh et al. 2006; Smeringaiova et al. 2017), graft structure and cellular viability and content modification (intact, or denuded AM) (Koizumi et al. 2000a, b; Hopkinson et al. 2006a, b; Duan-Arnold et al. 2015), the type of preparation and storage (freezing, air-drying, lyophilization) (Dhall et al. 2018; Memmi et al. 2022).

Finally, the effect of these factors on the effectiveness of the AM application is always additionally modulated by the individuality of the treated subject, i.e., by its physiological/pathological conditions, including its sensibility to the AM treatment at the moment of the AM application.

The closure kinetics of chronic wounds usually progresses in two phases; the first is characterized by relatively rapid progress and lasts for the first 5 to 20 weeks of healing with a closure level of more than 50%. The following phase of healing is characterized by a slower progression of wound closure with a less steep curve (Herbin et al. 1993; Venault et al. 2019; Becerra-Bayona et al. 2020). Herein, these two stadia are described as progressive (p-phase) and terminal (e-phase) (Svobodova et al. 2022).

In standard AM preparation for clinical use, several tens of AM sheets are typically prepared from one placenta without keeping exact track of the sub-region origin, except when the targeted region is very specific, e.g., the umbilical part (Cognard et al. 2022). Thus, the intra-placental variations are mostly impossible to survey in clinical applications. However, the track of AMs obtained from individual placentas is rigorous, as required by legislation, and therefore, should the inter-placental differences in AM healing features be prevailing the other factors, they could be potentially detectable by evaluating its healing effect, e.g., by assessing the wound closure rate (DiDomenico et al. 2016; Valiente et al. 2018; Johnson et al. 2021).

In this study, we evaluated the effect of the cryopreserved AMs retrieved from different donors on the efficiency of wound healing (wound closure), intending to understand whether the inter-placental variations could be dominant in wound healing progress or if they are suppressed by the processing/application chain and the individual patient status at the moment of application.

Materials and methods

The study followed the Ethics Committee's standards of three participating institutions (1st Medical Faculty of Charles University, General Teaching Hospital, University Hospital Motol, and Na Homolce Hospital, all in Prague) and adhered to the tenets set out in the Declaration of Helsinki.

AM grafts preparation

After obtaining informed consent from placenta donors, the placenta and blood for serological examination were retrieved. All donors were negative for hepatitis B and C, syphilis, and HIV, C-reactive protein was < 20 mg/l. The serology was repeated after 6 months. The AM grafts were prepared as described earlier (Svobodova et al. 2022). Shortly,

all placentas were obtained by elective cesarean section between 38 to 39 (from 38 weeks+1 day to 39 weeks+4 days) gestational week in the Motol University Hospital, Prague, from donors with no serious systemic or genetic diseases. Before further processing, placentas were visually inspected for injuries and visible pathologies. Then the tissue (placenta/AM) was decontaminated at room temperature using BASE•128 (Alchimia, Ponte San Nicolò, Italy) for 24 h (±2 h) at 37 °C. AM sheets were rinsed, stretched on Sanatyl support (Tylex, Letovice, Czech Republic), and cut into desired-sized patches (varying from 2×2 cm up to 7×11 cm). Finally, AM pieces were placed into Dulbecco's Modified Eagle Medium (Gibco™ DMEM 32,430,027, Thermo Fisher Scientific) in 50% glycerol (Dr. Kulich Pharma, Czech Republic) and stored at − 80 °C. After six months, tissues with negative microbiology and serology test results were released for grafting**.**

Patients

The presented study enrolled 16 patients suffering from chronic nonhealing wounds (lasting more than 6 weeks before AM application, range 6 to 1408 weeks, average 139 weeks). Twelve wounds were venous, one arterial, one diabetic origin, one wound was linked to fasciotomy, and one to physical trauma. The inclusion and exclusion criteria have been described previously (Svobodova et al. 2022), shortly, the inclusion criteria were: age≥ 18 years, the presence of resistant NHW with a duration of more than 6 weeks, and wound extending through the entire thickness of the skin. Exclusion criteria were: tendon or bone exposure in the wound, allergy to antibiotics used for AM decontamination, transcutaneous oximetry value below 30 mmHg for patients with diabetes mellitus, known history of AIDS or HIV, ankle-brachial index (ABI)<0.5, for all patients except those with diabetes mellitus, suspicious for cancer or history of radiation at the wound site, severe (uncontrolled) systemic disease, or planned surgical intervention in the next six months.

The average age of the patients was 66.8 years (33 to 82), with 4 females and 12 males. Altogether, 22 defects (D) were followed. Before starting the treatment using AM, the wound size varied between 0.99 and 50.51 cm^2, averaging 12.88 ± 14.54 cm^2. The wound resistance to treatments before the AM

application spanned from 6 to 1408 weeks, averaging 12.88 weeks. The complete healing lasted from 5 to 105 weeks, averaging 31.14 weeks.

Input data selection and measurement

The efficiency of AM grafts obtained from 9 placentas was analyzed. The mean age of placenta donors was 34 years (26–38). AM sheets from each placenta were distributed to at least three patients, and at least ten AM sheets from individual placentas had to be used to include the placenta in the evaluation. All patients (16 in total) reached complete healing. The data from the p-phase only were evaluated (for the p-phase description, see the introduction and discussion section), which in most cases represents the first 10 to 20 weeks of the treatment. The efficiency score was evaluated as the relative wound closure; the wound size on the day of AM application was used as the baseline (100%), and the percentage of wound area change 7 days after the AM application was evaluated. The size of the wound was assessed as described previously (Svobodova et al. 2022). Briefly, the wound was photo-documented with a scale in the proximity of the wound. The wound size was determined by manually tracing the wound border on calibrated images with an automatic determination of the area using NIS-Elements software (Laboratory Imaging, The Czech Republic). The mean efficiency for each placenta, expressed as an average of wound area reduction (in %), was calculated from at least 10 applications.

Statistical analysis

First, the data sets for individual placentas were checked for the normality by Saphiro-Wilk's test. The results showed that not all sets were of normal distribution, so the Kruskal–Wallis test was applied to check if a statistically significant difference could be detected. Finally, Dunn's test for performing multiple pairwise-comparison between the means of individual placentas was used. All the evaluations were performed using the R and RStudio package (RStudio 2020).

Results

The results represent the analysis of AM efficiency on non-healing wound treatment over 5 years (2017–2022). The treatment of the "non-healing" wounds using AMs included in the study led to a complete wound closure at the end of the treatment. For the evaluation of the AM efficiency, only the p-phase of the healing progress was used (for details, see the Discussion section). Our evaluation of the AM efficiency shows that the 7-day average wound closure (% of wound surface) in the p-phase of healing after the application of cryopreserved AMs varied from 5.7 to 20.99% (medians from 1.07 to 17.75). The values for individual placentas are summarized in Table 1, and statistics are visualized in Fig. 1. These results suggest that the average wound closure rate when using cryopreserved AM for non-healing wounds is $12.17 \pm 20.12\%$ (average± standard deviation) of the wound surface 7 days after AM application.

The records for individual defects treated by each placenta evaluated in this study are summarized in Table 2. The negative values represent a temporary worsening of the wound against the baseline. While the spread of the values measured after AM application was rather important for individual placentas (e.g., for placenta 4 ranging from − 38.20 to 72.73% of wound area closure one week after application, see Table 2), resulting in high values of standard deviations, the values of both mean and median were relatively coherent, ranging from 5.70 to 20.99 and 1.07 to 17.75 respectively.

Fig. 1 A statistical representation of the efficiencies of AMs originating from different placentas

The results of Saphiro-Wilk's test revealed dispersed values for the normality of individual sets. Therefore, Levene's test was performed to decide whether parametric analysis (ANOVA) could be used. The resulting p-value of 0.008 indicated the data's non-normal character; thus, the Kruskal–Wallis test was applied. Its result showed no statistically significant difference ($p = 0.492$) between individual placentas. Therefore, it is legitimate to conclude that, in general, there is no important difference in the efficacy of AMs originating from different placentas on wound healing.

Discussion

In this study, we aimed to determine whether some significant differences in the healing efficiency of AM applied to non-healing wounds can be traced between AM sheets prepared from different placentas and to establish mean wound closure. As mentioned in the introduction, the existing studies are somewhat controversial concerning the inter- and intra-placental variation in the presence/concentration of wound healing factors (Avila-Gonzalez et al. 2015; Centurione et al. 2018). However, if such differences can be detected in the AM clinical applications for wound healing, it would help to orient more targeted studies on how to evaluate the placentas healing potential

Table 1 The average healing efficiency of the placentas is expressed as wound area reduction in % seven days after AM application

	Average± SD	Median	Saphiro-Wilk test *p* value
Placenta 1	13.67± 12.98	17.75	0.19
Placenta 2	5.70± 14.47	1.07	0.18
Placenta 3	10.13± 8.66	10.24	0.63
Placenta 4	6.83± 32.75	12.29	0.60
Placenta 5	12.13± 17.65	9.65	0.77
Placenta 6	7.26± 29.11	7.02	0.33
Placenta 7	13.46± 14.13	11.87	0.33
Placenta 8	18.06± 13.07	12.87	0.01
Placenta 9	20.99± 17.19	16.21	0.50

Table 2 Effects of applications of AMs from selected placentas on individual defects seven days after application time

Placenta 1			Placenta 2			Placenta 3		
Change (%)	Defect	Application date	Change (%)	Defect	Application date	Change (%)	Defect	Application date
30.00	P1-D1	2017–10-05	− 1.32	P4-D1	2019–02-26	17.36	P6-D1	2018–07-31
14.01	P2-D1	2018–06-26	− 12.14	P4-D2	2019–02-26	11.38	P6-D1	2018–08-07
− 6.44	P3-D2	2018–07-10	− 6.25	P5-D1	2019–01-15	12.08	P2-D1	2018–07-10
30.00	P1-D1	2017–10-23	9.70	P6-D4	2019–01-02	29.23	P3-D2	2018–07-17
20.00	P1-D1	2017–10-28	− 1.25	P6-D4	2019–01-15	3.76	P3-D1	2018–07-17
20.00	P1-D1	2017–11-01	− 4.29	P5-D1	2019–01-02	11.80	P3-D1	2018–07-03
19.66	P3-D2	2018–07-24	39.66	P4-D2	2019–04-02	−4.72	P3-D2	2018–07-03
15.85	P3-D1	2018–08-07	21.71	P7-D1	2019–04-24	8.99	P5-D1	2018–09-11
2.24	P3-D2	2018–08-07	3.39	P8-D1	2019–04-24	9.09	P3-D2	2018–09-04
-8.60	P2-D1	2018–07-03	7.81	P8-D1	2019–04-17	2.30	P3-D1	2018–09-04

Placenta 4			Placenta 5			Placenta 6		
Change (%)	Defect	Application date	Change (%)	Defect	Application date	Change (%)	Defect	Application date
− 34.62	P5-D2	2018-10-16	8.73	P6-D4	2018-11-27	− 18.52	P8-D1	2019-04-10
− 8.48	P5-D1	2018-10-16	18.47	P5-D1	2018-12-11	− 13.60	P9-D1	2019-07-02
− 29.47	P5-D2	2018-10-02	4.07	P6-D4	2018-11-06	3.29	P9-D1	2019-07-09
− 38.20	P3-D1	2018-10-02	−2.45	P4-D1	2019-02-12	− 44.52	P9-D1	2019-06-11
19.37	P5-D2	2018-09-18	10.57	P6-D4	2018-11-13	− 0.90	P9-D1	2019-04-09
5.22	P3-D1	2018-10-16	−15.56	P5-D1	2018-11-13	7.02	P9-D1	2019-04-30
38.57	P6-D1	2018-09-25	42.25	P3-D1	2018-11-20	15.52	P8-D1	2019-04-30
19.77	P4-D1	2019-03-05	−5.17	P6-D4	2018-11-20	26.28	P7-D1	2019-04-30
21.66	P4-D2	2019-03-05	39.07	P5-D2	2018-10-30	14.04	P8-D1	2019-05-02
− 21.27	P5-D1	2018-10-02	21.34	P5-D1	2018-10-30	77.55	P8-D1	2019-05-07
36.66	P6-D1	2018-10-09				13.71	P4-D1	2019-06-25
72.73	P6-D2	2018-10-09						

Placenta 7			Placenta 8			Placenta 9		
Change (%)	Defect	Application date	Change (%)	Defect	Application date	Change (%)	Defect	Application date
10.21	P10-D1	2021-03-01	5.51	P14-D1	2022-03-15	16.28	P16-D1	2022-02-22
21.88	P11-D1	2021-03-22	36.50	P15-D1	2019-09-10	32.64	P16-D2	2022-02-22
14.41	P12-D1	2020-08-04	16.47	P14-D1	2022-03-01	4.38	P13-D1	2021-12-21
4.35	P11-D1	2021-04-12	9.66	P14-D1	2022-01-25	−8.61	P13-D1	2022-01-10
50.55	P12-D1	2020-10-27	5.89	P9-D1	2019-08-13	40.25	P16-D2	2022-02-15
23.55	P12-D1	2020-08-11	5.87	P4-D1	2019-07-23	0.67	P13-D1	2022-02-14
− 10.34	P11-D1	2021-03-17	12.87	P15-D1	2019-07-24	14.08	P13-D2	2021-12-13
24.06	P10-D1	2021-03-17	20.93	P15-D1	2019-07-29	11.99	P14-D1	2022-05-31
4.90	P11-D1	2021-03-01	7.31	P15-D1	2019-08-27	38.93	P16-D1	2022-02-01
− 4.11	P11-D1	2021-02-12	38.17	P9-D1	2019-08-27	37.73	P16-D2	2022-02-08
13.54	P10-D1	2021-04-12	39.44	P15-D1	2019-09-25	47.42	P16-D2	2022-01-03
19.15	P10-D1	2021-02-08				16.14	P14-D1	2022-05-17
9.64	P10-D1	2021-04-19						
6.67	P13-D1	2022-02-28						

P designates the subject number, *D* is the defect number of the given subject

(both in inter-placental and intra-placental respect) and perhaps avoid the use of less efficient placentas for their application, which could spare an important amount of preparative time and shorten the healing period.

Herein, we defined the placenta inclusion parameters at three different levels. First, the patient's positive reactive response to the AM application healing procedure was critical. Therefore, only patients with good healing progress and complete final healing were included. Second, only the first progressive phase of healing was included in the evaluation. As we reported previously, the healing progress of well-reacting patients in our clinical study could be fitted with asymptotic function (Svobodova et al. 2022). This is characterized by rather rapid progress in the initial phases, which is then progressively slowed down in the final healing period when the last few percent of the closure generally heal much slower than at the healing onset (Becerra-Bayona et al. 2020).

Moreover, the inaccuracies in the wound size determination increase with the smaller wound size and with the absolute differences in the wound size between the measurements. Therefore, our interest was to utilize the period when the wound size and its changes were the most important, typically in the first 10–20 weeks of healing. Furthermore, the patients with multiple wounds were preferred as this would allow us to, at least partly, evaluate the subject/defect status factor.

The rate of wound healing (% of wound closure per week) in the p-phase of our patients is consistent with the regularly observed one (Bull et al. 2022). Our results suggest that more than individual placentas' properties, patients' physiological status predominantly influences the wound closure progress. We suppose that important variation of obtained values found almost for each placenta (with one exception—Pl8) reflects the patient's or wound's immediate physiological/pathological condition. This is supported by the observation that the average healing efficiency of all 9 analyzed placentas did not statistically differ. However, it is necessary to consider the limitations of this study, such as the small number of placentas (9) and the variability in patients' parameters and their wounds.

The results show that although the average values of placenta efficiency may differ quite notably (more than double the value between Pl1 and Pl6), the analysis does not confirm the statistical significance. We have also observed case-by-case differences in reaction to the AM application. In some cases, we recorded different responses of two wounds of the same subject being treated by the AM from the same placenta. E.g., when treated with AMs from placenta 1 (Pl1), the reaction of the defects P3-D1 and P3-D2, which are the two defects of the same subject, was quite different even though they were treated on the same visit day (2018-08-07), closure 15.85 vs. 2.24%, respectively. A similar situation could be observed for the P5-D1 and P5-D2 (again two defects of the same patient) wherein two weeks, the defect P5-D1 changed its reaction from positive 21.34% (2018-10-30) to negative − 15.56% (2018-11-13) when treated by AMs from placenta 5 (Pl5). At the same time, the reaction of P5-D2 was twice as important as that of P5-D1 on the same application date (2018-10-30, 39.07% vs. 21.34%, respectively). Another example of reaction variation on the AM application can be detected for the defect P9-D1, which had a very different response on the AMs from placenta 6 in two months (2019-04-30 vs. 2019-06-11). All the data suggest that if there are intra- and inter-placental differences, they are overridden mainly by the actual health status of the subject or even the status of its individual wounds (due to the microbial, blood circulation, or other possible conditions, which may affect the healing process).

Declarations

Conflict of interest The authors declare no conflict of interest.

Open Access This article is licensed under a Creative Commons Attribution 4.0 International License, which permits use, sharing, adaptation, distribution and reproduction in any medium or format, as long as you give appropriate credit to the original author(s) and the source, provide a link to the Creative Commons licence, and indicate if changes were made. The images or other third party material in this article are included in the article's Creative Commons licence, unless indicated otherwise in a credit line to the material. If material is not included in the article's Creative Commons licence and your intended use is not permitted by statutory regulation or exceeds the permitted use, you will need to obtain permission directly from the copyright holder. To view a copy of this licence, visit http://creativecommons.org/licenses/by/4.0/.

References

Adinolfi M, Akle CA, McColl I, Fensom AH, Tansley L, Connolly P, Hsi BL, Faulk WP, Travers P, Bodmer WF (1982) Expression of HLA antigens, beta 2-microglobulin and enzymes by human amniotic epithelial cells. Nature 295(5847):325–327. https://doi.org/10.1038/295325a0

Allen CL, Clare G, Stewart EA, Branch MJ, McIntosh OD, Dadhwal M, Dua HS, Hopkinson A (2013) Augmented dried versus cryopreserved amniotic membrane as an ocular surface dressing. PLoS ONE 8(10):e78441. https://doi.org/10.1371/journal.pone.0078441

Avila-Gonzalez D, Vega-Hernandez E, Regalado-Hernandez JC, De la Jara-Diaz JF, Garcia-Castro IL, Molina-Hernandez A, Moreno-Verduzco ER, Razo-Aguilera G, Flores-Herrera H, Portillo W, Diaz-Martinez NE, Garcia-Lopez G, Diaz NF (2015) Human amniotic epithelial cells as feeder layer to derive and maintain human embryonic stem cells from poor-quality embryos. Stem Cell Res 15(2):322–324. https://doi.org/10.1016/j.scr.2015.07.006

Aykut V, Celik U, Celik B (2015) The destructive effects of antibiotics on the amniotic membrane ultrastructure. Int Ophthalmol 35(3):381–385. https://doi.org/10.1007/s10792-014-9959-z

Banerjee A, Weidinger A, Hofer M, Steinborn R, Lindenmair A, Hennerbichler-Lugscheider S, Eibl J, Redl H, Kozlov AV, Wolbank S (2015) Different metabolic activity in placental and reflected regions of the human amniotic membrane. Placenta 36(11):1329–1332. https://doi.org/10.1016/j.placenta.2015.08.015

Banerjee A, Lindenmair A, Steinborn R, Dumitrescu SD, Hennerbichler S, Kozlov AV, Redl H, Wolbank S, Weidinger A (2018) Oxygen tension strongly influences metabolic parameters and the release of interleukin-6 of human amniotic mesenchymal stromal cells in vitro. Stem Cells Int 2018:9502451. https://doi.org/10.1155/2018/9502451

Baradaran-Rafii A, Eslani M, Djalillian AR (2013) Complications of keratolimbal allograft surgery. Cornea 32(5):561–566. https://doi.org/10.1097/ICO.0b013e31826215eb

Becerra-Bayona SM, Solarte-David VA, Sossa CL, Mateus LC, Villamil M, Pereira J, Arango-Rodriguez ML (2020) Mesenchymal stem cells derivatives as a novel and potential therapeutic approach to treat diabetic foot ulcers. Endocrinol Diabetes Metab Case Rep. https://doi.org/10.1530/EDM-19-0164

Bomfim Pereira MG, Pereira Gomes JA, Rizzo LV, Cristovam PC, Silveira LC (2016) Cytokine dosage in fresh and preserved human amniotic membrane. Cornea 35(1):89–94. https://doi.org/10.1097/ICO.0000000000000673

Bull RH, Staines KL, Collarte AJ, Bain DS, Ivins NM, Harding KG (2022) Measuring progress to healing: a challenge and an opportunity. Int Wound J 19(4):734–740. https://doi.org/10.1111/iwj.13669

Centurione L, Passaretta F, Centurione MA, Munari S, Vertua E, Silini A, Liberati M, Parolini O, Di Pietro R (2018) Mapping of the human placenta: experimental evidence of amniotic epithelial cell heterogeneity. Cell Transpl 27(1):12–22. https://doi.org/10.1177/0963689717725078

Cognard S, Barnouin L, Bosc J, Gindraux F, Robin MC, Douet JY, Thuret G (2022) New devitalized freeze-dried human umbilical cord amniotic membrane as an innovative treatment of ocular surface defects: preclinical results. J Funct Biomater. https://doi.org/10.3390/jfb13030150

Curtis NE, Ho PW, King RG, Farrugia W, Moses EK, Gillespie MT, Moseley JM, Rice GE, Wlodek ME (1997) The expression of parathyroid hormone-related protein mRNA and immunoreactive protein in human amnion and choriodecidua is increased at term compared with preterm gestation. J Endocrinol 154(1):103–112. https://doi.org/10.1677/joe.0.1540103

Deihim T, Yazdanpanah G, Niknejad H (2016) Different light transmittance of placental and reflected regions of human amniotic membrane that could be crucial for corneal tissue engineering. Cornea 35(7):997–1003. https://doi.org/10.1097/ICO.0000000000000867

Dhall S, Sathyamoorthy M, Kuang JQ, Hoffman T, Moorman M, Lerch A, Jacob V, Sinclair SM, Danilkovitch A (2018) Properties of viable lyopreserved amnion are equivalent to viable cryopreserved amnion with the convenience of ambient storage. PLoS ONE 13(10):e0204060. https://doi.org/10.1371/journal.pone.0204060

DiDomenico LA, Orgill DP, Galiano RD, Serena TE, Carter MJ, Kaufman JP, Young NJ, Zelen CM (2016) Aseptically processed placental membrane improves healing of diabetic foot ulcerations: prospective, randomized clinical trial. Plast Reconstr Surg Glob Open 4(10):e1095. https://doi.org/10.1097/GOX.0000000000001095

Duan-Arnold Y, Gyurdieva A, Johnson A, Jacobstein DA, Danilkovitch A (2015) Soluble Factors released by endogenous viable cells enhance the antioxidant and chemoattractive activities of cryopreserved amniotic membrane. Adv Wound Care (new Rochelle) 4(6):329–338. https://doi.org/10.1089/wound.2015.0637

Elkhenany H, El-Derby A, Abd Elkodous M, Salah RA, Lotfy A, El-Badri N (2022) Applications of the amniotic membrane in tissue engineering and regeneration: the hundred-year challenge. Stem Cell Res Ther 13(1):8. https://doi.org/10.1186/s13287-021-02684-0

Farrugia W, Ho PW, Rice GE, Moseley JM, Permezel M, Wlodek ME (2000) Parathyroid hormone-related protein(1–34) in gestational fluids and release from human

gestational tissues. J Endocrinol 165(3):657–662. https://doi.org/10.1677/joe.0.1650657

Fenelon M, Catros S, Meyer C, Fricain JC, Obert L, Auber F, Louvrier A, Gindraux F (2021) Applications of human amniotic membrane for tissue engineering. Membranes (basel). https://doi.org/10.3390/membranes11060387

Fuchsluger TA, Steuhl KP, Meller D (2005) Neurotrophic keratopathy–a post-LASIK case report. Klin Monbl Augenheilkd 222(11):901–904. https://doi.org/10.1055/s-2005-858800

Garcia-Lopez G, Avila-Gonzalez D, Garcia-Castro IL, Flores-Herrera H, Molina-Hernandez A, Portillo W, Diaz-Martinez NE, Sanchez-Flores A, Verleyen J, Merchant-Larios H, Diaz NF (2019) Pluripotency markers in tissue and cultivated cells in vitro of different regions of human amniotic epithelium. Exp Cell Res 375(1):31–41. https://doi.org/10.1016/j.yexcr.2018.12.007

Germain AM, Attaroglu H, MacDonald PC, Casey ML (1992) Parathyroid hormone-related protein mRNA in avascular human amnion. J Clin Endocrinol Metab 75(4):1173–1175. https://doi.org/10.1210/jcem.75.4.1400890

Gicquel JJ, Dua HS, Brodie A, Mohammed I, Suleman H, Lazutina E, James DK, Hopkinson A (2009) Epidermal growth factor variations in amniotic membrane used for ex vivo tissue constructs. Tissue Eng Part A 15(8):1919–1927. https://doi.org/10.1089/ten.tea.2008.0432

Han YM, Romero R, Kim JS, Tarca AL, Kim SK, Draghici S, Kusanovic JP, Gotsch F, Mittal P, Hassan SS, Kim CJ (2008) Region-specific gene expression profiling: novel evidence for biological heterogeneity of the human amnion. Biol Reprod 79(5):954–961. https://doi.org/10.1095/biolreprod.108.069260

Herbin M, Bon FX, Venot A, Jeanlouis F, Dubertret ML, Dubertret L, Strauch G (1993) Assessment of healing kinetics through true color image processing. IEEE Trans Med Imaging 12(1):39–43. https://doi.org/10.1109/42.222664

Hopkinson A, McIntosh RS, Shanmuganathan V, Tighe PJ, Dua HS (2006a) Proteomic analysis of amniotic membrane prepared for human transplantation: characterization of proteins and clinical implications. J Proteome Res 5(9):2226–2235. https://doi.org/10.1021/pr050425q

Hopkinson A, McIntosh RS, Tighe PJ, James DK, Dua HS (2006b) Amniotic membrane for ocular surface reconstruction: donor variations and the effect of handling on TGF-beta content. Invest Ophthalmol vis Sci 47(10):4316–4322. https://doi.org/10.1167/iovs.05-1415

Hori J, Wang M, Kamiya K, Takahashi H, Sakuragawa N (2006) Immunological characteristics of amniotic epithelium. Cornea 25(10 Suppl 1):S53-58. https://doi.org/10.1097/01.ico.0000247214.31757.5c

Jirsova K, Jones GLA (2017) Amniotic membrane in ophthalmology: properties, preparation, storage and indications for grafting-a review. Cell Tissue Bank 18(2):193–204. https://doi.org/10.1007/s10561-017-9618-5

Johnson EL, Saunders M, Thote T, Danilkovitch A (2021) Cryopreserved placental membranes containing viable cells result in high closure rate of nonhealing upper and lower extremity wounds of non-diabetic and non-venous pathophysiology. Wounds 33(2):34–40

Kim SY, Romero R, Tarca AL, Bhatti G, Lee J, Chaiworapongsa T, Hassan SS, Kim CJ (2011) miR-143 regulation of prostaglandin-endoperoxidase synthase 2 in the amnion: implications for human parturition at term. PLoS ONE 6(9):e24131. https://doi.org/10.1371/journal.pone.0024131

Koizumi N, Inatomi T, Quantock AJ, Fullwood NJ, Dota A, Kinoshita S (2000a) Amniotic membrane as a substrate for cultivating limbal corneal epithelial cells for autologous transplantation in rabbits. Cornea 19(1):65–71. https://doi.org/10.1097/00003226-200001000-00013

Koizumi NJ, Inatomi TJ, Sotozono CJ, Fullwood NJ, Quantock AJ, Kinoshita S (2000b) Growth factor mRNA and protein in preserved human amniotic membrane. Curr Eye Res 20(3):173–177

Krabcova I, Jirsova K, Bednar J (2014) Rapid cooling of the amniotic membrane as a model system for the vitrification of posterior corneal lamellae. Cell Tissue Bank 15(1):165–173. https://doi.org/10.1007/s10561-013-9388-7

Lee DC, Romero R, Kim JS, Yoo W, Lee J, Mittal P, Kusanovic JP, Hassan SS, Yoon BH, Kim CJ (2010) Evidence for a spatial and temporal regulation of prostaglandin-endoperoxide synthase 2 expression in human amnion in term and preterm parturition. J Clin Endocrinol Metab 95(9):E86-91. https://doi.org/10.1210/jc.2010-0203

Lemke A, Castillo-Sanchez JC, Prodinger F, Ceranic A, Hennerbichler-Lugscheider S, Perez-Gil J, Redl H, Wolbank S (2017) Human amniotic membrane as newly identified source of amniotic fluid pulmonary surfactant. Sci Rep 7(1):6406. https://doi.org/10.1038/s41598-017-06402-w

Litwiniuk M, Radowicka M, Krejner A, Sladowska A, Grzela T (2018) Amount and distribution of selected biologically active factors in amniotic membrane depends on the part of amnion and mode of childbirth. Can we predict properties of amnion dressing? A-proof-of concept study. Cent Eur J Imunol 43(1):97–102. https://doi.org/10.5114/ceji.2017.69632

Meller D, Pauklin M, Thomasen H, Westekemper H, Steuhl KP (2011) Amniotic membrane transplantation in the human eye. Dtsch Arztebl Int 108(14):243–248. https://doi.org/10.3238/arztebl.2011.0243

Memmi B, Leveziel L, Knoeri J, Leclere A, Ribes O, Despiaux MC, Bouheraoua N, Nordmann JP, Baudouin C, Borderie V (2022) Freeze-dried versus cryopreserved amniotic membranes in corneal ulcers treated by overlay transplantation: a case-control study. Cornea 41(3):280–285. https://doi.org/10.1097/ICO.0000000000002794

Moraes J, Costa MM, Alves PCS, Sant'Anna LB (2021) Effects of preservation methods in the composition of the placental and reflected regions of the human amniotic membrane. Cells Tissues Organs 210(1):66–76. https://doi.org/10.1159/000515448

Nejad AR, Hamidieh AA, Amirkhani MA, Sisakht MM (2021) Update review on five top clinical applications of human amniotic membrane in regenerative medicine. Placenta 103:104–119. https://doi.org/10.1016/j.placenta.2020.10.026

Paolin A, Trojan D, Leonardi A, Mellone S, Volpe A, Orlandi A, Cogliati E (2016) Cytokine expression and

ultrastructural alterations in fresh-frozen, freeze-dried and gamma-irradiated human amniotic membranes. Cell Tissue Bank 17(3):399–406. https://doi.org/10.1007/s10561-016-9553-x

RStudio (2020) RStudio: Integrated Development for R. RStudio, PBC, Boston, MA URL: http://www.rstudio.com/

Ruiz-Canada C, Bernabe-Garcia A, Liarte S, Rodriguez-Valiente M, Nicolas FJ (2021) Chronic wound healing by amniotic membrane: TGF-beta and EGF signaling modulation in re-epithelialization. Front Bioeng Biotechnol 9:689328. https://doi.org/10.3389/fbioe.2021.689328

Singh R, Gupta P, Purohit S, Kumar P, Vaijapurkar SG, Chacharkar MP (2006) Radiation resistance of the microflora associated with amniotic membranes. World J Microbiol Biotechnol 22(1):23–27. https://doi.org/10.1007/s11274-005-2890-8

Skinner SJ, Campos GA, Liggins GC (1981) Collagen content of human amniotic membranes: effect of gestation length and premature rupture. Obstet Gynecol 57(4):487–489

Smeringaiova I, Trosan P, Mrstinova MB, Matecha J, Burkert J, Bednar J, Jirsova K (2017) Comparison of impact of two decontamination solutions on the viability of the cells in human amnion. Cell Tissue Bank 18(3):413–423. https://doi.org/10.1007/s10561-017-9636-3

Svobodova A, Horvath V, Smeringaiova I, Cabral JV, Zemlickova M, Fiala R, Burkert J, Nemetova D, Stadler P, Lindner J, Bednar J, Jirsova K (2022) The healing dynamics of non-healing wounds using cryo-preserved amniotic membrane. Int Wound J 19(5):1243–1252. https://doi.org/10.1111/iwj.13719

Svobodova A, Vrkoslav V, Smeringaiova I, Jirsova K (2023) Distribution of an analgesic palmitoylethanolamide and other N-acylethanolamines in human placental membranes. PLoS ONE. https://doi.org/10.1371/journal.pone.0279863

Tabatabaei SA, Soleimani M, Behrouz MJ, Torkashvand A, Anvari P, Yaseri M (2017) A randomized clinical trial to evaluate the usefulness of amniotic membrane transplantation in bacterial keratitis healing. Ocul Surf 15(2):218–226. https://doi.org/10.1016/j.jtos.2017.01.004

Tossetta G, Paolinelli F, Avellini C, Salvolini E, Ciarmela P, Lorenzi T, Emanuelli M, Toti P, Giuliante R, Gesuita R, Crescimanno C, Voltolini C, Di Primio R, Petraglia F, Castellucci M, Marzioni D (2014) IL-1beta and TGF-beta weaken the placental barrier through destruction of tight junctions: an in vivo and in vitro study. Placenta 35(7):509–516. https://doi.org/10.1016/j.placenta.2014.03.016

Tsubota K, Satake Y, Ohyama M, Toda I, Takano Y, Ono M, Shinozaki N, Shimazaki JUN (1996) Surgical reconstruction of the ocular surface in advanced ocular cicatricial pemphigoid and stevens-johnson syndrome. Am J Ophthalmol 122(1):38–52. https://doi.org/10.1016/s0002-9394(14)71962-2

Valiente MR, Nicolas FJ, Garcia-Hernandez AM, Fuente Mora C, Blanquer M, Alcaraz PJ, Almansa S, Merino GR, Lucas MDL, Alguero MC, Insausti CL, Pinero A, Moraleda JM, Castellanos G (2018) Cryopreserved amniotic membrane in the treatment of diabetic foot ulcers: a case series. J Wound Care 27(12):806–815. https://doi.org/10.12968/jowc.2018.27.12.806

Venault A, Bai YW, Dizon GV, Chou HE, Chiang HC, Lo CT, Zheng J, Aimar P, Chang Y (2019) Healing kinetics of diabetic wounds controlled with charge-biased hydrogel dressings. J Mater Chem B 7(45):7184–7194. https://doi.org/10.1039/c9tb01662g

Walkden A (2020) Amniotic membrane transplantation in ophthalmology: an updated perspective. Clin Ophthalmol 14:2057–2072. https://doi.org/10.2147/OPTH.S208008

Wassmer CH, Berishvili E (2020) Immunomodulatory properties of amniotic membrane derivatives and their potential in regenerative medicine. Curr Diab Rep 20(8):31. https://doi.org/10.1007/s11892-020-01316-w

Weidinger A, Pozenel L, Wolbank S, Banerjee A (2020) Subregional differences of the human amniotic membrane and their potential impact on tissue regeneration application. Front Bioeng Biotechnol 8:613804. https://doi.org/10.3389/fbioe.2020.613804

10.7. Appendix 7: Discontinuous transcription of ribosomal DNA in human cells

PLOS ONE

Discontinuous transcription of ribosomal DNA in human cells

Evgeny Smirnov[1]*, **Peter Trosan**[2], **Joao Victor Cabral**[2], **Pavel Studeny**[3], **Sami Kereïche**[1], **Katerina Jirsova**[2], **Dušan Cmarko**[1]

1 Laboratory of Cell Biology, Institute of Biology and Medical Genetics, First Faculty of Medicine, Charles University and General University Hospital in Prague, Prague, Czech Republic, 2 Laboratory of the Biology and Pathology of the Eye, Institute of Biology and Medical Genetics, First Faculty of Medicine, Charles University and General University Hospital in Prague, Prague, Czech Republic, 3 Ophthalmology Department of 3rd Faculty of Medicine, Charles University and University Hospital Kralovske Vinohrady, Prague, Czech Republic

*esmir@lf1.cuni.cz

Abstract

Numerous studies show that various genes in all kinds of organisms are transcribed discontinuously, i.e. in short bursts or pulses with periods of inactivity between them. But it remains unclear whether ribosomal DNA (rDNA), represented by multiple copies in every cell, is also expressed in such manner. In this work, we synchronized the pol I activity in the populations of tumour derived as well as normal human cells by cold block and release. Our experiments with 5-fluorouridine (FU) and BrUTP confirmed that the nucleolar transcription can be efficiently and reversibly arrested at +4°C. Then using special software for analysis of the microscopic images, we measured the intensity of transcription signal (incorporated FU) in the nucleoli at different time points after the release. We found that the ribosomal genes in the human cells are transcribed discontinuously with periods ranging from 45 min to 75 min. Our data indicate that the dynamics of rDNA transcription follows the undulating pattern, in which the bursts are alternated by periods of rare transcription events.

Introduction

Numerous studies show that genes in all kinds of organisms, from prokaryotes to mammals, can be transcribed in short bursts or pulses alternated by periods of silence (reviewed in Smirnov et al. [1]) The probability of such mode of expression was suggested long ago;[2] now it seems that the discontinuous transcription is a common feature of the gene expression, at least in mammalian cells.[3–12] The periodical switches of the promoter between the active and "refractory" states may be crucial in the efficient regulation of the gene expression.[13–17] General considerations suggest even more significant role of the phenomenon in the dynamic organization of the cell, since the pulsing mode of one process is likely to be a cause and a consequence of pulsing in other processes. Thus, RNA processing, which is closely linked to the RNA synthesis, seems to be discontinuous.[9] A spontaneous heterogeneity of gene expression occasioned by transcriptional fluctuations may influence cell behaviour in changing environmental conditions and in the course of differentiation.[18]

The discontinuous character of transcription has been detected by various methods (reviewed in Smirnov et al. [1]) The number of transcripts produced in a certain (sufficiently short) period of time may be determined with high precision by single molecule RNA fluorescence in situ hybridisation (smFISH).[19–21] The results of such quantification alone provide indirect, but valuable information for modelling the expression kinetics in a cell population or tissue, when the studied gene is supposed to be transcriptionally active in all the cells. Methods based on the allele-sensitive single-cell RNA sequencing also allow to reveal and characterize the transcription bursting.[22] To monitor gene expression in real time, cells are transfected with constructs providing a fluorescent signal that corresponds to the expression of a particular gene. In a gene trap strategy, a luciferase gene is inserted under the control of endogenous regulatory sequences. Since both the luciferase protein and its mRNA are short-lived, the method allows to calculate the key parameters of the transcriptional kinetics. Probably the most popular *in vivo* method is based on the use of bacteriophages derived fluorescent coat proteins, such as MS2 or PP7, fused with GFP, which allows to visualize a bunch of the nascent RNA molecules accumulated around one gene.[4, 23, 24]

So far, the pulse-like transcription is well documented only in the genes transcribed by RNA polymerase II. It is not clear yet whether ribosomal DNA (rDNA) is also expressed discontinuously. In human cells, the clusters of multiple rDNA repeats, known as Nucleolus Organizer Regions (NORs), are situated on the short arms of the acrocentric chromosomes. Each repeat includes a gene coding for 18S, 5.8S and 28S RNAs of the ribosomal particles and an intergenic spacer.[25–30] In the interphase nucleus the rDNA provides the basis for the formation of nucleoli. The transcription by pol I and the first steps of rRNA processing take place in the special nucleolar units (FC/DFC) composed of fibrillar centers (FC) and dense fibrillar components (DFC).[31–42] The units correspond in light microscopy to the "beads" forming nucleolar necklaces,[43–46] and each unit is believed to accommodate a single transcriptionally active gene.[33, 39, 47, 48] The intensity of the rDNA transcription is usually very high throughout the entire interphase, especially at the S and G2 phases.[49] Now most of the methods used for the detection of the transcription fluctuation are hardly applicable to the ribosomal genes, since one cell usually contains hundreds of such genes. An alternative method was designed for direct measurements of rDNA transcription in the live cells by using the label-free confocal Raman microspectrometry. [50] This work revealed an undulatory character of the ribosomal RNA production in the whole nucleoli. In our earlier study on tumour-derived cells expressing a GFP-RPA43 (a subunit of pol I) fusion protein, we have observed specific fluctuations of the fluorescence signal in the individual FC/DFC units.[51] We also found high correlation of pol I and incorporated FU signals within the units. These data suggested that the ribosomal genes are transcribed in a pulse-like manner.

In the present work we used a different approach to the study of the discontinuous transcription of ribosomal genes in human cells. In our experiments with 5-fluorouridine (FU) and BrUTP, we found that the nucleolar transcription can be efficiently arrested at +4°C and quickly restored at normal conditions. Based on this finding, we synchronized the pol I activity in the cell population by cold block and release. Then using specially designed software we measured the intensity of transcription signal (incorporated FU) in the nucleoli and individual FC/DFC units at different periods after the release. This enabled us to detect transcription fluctuations of ribosomal genes in tumour derived as well as normal human cells and to reveal special properties of this fluctuation.

Methods

Ethics

The study followed the standards of the Ethics Committees of the General Teaching Hospital and the First Faculty of Medicine of Charles University, Prague, Czech Republic (Ethics

Committee of General Univeristy Hospital, Prague approval no. 1570/11 S-IV (held on October 13, 2011, and updated January 18, 2018. The name of project: Pathogenesis of hereditary, degenerative and systemic diseases with manifestations in the eye, transplantology. Study of healthy and control tissue), and adhered to the principles set out in the Helsinki Declaration. We obtained human cadaver corneoscleral rims from 10 donors, which were surplus from surgery and stored in Eusol-C (Alchimia, Padova, Italy), from the Department of Ophthalmology, General University Hospital in Prague, Czech Republic, for the study. On the use of the corneoscleral rims, based on Czech legislation on specific health services (Law Act No. 372/2011 Coll.), informed consent is not required if the presented data are anonymous in the form."

Cell cultures

Human limbal epithelial cells (LECs) were obtained from XY cadaver corneoscleral rims after cornea grafting at University Hospital Kralovske Vinohrady, Prague, Czech Republic. The mean donor age ±standard deviation (SD) was 63.5 ±6.5 years. Tissue was stored in Eusol-C (Alchimia, srl., Ponte San Nicolò, Italy) preservation medium at +4˚C. The mean storage time ±SD (from tissue collection until explantation) was 7.2 ±3.6 days. The corneoscleral rims were prepared as described before.[52,53] Shortly, corneoscleral rims were cut into 12 pieces and placed in a 24-wellplate (TPP Techno Plastic Products AG, Trasadingen, Switzerland) on Thermanox plastic coverslips (Nunc, Thermo Fisher Scientific, Rochester, NY, USA). Explants were cultured in 1 ml of complete medium [1:1 DMEM/F12, 10% FBS, 1% AA, 10 ng/ml recombinant EGF, 0.5% insulin-transferrin-selenium (Thermo Fisher Scientific), 5 μg/ml hydrocortisone, 10 μg/ml adenine hydrochloride and 10 ng/ml cholera toxin (Sigma-Aldrich, Darmstadt, Germany)]. The culture media were changed every 2–3 days until the cells were 90–100% confluent (after 2–4 weeks).

HeLa cells were cultivated at 37˚C in Dulbecco modified Eagle's medium (DMEM, Sigma) containing 10% fetal calf serum, 1% glutamine, 0.1% gentamicin, and 0.85g/l $NaHCO_3$ in standard incubators. For the transcription synchronization, the cells were incubated in cold medium (+4˚C) for 1 h, then transferred to the normal conditions and fixed at different time points from 15 to 150 min with the interval of 15 min.

Plasmids and transfection

The GFP-RPA43 and GFP-Fibrillarin vectors were received from Laboratory of Receptor Biology and Gene Expression Bethesda, MD.[54] The constructs were transfected into HeLa cells using Fugene (Qiagen).

Labeling of the transcription sites

For visualization of the transcription sites, sub-confluent cells were incubated for 5 min prior to fixation with 5-fluorouridine (FU) (Sigma). The cells were fixed in pure methanol at -20˚C for 30 min and processed for FU immunocytochemistry. BrUTP (Sigma) was introduced into cells by the scratch procedure.[55, 56] Here we followed the same procedure as for the labelling of replication in the cited works. Briefly, the cells were grown on the coverslips; a drop of medium containing 20μg/ml BrUTP was applied upon each coverslip; then the latter was scratched by the tip of a syringe needle and incubated for 5 min at 37˚C. Thus permeabilized, the cells were incubated for 10 min in the usual medium and then fixed and processed as after the incorporation of FU.

Incorporated FU and BrUTP signal was visualized using a mouse monoclonal anti-BrdU antibody (Sigma) and secondary goat Cy3-conjugated anti-mouse antibody (Abcam).

Light microscopy

Confocal images were acquired by means of SP5 (Leica) confocal laser scanning microscope equipped with a 63×/1.4NA oil immersion objective. For *in vivo* cell imaging we used a spinning disk confocal system based on Olympus IX81 microscope equipped with Olympus UPlanSApo 100×/1.4NA oil immersion objective, CSU-X spinning disk module (Yokogawa) and Ixon Ultra EMCCD camera (Andor). The live cells were maintained in glass bottom Petri dishes (MatTek) at 37°C and 5% CO_2 within a microscope incubator (Okolab).

Software and data analysis

For measurement and counting of the transcription and other signals corresponding to individual FC/DFC units in 3D confocal images, we developed a MatLab based software.[51] The program identifies each unit by creating a maximum intensity projection of the confocal stack and blurring the projection with a Gaussian filter (σ= 8–10 pixels), defining the blurred image with a value obtained by Otsu's method for automatic threshold selection. After that, the optical section whereupon the unit had maximum intensity was identified. The final result contains 3D coordinates of each unit, its size (full-width half-maximum), the value of χ^2, and integral intensities in the spheres with radii 1.0, 1.5, 2.0, 2.5, 3.0, 3.5, and 4.0 pixels. The values corresponding to 1.5 pixels seemed to be the most resistant to noise and were used for presentation of the data. FC/DFC units were counted after deconvolution with Huygens software.

For measuring signals in the entire nucleoli we used a custom ImageJ plugin available at https://github.com/vmodrosedem/segmentation-correlation.[45] Based on the confocal stacks, the program identifies the regions occupied by the cell nuclei as well as nucleoli, measures their areas (in pixels), and the intensities, both integral and average, of the signal within these areas.

Results

1. Effects of low temperature on the nucleolar transcription

In the control the incorporated FU is accumulated predominantly in the nucleolar beads which, according to our earlier study,[55] correspond to the FC/DFC units of the nucleoli (Fig 1). The transcription signal in the nucleoplasm appeared as multiple small foci of much lower intensity. After 15 min of incubation at +4°C (without additional supply of CO_2), both HeLa and LECs lost the ability to incorporate 5-fluorouridin (FU). When the cells were returned to the normal conditions (37°C, 5% CO_2), transcription was partly restored in 15 min, and in 30 min the FU incorporation did not visibly differ from the control (Fig 1).

Since incorporation of FU is preceded by its penetration in the cell and phosphorylation, we performed an additional experiment with another RNA predecessor, BrUTP, which was introduced in the HeLa cells by the scratch procedure (Fig 1B).[55,56] When cells were permeabilized by scratching in the presence of BrUTP for 5 min and then immediately fixed (Fig 1B, left) or washed and incubated for further 10 min at +4°C (Fig 1B, middle), there was no significant incorporation of the nucleotide. But when the permeabilization was followed by 10 min incubation in the normal conditions (Fig 1B, right), the cells situated along the scratch track displayed the transcription signal in the nucleoli and nucleoplasm. This result confirmed that the transcription was efficiently arrested in our experiments at +4°C.

It is known that pol I and fibrillarin are particularly sensitive to stress, and their redistribution in the cell nuclei is a common symptom of nucleolar pathology. Therefore, to assess the effect of cold on the FC/DFC units, which are the centers of rDNA transcription and early rRNA processing, we transfected the cells with GFP-RPA43 or GFP-Fibrillarin. At the low
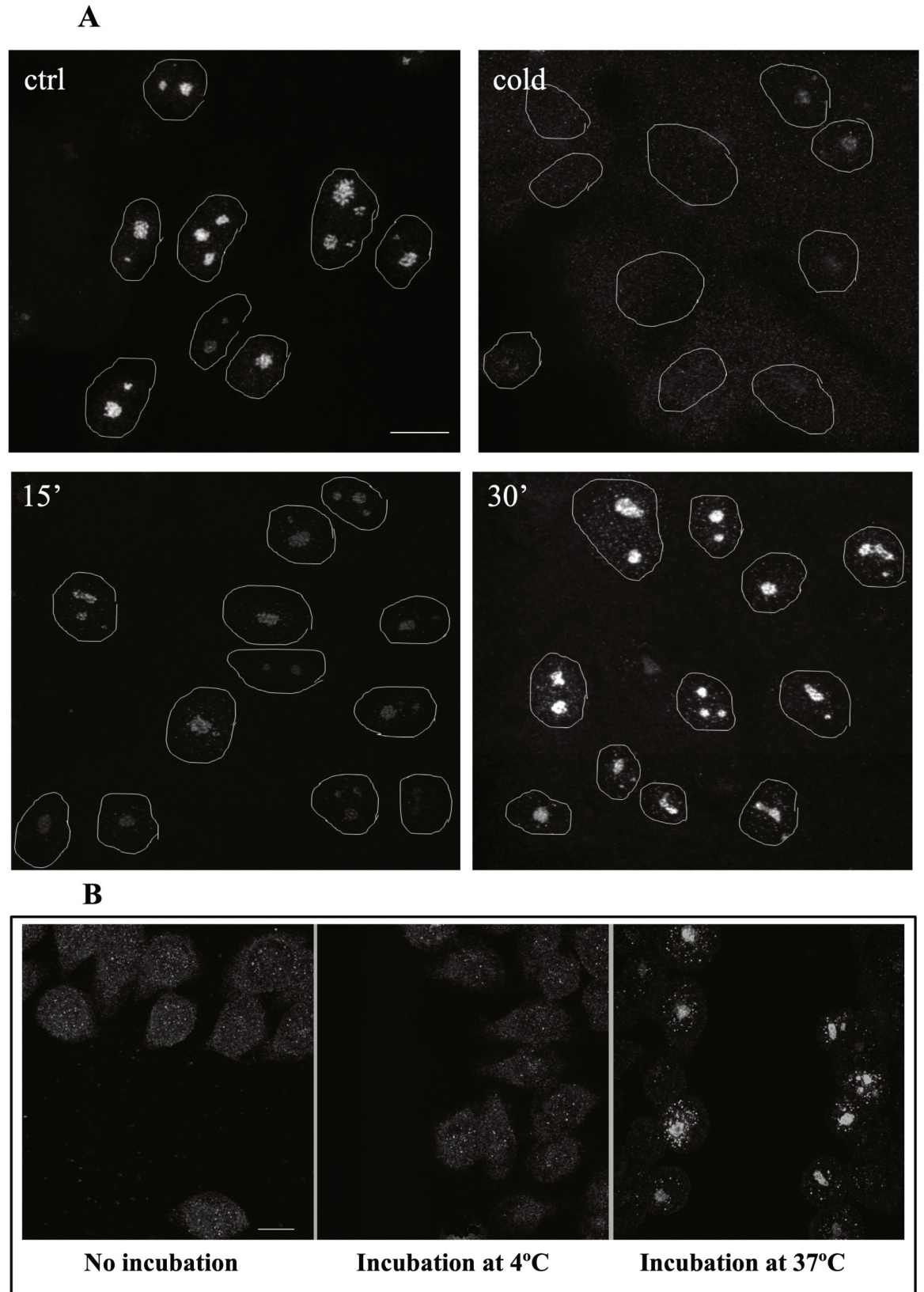
Fig 1. (A) Transcription in HeLa cells is quickly inhibited at +4°C and restored at the normal conditions. The transcription signal (FU incorporation) is accumulated in the nucleoli. The signal disappeared after 15 min of cold treatment (top right); when the cells were transferred to the normal conditions, the signal was partly restored in 15 min and appeared like in the control in 30 min (bottom). **(B) Incorporation of BrUTP.** No significant signal in the cells fixed after the permeabilization immediately (left) or following 10 min of incubation at +4°C (middle); when permeabilization was followed by 10 min incubation at +37°C, specifically labelled cells could be observed along the scratch track (right). Scale bar: 10μm.

temperature the GFP-Fibrillarin signal did not change significantly, but the intensity of the RPA43 signal was decreased as average to about 60% of the control level (Fig 2).

Observation of the individual cells also showed that after transferring the cells from the cold to the normal conditions, the intensity of GFP-RPA43 signal in all FC/DFC units increased, although the number of the detectable units did not change (Fig 3).

These experiments show that low temperature causes a quick inhibition of the rDNA transcription, as well as significant though not complete depletion of the pol I pools in the nucleoli.

On the other hand, we observe a quick recovery of the cells without any lasting symptoms of pathology.

2. Synchronization of the nucleolar transcription in HeLa and human limbal cells by cold treatment

The experiments described in the previous section indicate that at the low temperature the ribosomal genes are brought to a silent state with a diminished RPA-GFP signal within the FC/DFC units which implies a decreased number of pol I complexes bound to the genes. This synchronization procedure was used for the study of the discontinuous expression of the rDNA in HeLa and LEC cells. Namely, the cells were incubated in cold medium (+4°C) for 1 h, then transferred to the normal conditions and fixed at different time points from 15 to 150 min with the interval of 15 min. FU was added to the cultivation medium 5 min prior to each fixation. The transcription signal visualized by antibody was then measured in the nucleoli by means of the ImageJ plugin software (see Methods). The results are presented in Fig 4.

In all such experiments the intensity of the transcription signal increased during the first 30 min, then began to decrease. Altogether two cycles of rise and fall have been observed within the period of 150 min, the coefficient of variation (CV) was 0.26. The spectral analysis revealed a significant peak corresponding to the period of 60 min. Since the interval between the measurements was 15 min, the values of the period may be varying from 45 min to 75 min. An additional lower peak at 15 min probably reflected a high frequency noise. In the control, when the cells were kept at 37°C and fixed at different time points as in the experiment, the fluctuations of the transcription signal intensity were irregular. CV was only 0.07, and the periodogram had two peaks of low amplitude (compare the left and right parts of the Fig 4). In two experiments the period of observation was extended to 210 min, but between 150 and 210 min the fluctuations of the transcription signal appeared irregular with the CV values 0.06, i.e. just like in the control, which indicated that the synchrony in the cell population was lost. These results showed that in HeLa cells the activity of pol I transcription machinery was synchronized by the cold treatment for the period of 150 min, but not longer.

The same experimental procedure was applied to the LECs (Fig 5). In this case the first two cycles were more pronounced and the difference between control and experiment was more significant (compare Fig 5 and Fig 4). Otherwise, the dynamics of the transcription activity after the cold treatment proved to be similar in the studied cell lines. In the LECs, the periodogram had a more distinct peak at 60 min, but the synchronization also did not last longer than 150 min. CV was 0.29, i.e. slightly higher than in HeLa cells. It seems worth mentioning that
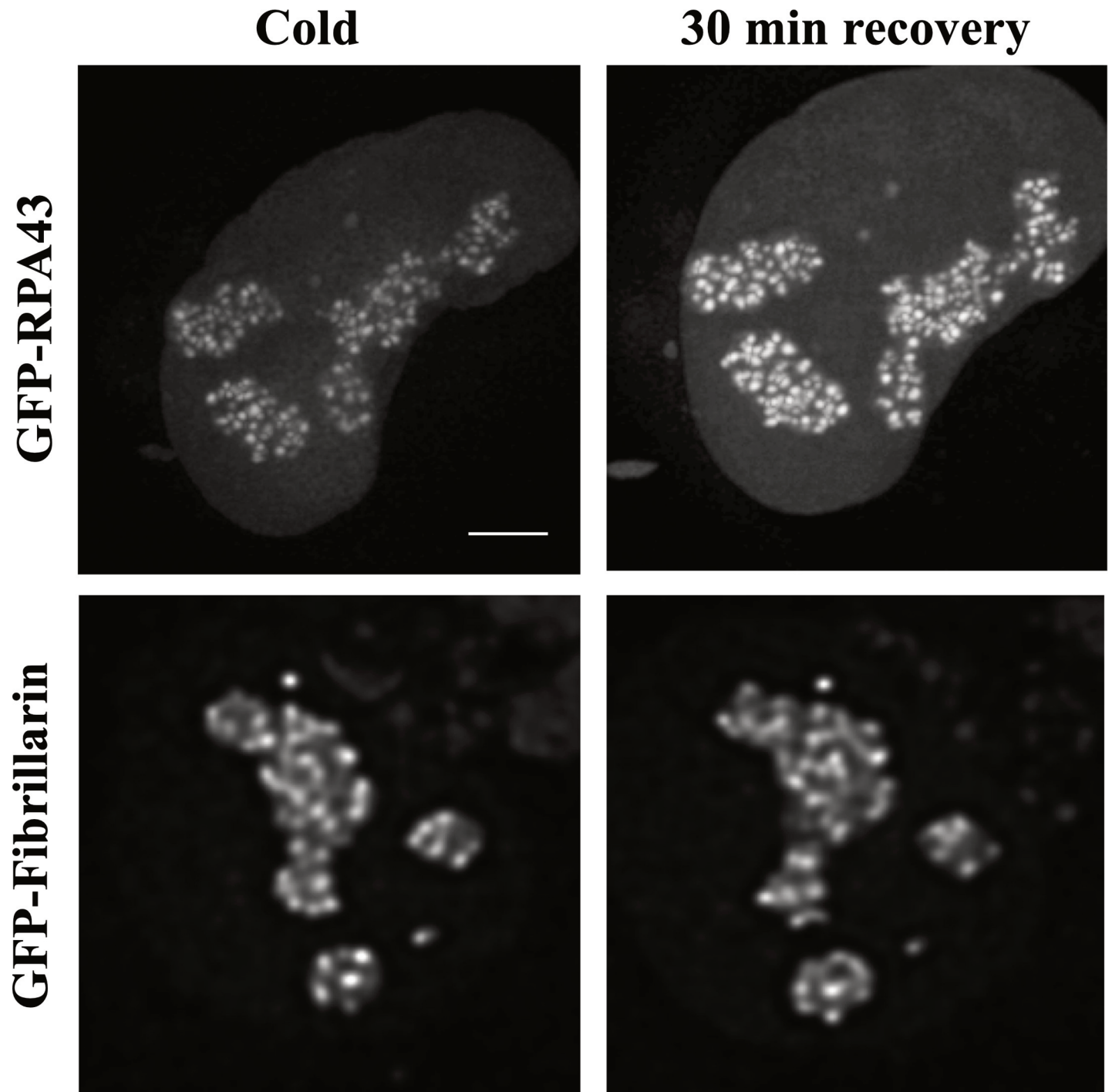
Cold

30 min recovery

Fig 2. Following GFP-RPA43 and GFP-Fibrillarin signals in the transfected HeLa cells *in vivo*. The intensity of the GFP-RPA43 signal is reduced after 15 min incubation at +4°C (left, top) and restored after subsequent 30 min incubation at normal conditions (top, right). The GFP-Fibrillarin signal was not significantly affected by the cooling/warming procedure (bottom). Scalebar: 5μm.

https://doi.org/10.1371/journal.pone.0223030.g002

our attempt to synchronize the transcription in human fibroblasts failed, for only a few of these cells recovered quickly enough after the cold treatment.
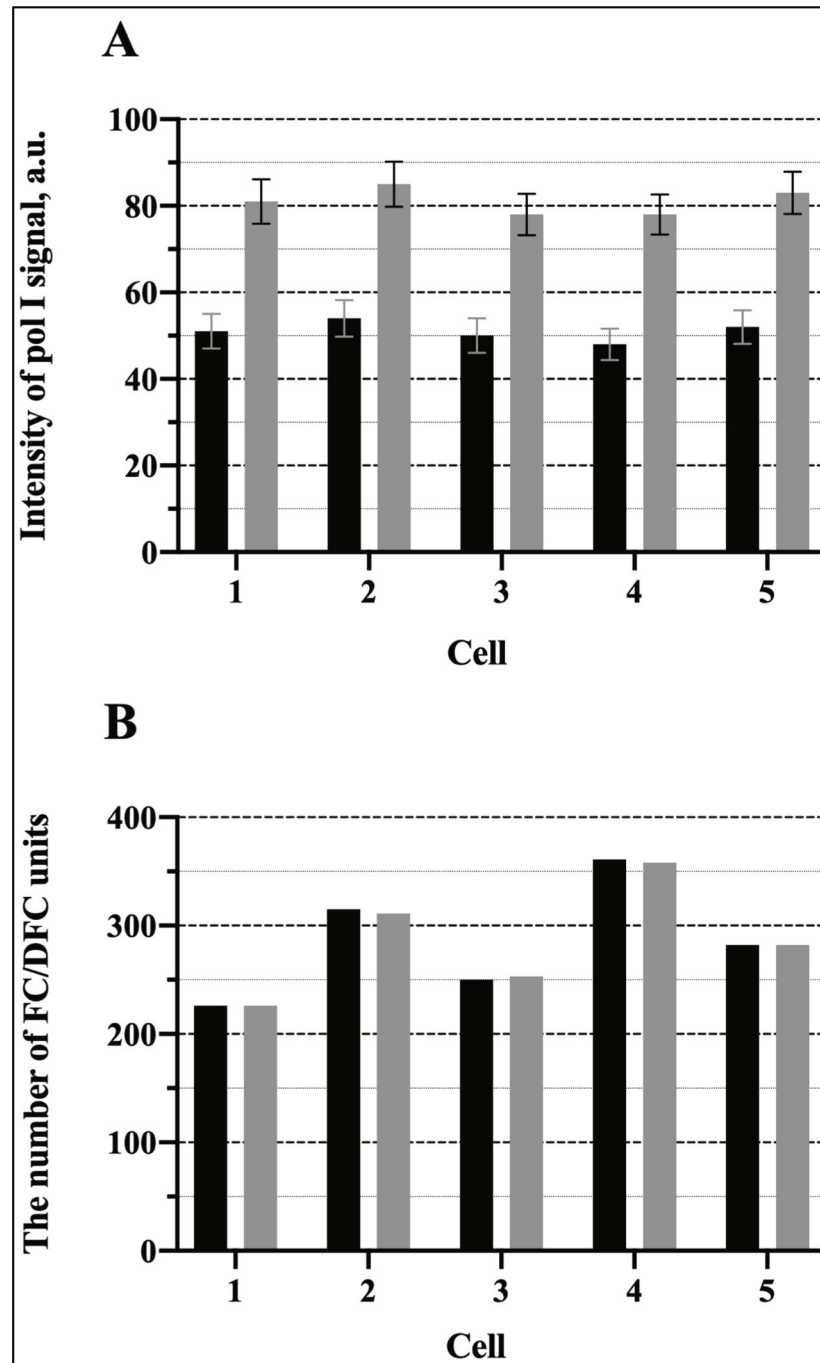
Fig 3. Effects of cooling/warming (as in Fig 2, top) on the FC/DFC units *invivo* in the transfected HeLa cells. (A) intensity of the GFP-RPA43 signal in the individual units after 15min incubation at +4˚C (black columns) and after subsequent 30 min incubation at 37˚C (grey columns). Five cells were observed, and five selected units were followed in each cell. The error bars show SEM. **(B)** the total number of the GFP-RPA43 positive units in five cells after 15min incubation at +4˚C (black columns) and after subsequent 30 min incubation at 37˚C (grey columns). The experiment indicates that at the low temperature pol I escapes from the FC/DFC units.
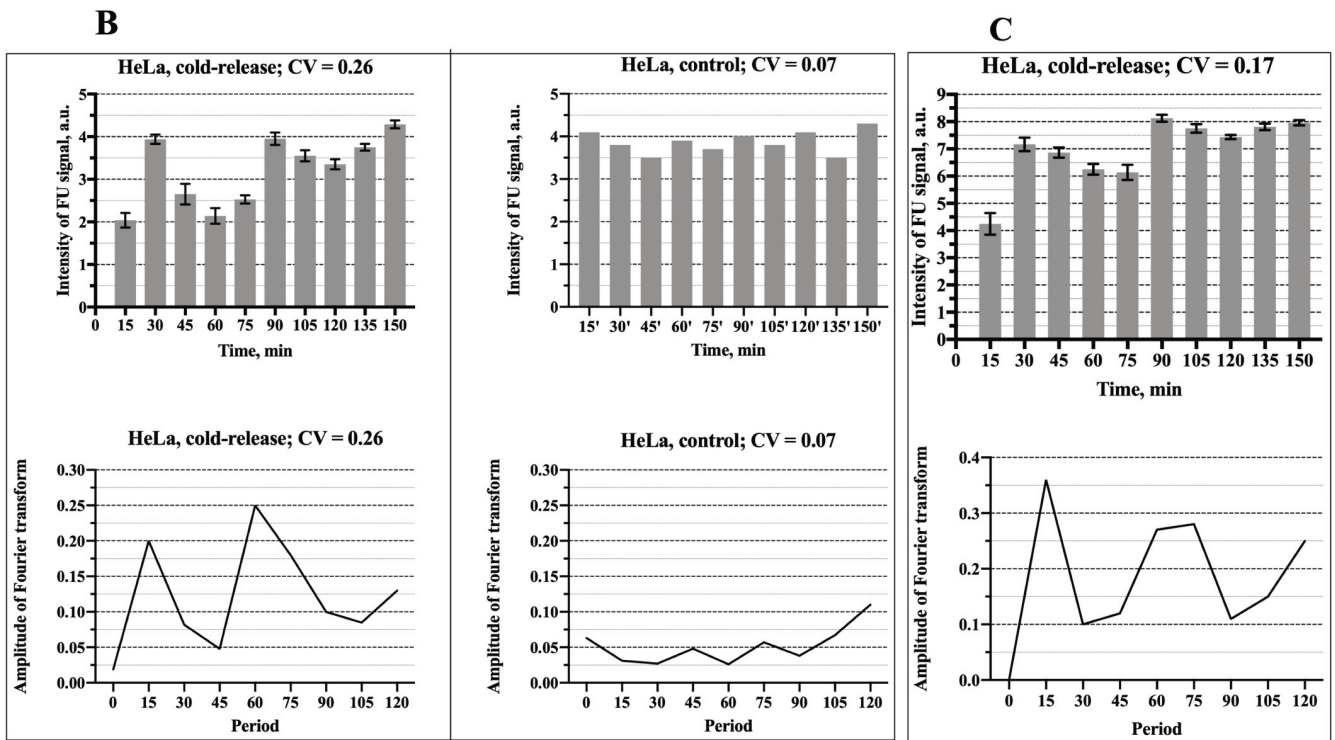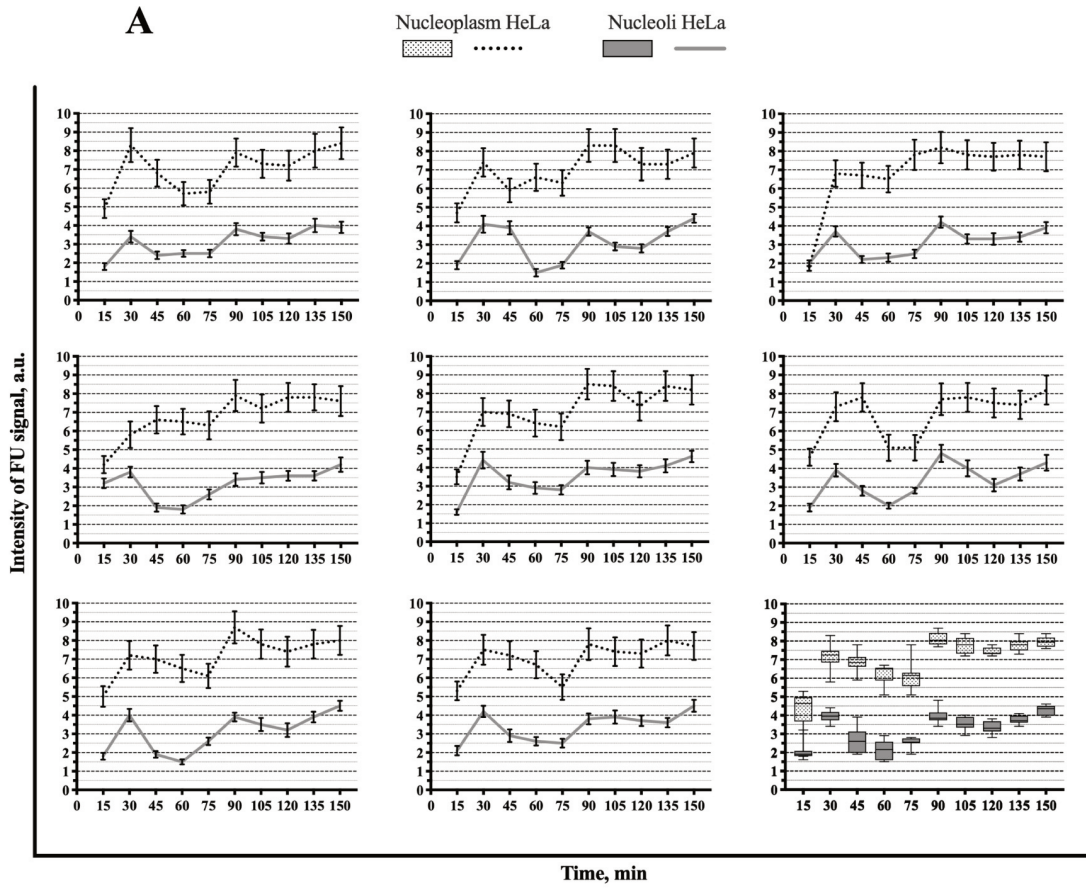
Fig 4. Fluctuation of the intensity of the transcription signal (incorporated FU) in the whole nucleoli and nucleoplasm of HeLa cells after release from the cold block. (A) Data of the individual experiments and the box-plot chart. **(B)** Mean values of the transcription signal intensity in the nucleoli after release from the cold block (left, top) and in the nucleoli of the control cells, i.e. without cold treatment (right, top) In the experiment the signal reaches maximal values at 30 min, 90 min, and 150 min. The graph shows mean values obtained from 50 cells in one experiment. Such experiment was repeated 8 times. CV- coefficient of variation. The error bars show SEM. The bottom graphs show the respective periodograms for the experiment (left) and control (right) calculated as amplitudes of the Fourier transforms. The x-axis represents the period (min). **(C)** Mean values of the transcription signal intensity in the nucleoplasm after release from the cold block (top) and the respective periodogram (bottom).

Thus, our experiments indicated that transcription of the ribosomal genes proceeds in a wave-like manner, although the employed synchronization procedure is not equally efficient in various cells.

3. Fluctuation of the pol I signal in the cells synchronized by chilling

To confirm our result by an independent set of data, we used chilling shock to synchronize HeLa cells transfected with GFP-RPA-43 (see Fig 6). Measuring the intensity of the pol I signal in the nucleoli of the individual cells, we observed fluctuations similar to those of the transcription signal (Figs 4 and 5). The fluctuations had a relatively low amplitude, and the distinct undulations persisted for no longer than two hours, apparently because only a minor portion of the pol I molecules within FC/DFC units are engaged in the current transcription, as was indicated, for instance, in our earlier work.[51] Nevertheless, the initial increase of the signal intensity during the first 30 min after the cold treatment was followed by a noticeable decrease during the next half hour, which could not be attributed to the effects of recovery. Together with the other results of the present study (Figs 4 and 5) this indicates, that fluctuations of the transcription intensity and pol I levels in the nucleoli are synchronous.

4. Synchronization of the transcription in the nucleoplasm by cold treatment

When the LECs or HeLa cells were incubated at +4˚C, the transcription ceased completely in their nucleoplasm as well as in the nucleoli. Measurement of the total FU signal after transferring the cells from the cold to the normal conditions showed symptoms of synchronization: the signal in the nucleoplasm increased for 30 min and then began to decrease (Figs 4A, 4C, 5A and 5C). The average intensity of the transcription signal in the nucleoli and nucleoplasm positively correlated, with the correlation coefficients 0.65 for the HeLa cells and 0.74 for the LECs. But, as one could expect, the total expression of the nucleoplasmic genes was less synchronized. After the initial recovery and subsequent decrease, the signal became rather noisy. The CV was 0.17 and 0.19 in the HeLa and LECs respectively. The periodograms showed a not very distinct peak at 75 min as well as a sharper peak corresponding to higher frequencies. The second peak probably reflects a noisier character of the fluctuations in the nucleoplasm as compared to the nucleoli.

5. The FC/DFC units in the course of the transcription fluctuation

Since the measurement of the transcription signal in the whole nucleoli is significantly affected by the fluorescence between the FC/DFC units, we measured the signal also within the units. According to the data presented in the sections 2 and 3 (Figs 4 and 5), the intensity of FU signal in the nucleoli at 15 min and 30 min after the cold treatment may be taken as representatives of the two extreme states of the transcriptional fluctuation in the synchronized cells. Measurement of the FU signal in the individual FC/DFC units of the LECs and HeLa cells using the MatLab based software (see Methods) showed an approximately threefold increase
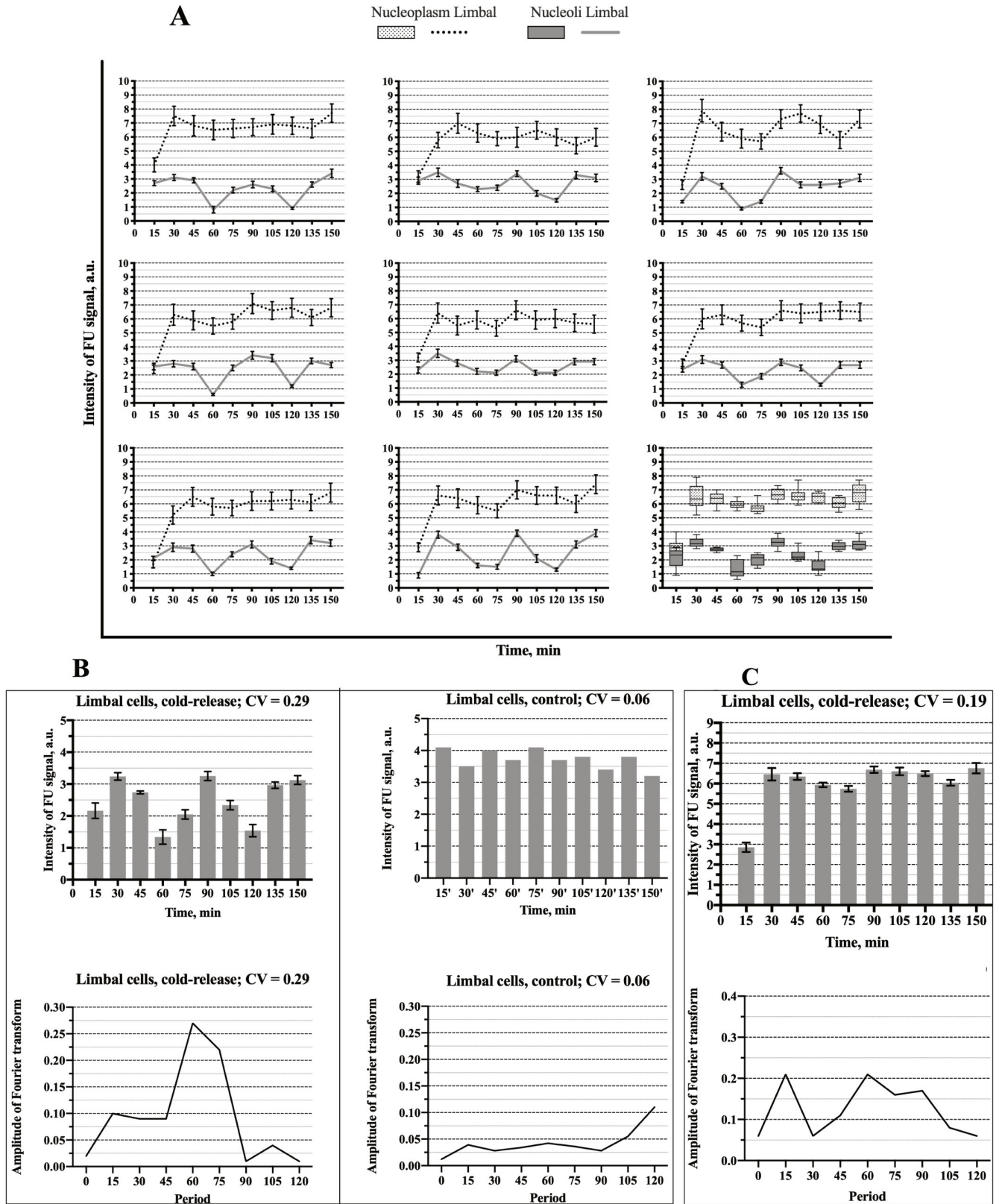
Fig 5. Fluctuation of the intensity of the transcription signal (incorporated FU) in the whole nucleoli and nucleoplasm of the limbal cells. (A) Data of the individual experiments and the box-plot chart as in Fig 4A. **(B)** Mean values of the transcription signal intensity in the nucleoli after release from the cold

block (left, top) and in the nucleoli of the control cells (right, top). The figure is analogous to the Fig 4. But in this case, the undulating pattern in the experiment (top, right) is more pronounced, and the periodogram related to the experiment (bottom, left) has a more distinct peak at 60 min. The data are obtained from 8 independent experiments, and in each of them 50 cells were measured. **(C)** Mean values of the transcription signal intensity in the nucleoplasm after release from the cold block (top) and the respective periodogram (bottom).

of the signal intensity between 15 min and 30 min (Fig 7). But the transcription signal never disappeared from the cells completely, so that the average number of the FU-positive FC/DFC units did not change significantly (Fig 7B, right chart).

Discussion

In our experiments, when the human derived cells were incubated at +4°C, transcription in their nuclei seemed to be arrested completely (Figs 1 and 7). At the same time the pol I signal in the FC/DFC units of the nucleoli was significantly reduced (Figs 2 and 6), whereas the amount of fibrillarin, which is an essential component of the early rRNA processing, did not change significantly (Fig 2). On the other hand, previous studies, including our own, indicate that the mobile fraction of pol I, apparently responsible for the actual transcription, constitutes less than a half of the entire pool of the enzyme in the units.[51, 54] Therefore, in all probability, the pol I complexes do not "freeze" on their matrices after the arrest of the transcription by the chill shock, but rather detach themselves and escape from the units. After returning to normal conditions, the pools of the enzyme are swiftly restored, and the rRNA synthesis in the cells is synchronized. This effect was used in our work for detection of the pulse-like transcription.

In our previous work we studied the fluctuations of pol I signal, but could not speak about the discontinuous transcription otherwise than hypothetically, since the dynamics of this signal does not necessarily reflect the transcription.[55] Therefore, only after developing the cold/release method of cell synchronization, we obtained the data related to the transcription fluctuations directly.

In thus synchronized HeLa and LEC cells, we observed a wave-like modification of the nucleolar transcription signal with two successive peaks (Figs 4 and 5). It should be mentioned, that the recovery process, which seemed to be limited to the first 30 min after the cold treatment, could not account for the observed dynamics, especially the regularly observed decrease of transcription intensity after the initial increase, as well as more or less distinct second peak. In both kinds of cells, the predominant fluctuation period estimated by the spectral analysis was about 60 min. A similar value of the period was obtained in our previous work for the fluctuations of the GFP-RPA43 signal.[51]. After the two distinct cycles, the waves were damped; probably because of their irregularity and variability in the individual cells. Nevertheless, our data indicate that the ribosomal genes are expressed discontinuously, with intervals of 45–75 min between the bursts.

In our review on the discontinuous transcription, we indicated what seemed to be four main patterns in which this phenomenon may be manifested: the typical busts; the undulating pattern; the regular pulsing; and the rare transcription events.[1] As mentioned above, the fluctuations observed in our study do not seem to belong to the regular type. Rare events also must be excluded, since rDNA transcription is very intensive throughout the entire interphase. The typical bursts are separated by the relatively long periods of silence. But we observed no diminishing of the number of FU positive (Fig 7B) or pol I positive (Fig 3) FC/DFC units in the course of the experiment, although the mean intensity of the incorporated FU signal in the individual units was greatly reduced at the points of minimal transcription activity (Fig 7B).
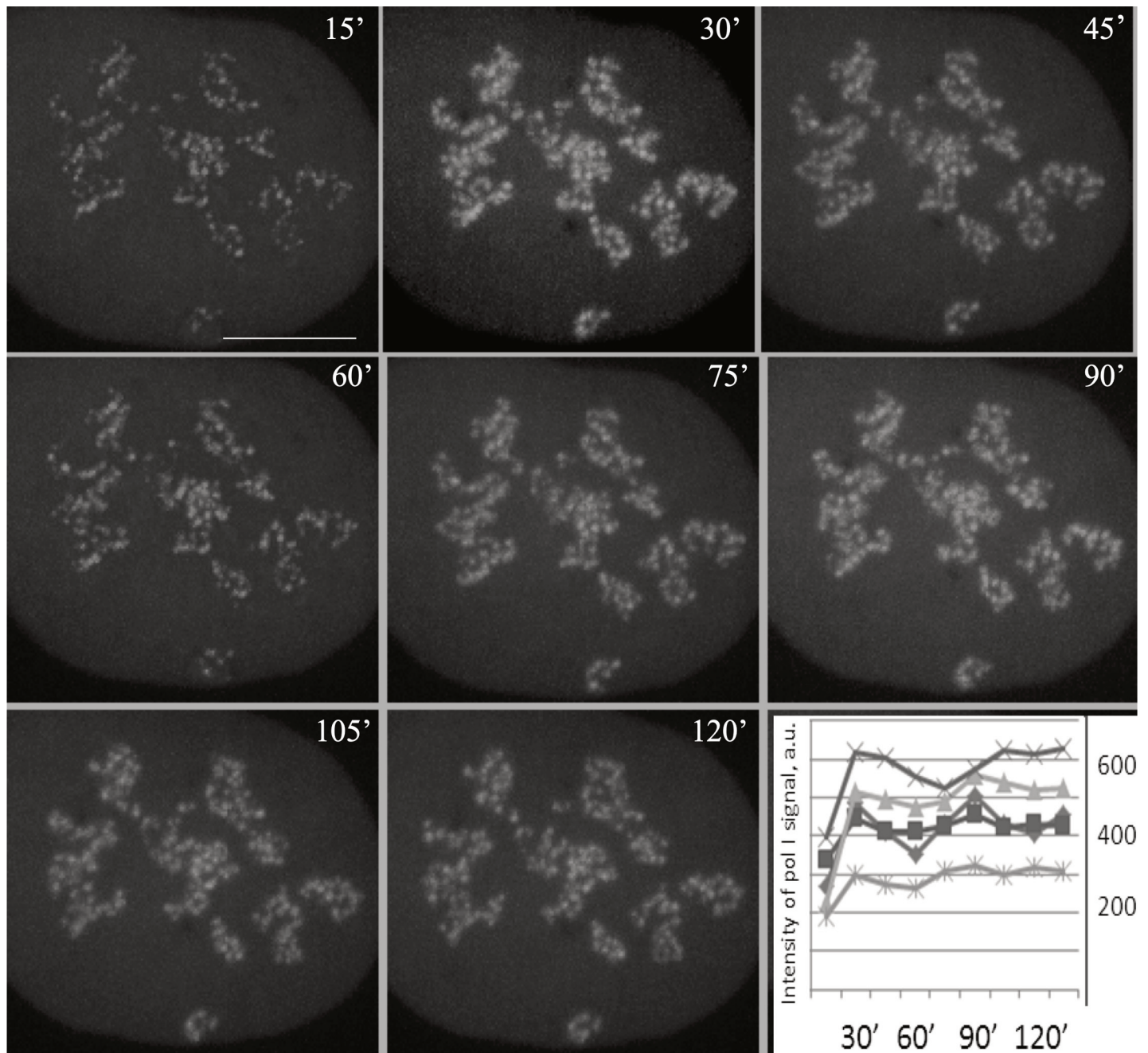
Fig 6. Fluctuation of the intensity of GFP-RPA43 signal in the nucleoli of HeLa cells after the cold treatment. The eight successive images of the same transfected cell photographed every 15 min after the release from the cold block. The intensity of the signal at 15 min as well as at 60 min after the release is visibly lower than at other points. The graph at the bottom right shows records of the pol I signal intensity in five cells at different time points after the release. Each curve represents one cell. All curves have two peaks at 30 min and at 90 min or close to it, as in the case of FU incorporation (Figs 4 and 5). Scalebar: 5μm.

Therefore, the observed fluctuation of rDNA transcription most likely belongs to the undulating pattern, in which the bursts are alternated by periods of relatively rare transcription events.

Additionally, our method of synchronization allowed us to obtain averaged data concerning the fluctuations in the nucleoplasmic genes, since their expression was also inhibited by the cold treatment. After this procedure, the total transcription signal in the nucleoplasm
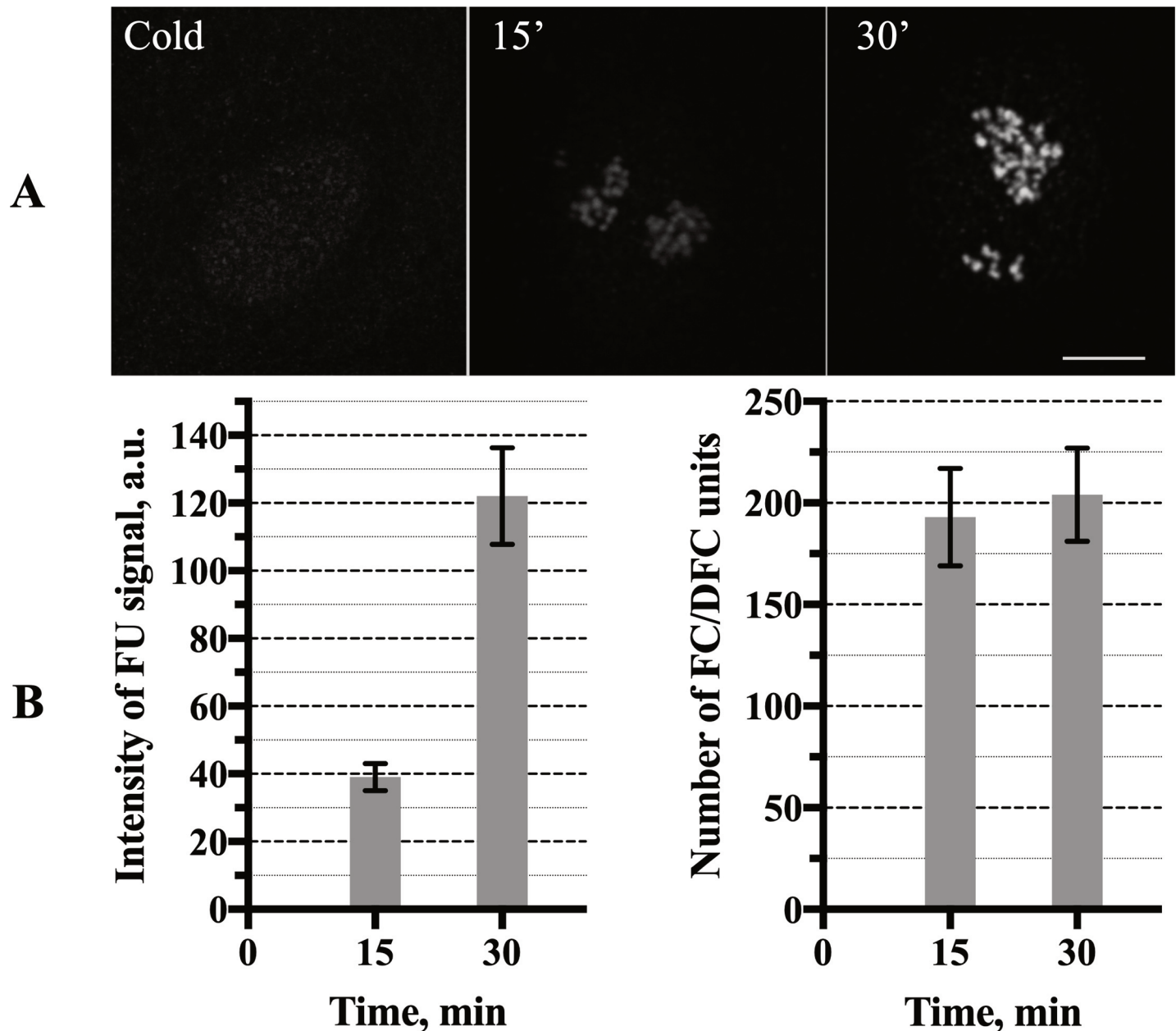
Fig 7. The transcription signal (incorporated FU) in the FC/DFC units of the limbal epithelial cells after the cold treatment. **(A)** no FU incorporation in the cells incubated at +4°C for 15 min (left); a weak FU signal in the cell incubated at 37°C for 15 min after the chilling (middle); 30 min; completely recovered FU signal in the cell incubated at 37°C for 30 min after the chilling (right). Scale bar: 5 μm. **(B)** the average (from 50 cells) intensity of the FU signal in the individual FC/DFC units measured in the cells incubated at 37°C for 15 min and 30 min after the chilling. The increase is statistically significant (P < 0.0001, according to the Student's t-test) (left). The average (from 50 cells) number of the FU positive FC/DFC units in the cells incubated for 15 min and 30 min at +37°C after the cold treatment; the differences are statistically insignificant (right). The data show an initial quick recovery of the transcription in the units without changing their number (see Fig 5).

showed symptoms of fluctuations with two discernible, though not very distinct, peaks (Figs 4A, 4C, 5A and 5C). Evaluating these results, we have to keep in mind that various nucleoplasmic genes in the same cell display a wide range of transcriptional kinetic behavior (reviewed in Smirnov et al. [1]).[4, 10, 57, 58] Moreover, some of these genes are expressed in typical bursts with long periods of silence, during which they cannot be detected by FU incorporation. We should also mention that the status of the nucleoplasmic RNA polymerases at the low temperature

was not examined in our experiments, and thus we do not know how efficiently the transcription was synchronized. Nevertheless, the presence of two significant peaks on the periodograms (Figs 4C and 5C) suggests that numerous genes in the nucleoplasm were transcribed in a pulse-like manner with periods close to 15 min and 75 min.

Thus, our results indicate that ribosomal genes in human cells are expressed discontinuously, and their transcription follows undulating pattern with predominant period of about 60 min.

Acknowledgments

Author Contributions

Conceptualization: Evgeny Smirnov.

Data curation: Peter Trosan, Pavel Studeny, Katerina Jirsova.

Formal analysis: Evgeny Smirnov, Joao Victor Cabral, Sami Kereïche.

Investigation: Evgeny Smirnov, Joao Victor Cabral, Katerina Jirsova, Dušan Cmarko.

Methodology: Evgeny Smirnov, Peter Trosan.

Software: Sami Kereïche.

Supervision: Evgeny Smirnov, Dušan Cmarko.

Validation: Evgeny Smirnov, Joao Victor Cabral.

Writing – original draft: Evgeny Smirnov.

Writing – review & editing: Peter Trosan, Joao Victor Cabral, Pavel Studeny, Sami Kereïche, Katerina Jirsova, Dušan Cmarko.

References

1. Smirnov E, Hornáček M, Vacík T, Cmarko D, Raška I. Discontinuous transcription. Nucleus. 2018; 9 (1):149–60. https://doi.org/10.1080/19491034.2017.1419112 PubMed Central PMCID: PMC5973254. PMID: 29285985

2. McKnight SL, Miller OL. Post-replicative nonribosomal transcription units in D. melanogaster embryos. Cell. 1979; 17(3):551–63. https://doi.org/10.1016/0092-8674(79)90263-0 PMID: 113103

3. Bahar Halpern K, Tanami S, Landen S, Chapal M, Szlak L, Hutzler A, et al. Bursty gene expression in the intact mammalian liver. Mol Cell. 2015; 58(1):147–56. https://doi.org/10.1016/j.molcel.2015.01.027 PubMed Central PMCID: PMC4500162. PMID: 25728770

4. Chubb JR, Trcek T, Shenoy SM, Singer RH. Transcriptional pulsing of a developmental gene. Curr Biol. 2006; 16(10):1018–25. https://doi.org/10.1016/j.cub.2006.03.092 PubMed Central PMCID: PMC4764056. PMID: 16713960

5. Dar RD, Razooky BS, Singh A, Trimeloni TV, McCollum JM, Cox CD, et al. Transcriptional burst frequency and burst size are equally modulated across the human genome. Proc Natl Acad Sci USA. 2012; 109(43):17454–9. https://doi.org/10.1073/pnas.1213530109 PubMed Central PMCID: PMC3491463. PMID: 23064634

6. Golding I, Paulsson J, Zawilski SM, Cox EC. Real-time kinetics of gene activity in individual bacteria. Cell. 2005; 123(6):1025–36. https://doi.org/10.1016/j.cell.2005.09.031 PMID: 16360033

7.   Nicolas D, Phillips NE, Naef F. What shapes eukaryotic transcriptional bursting? Mol Biosyst. 2017; 13 (7):1280–90. https://doi.org/10.1039/c7mb00154a PMID: 28573295

8.   Nicolas D, Zoller B, Suter DM, Naef F. Modulation of transcriptional burst frequency by histone acetylation. Proc Natl Acad Sci USA. 2018; 115(27):7153–8. https://doi.org/10.1073/pnas.1722330115 PubMed Central PMCID: PMC6142243. PMID: 29915087

9.   Raj A, Peskin CS, Tranchina D, Vargas DY, Tyagi S. Stochastic mRNA synthesis in mammalian cells. PLoS Biol. 2006; 4(10):e309. https://doi.org/10.1371/journal.pbio.0040309 PubMed Central PMCID: PMC1563489. PMID: 17048983

10. Suter DM, Molina N, Gatfield D, Schneider K, Schibler U, Naef F. Mammalian genes are transcribed with widely different bursting kinetics. Science. 2011; 332(6028):472–4. https://doi.org/10.1126/ science.1198817 PMID: 21415320

11. Suter DM, Molina N, Naef F, Schibler U. Origins and consequences of transcriptional discontinuity. Curr Opin Cell Biol. 2011; 23(6):657–62. https://doi.org/10.1016/j.ceb.2011.09.004 PMID: 21963300

12. Wang Y, Ni T, Wang W, Liu F. Gene transcription in bursting: a unified mode for realizing accuracy and stochasticity. Biol Rev Camb Philos Soc. 2018. https://doi.org/10.1111/brv.12452 PMID: 30024089

13. Li C, Cesbron F, Oehler M, Brunner M, Höfer T. Frequency modulation of transcriptional bursting enables sensitive and rapid gene regulation. Cell Syst. 2018; 6(4):409–23.e11. https://doi.org/10.1016/ j.cels.2018.01.012 PMID: 29454937

14. Ochiai H, Hayashi T, Umeda M, Yoshimura M, Harada A, Shimizu Y, et al. Genome-wide analysis of transcriptional bursting-induced noise in mammalian cells. BioRxiv. 2019. https://doi.org/10.1101/ 736207

15. Coulon A, Ferguson ML, de Turris V, Palangat M, Chow CC, Larson DR. Kinetic competition during the transcription cycle results in stochastic RNA processing. elife. 2014;3. https://doi.org/10.7554/eLife. 03939 PubMed Central PMCID: PMC4210818. PMID: 25271374

16. Eldar A, Elowitz MB. Functional roles for noise in genetic circuits. Nature. 2010; 467(7312):167–73. https://doi.org/10.1038/nature09326 PubMed Central PMCID: PMC4100692. PMID: 20829787

17. Raj A, van Oudenaarden A. Nature, nurture, or chance: stochastic gene expression and its consequences. Cell. 2008; 135(2):216–26. https://doi.org/10.1016/j.cell.2008.09.050 PubMed Central PMCID: PMC3118044. PMID: 18957198

18. Chubb JR. Gene regulation: stable noise. Curr Biol. 2016; 26(2):R61–R4. https://doi.org/10.1016/j.cub. 2015.12.002 PMID: 26811888

19. Bahar Halpern K, Itzkovitz S. Single molecule approaches for quantifying transcription and degradation rates in intact mammalian tissues. Methods. 2016; 98:134–42. https://doi.org/10.1016/j.ymeth.2015.11. 015 PMID: 26611432

20. Femino AM, Fay FS, Fogarty K, Singer RH. Visualization of single RNA transcripts in situ. Science. 1998; 280(5363):585–90. https://doi.org/10.1126/science.280.5363.585 PMID: 9554849

21. Mueller F, Senecal A, Tantale K, Marie-Nelly H, Ly N, Collin O, et al. FISH-quant: automatic counting of transcripts in 3D FISH images. Nat Methods. 2013; 10(4):277–8. https://doi.org/10.1038/nmeth.2406 PMID: 23538861

22. Larsson AJM, Johnsson P, Hagemann-Jensen M, Hartmanis L, Faridani OR, Reinius B, et al. Genomic encoding of transcriptional burst kinetics. Nature. 2019; 565(7738):251–4. https://doi.org/10.1038/ s41586-018-0836-1 PMID: 30602787

23. Bensidoun P, Raymond P, Oeffinger M, Zenklusen D. Imaging single mRNAs to study dynamics of mRNA export in the yeast Saccharomyces cerevisiae. Methods. 2016; 98:104–14. https://doi.org/10. 1016/j.ymeth.2016.01.006 PMID: 26784711

24. Bertrand E, Chartrand P, Schaefer M, Shenoy SM, Singer RH, Long RM. Localization of ASH1 mRNA particles in living yeast. Mol Cell. 1998; 2(4):437–45. https://doi.org/10.1016/s1097-2765(00)80143-4 PMID: 9809065

25. Henderson AS, Warburton D, Atwood KC. Location of ribosomal DNA in the human chromosome complement. Proc Natl Acad Sci USA. 1972; 69(11):3394–8. https://doi.org/10.1073/pnas.69.11.3394 PubMed Central PMCID: PMC389778. PMID: 4508329

26. Long EO, Dawid IB. Repeated genes in eukaryotes. Annu Rev Biochem. 1980; 49:727–64. https://doi. org/10.1146/annurev.bi.49.070180.003455 PMID: 6996571

27. Moss T, Mars J-C, Tremblay MG, Sabourin-Felix M. The chromatin landscape of the ribosomal RNA genes in mouse and human. Chromosome Res. 2019; 27(1–2):31–40. https://doi.org/10.1007/s10577-018-09603-9 PMID: 30617621

28. Puvion-Dutilleul F, Bachellerie J-P, Puvion E. Nucleolar organization of HeLa cells as studied by in situ hybridization. Chromosoma. 1991; 100(6):395–409. https://doi.org/10.1007/bf00337518 PMID: 1893795

29. Raska I, Shaw PJ, Cmarko D. New insights into nucleolar architecture and activity. Int Rev Cytol. 2006; 255:177–235. https://doi.org/10.1016/S0074-7696(06)55004-1 PMID: 17178467

30. Sharifi S, Bierhoff H. Regulation of RNA polymerase I transcription in development, disease, and aging. Annu Rev Biochem. 2018; 87:51–73. https://doi.org/10.1146/annurev-biochem-062917-012612 PMID: 29589958

31. Bártová E, Horáková AH, Uhlírová R, Raska I, Galiová G, Orlova D, et al. Structure and epigenetics of nucleoli in comparison with non-nucleolar compartments. The Journal of Histochemistry and Cytochemistry. 2010; 58(5):391–403. https://doi.org/10.1369/jhc.2009.955435 PubMed Central PMCID: PMC2857811. PMID: 20026667

32. Bersaglieri C, Santoro R. Genome Organization in and around the Nucleolus. Cells. 2019; 8(6). https://doi.org/10.3390/cells8060579 PubMed Central PMCID: PMC6628108. PMID: 31212844

33. Casafont I, Navascués J, Pena E, Lafarga M, Berciano MT. Nuclear organization and dynamics of transcription sites in rat sensory ganglia neurons detected by incorporation of 5'-fluorouridine into nascent RNA. Neuroscience. 2006; 140(2):453–62. https://doi.org/10.1016/j.neuroscience.2006.02.030 PMID: 16563640

34. Cmarko D, Smigova J, Minichova L, Popov A. Nucleolus: the ribosome factory. Histology and Histopathology. 2008; 23(10):1291–8. https://doi.org/10.14670/HH-23.1291 PMID: 18712681

35. Cmarko D, Verschure PJ, Rothblum LI, Hernandez-Verdun D, Amalric F, van Driel R, et al. Ultrastructural analysis of nucleolar transcription in cells microinjected with 5-bromo-UTP. Histochemistry and Cell Biology. 2000; 113(3):181–7. https://doi.org/10.1007/s004180050437 PMID: 10817672

36. Koberna K, Malínský J, Pliss A, Masata M, Vecerova J, Fialová M, et al. Ribosomal genes in focus: new transcripts label the dense fibrillar components and form clusters indicative of "Christmas trees" in situ. The Journal of Cell Biology. 2002; 157(5):743–8. https://doi.org/10.1083/jcb.200202007 PubMed Central PMCID: PMC2173423. PMID: 12034768

37. Lam YW, Trinkle-Mulcahy L. New insights into nucleolar structure and function. F1000Prime Rep. 2015; 7:48. https://doi.org/10.12703/P7-48 PubMed Central PMCID: PMC4447046. PMID: 26097721

38. Scheer U, Benavente R. Functional and dynamic aspects of the mammalian nucleolus. Bioessays: News and Reviews in Molecular, Cellular and Developmental Biology. 1990; 12(1):14–21. https://doi.org/10.1002/bies.950120104 PMID: 2181998

39. Shaw PJ, McKeown PC. The Structure of rDNA Chromatin. In: Olson MOJ, editor. The Nucleolus. New York, NY: Springer New York; 2011. p. 43–55.

40. Sirri V, Urcuqui-Inchima S, Roussel P, Hernandez-Verdun D. Nucleolus: the fascinating nuclear body. Histochemistry and Cell Biology. 2008; 129(1):13–31. https://doi.org/10.1007/s00418-007-0359-6 PubMed Central PMCID: PMC2137947. PMID: 18046571

41. Raška I, Reimer G, Jarník M, Kostrouch Z, Raška K Jr. Does the synthesis of ribosomal RNA take place within nucleolar fibrillar centers or dense fibrillar components? Biology of the cell. 1989; 65(1):79–82. PMID: 2539876

42. Correll CC, Bartek J, Dundr M. The Nucleolus: A Multiphase Condensate Balancing Ribosome Synthesis and Translational Capacity in Health, Aging and Ribosomopathies. Cells. 2019; 8(8):869.

43. Cheutin T, O'Donohue M-F, Beorchia A, Vandelaer M, Kaplan H, Deféver B, et al. Three-dimensional organization of active rRNA genes within the nucleolus. Journal of Cell Science. 2002; 115(Pt 16):3297–307.

44. Haaf T, Hayman DL, Schmid M. Quantitative determination of rDNA transcription units in vertebrate cells. Experimental Cell Research. 1991; 193(1):78–86. https://doi.org/10.1016/0014-4827(91)90540-b PMID: 1995304

45. Smirnov E, Borkovec J, Kováčik L, Svidenská S, Schröfel A, Skalníková M, et al. Separation of replication and transcription domains in nucleoli. J Struct Biol. 2014; 188(3):259–66. https://doi.org/10.1016/j.jsb.2014.10.001 PMID: 25450594

46. Haaf T, Ward DC. Inhibition of RNA polymerase II transcription causes chromatin decondensation, loss of nucleolar structure, and dispersion of chromosomal domains. Experimental Cell Research. 1996; 224(1):163–73. https://doi.org/10.1006/excr.1996.0124 PMID: 8612682

47. Tollervey D, Kiss T. Function and synthesis of small nucleolar RNAs. Curr Opin Cell Biol. 1997; 9 (3):337–42. https://doi.org/10.1016/s0955-0674(97)80005-1 PMID: 9159079

48. Tollervey D, Lehtonen H, Jansen R, Kern H, Hurt EC. Temperature-sensitive mutations demonstrate roles for yeast fibrillarin in pre-rRNA processing, pre-rRNA methylation, and ribosome assembly. Cell. 1993; 72(3):443–57. https://doi.org/10.1016/0092-8674(93)90120-f PMID: 8431947

49. Iyer-Bierhoff A, Grummt I. Stop-and-Go: Dynamics of Nucleolar Transcription During the Cell Cycle. Epigenet Insights. 2019; 12:2516865719849090. https://doi.org/10.1177/2516865719849090 PubMed Central PMCID: PMC6537492. PMID: 31206100

50. Pliss A, Kuzmin AN, Kachynski AV, Baev A, Berezney R, Prasad PN. Fluctuations and synchrony of RNA synthesis in nucleoli. Integrative Biology: Quantitative Biosciences from Nano to Macro. 2015; 7 (6):681–92. https://doi.org/10.1039/c5ib00008d PMID: 25985251

51. Hornáček M, Kováčik L, Mazel T, Cmarko D, Bártová E, Raška I, et al. Fluctuations of pol I and fibrillarin contents of the nucleoli. Nucleus. 2017; 8(4):421–32. https://doi.org/10.1080/19491034.2017.1306160 PubMed Central PMCID: PMC5597295. PMID: 28622108

52. Brejchova K, Trosan P, Studeny P, Skalicka P, Utheim TP, Bednar J, et al. Characterization and comparison of human limbal explant cultures grown under defined and xeno-free conditions. Experimental Eye Research. 2018; 176:20–8. https://doi.org/10.1016/j.exer.2018.06.019 PMID: 29928900

53. Stadnikova A, Trosan P, Skalicka P, Utheim TP, Jirsova K. Interleukin-13 maintains the stemness of conjunctival epithelial cell cultures prepared from human limbal explants. Plos One. 2019; 14(2): e0211861. https://doi.org/10.1371/journal.pone.0211861 PubMed Central PMCID: PMC6370187. PMID: 30742646

54. Dundr M, Hoffmann-Rohrer U, Hu Q, Grummt I, Rothblum LI, Phair RD, et al. A kinetic framework for a mammalian RNA polymerase in vivo. Science. 2002; 298(5598):1623–6. https://doi.org/10.1126/science.1076164 PMID: 12446911

55. Smirnov E, Hornáček M, Kováčik L, Mazel T, Schröfel A, Svidenská S, et al. Reproduction of the FC/DFC units in nucleoli. Nucleus. 2016; 7(2):203–15. https://doi.org/10.1080/19491034.2016.1157674 PMID: 26934002

56. Schermelleh L, Solovei I, Zink D, Cremer T. Two-color fluorescence labeling of early and mid-to-late replicating chromatin in living cells. Chromosome Res. 2001; 9(1):77–80. https://doi.org/10.1023/a:1026799818566 PMID: 11272795

57. Golding I, Cox EC. RNA dynamics in live Escherichia coli cells. Proc Natl Acad Sci USA. 2004; 101 (31):11310–5. https://doi.org/10.1073/pnas.0404443101 PubMed Central PMCID: PMC509199. PMID: 15277674

58. Lionnet T, Czaplinski K, Darzacq X, Shav-Tal Y, Wells AL, Chao JA, et al. A transgenic mouse for in vivo detection of endogenous labeled mRNA. Nat Methods. 2011; 8(2):165–70. https://doi.org/10.1038/nmeth.1551 PubMed Central PMCID: PMC3076588. PMID: 21240280